C U R S O S E C O N G R E S O S

RSME2011

Transfer and Industrial Mathematics

PROCEEDINGS OF THE RSME CONFERENCE ON TRANSFER AND INDUSTRIAL MATHEMATICS

Santiago de Compostela
July, 12th-14th, 2011

EDITED BY
P. Quintela
M. J. Esteban
W. González
M. C. Muñiz
J. Rubio
J. J. Salazar

UNIVERSIDADE DE SANTIAGO DE COMPOSTELA
publicacións

RSME2011

Transfer and Industrial Mathematics

Proceedings of the RSME Conference
on Transfer and Industrial Mathematics

Santiago de Compostela, July 12-14, 2011

Edited by
P. Quintela ● M. J. Esteban
W. González ● M. C. Muñiz
J. Rubio ● J. J. Salazar

2011

UNIVERSIDADE DE SANTIAGO DE COMPOSTELA

CURSOS E CONGRESOS DA
UNIVERSIDADE DE SANTIAGO DE COMPOSTELA
Nº 204

TRANSFER and Industrial Mathematics : proceedings of the RSME Conference on Transfer and Industrial Mathematics : Santiago de Compostela, July 12-14, 2011 / edited by P. Quintela, … [et al.]. – Santiago de Compostela : Universidade, Servizo de Publicacións e Intercambio Científico, 2011. -- p. ; cm. – (Cursos e congresos da Universidadade de Santiago de Compostela ; 204). – ISBN 978-84-9887-715-1

1. Matemáticas para enxeñeiros -- Congresos. 2. Modelos matemáticos -- Congresos. I. Quintela Estévez, Peregrina, 1960- , ed. II. Real Sociedad Matemática Española (Madrid). III. Universidade de Santiago de Compostela. Servizo de Publicacións e Intercambio Científico, ed.

51:62
62:51

Edita
Servizo de Publicacións e Intercambio Científico
Campus Vida
15782 Santiago de Compostela
www.usc.es/publicacions

ISBN 978-84-9887-715-1 (edición dixital .pdf)

PREFACE

The RSME Conference on Transfer and Industrial Mathematics is supported by the Royal Spanish Mathematical Society, a scientific society for the promotion of mathematics and its applications as well as the encouragement of research and teaching at all educational levels.

The three-day conference presents successful experiences in the field of mathematical knowledge transfer to industry and focuses on the following issues:

- Showing how collaboration with industry has opened up new lines of research in the field of mathematics providing high quality contributions to international journals and encouraging the development of doctoral theses.
- How the promotion of existing infrastructures has contributed to enhance the transfer of mathematical knowledge to industry.
- The presentation of postgraduate programs offering training in mathematics with industrial applications.

The conference includes talks from researchers and industry representatives who present their different points of view and experiences with regards to the transfer of mathematical knowledge to industry.

We would like to sincerely thank the invited speakers for coming to Santiago and motivating the audience with their interesting contributions. We are greatly indebted to the Scientific Committee (Alfredo Bermúdez de Castro, Mikel Lezaun, Justo Puerto, Peregrina Quintela, Joan Solá-Morales) for reviewing all the contributed material.

We gratefully acknowledge the financial support provided by the Spanish Ministerio de Ciencia e Innovación (MICINN), the Ingenio Mathematica Consolider Project, the Royal Spanish Mathematical Society, the Consulting and Computing Network and, especially, the Universidade de Santiago de Compostela, which has allowed us to host this event in its buildings.

Finally, we would like to thank Elisa Eiroa and Guadalupe Parente for their administrative support and all the speakers and participants in this conference, without which the event would not have taken place.

We hope that this conference and its collection of proceedings provide a good contribution to the most recent research in transfer and industrial mathematics.

Santiago de Compostela, Spain
July 2011

Peregrina Quintela
María J. Esteban
Wenceslao González
MCarmen Muñiz
Julio Rubio
Juan José Salazar

Contents

POSTERS

Invited Lecture.

Numerical simulation of metallurgical processes in silicon production

Javier Bullón

Ferroatlántica I+D
Polígono Industrial de Sabón, Arteixo, A Coruña, Spain.
e-mail: jbullon@ferroatlantica.es

Pilar Salgado

Departamento de Matemática Aplicada
Universidade de Santiago de Compostela, Escola Politécnica Superior, Lugo, Spain.
e-mail: mpilar.salgado@usc.es

Abstract

The objective of this work is to describe the collaboration between the company Ferroatlántica I+D and the research group in Mathematical Engineering of the University of Santiago de Compostela (Spain) on the numerical simulation of metallurgical processes.

1.1 Introduction

Ferroatlántica Group is composed by different companies devoted to the the production of ferroalloys and, in particular, of silicon. The research activity of the group is coordinated by Ferroatlántica I + D which keeps a fluid collaboration with different universities and research centers. From 1996, Ferroatlántica I+D has maintained an intensive collaboration with the research group in Mathematical Engineering in order to understand and develop different technological innovations in silicon production by using numerical simulation. This collaboration has been financed by the company under annual contracts and also supported from public funds. An important number of people has participated in this experience: Javier Bullón, the manager of Ferroatlántica I+D has supervised the company group which has been integrated by M. Lage, A. Lorenzo, J. M. Míguez, A. Miranda, A. Pérez and R. Ordás; the professor Alfredo Bermúdez has been the director of the university group, where D. Gómez, R. Leira, M.C. Muñiz, C. Naya, F. Pena, M. Piñeiro, P. Salgado, A. Varela and R. Vázquez have participated.

The numerical simulation has been used to study different industrial applications; namely:

- Modeling of thermoelectrical and thermomechanical behavior of metallurgical electrodes.
- Modeling of the thermo-magneto-hydrodynamic behavior of an induction heating furnace.
- Thermoelectrical modeling of innovative casting systems.

The used methodology to analyze these problems can be summarized in the following steps: to understand the physical phenomena involved in the metallurgical process, to develop suitable mathematical models, to analyze efficient numerical techniques to approximate its solution and elaborate a software package to simulate the full process. In this work, we will focus in the two first applications cited above. Thus, Section 2 is devoted to the description of the physical problem involved in an electric arc furnace,

the role of metallurgical electrodes and the key points of its numerical simulation. In Section 3, we explain the working of an induction heating furnace and the goal of its modeling. The software developed to simulate these applications is also described in the corresponding sections. Finally, in Section 4, we show the main research lines in the field of mathematical modeling and numerical analysis opened as a consequence of the collaboration with Ferroatántica I+D.

1.2 Numerical simulation of metallurgical electrodes

Silicon is produced industrially by reduction of silicon dioxide, as quartz or quartzite, with carbon, by a reaction which can be written in a simple way as $\mathrm{Si\,O_2} + 2\mathrm{C} = \mathrm{Si} + 2\mathrm{CO}$. This reaction takes place in a submerged "arc" furnace which uses three-phase alternating current. A simple sketch of the furnace can be seen in Figure 1.1; it consists of a cylindrical pot containing charge materials and three electrodes disposed conforming an equilateral triangle. Electrodes are the main components of reduction furnaces and their purpose is to conduct the electric current to the center of the furnace; the current enters the electrode through the "contact clamps" and goes down crossing the column generating heat by Joule effect. At the tip of the electrode an electric arc is produced, generating the high temperatures that activate the chemical reaction.

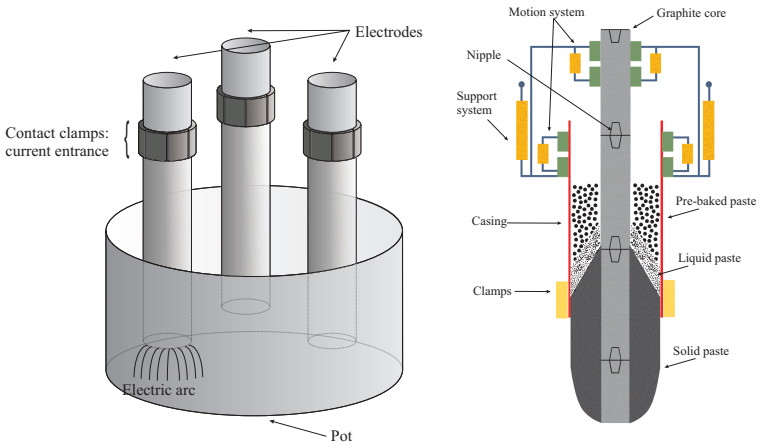

Figure 1.1: A reduction furnace (left). Skecth of an ELSA electrode (right).

The electrodes can be of different kinds, depending on the type of production; namely, ferro-silicon or silicon metal (silicon with metallurgical quality). For many years, graphite or prebaked electrodes have been the only kind of electrodes used in silicon metal production. In the early 1990s, Ferroatlántica S.L. patented a new type of electrode named ELSA [2], that serves for the production of silicon metal at a lower cost of the classical electrodes; nowadays, this electrode is used in a great part of the world's silicon production.

An ELSA electrode consists of a central column of baked carbonaceous material, graphite or similar, surrounded by a Søderberg-like paste (see Figure 1.1). There is a steel casing that contains the paste until it is baked and the baking of paste is a crucial point in the working of this type of electrode. In general, the design and control parameters of electrodes are very complex and numerical simulation plays an important role at this point; modeling the involved phenomena in a computer allows us to analyze the influence of changing a parameter without the need of expensive and difficult tests. Thus, Ferroatlántica started its collaboration with the university group in order to simulate the behavior of the

ELSA electrode to improve its design and operation conditions; the main objectives in this simulation have been: to know and control the parameters involved in the baking of paste and to improve the design of the nipple-joints which connect the graphite bars. In this framework, the group has developed mathematical models which allow to compute the temperature distribution, the current density and the stresses produced in an electrode under different operation conditions. The first works deal with the thermoelectrical and thermomechanical modeling of a single electrode by assuming cylindrical symmetry and solving the problem in a vertical section of the electrode [3]. The mathematical models involve the coupling between the eddy current problem obtained from Maxwell equations, the heat transfer equation in transient or steady state and the elasticity equations.

In despite of the simplifications, the axisymmetric models have given valuable information on important electrode parameters and have been used for specific purposes with promising results. For instance, the position of the baked zone, the distribution of stresses, the behavior of the electrode varying parameters such us, electric current intensity, slipping rate, shut-down/start-up procedures, material properties, etc, have been extensively studied with these models. The main advantage of the axisymmetric models compared with three-dimensional ones is the saving in computing time. However, a more realistic modeling of the reduction furnace requires to consider three-dimensional models which have been developed by the group in a second phase [8, 9]. From the numerical point of view, the finite element method has been a common tool to solve the different models, while the coupled aspects have been dealt with iterative algorithms. All the numerical methods have been implemented in Fortran and MATLAB codes; furthermore, it has been developed a graphical user interface called ELSATE which can be used by the the company to simulate the ELSA electrode by introducing the data and plotting the results in an easy way.

1.3 Numerical simulation of an induction heating furnace

Induction heating is a physical process extensively used in metallurgy for several purposes such us heating or stirring. An induction heating system consists of one or several inductors supplied with alternating electrical current and a conductive workpiece to be heated. The alternating current traversing the inductor generates eddy currents in the workpiece, and through the Ohmic losses the workpiece is heated (see Figure 1.2). Different furnaces can be designed depending on its application. In the last years, Ferroatlántica I+D has been interested in modeling the behavior of a cilyndrical induction furnace used for melting and stirring. This furnace consists of an helical copper coil and a workpiece, which is formed by the crucible and the load within; the load is the material to melt and the crucible is usually a refractory material which can resist very high temperatures.

In induction heating it is crucial to control the distribution of Ohmic losses or to choose a suitable frequency and intensity of the alternating current to achieve the stirring. Thus, the numerical simulation represents a powerful tool to optimize the design and the operation conditions of the furnace. The overall process in an induction heating system is very complex and involves different physical phenomena, electromagnetic, thermal with change of phase and hydrodynamic in the liquid region. In order to perform a realistic numerical simulation of the furnace, the research group has developed a thermo-magneto-hydrodynamic model based on cylindrical symmetry [4, 12]; this model leads to a coupled nonlinear system of partial differential equations and allows us to compute the electromagnetic fields, the temperature and the velocity of the liquid part in a vertical section. From a numerical point of view, the problem is discretized by using a mixed boundary element/finite element method, while the coupling aspects and the non-linearities are dealt with iterative algorithms. The group has developed a Fortran code to solve the coupled problem integrated in a graphical user interface called THESIF;

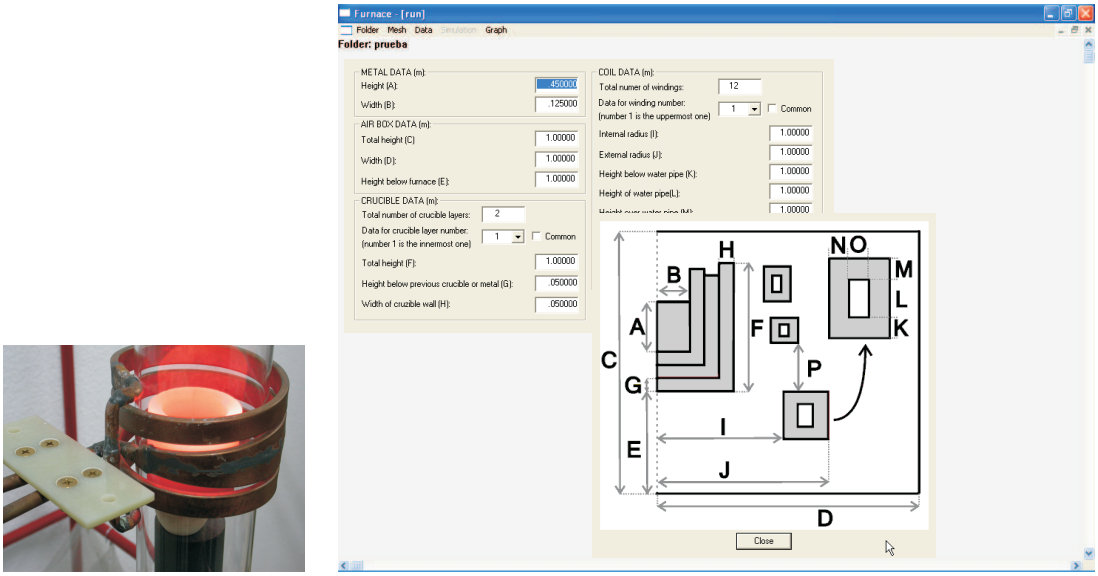

Figure 1.2: A simple induction furnace (left). Sketch of the graphical interface THESIF (right).

Figure 1.2 (right) shows an example of menus of this interface. The numerical method has been applied to simulate the induction heating furnace used by Ferroatlántica I+D under different conditions.

1.4 Research lines in mathematical modeling and numerical analysis

The collaboration with the industry opened interesting research lines for the university group in several topics, specially in electromagnetism and thermoelectrical and magneto-hydrodynamic problems. There are still many open questions related to the mathematical and numerical analysis of these models, which are present in many other industrial applications. The electromagnetic model, based on the eddy current equations represents itself an enough complex problem, specially in three-dimensional domains [1]. Thus, in the last years the group has developed an important research line which relies on the mathematical and numerical analysis of the eddy current model in the axisymmetric and three-dimensional case [4, 7, 8, 9, 11]; on the other hand, questions related to the analysis of the thermoelectrical problem are studied in [5, 10], while the magneto-hydrodynamic model is analyzed in [6, 12]. The theoretical research was funded by the Galician and Spanish Administrations and allowed to several members of the group the development of its doctoral thesis. Besides the reference works included in the literature, many of the results have been presented in metallurgical and numerical conferences in collaboration with personal of Ferroatlántica I + D.

Bibliography

[1] A. Alonso and A. Valli, *Eddy current approximation of Maxwell equations,* Springer-Verlag, 2010.

[2] J. Bullón and V. Gallego, *The use of a compound electrode for the production of silicon metal.* Electric Furnace Conference Proceedings, Vol. 52, Iron & Steel Society, Warrendale, PA, 371–374, 1994.

[3] A. Bermúdez, J. Bullón, F. Pena and P. Salgado, A numerical method for transient simulation of metallurgical compound electrodes, Finite Elem. Anal. Des. 39, (2003), 283-299.

[4] A. Bermúdez, D. Gómez, M. C. Muñiz, P. Salgado and R. Vázquez, Numerical simulation of a thermo-electromagneto-hydrodynamic problem in an induction heating furnace, Appl. Numer. Math. 59 (9), (2009), 2082-2104.

[5] A. Bermúdez, R. Muñoz-Sola and F. Pena, A nonlinear partial differential system arising in thermoelectricity, European J. Appl. Math. 16 (6), (2005), 683-712.

[6] A. Bermúdez, R. Muñoz-Sola and R. Vázquez, Analysis of two stationary magnetohydrodynamics systems of equations including Joule heating, J. Math. Anal. Appl. 368, (2010), 444-468.

[7] A Bermúdez, C. Reales, R. Rodríguez and P. Salgado, Numerical analysis of a finite-element method for the axisymmetric eddy current model of an induction furnace IMA J. Numer. Anal. 30, (2010), 654-676.

[8] A. Bermúdez, R. Rodríguez and P. Salgado, A finite element method with Lagrange multipliers for low-frequency harmonic Maxwell equations, SIAM J. Numer. Anal., 40 (5), (2002), 1823-1849.

[9] A. Bermúdez, R. Rodríguez and P. Salgado, Finite element methods for 3D eddy current problems in bounded domains subject to realistic boundary conditions. An application to metallurgical electrodes. Arch. Comput. Meth. Engng., 12 (1), (2005), 67-114.

[10] F. Pena, *Contribución al modelado matemático de algunos problemas en la metalurgia del silicio.* Ph.D. Thesis, Universidade de Santiago de Compostela, 2003.

[11] P. Salgado, *Mathematical and numerical analysis of some electromagneitc problems. Application to the simulation of metallurgical electrodes.* Ph.D. Thesis, Universidade de Santiago de Compostela, 2002.

[12] R. Vázquez, *Contributions to the mathematical study of some problems in magnetohydrodynamics and induction heating,* Ph.D. Thesis, Universidade de Santiago de Compostela, 2009.

Invited Lecture.

Risk Modeling in Finance

José L. Fernández

Departamento de Matemáticas, Universidad Autónoma de Madrid, 28049 Madrid, Spain
joseluis.fernandez@uam.es

Paul MacManus

Afi, Españoleto 19, 28010 Madrid, Spain, pmacmanus@afi.es

In the aftermath of this Great Recession, the use of mathematics and statistics in financial risk management is being thoroughly revised. From the academic standpoint, better models and new approaches are needed to address, in particular, feedback effects and the overall complexity of the financial system. However, besides the need for better modeling tools, it is clear that all parties involved in risk management need to be keenly aware of the limitations of mathematical modeling in the social sciences.

2.1 Introduction

Risk models are essential for understanding and managing financial risk but their intrinsic limitations need to be properly understood and their underlying hypotheses have to be clear and transparent to those who are going to use them as management and decision tools. Unrealistic claims on their accuracy and on the their range of application have to be avoided.

Commonly used models need be improved, starting with using the best academic approaches available and avoiding "simplicity for convenience". As the saying goes, models should be as simple as possible, but no simpler. More advanced models which are able to encompass feedback effects and the inherent complexity of the financial system have to be developed, tested (as far as possible), and, of course, properly used.

It should be clearly understood by all involved that most mathematical models in this context are designed to help management in their decisions and that most of them will not be fully scientific models which can be properly verified and back-tested.

> *Personally I ought to say that there is, in my own opinion, considerable danger in applying the methods of exact science to problems in descriptive science, whether they be problems of heredity or of political economy; the grace and logical accuracy of the mathematical processes are apt to so fascinate the descriptive scientist that he seeks for sociological hypotheses which fit his mathematical reasoning and this without first ascertaining whether the basis of his hypotheses is as broad as that human life to which the theory is to be applied.*

This warning comes from a lecture that Karl Pearson delivered at the Men's and Women's Club in 1889; from [9]. And, here is a sample of what Daniel Innerarity, a professor of social and political philosophy from the Basque country, has to say about models, statistics and crises in [8]:

Nos hace falta una verdadera revolución epistemológica para abandonar la ilusión de que podemos vivir en un mundo calculable, que resultaría de aplicar ilimitadamente el modelo científico que hemos heredado de las ciencias de la naturaleza a las realidades sociales. Este modelo debe su exactitud a que mide realidades objetivas, exteriores a los sujetos, pero es muy limitado a la hora de calcular comportamientos humanos como el del sistema financiero, que no es algo exterior a la sociedad, que pudiera ser controlado por el saber y la tecnología, sino que resulta de la suma de nuestras acciones.[1]

2.2 Risk models in finance and their limitations.

The output of a (statistical) risk model in finance is the joint probability distribution of the values of a number of financial variables (or risk factors). The structure of such a distribution is obtained from statistical analysis of the past joint behavior of those variables. That distribution is then applied to an investment portfolio, to a portfolio of mortgages, to the whole balance of the institution,..., to obtain a probability distribution of market value, or of loss arising from defaults, or of the mismatch between assets and liabilities, ..., so that extreme (negative) variations can be anticipated and managed.

It is important to distinguish between internal models, those that institutions create for their own use, and regulatory models, standardized models used in the calculation of regulatory capital.[2]

In 2001, Danielsson, Embrecths, Goodhart *et al.* [4], exposed the **fundamental limitations and foundational problems** of the current practice of risk modeling. So nothing is new, except that the current crisis has unveiled just how very important these limitations are and the urgency of finding alternatives and improvements that go beyond current practice. We will concentrate on two of these areas in order to focus on some interesting and relevant modeling questions.

2.2.1 Statistics and probability, limitations

Most models used in risk management are parametric models. The parameters are chosen – in the process of calibration – so that the models match as accurately as possible relatively long series of data. One important exception is the widely used process of historical simulation, which simply uses the actual historical series to create samples of futures scenarios without imposing any model whatsoever,

The main outputs of statistical risk models are estimates of very extreme percentiles. For a 1-month VaR at 99,9%, a model is supposed to accurately estimate the largest fall that a portfolio might experience over the course of a month at the 99,9% percentile. In other words, the model is supposed to capture events that will happen only once in 1000 months. These unrealistic demands on the models are plainly impossible to test in practice. This violates a fundamental tenet of the scientific method: model predictions, whether deterministic or probabilistic, should be properly verified and backtested.

Any statistical model that tries to estimate the kinds of extreme percentiles we are considering assumes that there is some unknown *stable* source of risk that generates the values of the relevant variables along with a long series of data of sufficient quality to calibrate the model. Neither of these conditions are met

[1] Amen! The whole article is well worth reading.

[2] In addition, there are the models that investment banks and ratings agencies *were* using for valuing securitizations of mortgages, subprime and not so subprime. These models were grossly naive, if, as claimed, their purpose was to determine the level of protection of the so called senior tranches. More importantly, they provided a false sense of confidence and hid the lack of any real understanding of the nature of the risks involved. This abuse created very opaque and unstable instruments, understood by nobody, but sold by a few and bought by many. The misuse of (statistical, mathematical) models for this purpose ignited the crisis, although it did not cause it; like a match in a gas filled room.

in practice. The financial markets are constantly changing: new instruments, new markets, new agents, new financing needs, new liquidity context, new.... Change happens all the time. The sources of risk are far from stable and, moreover, the causes of structural change in these rapidly evolving markets are unknown.

Regarding historical data series, for many market variables these are no more than a couple of decades long at the very most and, in any case, data from a decade or more ago is usually dismissed as irrelevant for generating scenarios of future behaviour because, as described above, it comes from a different world. This means that we have even less data available to us for calibrating our model. It is clear that we are modelling an ever-changing reality and that this will change, soon, unexpectedly, precisely during the future time horizon that the model is trying to understand. Even when using relatively recent data to calibrate, one is (in some sense) trying to understand how a disappearing world behaves.

Auto insurance, for example, serves as a good contrast. Calculation of insurance premiums is based on statistical distributions of the severity of accidents. Those distributions are reasonably stable. Of course, one has to try to anticipate how they may change, whether due to new safety standards (airbags, city safety, ...), new regulation (enforcement of traffic rules, speed limits, ...), ..., and estimate their impact on the severity distributions. But, in any case, these changes are signalled well in advance. This stability and anticipation of change are simply not present in the context of financial markets and this fact cannot be overlooked.

This does not mean that the estimates obtained in a carefully designed and calibrated model are useless, far from it. A (good) risk model can be a very useful risk management tool. For example, if the VaR estimate increases, this indicates that the risk of the portfolio has increased, and it helps to identify where the extra source of risk is coming from. Capital allocation based on risk modelling is extremely useful for identifying sources of risk and risk concentration in a portfolio, and risk modelling can provide very important insights into the interactions between different risk factors (correlation) and the degree of diversification provided by different asset allocations and investment strategies. But note that these uses are more qualitative than quantitative in nature: this is important. The exact numbers produced by these models are neither as reliable nor as important as they often presented as being. [3] We should not place the same faith in risk models that we place on predictive scientific models; they are not the same thing. Regulators are, of course, well aware of these limitations and the regulations they develop try to compensate for this lack of accuracy by including buffers of varying types, including the use of very high VaR percentiles, multiplying the outputs of the risk models by scaling factors and fixing various model parameters at conservative levels

Risk models are intended to anticipate extraordinary situations but the standard risk models in use currently, with the shortcomings just described, are not prepared for that. Crises are unique events, each one is different, and our basic models are ill-prepared for handling them.

2.2.2 Regulation, feedback and systemic risks

GOODHART'S LAW. *Any observed statistical regularity will tend to collapse once pressure is placed upon it for control purposes.*

DANIELSSON'S COROLLARY. *A risk model breaks down when used for regulatory purposes.*

[3] Simply think for a few seconds, as a scientist, about the meaning of the phrase "once in a thousand months".

The financial system is an extremely complex and interconnected network. This means that built into it, there is the germ of chaotic behavior and nonlinear effects, which are not easy to manage.

An illustrative example, is the effect that floods in Central Europe a few years ago had on the stocks markets in Spain. In general, extreme events that require important payment compensations on the part of insurance companies affect stock and debt markets. Insurance premiums are invested in those market and have to be materialized to meet those payments; if that unavoidable selling is massive, prices will go down. Another example, at the heart of the current crisis, is the default of Lehman Brothers. The default itself was certainly an important event but what really turned it into a massive global shock was the web of real and perceived connections spreading from Lehman throughout the global financial system and the knock-on effects caused by the breaking of these links.

The interconnection of agents and their actions could be modelled. We are talking here of first level models, models intended for understanding but that cannot be directly verified and backtested. These models could help regulators in designing better and more appropriate regulation, and in calculating levels of capital reserves which reflect the systemic relevance of an institution. This is very interesting and challenging mathematics and is not easy. See, for instance, [3] or [1].

Regulation of the financial system itself leads to all types of feedback effects. For example, our current regulatory structure tends to be pro-cyclical. In other words, it requires more capital when the situation is already bad but less when conditions are not so bad. Developing good anti-cyclical risk models (a very desirable goal) is an important area of research.[4]

Endogenous risk is the risk that arises when shocks to a system are amplified within the system. The oscillations of London's Millenium Bridge, [5], provide a very apt engineering illustration of this phenomenon[5]. Current regulation (Basel II, Basel III, Solvency II) generates systemic, endogenous risk: if every institution uses the same risk models[6] with the same metrics (such as VaR) and with the same management tools (such as incremental VaR), every institution will react in the same way to the same shock and that common reaction will amplify its effect. To avoid generating systemic risks while regulating institutional risk, these feedback effects have to be taken into consideration and properly modelled. This is a crucial and fascinating area of research involving equilibrium models from game theory and other advanced mathematical models [7].

If the financial system is so complex that it is almost impossible to manage, one obvious proposal is to *simplify it*. Restrictions on financial instruments and financial agents, improved supervision, anti-cyclical capital requirements, capital requirements for systemic risk: these are all feasible and, provided that they are implemented in an appropriate way, would not unduly restrict the freedom of action of market participants.

Bibliography

[1] K. Anand, S. Brennan, P. Gai, S. Kapadia, M. Wilson. *Complexity and crisis in financial systems.* Bank of England, preprint, 2002

[2] J. P. Bouchad. *The (unfortunate) complexity of the economy.*

[4] The implementation of these would be politically difficult, it is akin to " taking away the punchbowl just as the part is getting going."

[5] Visit Danielsson's web page: `http://www.riskresearch.org/`

[6] No matter how *good* these models are.

[3] R. Cont, A. Moussa, E. Bastos-Santos. *Network Structure and Systemic Risk in Banking Systems Endogenous risk.* Columbia University, preprint, 2010

[4] J. Danielsson, P. Embrechts, *et al*. *An academic response to basel II.* London School of Economics, preprint, 2001

[5] J. Danielsson, H. S. Shin. *Endogenous risk.* London School of Economics, preprint, 2002

[6] *Conclusions of the Financial Crisis Inquiry Commission.* `http://fcic.law.stanford.edu/`

[7] J. Danielsson, H. S. Shin, J.P. Zigrand. *Endogenous and Systemic Risk.* London School of Economics, preprint, 2011

[8] D. Innerarity. *La política y los riesgos del futuro,* diario EL PAIS, 27 de agosto de 2009

[9] R. Rebonato. *The plight of the fortune tellers.* Princeton University Press, 2007

Invited Lecture.

LATENT-BASED MULTIVARIATE ANALYSIS FOR PROCESS UNDERSTANDING, MONITORING AND IMPROVEMENT

Alberto Ferrer

Universidad Politécnica de Valencia
Dpto. Estadística e I.O. Aplicadas y Calidad
Grupo de Ingeniería Estadística Multivariante
Camino de Vera s/n, Edificio 7 A, 46022 Valencia - Spain
aferrer@eio.upv.es - http://mseg.webs.upv.es/index.html

Estela Espinós

Process Engineering Department
UBE CORPORATION EUROPE, S.A.
P.O. Box, 118 - 12080 Castellón - Spain
e.espinos@ube.es - www.ube.es

Abstract

In modern industries, massive amounts of multivariate data are routinely collected through automated in-process sensing. These data often exhibit high correlation, rank deficiency, low signal-to-noise ratio and missing values. Conventional univariate and multivariate statistical techniques are not suitable to be used in these environments. Data from a chemical process owned by UBE Corporation Europe, S.A. are used to discuss these issues and show the potential of latent-based multivariate analysis as an efficient statistical tool for process understanding, monitoring and improvement.

3.1 Introduction

Nowadays, massive amounts of data are routinely collected from processes in modern highly automated industries. Extracting useful information from these data is essential for making sound decisions for process improvement and optimization. This is a strategic issue for industrial success in the tremendous competitive global market.

Although conventional statistical tools such as ordinary least squares-based predictive models, linear discriminant analysis, classical univariate and multivariate statistical process control (SPC) are well sounded from a statistical point of view, they suffer from lack of applicability in data-rich environments, typical of modern processes. Univariate SPC methods ignore the multivariate structure of the data yielding poor performance. Conventional multivariate statistical methods involve the inversion of a covariance matrix. To avoid problems with this inversion, the number of multivariate observations or samples (N) has to be larger than the number of variables (K) and covariance matrix has to be well conditioned (slightly correlated variables). In addition, complete data (no missing values) are required. Nevertheless, these requirements are not met in highly automated processes where not only a few product quality variables but also hundreds (or even thousands) of process variables are measured at a higher frequency rate [1]. In an attempt to avoid the mentioned problems, a bad practice is to select

a priori which variables to be analyzed. This approach is completely inadvisable due to the potential risk of wasting critical and useful information.

For treating large and ill-conditioned data sets that are not full statistical rank ($N < K$), we advocate the use of multivariate statistical projection methods such as principal component analysis (PCA) [2, 3] and partial least squares (PLS) [4, 5]. These are latent-based methods that exploit the correlation structure of the original variables by revealing the few independent underlying sources of variation (latent variables, not observable) that are driving the process at any time. The high dimensionality of the original space, specified from the measured information, is reduced by projecting the information in the original variables down onto low-dimensional subspaces defined by a few latent directions. From these latent subspaces new latent variables and residuals (i.e. deviations from the model) are worked out. The statistical properties of these new latent variables are quite similar to those assumed in classical statistical methods (i.e. normality, independence...) and then process understanding, discrimination, classification and prediction can be done by using standard statistical methods. Instead of selecting variables, latent-based methods advocate for compressing information, and so original variables are not deleted but can be recovered whenever the analyst wants.

3.2 Case study

Data from a petrochemical continuous process have been analyzed to diagnose the causes of variability of one of the critical to cost characteristics: the yield of the reaction. This process takes place in several units. Data base includes: 72 process variables (temperatures, flows, tank levels, etc.) measured every hour from on-line electronic sensors located in the different units, 5 yield variables (%) measured every 8 hours, and 3 yield variables (%) measured every day from off-line laboratory analyses during two campaigns of approximately 4 months each.

Figure 3.1 shows the evolution of the most critical yield (%) in the two campaigns analyzed. Practically, both campaigns have similar performance in process yield (no statistical significance mean difference, p-value < 0.05).

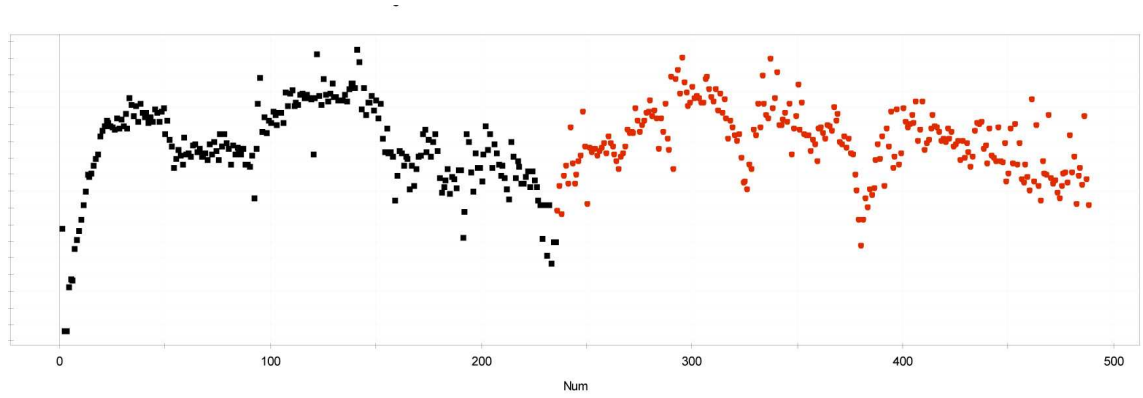

Figure 3.1: Most critical yield (%) in two campaigns

A question arises: does similar behavior in output means similar (i.e., consistent) process? The answer in this case is: no. Figure 3.2 shows the score plot (plot of latent variables) of the two components of

the partial least squares discriminant analysis (PLS-DA) [6] fitted by using only process data (measured every hour). Each one of the points shown summarizes the information of the process at a particular hour. By looking at the swarm of points corresponding to each campaign it is clear that campaign in black is more stable (consistent) than campaign in red.

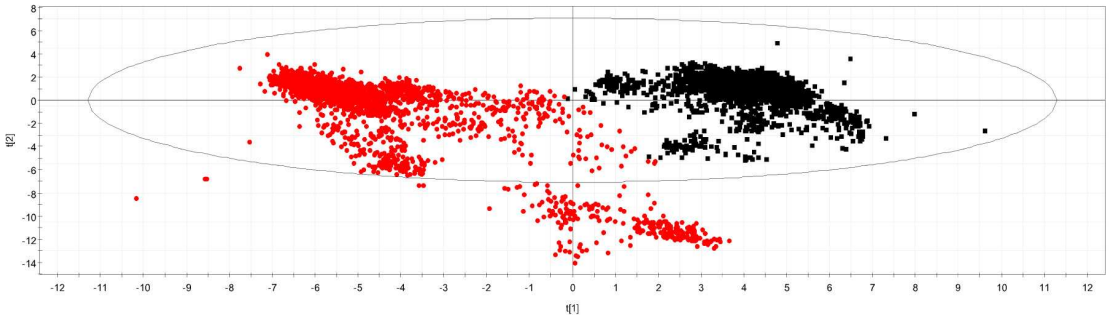

Figure 3.2: Score plot of the two components of the PLS-DA model.

Figure 3.3: Coefficient plot of the PLS-DA model.

To understand which of the process variables has been operated in a different way in the two campaigns, the coefficient plot shown in Figure 3.3 is a useful tool. Those variables with higher coefficients (in absolute value) have different behavior in both campaigns. Figure 3.4 shows a time series chart of one of these discriminating variables showing a higher variability and a different mean in campaign in black than campaign in red.

Process engineers realized that both campaigns yielded similar performance in the critical-to-cost characteristic analyzed under different operational policies. Therefore, same output variable does not necessarily mean similar process. Contrary to the common belief, this case study revealed that operators were implementing different operational rules, causing differences between campaigns in terms of cost and safety.

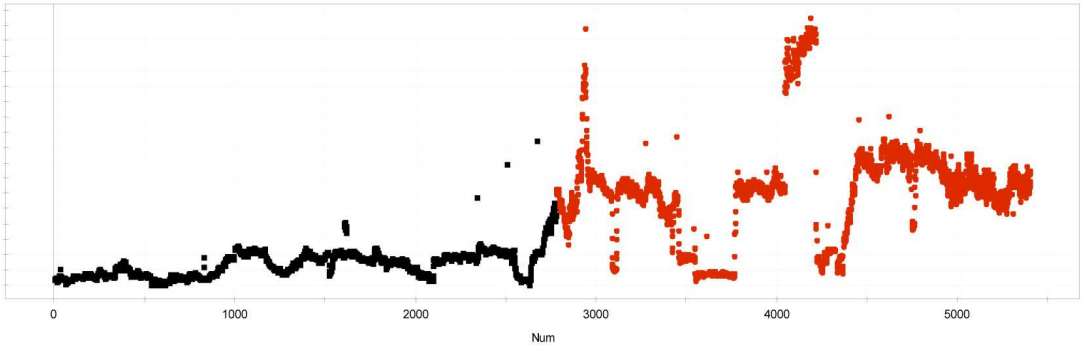

Figure 3.4: Time series plot of one process variable with different behavior in campaigns.

3.3 Summary

Multivariate statistical projection methods helped to detect inconsistent operating policies between campaigns and to diagnose which process variables should be analyzed for a better process control. A latent-based multivariate statistical monitoring scheme was designed to define a normal operating process space and to detect potential deviations in future campaigns.

Bibliography

[1] A. Ferrer, Multivariate statistical process control based on principal component analysis (mspc-pca): Some reflections and a case study in an autobody assembly process, *Quality Engineering* 19 (4), (2007), 311-325.

[2] J.E. Jackson, A UserÕs Guide to Principal Components, Wiley: New York, 2003.

[3] S. Wold, K. Esbensen, P. Geladi, Principal Component Analysis, *Chemometrics and Intelligent Laboratory Systems* 2, (1987), 37-52.

[4] H. Martens, T.Naes, Multivariate Calibration, *Analytica Chimica Acta* 185, (1986), 1-17.

[5] P. Geladi, B.R. Kowalsk, Partial least-squares regression: a tutorial, *Analytica Chimica Acta* 185, (1986), 1-17.

[6] M. Sjšstršm, S. Wold, B. Sšderstršm, PLS discriminant plots,, Proceedings of PARC in Practice, Amsterdam, June 19-21, 1985, Elsevier Science Publishers B.V., North-Holland, 1986.

Invited Lecture.

Successful Transfer of Mathematics to Industry
Open Grid Europe's Project
"Research Cooperation Network Optimisation"

Uwe Gotzes

Open Grid Europe GmbH, Kallenbergstrasse 5, 45141 Essen
uwe.gotzes@open-grid-europe.com, www.open-grid-europe.com

Abstract

Open Grid Europe is Germany's leading gas network operator. With 75 years experience in the gas business, we operate one of the most efficient gas transmission systems in Europe. Today this pipeline network covers some 12,000 km. Our customers book capacities on the Open Grid Europe network and we transport their gas for them. The liberalisation of gasmarkets led to far reaching changes over recent years and network and capacity planning became a more and more complex task. Therefore in 2008 our network planning department initiated a research cooperation to make use of contemporary mathematics in our applications. Currently, we cooperate with around 40 researchers from 5 universities and 2 research institutes. We report on our experiences with the cooperation and on its benefits for the company.

4.1 Introduction

Open Grid Europe applies an entry/exit model, meaning that the tariffs for bookable capacities only depend on the entry or exit point, but not on the routing through the network. Moreover, capacities are freely allocable, i. e., gas can be traded between entering and leaving the network and if a customer has flexible entry contracts, he can intradaily decide which entries he wants to use to supply his consumers. See figure 4.1 to get an impression of the Open Grid Europe network.

Today, network planning is done more or less manually at Open Grid Europe. Based upon the known historical gas flows and on the contractual situation, the network planning department tries to identify a small set of restrictive, that is, pessimistic, but still realistic (static) transport scenarios. Those expertise-based scenarios are simulated with standard gas network simulation software SIMONE to stress the network and to gain information regarding network capacities. Before the simulation can come to a feasible network state, the network planner has to manually adjust many of the numerous active elements of the network to a suitable configuration for the current scenario. Acitve elements include valves, control valves and compressors. If the simulation does not reach a steady state or if certain limit values such as temperatures or contractual pressure conditions are not fulfilled when the simulation process has finished, the planner can reconfigure some active elements and rerun the simulation or he can decide that there is no feasible configuration.

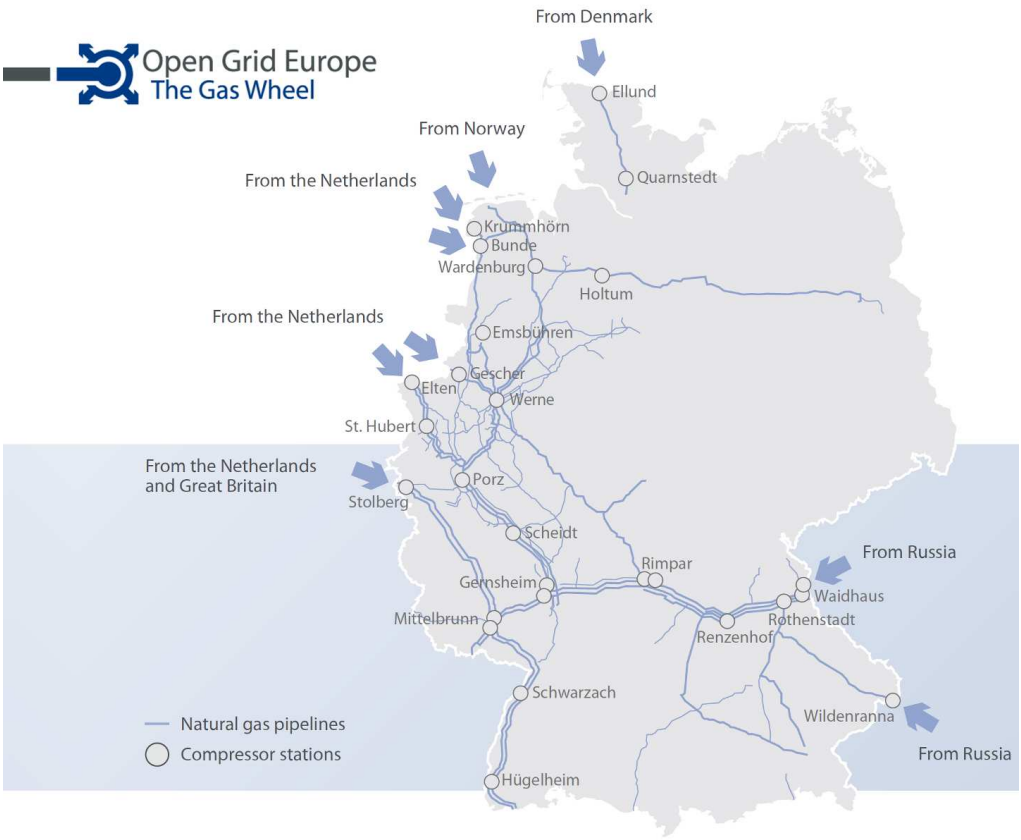

Figure 4.1: The network has a few tens entry points and around 1000 exit points in the high pressure distribution system. 27 compressor stations with 96 compressor units pump the gas with up to 100 bar gauge pressure through the network. Additionally hundereds of metering and pressure controlling plants control the gas flow.

4.2 Tasks of the network planning department

Amongst others, our network planning department is responsible for the determination of most favorable network expansions to increase the network's transportation capacity if needed. Furthermore, the amount of freely allocable capacities has to be maximised and when a customer requests freely allocable capacity at some point, the planners have to decide whether this capacity is available or not. If such a capacity request is denied, congent justifications have to be given.

Today, from the planner's perspective, all those tasks boil down to the generation and simulation of meaningful scenarios and to draw the correct conclusions from results obtained by simulation.

4.3 Approaches of our scientific partners

From a mathematician's point of view, the tasks from the last section are easily formulated, but lead to extremly complicated very large-scale mixed-integer nonlinear stochastic programs. As a basic tool to tackle these challanging tasks with modern mathematics, our experienced scientific partners developed

a model kit for the validation of nominations (see figure 4.2). Nomination validation stands for an automised procedure to decide, if for a given set of boundary values, there exists a feasible configuration of the active elements.

Concrete nomination validation model specifications which were implemented by the different research groups are a mixed-integer linear program, a reduced nonlinear program, a mixed-integer nonlinear program and a mathematical program with equilibrium constraints. Each such mathematical model uses different modules of the model kit and features different advantages. Last but not least, a very detailed, technically and physically accurate nonlinear programming model was developed. While the first four models are supposed to automatically find reasonable suggestions for the integer and binary decisions in the network at a given nomination, the precise nonlinear programming model serves as a validator for those suggestions and delivers the exact pressures and flows in the network in case of convergence.

Recently this framework (generate starting points by four different approaches and validate them with a physically accurate network model) was made available to Open Grid Europe as a server solver via a browser-based frontend. The network planner can upload networks and scenarios and if everything works fine, the solver framework returns flows and pressures for the whole network as well as the underlying feasible configuration of the active elements. After having gained a bit more experience with this solver, another part of our manual work will be computer-aided.

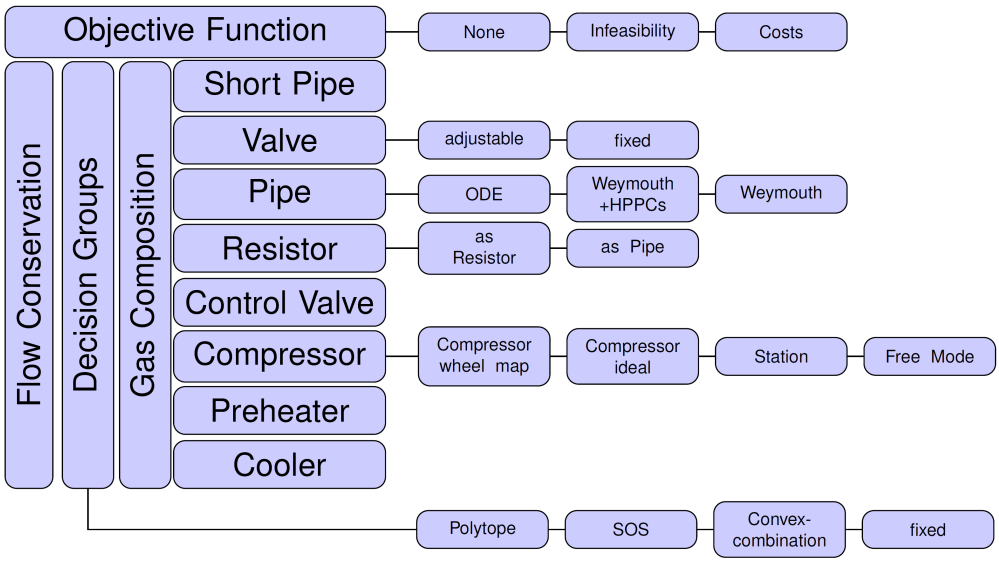

Figure 4.2: Model kit to deal with the basic nomination validation problem in different approaches.

4.4 Future Goals

Future goals that we hope to achieve together with our partners are booking validation, boundary value optimisation, topology optimisation and optimal network integration. All these aims rely on fast and reliable nomination validation algorithms, since all of these objectives have in common that tons of nomination validation problems have to be solved. For instance a booking situation can be considered

to be valid, if a significant set of intelligently sampled nominations is feasible. Regarding topology optimization, computations always start with a set of infeasible nominations. A cost optimal topology expansion taken from a large set of reasonable expansions, that makes the former infeasible nominations feasible, can be considered to be practically optimal.

Bibliography

[1] P. Domschke, B. Geißler, O. Kolb, J. Lang, A. Martin, A. Morsi, Combination of Nonlinear and Linear Optimization of Transient Gas Networks, INFORMS Journal on Computing, Articles in Advance, pp. 1-13, ISSN 1091-9856, 2010.

[2] R. Mirkov, H. Friedl, H. Leövey, W. Römisch, I. Wegner-Specht, Sigmoid Models Utilized in Optimization of Gas Transportation Network, A.W. Bowman: Proceedings of the 25th International Workshop on Statistical Modelling, 381-385, 2010.

[3] B. Geißler, A. Martin, A. Morsi, L. Schewe, Using Piecewise Linear Functions for Solving MINLPs, Accepted for publication in the upcoming IMA Volume on MINLP.

[4] B. Geißler, O. Kolb, J. Lang, G. Leugering, A. Martin, A. Morsi, Mixed Integer Models for the Optimization of Dynamical Transport Networks, Submitted to Mathematical Methods of Operations Research, 2010.

[5] H. Friedl, R. Mirkov, W. Römisch, Forecasting Gas Flow on Exits of Gas Transmission Networks, Planned for a Special Issue of the ISR on Energy Statistics.

[6] T. Göllner, Preprocessing-Techniken für die Optimierung stationärer Gasnetzwerke, Diploma Thesis, Technische Universität Darmstadt, 2010.

[7] D. Oucherif, Approximationen der stationären Impulsgleichung realer Gase in Pipelines, Diploma Thesis, Leibniz Universität Hannover, 2009.

[8] D. Schuman, Approximation des adiabatischen stationären Gasflusses in Pipelines, Diploma Thesis, Leibniz Universität Hannover, 2010.

[9] SIMONE Research Group s.r.o., SIMONE Software, http://www.simone.eu

Invited Lecture.

Modelling solidification and melting with a flowing liquid layer

T.G. Myers, M.M. de Decker, F. Font, J. Low

Centre de Recerca Matemática, Campus de Bellaterra, Edifici C, 08193 Bellaterra, Barcelona, Spain
tmyers@crm.cat, http://www.crm.cat/tmyers/

Abstract

The focus of this paper is on phase transitions in the presence of a flowing liquid. First the basic mathematical theory will be described. This theory will then be briefly discussed in the context of three practical applications, namely: aircraft icing; contact melting; solidification in microchannels.

5.1 Introduction

Phase transitions occur in a multitude of natural and industrial situations, for example in ice formation and melting, steel production, laser drilling, melting of heat shields, drying of coatings or in the food industry in applying molten chocolate or manufacturing ice cream. The mathematical theory for one-dimensional phase change, commonly termed a Stefan problem, is well established. However, there are many theoretical and practical challenges remaining when the Stefan problem is coupled to models for fluid flow. In this paper we outline the theory and then briefly show how it may be applied to three different industrial areas. All of these areas have been studied by members of the Industrial Mathematics group at the CRM and in the case of aircraft icing and solidification in a channel have been applied to industrial situations.

5.2 Stefan problem and flow definition

Consider a semi-infinite solid occupying $z \geq 0$ and at a constant temperature $T = T_\infty$, where T_∞ is below the melting temperature T_m. A heat source at $z = 0$ suddenly raises the temperature there to $T_0 > T_m$ and melting commences. There are now two material phases, liquid and solid. The liquid occupies the region $z \in [0, s(t)]$ whilst the solid is in $z \geq s(t)$. To model this process, and so determine how the melting progresses, requires solving heat equations in the two regions. However this is not enough, the domain over which the heat equations apply (the position of the moving boundary $s(t)$) is unknown and so we require a further equation: an energy balance known as the Stefan condition. The classical one-dimensional *Stefan problem* may now be written down as

$$\frac{\partial \theta}{\partial t} = \alpha_l \frac{\partial^2 \theta}{\partial z^2}\,, \qquad 0 < z < s(t) \qquad \frac{\partial T}{\partial t} = \alpha_s \frac{\partial^2 T}{\partial z^2}\,, \qquad z > s(t) \tag{5.1}$$

$$\rho_s L_m \frac{ds}{dt} = k_s \frac{\partial T}{\partial z} - k_l \frac{\partial \theta}{\partial z}\,, \qquad \text{at } z = s(t) \tag{5.2}$$

where θ, T are the temperatures in the liquid and solid respectively, α is the thermal diffusivity, ρ the density, L_m the latent heat (a measure of the energy release when the phase change occurs) and k the

thermal conductivity. Subscripts l, s denote liquid and solid respectively. Typical boundary conditions are

$$\theta(0,t) = T_0 \qquad \theta(s,t) = T(s,t) = T_m \qquad T \to T_\infty \,, \qquad \text{as } z \to \infty \,, \tag{5.3}$$

$$T(z,0) = T_\infty \,, \qquad s(0) = 0 \,, \tag{5.4}$$

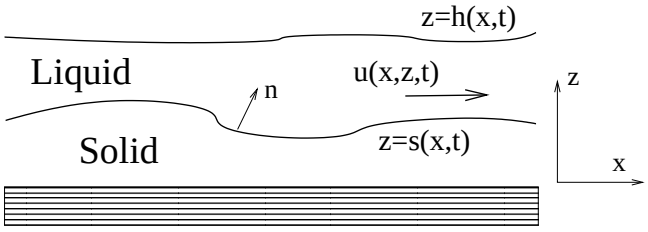

Figure 5.1: Typical problem configuration.

In practical situations one is seldom lucky enough to come across the classical semi-infinite one-dimensional Stefan problem. A more common scenario involves a finite, flowing liquid layer, as shown in Figure 5.1, then the two-dimensional thermal problem becomes

$$\left(\frac{\partial \theta}{\partial t} + \mathbf{u}\cdot\nabla\theta\right) = \alpha_l \nabla^2\theta \,, \qquad s(x,t) < z < h(x,t) \qquad \frac{\partial T}{\partial t} = \alpha_s \nabla^2 T \,, \qquad 0 < z < s(x,t) \tag{5.5}$$

$$\rho_s L_m \frac{\partial s}{\partial t} = \mathbf{n}\cdot(k_s \nabla T - k_l \nabla\theta) \,, \qquad \text{at } z = s(x,t) \,, \tag{5.6}$$

where $\mathbf{n}$ is the unit normal to the surface $z = s(x,t)$. Obviously this also holds for three-dimensional problems (except for the dependence of s, h). The boundary conditions at $z = 0, s$ are the same as before. We must also specify conditions at $z = h(x,t)$ and $x = 0$. The velocity vector $\mathbf{u}$ is another unknown which may be determined through the Navier-Stokes equation

$$\rho_l \left(\frac{\partial \mathbf{u}}{\partial t} + \mathbf{u}\cdot\nabla\mathbf{u}\right) = -\nabla p + \mu_l \nabla^2 \mathbf{u} \,, \qquad s(x,t) < z < h(x,t) \,, \tag{5.7}$$

where p is the fluid pressure and μ the viscosity.

Obviously this is a daunting system, consisting of coupled heat and fluid flow equations applied over an unknown, time-dependent domain. However, in certain situations and with certain materials it may be simplified significantly. In this paper we will focus on the common situation where the flow is laminar and the length-scale L is much greater than the height-scale H. In this case quantities such as $\frac{\partial^2 u}{\partial z^2} \sim U/H^2$ are much larger than $\frac{\partial^2 u}{\partial x^2} \sim U/L^2$. Following this line of argument we end up reducing the Stefan problem above to a much simpler system

$$0 = \frac{\partial^2 \theta}{\partial z^2} \,, \qquad s(x,t) < z < h(x,t) \qquad 0 = \frac{\partial^2 T}{\partial z^2} \,, \qquad 0 < z < s(x,t) \,. \tag{5.8}$$

This involves neglecting terms of $\mathcal{O}(\epsilon^2, \epsilon^2 Pe)$ where $\epsilon = H/L \ll 1$ and $Pe = UH^2/(\alpha_l L)$ (which reflects the relative importance of advection to conduction). The two-dimensional Stefan condition

reduces to the one-dimensional version (5.2). The Navier-Stokes equations reduce to the familiar lubrication approximation

$$0 = -\frac{\partial p}{\partial x} + \mu_l \frac{\partial^2 u}{\partial z^2}\,, \qquad 0 = \frac{\partial p}{\partial z}\,, \qquad s(x,t) < z < h(x,t)\,. \tag{5.9}$$

Here we neglect terms of $\mathcal{O}(\epsilon^2, \epsilon^2 Re)$ where the Reynolds number $Re = \rho_l U L/\mu_l$. Applying appropriate boundary conditions the problem may finally be reduced to two coupled partial differential equations to determine the unknown heights $h(x,t), s(x,t)$, see [6]–[9] for example. Once these are solved all other quantities, such as velocities, temperatures and pressure may be found analytically.

5.3 Aircraft Icing

Water can remain in liquid form down to around -42°C (at atmospheric pressure) if there are no available nucleation sites. This is why clouds of water droplets can exist even when the surrounding air is well below the freezing temperature. When an aircraft flies through a cloud of *supercooled* droplets it provides a large nucleation site and so ice accretion is a significant and very dangerous problem. Passengers remain blissfully aware of this issue due to the fact that all commercial aircraft incorporate some form of ice prevention and so ice should never appear on an in-flight aircraft. Typically critical surfaces are heated around 100°C above the ambient temperature to prevent any ice formation. However, this is an expensive strategy and so there is a great deal of research not only to improve aircraft safety during icing incidents but also to reduce energy consumption.

With no heating, when supercooled droplets impact on an aircraft surface they will first freeze. However, after some time a portion of the incoming droplets will stay liquid and then join to form a rivulet or thin film: thicknesses of around $H = 10^{-4}$m have been recorded. Since the length-scale is typically of the order centimetres the problem is well described by the system (5.8,5.9). After some manipulation the problem may be reduced to solving a fourth-order non-linear PDE for h and a first-order non-linear ODE for s. Their numerical solution and derivation is detailed in [6, 7, 8].

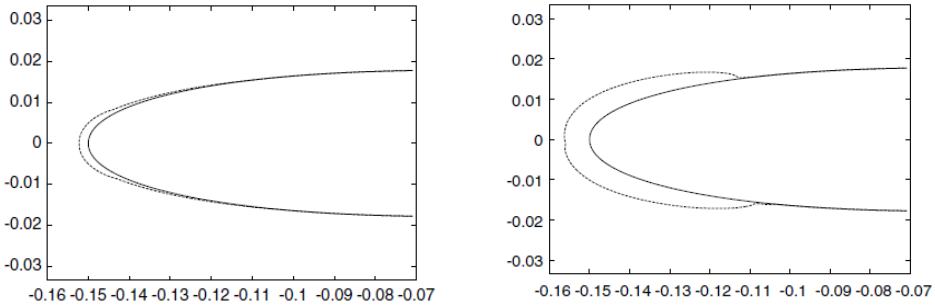

Figure 5.2: Ice accreting on a NACA0012 aerofoil at two different times.

This approach was applied in the development of a commercial aircraft icing code, ICECREMO that was developed jointly between British Aerospace (now BAe Systems), DERA (now Qinetiq), Westland Helicopters (now AgustaWestland), Rolls-Royce PLC (now Rolls-Royce PLC) and Cranfield University (still Cranfield University). Academic researchers at Cranfield were responsible for developing the mathematical models and then incorporating them into a code modelling air flow and water droplet trajectories around aircraft components. A sample result is shown in Figure 5.2, which shows ice

accreting on one of the standard aerofoil shapes (the NACA0012 is symmetric and used as a base test case for simulations). The ICECREMO code has become an essential tool in the development of new aircraft, for example, in a single development program it was estimated that the computer model saved the company £300,000 by reducing the number of flight trials, see [2].

5.4 Contact melting

Contact melting is the process whereby a phase change material (PCM) is placed on a surface that is maintained above the phase change temperature. The heat from the surface causes the PCM to melt and it then rests on its own melt layer. The process may be easily observed by placing a piece of ice on a warm surface: after a short time the ice will sit on a thin layer of water as it slowly melts. The Leidenfrost effect, where a liquid droplet placed on a hot surface floats on a vapour layer is another well-known example.

The mathematical description of contact melting is detailed in another paper in this issue [3] and so we refer the reader there for further information. Since the melt layer is always thin the approximation of (5.8b,5.9) holds. With an initially flat based material, placed on a flat surface a full one-dimensional heat equation applies in the solid (even for the three-dimensional melting scenario). The heat and flow equations must also be coupled to a force balance between the solid weight and the fluid pressure (acting over the base of the solid) and in the case of Leidenfrost the fluid shape must also be determined through the Young-Laplace equation (which balances surface tension with gravity)

In Figure 5.3 we show results obtained through this type of mathematical model applied to Leidenfrost and compared to experimental data of [1]. The results are for a water droplet resting on a vapour layer. The solid line in Figure 5.3 shows the model prediction for the vapour layer thickness, the stars with error bars represent the experimental data.

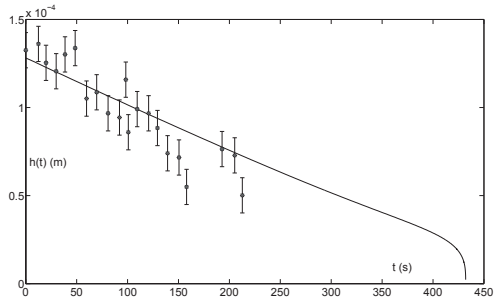

Figure 5.3: Comparison of vapour layer thickness against time using the mathematical model of [9] (solid line) and experimental data of [1] .

5.5 Solidification in microchannels

Understanding the process of solidification when a fluid flows through a narrow channel is important in many fields. For example, in microfluidic devices, such as micro PCR chips, due to the difficulty of

incorporating a valve within the device a section of fluid may be frozen to stop the flow. The change in density upon freezing, and thus volume variation, is key to the success of cryopreservation and is also a well-known problem with any system of pipes exposed to sub-freezing temperatures.

The mathematical description of this scenario shows one significant difference to the previous two in that advection often plays an important role. This requires us to include the previously neglected $\mathcal{O}(\epsilon^2 Pe)$ terms in the heat equation in the liquid. However, analytical progress is still possible, allowing the initially complex system of equations to be reduced to a single first-order integro-differential equation. In Figure 5.4a we show a typical plot for an initially warm fluid entering a cooled section of

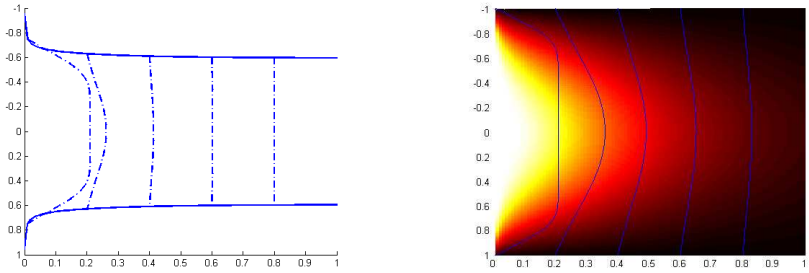

Figure 5.4: Fluid temperature profiles through a solidifying channel. Right plot is scaled so the fluid occupies $z \in [-1, 1]$.

pipe, see [10, 4]. The solid line represents the position of the freezing front, $z = \pm s(x, t)$, the dashed lines represent the temperature at different x co-ordinates. This fluid temperature is shown more clearly in Figure 5.4b (where now the vertical axis is scaled with $\hat{z} = z/s$ so that the fluid occupies $\hat{z} \in [-1, 1]$), lighter colours represent higher temperatures.

5.6 Conclusion

In this paper we have briefly detailed the basic mathematical model for solidification in the presence of a thin layer of moving liquid. The full model involves PDEs in the solid and liquid layers coupled to flow equations and all applied over *a priori* unknown domains. The mathematical reduction of the initially complex system significantly simplifies the problem and is relevant to a number of physically important situations. Through extensive comparison with experimental data this approach has been shown to be highly accurate.

Bibliography

[1] A.-L. Biance, C. Clanet and D. Quere, Leidenfrost drops, Phys. Fluids 15, (2003), 1632-

[2] Cool computer model predicts ice build up on aircraft, `http://www.baesystems.com/Businesses/SharedServices/Divisions/AdvancedTechnologyCentre/FeatureArchive/bae_feat_atc_3dice.html` Last accessed 9th June 2011.

[3] M.M. de Decker and T.G. Myers, Contact melting of a three-dimensional phase change material on a flat substrate, This volume.

[4] J. Low and T.G. Myers, Modelling the solidification of a power-law fluid flowing through a narrow pipe, In preparation.

[5] M.K. Moallemi, B.W. Webb and R. Viskanta, An experimental and analytical study of close-contact melting, Int. J. Heat Trans.108, (1986), 894 - 899.

[6] T.G. Myers, J.P.F. Charpin and C.P. Thompson, Slowly accreting ice due to supercooled water impacting on a cold surface, Phys Fluids 14(1), (2002), 240-256.

[7] T.G. Myers, J.P.F. Charpin and S.J. Chapman, The flow and solidification of a thin fluid film on an arbitrary three-dimensional surface, Phys Fluids 14(8), (2002), 2788-2803.

[8] T.G. Myers and J.P.F. Charpin, A mathematical model for atmospheric ice accretion and water flow on a cold surface, Int. J. Heat Mass Trans. 47, (2004), 5483-5500.

[9] T.G. Myers and J.P.F. Charpin, A mathematical model of the Leidenfrost effect on an axisymmetric droplet, Phys. Fluids 21, (2009) DOI: 10.1063/1.3155185.

[10] T.G. Myers and J. Low, An approximate mathematical model for solidification of a flowing liquid in a microchannel, Microfluid. Nanofluid., (2011), DOI 10.1007/s10404-011-0807-4.

Special Sessions: Presentation of Posgraduate Experiences in Industrial Mathematics.

An international master programme in industrial mathematics. Difficulties and rewards

Aureli Alabert

Universitat Autònoma de Barcelona
Edifici C, 08193-Bellaterra, Catalonia
e-mail: Aureli.Alabert@uab.cat

Abstract

This note describes some aspects of starting and running an international Erasmus-Mundus master from the point of view of a local coordinator in Barcelona. Difficulties are especially stressed, but I believe that the benefits, shortly addressed in the last section, give rise to a very positive balance.

6.1 Introduction

MathMods is an international master programme on industrial mathematics run by a consortium of five European universities. Its full name is "Mathematical Modelling in Engineering: Theory, Numerics, Applications" and it is coordinated by the Università degli Studi dell'Aquila. It was born in the academic year 2008-09 under the Erasmus-Mundus action of the EU Education, Audiovisual and Culture Executive Agency (EACEA). The aim of the Erasmus-Mundus initiative is to enhance the quality of higher education and promote dialogue and understanding between people and cultures through mobility and academic cooperation, not only among European cultures but, more importantly, between third-country and European people. Among other specific objectives, it intends to promote the European Union as a centre of excellence in learning around the world.

EACEA provides financial support to implement joint international programmes at the postgraduate level (master and doctorate) as well as grants and scholarships to individual students, researchers and university staff who wish participate in those joint programmes.

To date, two programmes in Industrial Mathematics / Mathematical Engineering have been supported: *ESIM* (European School for Industrial Mathematics), started in 2005 by Technische Universiteit Eindhoven, Technische Universität Kaiserslautern, and Johannes Kepler Universität (Linz); and MathMods, by Università dell'Aquila, Université de Nice Sophia-Antipolis, Universität Hamburg, Politechnika Gdańska and Universitat Autònoma de Barcelona. Both are two-year masters (120 ECTS of learning load).

Starting and maintaining international master degrees involves some difficulties and it also pays some rewards. I will present an overview of those difficulties and rewards, from the point of view of my personal experience as coordinator in the Catalan node of *MathMods*, and with some emphasis in the Erasmus-Mundus case.

6.2 MathMods structure

MathMods is a two year master with a common curriculum of one academic year for all students, run in L'Aquila (first semester) and Nice or Hamburg (second semester), and five different tracks in each of the partner institutions in the second year.

The general emphasis of the first semester is on theoretical background, whereas the second semester is devoted to numerical methods and includes a short internship in an enterprise. The second year consists of a semester of courses geared towards practical modelling and particular applications and a final semester devoted to the 30 ECTS worth master thesis.

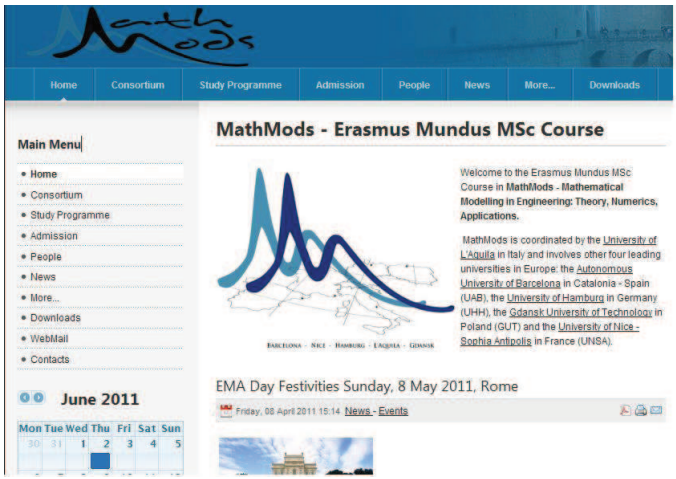

Figure 6.1: MathMods web page

The master receives a notable number of applications. Around 700 registrations are completed, with all required documentation. Except in rare cases, all the applicants ask for the Erasmus-Mundus grant. Between 100 and 150 students are admitted, based on their curricula and other documentation, and about 30 get finally enrolled and start the master. The main reason for the low enrolment is the difficulty for third-country students to live in Europe without a substantial economic aid.

6.3 Creating the master

It is not difficult to coincide with colleagues of other European universities to envision and design a post-degree. The main problem is to conceive a structure which conform and satisfy all local regulations at the same time. Despite our common European framework, one must not forget that local laws are always in force in each country, hence the endorsement of an European agency does not exempt from complying with those regulations.

A typical problem with Spanish universities is the "4 years degree + 1 year post-degree" structure to achieve the final goal of 300 ECTS, as opposed to the 3+2 structure of most European countries. At the very least, this conflict poses a difficulty to Spanish students to enrol a 2-year master, since in principle the total cost of their diploma would rise to 360 ECTS.

Deciding between awarding a joint diploma or a multiple diploma is another delicate point. Each country has its own recommended policy, and the universities themselves may apply some internal

rules. In the MathMods case, three of the universities have been able to sign a joint diploma agreement, whereas the other two can only resort to multiple diplomas. It is therefore possible to mix both kind of diplomas inside the same master, though this is better avoided, because it leads to confusion and more administrative work.

Local country rules may also have an impact on the protocol to validate the master. Mere approval by the European agency is not enough to get local approvals. In our case, a full application as any other new master had to be conducted. The new master had to be validated first by the university and the Catalan University Quality Assurance Agency (AQU), and later by the corresponding Spanish agency.

The multiple validation filters have no doubt a positive impact in the overall design of the master, and the assurance of its viability in all aspects, but the extra administrative work can be overwhelming. It is advisable to first look for help inside the university. If there are other international joint masters, some roads may have already been constructed. It is also worth looking at the ECMI recommendations: Conformity to ECMI standards can lead to additional recognition and rewards.

6.4 Students

Selection of students is not an easy task. There is a non-negligible difficulty in comparing academic transcripts from different countries and universities. Marks can be found in very different systems (F to A, 0 to 100, 5 to 1, ...), and even comparable scales are subject to the different demands of each university and country. Other than transcripts, very little can be learnt from the résumé, since in most cases students are too young to have a record of achievements to stand out of others. Also, very experienced candidates, usually older, may not be the best choice as master students. Finally, it is very difficult to assert the authenticity of scanned documents.

At MathMods, we found useful to establish a two stage selection. In the first stage, applications which are clearly weak are disregarded; in the second stage, all surviving applications (some 150 or 200) are examined by all members of the academic committee. Applications are marked following specified criteria, and put together in a spreadsheet, sorted by country of origin. This allows first an easier comparison of applications from the same country, and then a comparison among best applicants from each country. The result is a final list of admitted students, with the first places awarded with the Erasmus-Mundus grant, and the rest serving as "waiting list" for the grants in case of renounces.

When different universities implement different tracks of the master, it becomes a problem to keep the equilibrium of students among universities, since some specialities can be more demanded that others. Even in case of common tracks, different locations inside Europe have different appeal to both European and non-European students. The policy adopted may will have an impact in the internal economic agreement of the consortium.

My personal recommendation is to enforce a more or less strong equilibrium between partner universities. This can be achieved through the proposal of a double compromise in the acceptation letter sent to the students: The consortium guarantees to the student a specific track and a specific university routing, and the student takes the compromise to follow the assignment without complains. This does not preclude a posteriori changes agreed by all parties.

Students expect some extra value from the part of the coordinators and hosting universities, since their fees are probably higher than for local students. They also feel as high-profile students, because of the possibly very competitive selection process. The additional effort of the coordinators is at times non-negligible, especially when students away from home undergo health or legal difficulties. These

are good reasons for the coordinators to secure in advance the endorsement of their departments and the help of the administrative staff.

6.5 Running the master

The master should have from the very beginning a solid business plan, identifying all expenses that may be incurred during its expected lifetime. In the case of Erasmus-Mundus masters, there is a substantial initial sum contributed by the EACEA, but this contribution decreases year after year, and reduces to zero after five years. The master is supposed to be self-financing after this start-up time. A clear economic model between members of the consortium to distribute incomes and expenses should also be signed.

One especially delicate point regards the very different official university fees. Usually, the consortium must pay to the universities a fixed fee for every student and semester hosted by the university. The fees may range from zero (for example in Poland) to the high level of Spain, or to the prohibitive British fees. The economic model should definitely address this point.

A local coordinator must not hesitate to use his budget to pay for administrative help. A part-time person will suffice, as long as he/she is readily available for urgent issues. Institutional help in Spain can be found for example in the Erasmus-Mundus Secretary in the Ministry of Education. I must also mention the unvaluable help that I received from the International Welcome Point of the UAB, mainly in solving visa, accommodation and settlement problems raised by new students.

It is absolutely necessary to maintain a well designed web page, for publicity, visibility, managing, relation with students, registration and uploading of application documents. A content management system is advisable, to turn the site dynamic and collaborative.

6.6 Benefits

Society demands more knowledge transfer from the universities. In mathematics, there is a huge potential for applications, because of a transversality that intersects with almost all industry sectors. This transfer may in turn help to finance and guide new research of direct value. New opportunities will arise for graduates in the enterprise and in university departments, to the advantage of our mathematics degrees, that should attract more and stronger students. And more potential for technology transfer in consequence.

A master in industrial mathematics can boost the above circle. It can be started even without the support or preliminary contact with enterprises. Typically, master thesis have to be connected to industrial problems, pushing us to look for interesting projects. Enterprises, especially those that provide private consulting to other businesses, are usually open to host students or propose some part of their projects for a thesis. Problems for modelling seminars of even collaboration contracts can be found starting with a student-enterprise relation.

The master can also put industrial mathematics and interdisciplinary science closer to our colleagues more pure-math oriented, helping t overcome the fences that sometimes we perceive among mathematicians.

Some successful master students will like to pursue a Ph.D., building upon their new acquired knowledge. This will challenge our capacity to advise such kind of theses, but will in turn represent a huge advancement in the visibility of mathematics and the recognition of doctors in the industry world.

The degrees in mathematics should also adapt to the fact that at present the majority of students will have to look for a job outside academia and high schools. The degrees must provide the necessary background to follow the master successfully The existence of such a master in industrial mathematics will steer the undergraduate programmes towards this goal.

Bibliography

[1] MathMods web page, http://www.mathmods.eu

[2] ECMI web page, http://www.ecmi-indmath.org

[3] International Welcome Point presentation,
http://www.uab.cat/Document/79/1020/InternationalWelcomePoint.pdf

[4] EACEA web page,
http://eacea.ec.europa.eu

Special Sessions: Presentation of Infrastructures related to knowledge Transfer.

Technocampus EMC^2: a large joint technological center on composites structures

Francisco Chinesta

EADS Corporate Foundation International Chair
Ecole Centrale de Nantes, 1 rue de la Noe, BP 92101, F-44321 Nantes cedex 3, France
e-mail: Francisco.Chinestaz@ec-nantes.fr

Abstract

We describe in what follows a particular research transfer structure involving industry, academia and an industrial chair in order to develop a fundamental research able to be solve some challenging and recurrent scientific and technological issues.

7.1 An exceptional local framework

First, we are describing a specific local framework which enabled us, in the past 10 years, to create a particularly strong partnership between our laboratories and industries, not only through collaborative projects, but also through the development of large experimental platforms. This dedicated framework emerged in Nantes in two steps.

- First step: Techno'Campus agreement and EMC2/ID4CAR clusters.
  - In 2002, Pays de la Loire Region decided to help reinforce the research cooperation between Airbus and local partners (universities and industrial subcontractors) through the funding of finalised research projects at a relatively large scale in the field of manufacturing processes. In this framework, in order to move EADS researchers from Suresnes (near Paris) closer to Airbus industrial plants, EADS proposed to relocate in Nantes several researchers working in composite forming, robotics, machining, process modelling and non destructive testing (NDT). To strengthen the links with academics, the choice was done to install these EADS researchers in the Ecole Centrale buildings and to take this opportunity to build an official broader cooperation research network including other laboratories. This network agreement was called Techno'Campus.
  - At the same time, the French government decided, in 2005, to create clusters ("poles de compétivités"). In the vicinity of Nantes such clusters project were thus created: (i) EMC2 cluster (i.e. cluster for composite and metallic large assemblies) was initiated by 4 large companies (Airbus, Chantier de l'Atlantique - presently integrated into STX group -, DCNS - mainly active in military naval structures - and Beneteau) and (ii) ID4CAR cluster initiated around the automobile industry (PSA for example). These two clusters are concerned with a broad spectrum of applications, mainly related to the manufacturing of large structures.

- Second step: development of Technocampus EMC2: a large joint technological center on composites structures

  The benefits of Technocampus agreement turned out to be much more important than what was anticipated:

  - Development of an increasing number of scientific projects with EADS, Airbus as well as with smaller companies which were or became, because of these projects, subcontractors of aeronautics,
  - Mutual acquaintance between partners (”coffee machine effect”),
  - Domino effect inside our laboratories and extra-support by our institutions (in particular Ecole Centrale de Nantes, University of Nantes, CNRS, ...).

  The idea of the Technocampus EMC2 center emerged during spring 2006. From a political point of view it was necessary to strengthen Nantes' place during the Power 8 Airbus plan aimed at minimizing the dispersion of activities of Airbus in Europe. Scientifically this was an opportunity for us (i) to focalise the scientific field of research of Technocampus agreement on composite materials only and (ii) to enlarge the number of applications in addressing all aspects of composite forming including their applications to automobile industry, energy and transport. The Technocampus consists in a wide technological center (20 000 m2) of research equipments on composite forming. Located near the airbus site, it enables to test demonstrators on a scale of near to one. The founding members are EADS IW, Airbus, CETIM (French technical center for mechanical industry) as well as GeM, LTN and IRCCyN. The operational working conditions are:

  - Buildings have been jointly funded by regional collectivities, the state and Europe. These buildings are rent at a market price to different partners, viz (i) industries like Airbus, EADS, CETIM and Small and medium size companies, (ii) academic partners like GeM, LTN (or more precisely the institutions they belong to: Ecole Centrale de Nantes, University of Nantes, CNRS).
  - The occupants commit themselves to mutualizing their equipments for at least 20% time.

  The Technocampus EMC2 center was opened in september 2009. This opening was anticipated with many joint research projects between the partners which now take place in Technocampus EMC2. To give an order of magnitude of the academic activity inside, the numbers of PhD students has now reached 30. Furthermore, owing to this opportunity, we proposed to CNRS the creation of a national network on composite forming. This idea was effectively supported and granted by the creation of a GDR called MIC. A specific teaching activity was also initiated. In particular, each year, a ”mastère spécialisé” (i.e. something between a classical master degree and an industrial PhD thesis) brings together around ten engineers (freshly graduated from university with an engineering master degree or coming for a specialization after a few years in industry). The overall operation has been also considerably strengthened by the opening of the international EADS chair on ”advanced modelling of composite forming” held by F. Chinesta.

7.2 The EADS Corporate Foundation International Chair

EADS and Ecole Centrale de Nantes announced the creation of the EADS Foundation-Centrale Nantes Research Chair at the Technocampus EMC2 on 21 September 2009. The Chair goal is to develop and

structure courses and to define research projects, involving advanced numerical models for composite manufacturing processes for the aerospace industry, at a national and an European scale. This Chair has been endowed with a 1 million of euros budget for 4 years .The Chair research work will focus on two main areas:

- Modelling of materials and processes.
- Propose new advanced numerical strategies for solving the resulting multi-scale and multi-physic models, non-linear, strongly coupled, exhibiting space and time localization, of very large size and defined in very complex geometries. If we summarize in one sentence: we should solve **real industrial problems** with all the geometrical complexity and modelling richness, very fast and if possible **in real time** and using **light computing platforms** (e.g. smartphones) to spread those research developments to medium and small industries. This solvers should be used by non-specialize users.

The main aims of the Chair are:

- Support students finishing their studies in areas involving composites manufacturing and process simulation.
- Offering a scholarship to a student involved in the Erasmus Mundus European MasterÕs degree in Computational Mechanics (in which the Ecole Centrale of Nantes is one of the partners with the Swansea, Stuttgart and Barcelona universities).
- Provide an outstanding Master level course in Composite Structures Advanced Modelling for engineers concerned by this topic.
- Promote exchanges through networks and encourage experience sharing among researchers and other experts around the world, focusing on the scientific and technological hurdles and challenges in this area, by organizing an international conference every year, and several workshops and symposia.
- Promote the creation of a CNRS (French National Centre for Scientific Research) GDR (Research Group) focusing on modelling composite manufacturing processes, with a view to growing it into a European research group.
- Publish books and journal special issues.
- Define regional, national, european and international research projects.
- Improve the dialog between industry and academia.

7.3 A challenging research

Physical dynamical systems are usually modelled through a set of differential equations describing some quantity of interest as a function of space and time. Additionally, the model usually contains some parameters that are traditionally fixed before the model is solved numerically. The dimensionality of the model is therefore at most 4: 3 space coordinates and time. However a higher dimensional model containing some parameters as extra-coordinates, allows us to compute the quantity of interest

as a function of space, time and the model parameters now considered as coordinates. There is no conceptual limitation to the nature of the parameters that can be considered as new coordinates of the model: material parameters, initial or boundary conditions, command of actuators used to steer the system, geometrical parametersÉ The only limitation lies in the ability to solve the high dimensional model.

Having computed, in an off-line step, the solution of the high dimensional model, it is straightforward and numerically inexpensive to obtain, in an on-line step, the solution of the original model for any value of the parameters, as one only needs to particularize the solution with specific parameters values. Parameter identification or inverse problems are also efficiently solved: The solution of an inverse problem usually requires numerous solution of the so-called direct problem with different values of the parameters to identify. Here one can substitute the solutions of the direct problem with a simple evaluation of the multidimensional solution.

From this general solution computed only once and off-line one can therefore perform on-line and in real time all the post-processing task involved in optimization, inverse analysis, analysis of sensibilities, stochastic analysis, É required for the model based control of system that are computationally expensive to simulate or in dynamic data driven application systems where the simulation should run at the same speed that the simulated system itself.

The price to pay is the solution of parametric models defined in high dimensional spaces that could involve hundreds of coordinates. Models that are defined in high dimensional spaces suffers the so-called curse of dimensionality: If one proceeds to the solution of a model defined in a space of dimension N by using a standard mesh based discretization technique, where M nodes are used for discretizing each space coordinate, the resulting number of nodes reaches the value of M^N . As computers at present can handle about 10^{12} nodes, the mere storage of the solution of multi-dimensional models is a challenge. Computing this solution can be even more challenging with respect to computation time. Different techniques have been proposed to circumvent the curse of dimensionality, Monte Carlo simulations being the most widely used technique. Their main drawback is the statistical noise. To our knowledge there are few precedents of deterministic techniques (other than sparse grid techniques, that work well up to some 20 dimensions) able to circumvent efficiently the curse of dimensionality. We proposed recently a technique based on a separated representation of the solution that proceeds by expressing any generic multidimensional function in a separated form:

$$u(x_1, \cdots, x_N) \approx \sum_{i=1}^{i=Q} \prod_{j=1}^{j=N} F_i^j(x_j) \tag{7.1}$$

The method, known as Proper Generalized Decomposition, is still being intensively developed and allows the efficient solution of highly multidimensional models. Thanks to the separated representation of the unknown fields the computational complexity scales only linearly with the dimensionality, instead of exponential growing characteristic of mesh-based discretization techniques. This technique opens unimaginable possibilities for simulating the complex models involved in the description of composite manufacturing processes.

Special Sessions: Presentation of Posgraduate Experiences in Industrial Mathematics.

Master in mathematical engineering: from models to virtual simulations through mathematical analysis, numerical methods and computational resources

J. Durany

Dep. Matemática Aplicada II, Universidad de Vigo, Campus Marcosende, 36310 Vigo, Spain
email: durany@dma.uvigo.es - URL: http://www.dma.uvigo.es

Abstract

The rapid evolution of technology and applied sciences highlights the need for training technical experts in modeling and numerical simulation of problems from the industrial or business area. Therefore, it seems adequate to promote a training directed to the research, development, and innovation in these areas, trying to optimize processes, reduce costs, improve product quality, design new technologies, enhance safety, reduce environmental pollution, etc.

To fulfill this demand, the three Universities of Galicia (Spain) offer a Master in Mathematical Engineering focused on the modeling of real problems and the management of specific software, but without forgetting the training component in numerical and computational methods and equations that allows the use of models and software based on serious criteria. In particular, specific skills and competencies to be acquired through this Master are the following:

- To know and understand the problems that arise in the field of engineering and applied sciences as a starting point for appropriate mathematical modeling.
- To be able to determine whether a model for a process is well designed or not and mathematically formulate it in the appropriate working framework.
- To be able to choose the most appropriate selection of numerical techniques in order to solve a mathematical model.
- To know the languages and computational tools for implementing numerical methods.
- To identify and use the most common professional software tools for process simulation in industry and business.
- To acquire skills to integrate the specific knowledge in the numerical simulation of processes or devices appearing in industry or business, and to be able to develop new computer applications for numerical simulation.
- To acquire learning skills to enable integration in research and development teams within the industrial and business world.
- To set an initial stage of research to pursue doctoral studies.

In order to achieve the above-mentioned objectives, the Master's degree program is organized in six modules of courses: Modelization, Equations, Numerical Methods, Computation, Numerical Simulation and concludes with a tutored Project focused on simulation of processes or mechanisms previously defined by industries or business in general.

Special Sessions: Presentation of Infrastructures related to knowledge Transfer.

On the Forward Look "Mathematics and industry" (ESF & EMS)

Maria J. Esteban
CNRS and Université Paris-Dauphine
esteban@ceremade.dauphine.fr
http://http://www.ceremade.dauphine.fr/∼esteban

Abstract

In this talk will be presented the main results of the Forward Look project "Mathematics & Industry" of the European Science Foundation (ESF). This project has been coordinated by the Applied Mathematics Committee of the European Mathematical Society and it has involved mathematicians and people from industry of almost all european countries. This study has produced a report where the current situation is analyzed and where a series of recommendations are made to the European Commission, the national governments, the mathematics community and the industry.

A book of success stories will be published and a large survey has been answered by a large number of both mathematicians and people working in companies. All this will be presented in this talk.

9.1 Introduction

The Forward Look project on Mathematics and industry was launched by the European Science Foundation (ESF) and has involved representatives from all domains of European Mathematics: this project has been carried out with a strong involvement of the European Mathematical Society (EMS) and in particular of its Applied Mathematics Committee. Moreover, all national mathematical societies in Europe have been directly involved at different stages. In addition, an online survey has been launched among mathematicians in academia and researchers working in companies, and more than 500 answers were gathered. The results of the survey are reflected in a report which was made public in Brussels in december 2010.

The Forward Look springs from the strong belief that European Mathematics has the potential to be an important economic resource for European industry, helping its innovation and hence its capacity of competing on the global market. To fulfil its potential, special attention has to be paid to the reduction of the geographical and scientific fragmentation in the European Research Area. Overcoming this fragmentation will require the involvement of the entire scientific community. Europe needs to combine all experiences and synergies at the interface between mathematics and industry and create strong areas of interaction to turn challenges into new opportunities.

The need to consider this issue has been the main engine behind this Forward Look exercise, where were identified the groups that have significant activities in the field of industrial mathematics and have invited all mathematicians (through mathematical societies and general communication means) to submit short summaries of their experience and success stories in their cooperation with industry. These "success stories" have been gathered in a separate booklet that represents a snapshot of the impact and value created by active European groups in industrial mathematics.

Although there is a clear need in all areas of industry throughout Europe to use knowledge-based technologies in the development and improvement of products and services, it can be clearly seen that the level of cooperation between academia and industry needs to be increased and that is not equally well established throughout Europe. Strong efforts are necessary to correct this and deliver high-value collaborations across Europe.

9.2 Main conclusions of the Forward Look on "Mathematics and Industry (ESF & EMS)

STRATEGIC OBJECTIVES

Europe's competitiveness is to be achieved in a multilateral international environment through a common strategy for European Industrial mathematics by setting up the following key strategic objectives.
Strategic Objectives to build the community:

- To foster a European Network in applied mathematics towards a Smart Economy.
- To allow Member States to build up a common strategy for European mathematics.
- To establish mathematics as a necessary component of European innovation.

Strategic Objectives to develop the community:

- To overcome geographical and scientific fragmentation.
- To encourage the exchange of knowledge and information between Academia and industry.
- To facilitate the mobility between industry and Academia.

Strategic Objectives to empower the community:

- To harmonise the curriculum and educational programmes in industrial mathematics.
- To encourage the exchange of knowledge and information between Academia and industry.
- To promote and improve the career path in industrial mathematics.

RECOMMENDATIONS

Recommendation 1: Policy makers and funding organisations should join their efforts to fund mathematics activities through a European Institute of Mathematics for Innovation.

Roadmap implementation:

- EU and National funding agencies should coordinate clusters of excellence in industrial mathematics and create a European Institute of Mathematics for Innovation (EIMI) for mathematicians and users of mathematics.
- EU and European governments should set up a Strategy Taskforce for Innovation and Mathematics (STIM) in order to develop a European strategy for mathematics.

- EU must identify industrial and applied mathematics as an independent cross-cutting priority for the Framework Programme 8.
- Policy makers should put in place a Small Business Act in Mathematics (SBAM) to encourage spin-off companies explicitly using mathematics.

Recommendation 2: In order to overcome geographical and scientific fragmentation, academic institutions and industry must share and disseminate best practises across Europe and disciplines via networks and digital means.

Roadmap implementation:

- Researchers in academia and industry must adapt their mentalities to the different mathematical and scientific domains they interact with, and disseminate best practises.
- The mathematical community in collaboration with industry should create a journal devoted to industrial mathematics and contribute to a European Digital Mathematics Library.
- Academic institutions and industry must facilitate the employment mobility between academy and companies.
- The mathematics community and industry should work together on real opportunities in application-themed competitions.

Recommendation 3: Mathematical Societies and academic institutions must harmonise the curriculum and educational programmes in industrial mathematics at European level.

Roadmap implementation:

- Academia must create a European Curriculum for industrial mathematics and set up a pool of industrial mathematics engineers.
- Academia must develop new criteria to assess and recognise careers in industrial mathematics.

CONCLUSION

The basic message of this Forward Look report is that if Europe is to achieve its goal of becoming the leading knowledge-based economy in the world, mathematics has a vital role to play. In many industrial sectors the value of mathematics is already proven, in others its potential contribution to competitiveness is becoming apparent. The benefits resulting from a dynamic mathematics community interacting actively with industry and commerce are considerable and certainly far outweigh the rather modest costs required to support such a community. Nevertheless, such benefits will not be realized unless action is taken to develop mathematics and a coordinated community of industrial and applied mathematicians needed for the future success and global competitiveness of the European economy and prosperity.

REFERENCES : the final report of this Forward Look and the book of success stories can be downloaded at the webpage http://www.ceremade.dauphine.fr/FLMI/FLMI-frames-index.html. In the final report many references can be found.

Special Sessions: Presentation of Posgraduate Experiences in Industrial Mathematics.

Mathematics and Knowledge Transfer, a Challenge for Education

Matti Heilio
Lappeenranta University of Technology Box 20, 53851 Lappeenranta, Finland
matti.heilio@lut.fi

Abstract

The development of technology has modified in many ways the expectations facing mathematics education and practices of applied research. The increased role of mathematics calls for efforts to enhance knowledge transfer between universities, industry and public governance. This means a challenge for universities and educational programmes. This talk will review the recent development of educational programmes in Europe and efforts to make academia-industry interaction and European networking as an integral part in knowledge transfer and educating new generation of mathematics students.

10.1 Introduction

Mathematics is a vital resource in knowledge based industry, innovation and development of society. Today's industry is typically high-tech production but computationally intensive methods are also used in ordinary production chains. Terms like mathematical technology, industrial mathematics, computational modelling or simulation are used to describe this two-way knowledge transfer between technology, computing and mathematics. The communication of mathematical knowledge to industry can be facilitated in several interconnected ways.

10.1.1 OECD Survey

OECD sponsored in 2007 a survey to assess the intimate connection between innovation, science, and mathematics and to identify mechanisms for strengthening the connection. A report [1] summarized significant trends in research and the mathematical challenges faced by industry and implications for the academia-industry exchange. The report listed action-oriented practical recommendations for the main stakeholders, academia, industries and governments. Subsequently a follow-on report was written about the mechanisms available for facilitation of academia industry interaction in mathematics. The results are published in *Report on Mechanisms for Promoting Mathematics-in-Industry* [2]. Some notes from these reports and from experience collected during 25 years within the European network ECMI are listed below.

10.1.2 Talk to people

Casual interaction is important but organizational arrangements are helpful. University departments should build network of contacts and acquaintances in both organized and ad hoc way to companies, professions, organization, public governance. Industrial research is multidisciplinary and also industrial mathematics is of interdisciplinary character. Hence the appropriate mechanisms need to involve also researchers in other areas, both in academia and industry, who are motivated to search mathematical approaches.

10.1.3 IM days

When a country or region wants to start building academia-industry collaboration in the area of mathematical knowledge transfer one beneficial and recommended activity is to organize Industrial Mathematics Days. This would mean a 1-3 day workshop having balanced participation from academic research groups and people from industry. Industrialist are invited to describe problems from the R&D sector, design, quality control, logistics, research management etc where mathematical approach, simulation, modeling and computational means could be tried. Academic people would present talks on existing mathematical methods, tools, theoretical ideas and research questions which have direct relevance to current topics in industry and challenges of modern society.

10.1.4 Mathematical consultancy

One of the signs of progress in industrial mathematics is the growth of science based entrepreneurship. Since late 80ies several small companies have been established in different countries in the field of mathematical consulting and software development. The increasing potential of mathematics based knowledge in industrial R&D has opened the opportunity for applied mathematicians to exploit commercially their specialized expertise in mathematical modelling, simulation, modern mathematical techniques, advanced computational methods and scientific software skills. Typical examples are spin-offs starting from the pre-commercial software development in the research laboratories of applied mathematics and numerical analysis.

10.1.5 Curriculum development

A crucial thing in the strategy of knowledge transfer is educational culture and structures. Many universities nowadays offer specialized MS-programs that equip the students with skills that are needed in the mathematical projects in the R&D-sections in industry. The job title in industry is seldom that of a mathematician. It can be a researcher, an engineer, a research engineer, systems specialist, development manager. Industrial mathematics is team-work. Success stories are born when a group of specialists can join their expertise in a synergic manner. The requirement of team-work makes communications skills necessary. It would be very important to train oneself to work in a project, where interpersonal communication is continuously present.

The educational challenge is to find ways to make the theoretical content transparent and communicate to the students the end-user perspective of mathematical knowledge. The quest for novel ideas should be visible in curriculum development, up-to-date contents, innovative teaching methods and educational programs tailored to the needs of modern industy and concerns of sustainable development, smart growth and competitiveness through innovation.

Innovative practices have been adopted to facilitate the knowledge transfer into real world. Examples include the introduction of Modeling workshops and the European Study Group with Industry concept as an environment to combine applied research, mathematical R&D challenge in industry and post graduate education. For successful transfer of mathematical knowledge to client disciplines the theme of mathematical modelling is a crucial educational challenge. Maturing into an expert can only be achieved by treating real patients.

10.1.6 Modelling as a Course Subject

Many departments have introduced modelling courses in the curriculum. The challenge and fascination is the students' exposure to open problems, addressing questions arising from real context. The real world questions may be found from the student's own fields of activity, hobbies, summer jobs etc. Reading newspapers and professional magazines with a mathematically curious eye may find an idea for a modelling exercise. A good modelling course should

(a) contain an interesting collection of case examples which stir students' curiosity
(b) give an indication of the diversity of model types and purposes
(c) show the development from simple models to more sophisticated ones
(d) stress the interdisciplinary nature, teamwork aspect, communication skills
(e) tell about the open nature of the problems and non-existence of r̈ightsolutions
(f) help to understand the practical benefits of the model
(g) tie together mathematical ideas from different earlier courses

10.1.7 Modelling weeks

One of the innovative educational practices introduced in the recent decades is Modelling Week, an intensive mathematical problem solving workshop which simulates the real life R&D procedures. Modelling week mimics the Study Group format at the level of MS students.

Students come together and work in teams of five or six on real world problems. The cases originate from industry, various organisations or branches of society. The teams are guided by a group of academic staff members who as instructors play the role of the problem owners. The week starts with the problem owner giving a brief outline of the problem, the industrial context and the relevance of the problem for his/her company. The team questions the problem owner about the problem and the expectations.

To identify and understand the real problem may take some time. The students must formulate a model and recognize the typically non-unique mathematical problem. The analysis follows leading to analytical studies and efforts to find techniques for numerical solutions. Typically the group arrives at an approximate solution. At the end of the week the student groups have to present their findings in public. Further they are assumed to produce a decent written report, often a short article that will be published in the proceedings of the Modelling Week.

10.1.8 Study Groups with Industry

Oxford Study Group with Industry concept was pioneered at University of Oxford in 60ies. Later renamed as European Study Groups with Industry it has become a successful model copied worldwide. ESGI has been organized recently 1-3 times a year. It means an intensive problem seminar based on cases from industry. It brings the flavour real life problems into the campus and integrates the industrial R&D questions into the educational process. Study Group provide a forum for industrialists to work alongside established academic mathematicians, postdoctoral researchers and postgraduate students on problems of direct industrial importance.

Study Group last for a week and is focussed on 3-8 industrial problems. On the first day, each problem is presented by an industry representative . The academic participants allocate themselves to the groups who will work for the week on a given problem. Reports are presented on the final day and later a final

report is composed containing the results, comments, ideas and suggestions. Prior communication with the company and also during the week is important.

The success of a study group is due to the following

- they help to build contacts between academia and industry and may lead to research colaboration
- new research areas may be identified
- they provide source of research topics MS andf PhD for students
- companies meet students and may evaluate them for employment
- brain storming may be really helpful for the company, even if the problem will not be completely solved.

10.1.9 Interdisciplinary institutes

Several universities have set up interdisciplinary research institutes, centres on expertise on industrial mathematics to foster the interaction. Such institutes have been founded in several countries with the common aim to foster the university industry transfer of mathematical knowledge and computational technology. A few examples are INRIA France, OCIAM Oxford, ZIB Berlin. WIAS Berlin, ITWM Kaiserslautern. IWRMM Karlsruhe. ZeTeM, Bremen, MIRIAM Milan, CIMNE Barcelona, CASA Eindhoven, ITM FCC Gothenburg and RICAM Linz. The emergence of such network of institutes and their research agenda is a vivid indication of the intense development. It also gives a panorama view of the prolific field of industrial mathematics today.

10.1.10 Outreach for society, industry and educators

One challenge for mathematics community today is to make publicity about the importance and relevance of mathematical technology to the general public, educators, various professions and especially school children and future students. Special public outreach campaigns are called for. They could be organized in collaboration with universities, teacher's associations, companies, government and regional actors. The objective of such campaigns would be to tell about the various roles that mathematics has in the progress of industry, governance, logistics, economy and global concerns in energy, environment, ecosystem etc.

Bibliography

[1] Report on Mathematics in Industry 2008 http://www.oecd.org/dataoecd/47/1/41019441.pdf

[2] Report on Mechanisms for Promoting Mathematics-in-Industry 2009 http://www.oecd.org/dataoecd/31/19/42617645.pdf

Special Sessions: Presentation of Posgraduate Experiences in Industrial Mathematics.

THIRTY YEARS OF BIOSTATISTICS EDUCATION AT MASTER AND PHD LEVEL

Geert Molenberghs

Interuniversity Institute for Biostatistics and statistical Bioinformatics, Hasselt University, Diepenbeek, Belgium & Katholieke Universiteit Leuven, Belgium
geert.molenberghs@uhasselt.be, geert.molenberghs@med.kuleuven.be; www.ibiostat.be

Abstract

Biostatistics, medical statistics, bioinformatics, epidemiology, genetics, and related fields are both in rapid evolution and multi-faceted. It is important to grasp the full realm of aspects in order to move to successful educational initiatives. We sketch the professional arena for the field, also from a historical context, and then move on to contemporary educational initiatives.

11.1 The Bio-X Profession

As brought forward in [1], in the fields of medicine, public health, agriculture, the environment, and biology, we are faced with crucial challenges in the period ahead of us. Addressing these requires a strong quantitative component, i.e., biostatistics (also known as statistics in the life sciences, biometry, medical statistics) and statistical bioinformatics. These fields have stably developed in the Anglo-Saxon world but less so in continental Europe. The discipline is directed towards use and development of statistical theory and methods to address design, analysis, and interpretation of information in the biological sciences. This is a challenging, since multi-faceted, and interdisciplinary profession.

The profession is at a critical juncture. The biostatistician´s work has always been of great importance in the conduct of scientific investigations in agriculture, life sciences in general, ecology, forestry, medicine, public health, etc. This has never been more pressing than in current times, with advances in technology that have allowed amazing amounts of information to be collected and stored and with an increasingly complex health-care and public health landscape associated with dizzying arrays of new pharmaceutical products and medical procedures and growing interest among the public in assessing their risks and benefits.

In 1948, Chester Bliss, one of the first presidents of the International Biometric Society, edited a proceedings volume entitled "Biometrical Clinic on Entomological Problems." The title page is reproduced in Figure 11.1. While over 50 years old, the message is remarkably fresh and relevant, as we can read from the foreword:

> "The advances in biometry have developed through the close cooperation of biologists confronted with problems and of statisticians who develop methods for solving them. Both have gained from this collaboration. One medium for maintaining contact is the "biometrical clinic", in which questions are asked by the biologist and answered informally by the statistician. The meeting recorded here followed this pattern. Even when the answers can be found in the textbooks or in scientific journals, the method which is most relevant to a

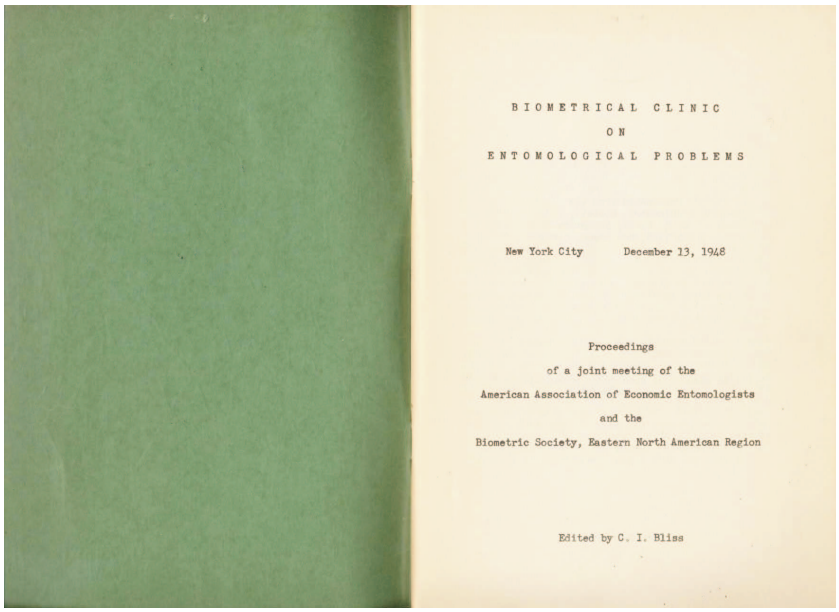
BIOMETRICAL CLINIC
ON
ENTOMOLOGICAL PROBLEMS

New York City December 13, 1948

Proceedings
of a joint meeting of the
American Association of Economic Entomologists
and the
Biometric Society, Eastern North American Region

Edited by C. I. Bliss

Figure 11.1: Title page of "Biometrical Clinic on Entomological Problems" proceedings.

> specific problem may not be apparent to the uninitiated. If a question cannot be answered, its asking may guide the statistician into a new and interesting field of study. Hence the session is of interest to both the biologist and the statistician."

This text provides food for reflection, especially at times where we are confronted, in addition to our traditional collaborators in agricultural, environmental, medical, biological, and epidemiological sciences, with colleagues from various new fields including molecular biology, bioinformatics, genomics, proteomics, even from security biometrics.

It is increasingly clear that the future is bright for interdisciplinary and multidisciplinary efforts. It is also clear that academic institutions should prepare themselves for this trend. A nice example is the Bio-X initiative in Stanford, a new entity in a new building, encompassing molecular biology, life sciences, biosciences, biostatistics and bioinformatics.

All of this underscores the need for top-notch, highly trained professionals.

11.2 Education in Bio-X

The field, as sketched in the previous section, is based upon strong Anglo-Saxon roots: Fisher´s pioneering work at the Britain-based Rothamsted Experimental Station on the one hand and the Food and Drug Act in the United States on the other. This has led to the inception of strong master and doctoral programs in statistics in the Anglo-Saxon world, including but not limited to the University of Reading, the London School of Hygiene and Tropical Medicine, Lancaster University, Harvard University, Johns Hopkins School of Public Health, University of Washington, Waterloo, North Carolina State University, etc. Also the presence of strong government-sponsored biomedical research institutions and regulatory bodies has contributed in important ways, such as the National Institutes of Health, the Centers for Disease Control and Prevention, and the Food and Drug Administration. The Anglo-Saxon tradition also lives in Commonwealth countries, such as South Africa, India, Australia, New Zealand, etc.

Continental Europe has followed suit, with some delay. Some thirty years ago, Hasselt University established a master program in biostatistics, inspired by the Anglo-Saxon model, through the late Steve Lagakos from the Harvard School of Publich Health, and Sir David Cox. The program now encompasses lines in biostatistics, bioinformatics, and epidemiology and public health. There are a number of key ingredients. First, the link with the rest of the world is crucial. This is seen through visiting faculty, students, and staff from all over the world. Second, and related, there is a strong link with South countries, with formal and informal collaboration with, for example: Cuba, Brazil, Ethiopia, Kenya, Mozambique, Suriname, etc. Third, biostatistics education cannot thrive without strong links with the organizing department´s research and statistical consulting lines. There ought to be a constant cross-fertilization between all of these pillars. Fourth, there should be symbiosis between the master and doctoral level education programs.

The University of Leuven established its program slightly more recently. Apart from biometry, there are lines in statistical methodology, social and behavioral statistics, and industrial statistics. Apart from through a strong collaboration with Hasselt University, there is a strong advantage in the close interaction between various application areas in statistics, as well as with methodology.

Students of these programs invariably find a satisfying job, with a healthy mix between industry, academe, and the government. About half continue towards a doctorate, in Belgium, the rest of Europe, and worldwide.

It is essential that a successful program prepares students, not only for the purely technical aspects of their job, but also for its interdisciplinary component. This implies that communication, oral and written, and boardroom-type interaction, should be integrated components of a program. Students should be exposed to teaching staff from the alma mater and beyond, preferably also from research institutes and industry. Biostatisticians, in the broad sense, are unique in the sense that they can keep an eye, at the same time, on the big picture and the fine details; the first, due to their ability for logical reasoning, the second, due to the very mathematical foundation of the statistical profession.

It is pleasing to see that others, most notably in the Hispanic world, follow the examples set out and offer state of the art training initiatives.

Bibliography

[1] Molenberghs, G. (2005) Presidential Address: XXII International Biometric Conference, Cairns, Australia, July 2004: Biometry, biometrics, biostatistics, bioinformatics,... Bio-X. *Biometrics* **61**, 1–9.

Special Sessions: Presentation of Industry Related Theses.

Artificial intelligence for surface-finish prediction and control in high speed milling processes

Maritza Correa Valencia

Automatic and Robotic Centre (CAR), UPM-CSIC, Km. 0.200 La Poveda,
Arganda del Rey, 28500, Madrid, Spain.
maritza.correa@car.upm-csic.es - http://www.iai.csic.es/users/mcorrea

Abstract

This thesis develops a methodology for analyzing and designing an intelligent surface-finish prediction and control system for high-speed milling processes. The system consists of: 1) a model learned with experimental data that uses Bayesian networks, which shed light on the dynamic processes involved in machining and the interactions between relevant variables; 2) an explanatory method, which generates a set of rules obtained from decision trees. These trees are induced from a set of simulated data generated from the posterior probabilities of the class variable, calculated with the Bayesian network learnt in the previous step, as Bayesian classifiers are especially useful when resolving problems that arise from probability tables; 3) and, finally, multiobjective optimization is completed, in case some goals may be quantified as ranges rather than real numbers. This often occurs in machine learning applications, especially those based on supervised classification; situations in which, conceptual extensions of dominance and Pareto frontier are applied. We analyze their application to the prediction of surface roughness in the case of study, while maximizing the sensitivity and the specificity of induced Bayesian classifiers, rather than only maximizing correct classification rates.

12.1 Introduction

Over recent years, great interest has been expressed in machine tooling techniques and their specific benefits. The product of automotive, aerospace and general engineering skills and a key element in manufacturing technology, machine tools are essential to the main industrial sectors. In machining, the new paradigm should be to maximize production while minimizing the rate of tool wear and maintaining the quality of each part [3]. Productivity is no longer the only requirement in the process. Today, quality is a key objective. So far there is no known system that provides real solutions to the problems of in-process surface-finish prediction for high-speed milling.

12.2 Contributions

The main contributions of this work are reflected in three areas: classification, explanation, and optimization. Classification, introduced into Bayesian classifiers for the prediction of Ra (average value of surface roughness), implies inclusion of novel variables (such geometric patterns basic and material hardness) for modeling Ra using the naïve Bayes and TAN structures. This contribution was published in [1]. In addition, a comparative analysis between two models for the prediction of Ra was developed using artificial neural networks (ANNs) (*Multi Layer Perceptron*) and Bayesian networks (BNs) (*Tree*

Augmented Network). This contribution is published in [2]. After validation of both models with the same dataset and method (K-fold cross-validation), the BNs produced better results in terms of classifier goodness-of-fit, when applied to the problem of surface quality prediction in high-speed milling processes. These results have been confirmed by several tests of the hypotheses. A summary of the measures of merit calculated for both classifiers are shown in Table 12.1.

Table 12.1: Summary of measures of merit calculated for each classifier

Measure	ANN	BN
Examples incorrectly classified	65 (5.15%)	46 (3.64%)
Examples correctly classified	1197 (94.84%)	1216 (96.35%)
Kappa statistic	0.92	0.94
Mean absolute error (MAE)	0.04	0.03
Root mean absolute error (RMSE)	0.14	0.13
Relative absolute error (RAE)	13.05%	10.41%
Root relative squared error (RRSE)	33.70%	32.66%
Construction time	12.69 s	0.08 s
Interpretability	Can not ask questions	Understandable, support inference in any direction

The explanation method is presented at a micro level through rules taken from a decision tree. It manages to simplify and explain the complexity of posterior probability tables computed with a BN and a very important aspect is that the meaning of the explanation is generally applicable to any environment, and is not restricted to a specific vocabulary. This contribution is published in [4]. The methodology is summarized in Figure 12.1.

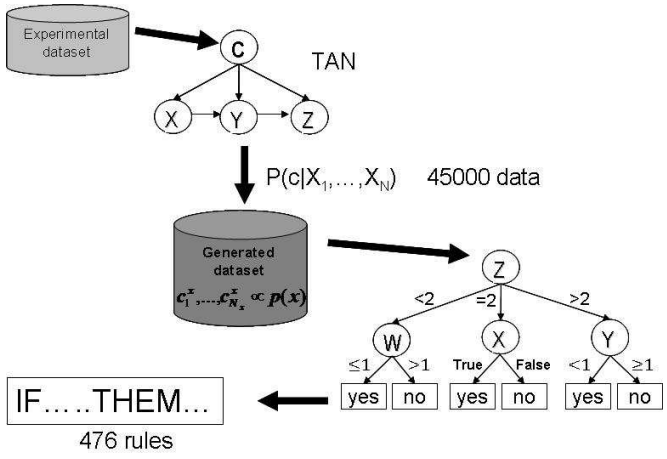

Figure 12.1: Outline of the methodology proposed for the explanation.

In the optimization area, an extension is made of the dominant ideas from the optimization multiobjetive to the case of interval-valued targets, as the methodology uses supervised classification models in which the model solutions have at least 2 goals (maximize sensitivity and specificity), which additionally may not be quantified (for validation purposes) as a single real number. The intervals of the goals may be the result of a confidence interval estimate. The effect of overlap and the confidence level is examined

and is converted into an extension of the concepts of Pareto's theory applied to the field of supervised classification.

Definition 1 ***(Pareto dominance of degree α for interval-valued objectives)***

1. *Pareto dominance of degree $\alpha(\alpha \in [0,1])$. A solution $\boldsymbol{x}$ is said to Pareto-dominate a solution $\boldsymbol{y}$ with degree α ($\alpha \in [0,1]$), or $\boldsymbol{x}$ α-dominates $\boldsymbol{y}$ for short, denoted as $\boldsymbol{x} \succ_\alpha \boldsymbol{y}$, iff*

$$\forall i \in M_P : f_i(\boldsymbol{x}) \leq f_i(\boldsymbol{y}) \quad \textit{and} \quad \forall i \in M_I : 1 - \frac{\sup f_i(\boldsymbol{x}) - \inf f_i(\boldsymbol{y})}{\sup f_i(\boldsymbol{x}) - \inf f_i(\boldsymbol{x})} \geq \alpha, \textit{ and}$$
$$\exists j \in M_P : f_j(\boldsymbol{x}) < f_j(\boldsymbol{y}) \quad \textit{or} \quad \exists j \in M_I : 1 - \frac{\sup f_j(\boldsymbol{x}) - \inf f_j(\boldsymbol{y})}{\sup f_j(\boldsymbol{x}) - \inf f_j(\boldsymbol{x})} > \alpha$$

2. *Pareto optimal solution of degree α. A solution $\boldsymbol{x}$ is said to be Pareto optimal of degree α iff $\nexists \boldsymbol{y}$ with $\boldsymbol{y} \succ_\alpha \boldsymbol{x}$.*

3. *Pareto optimal set of degree α. It is the set $\mathcal{P}_S^\alpha$ of all Pareto optimal solutions of degree α: $\mathcal{P}_S^\alpha = \{\boldsymbol{x} | \nexists \boldsymbol{y}$ with $\boldsymbol{y} \succ_\alpha \boldsymbol{x}\}$.*

4. *Pareto optimal front of degree α. It is the set $\mathcal{P}_F^\alpha$ of all objective function values corresponding to the solutions in $\mathcal{P}_S^\alpha$:*

$$\mathcal{P}_F^\alpha = \{(f_1(\boldsymbol{x}), ..., f_r(\boldsymbol{x}), (\inf f_{r+1}(\boldsymbol{x}), \sup f_{r+1}(\boldsymbol{x})), ..., (\inf f_m(\boldsymbol{x}), \sup f_m(\boldsymbol{x}))) | \boldsymbol{x} \in \mathcal{P}_S^\alpha\}.$$

Note that if $\sup f_i(\mathbf{x}) \leq \inf f_i(\mathbf{y})$, then the quotient is non-positive and the result is greater or equal to 1. In this case, we set $\alpha = 1$. Therefore, Strict Pareto dominance definition is embedded in the more general Definition 1 when $\alpha = 1$. Also, note that

$$1 - \frac{\sup f_i(\mathbf{x}) - \inf f_i(\mathbf{y})}{\sup f_i(\mathbf{x}) - \inf f_i(\mathbf{x})} \geq \alpha \Leftrightarrow \frac{\inf f_i(\mathbf{y}) - \inf f_i(\mathbf{x})}{\sup f_i(\mathbf{x}) - \inf f_i(\mathbf{x})} \geq \alpha$$

An intuitive idea of the meaning of different values of α, using this last quotient, is shown in Figure 12.2. A more general definition would allow different α values for different interval-valued objectives.

12.3 Structure

The thesis is organized into 7 chapters. Chapter 1 presents a brief introduction to its framework, objectives and methodology as well as and introduction to the structure that the memory will have. Chapter 2 conducts an in-depth study of some basic notions from high-speed machining. It seeks to show the inherent difficulties of the problem due to the great complexity of the machining process, the difficulty of in-process measuring of surface quality and the solutions that have been proposed to date.

Chapter 3 makes a detailed analysis of the methodology for predictive modeling of surface quality in high-speed milling processes. The data acquisition system is described: sensors and data processing of signals. The first experimental phase is detailed, followed by a theoretical introduction to BNs, the presentation of the empirical model and its solution for in-process surface-quality prediction based on BNs.

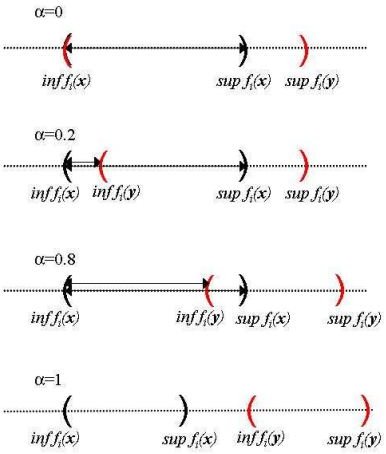

Figure 12.2: Different situations of α-dominance

Chapter 4 describes the second and third phase of experimentation beginning with two experimental designs: the fractional and the Response Surface Method (RSM) method which provide the data for modeling. Two models were developed: the results of an ANN model were compared with those from a BN-based model, which is a novel tool in this environment. Chapter 5 develops a method to explain the output of Bayesian classifiers from a group of rules obtained with decision trees.

In chapter 6 a novel solution to multi-objective optimization problems is presented, where objectives are quantified as intervals instead of a real number. Specifically, dominance ideas and the Pareto frontier are further explained in this context and their application to surface-finish in the case of study is formulated. Only two objectives -sensitivity and specificity- are maximized in this approach, instead of only the percentage of good classified cases. The interval-valued probabilities are calculated by means of a 10-fold cross validation.

Lastly, in chapter 7, the summations and some possible interesting lines of future research are presented.

12.4 Conclusions

The main tools described in the most recent literature to predict surface roughness are linear or multiple regression, and ANNs. The models using such tools all too often fail to include either a mechanical analysis of cutting processes or process expertise (of operators, production engineers or mechanical engineers). This was a key consideration in our choice of tool to develop a good predictor for Ra. To achieve this objective, the use of Bayesian classifiers have been introduced to model surface roughness in the milling process. This appears to represent an important advance towards optimal machining, because of the interesting inter-nodal relationships identified by these classifiers. Expert knowledge suggests that such relationships are evident in the process, even though they do not have any mathematical relationship in the formulas that define the metal-cutting process. BNs achieve better results than their strongest competitor (ANNs), from the point of view of quality prediction in high-speed milling. These results have been confirmed by several hypothesis tests.

One of the main problems with modelling is to understand the results and to arrive at generalizations. An explanation method is introduced that generates a set of rules obtained from decision trees. This methodology is a useful way of reducing and explaining the complexity of what are posterior probability

tables calculated by means of a Bayesian network. In this way, the information is conveyed more clearly to the expert, who finds it easier to understand the results. The methodology provides a compact form of the huge probability table for Ra prediction, applying only a few rules, where each rule leads to a deeper understanding and facilitates interpretation. The rules were validated using expert knowledge.

The ideas of dominance, which are borrowed from multiobjective optimization, will be applied to the case of interval-valued objectives. Theoretical results applied to the supervised classification field will be proven, where there are several real and interval-valued performance evaluation metrics. The best possible classification model is found on the basis of the one that identifies the best selection, in terms of Pareto optimality.

Finally, with regard to monitoring and control, it should be noted that the models developed to predict surface roughness provide open-loop control, as the control actions are presented in the form of suggestions that the operator may decide to put into practice.

Bibliography

[1] M. Correa, C. Bielza, M. de J. Ramírez & J.R. Alique, A Bayesian network model for surface roughness prediction in the machining process, International Journal of Systems Science 39 (12), (2008), 1181-1192.

[2] M. Correa, C. Bielza & J. Pamies-Teixeira, Comparison of Bayesian networks and artificial neural networks for quality detection in a machining process, Expert Systems with Applications 36, (2009), 7270-7279.

[3] L.N. López de Lacalle, J.A. Sánchez & A. Lamikiz, Mecanizado de Alto Rendimiento, Ediciones Técnicas Izaro S.A., 2004.

[4] M. Correa & C. Bielza, Explanation of a Bayesian network classifier by means of decision trees, Universidad Politécnica de Madrid, UPM-FI/DIA/2009-3, 2009. Submitted to International Journal of Pattern Recognition and Artificial Intelligence

Numerical resolution of water quality models: application to the closure of open pit mines

Luz María García García

Instituto Español de Oceanografía
luz.garcia@co.ieo.es

Abstract

By the end of 2007 the mining company Lignitos de Mirama, S.A (Limeisa, from now on) faced one important problem: the coal that they had been extracting for more than 25 years from an open pit coal mine in Cerceda (A Coruña, NW Spain) became exhausted. This situation was anticipated some years before and different closing scenarios were studied, being the flooding of the mining void with river water the selected one due to environmental and landscape recovery reasons.

Lakes that are formed by flooding open pit mines may present certain environmental problems associated with the presence of iron sulfides at the pit walls. When these materials are oxidized, acidity and heavy metals are released and accumulated in the water, becoming hazardous for the environment (see [5], [4]). Waters of this type may trigger a chain of chemical reactions whose relative importance will determine the final water quality of the lake.

The vertical circulation patterns of the lake contributed to increase the complexity of predicting the future lake water quality, which was the task that the Department of Applied Mathematics at the University of Santiago de Compostela carried out during the development of this thesis. The aim was determining by means of numerical modeling if the lake would satisfy some water quality standards at the end of the flooding period.

13.1 Introduction

Predicting the water quality of a future lake implies following the concentration of certain chemical species with time. For this purpose, the most relevant reactions in which these species are involved must be identified.

For the particular case of the pit lake whose water quality we want to predict, chemical reactions that are fast in comparison to the time scale of the problem coexist with others that are slower. Fast reactions are generally treated according to the theory of chemical kinetics, whereas slow ones are considered to be in equilibrium ([6]). A review of all the theoretical fundamentals regarding kinetics and equilibrium can be found, for instance, in [1] or [2], but we will focus here on the problem of coexistence.

13.2 The geochemical model: coexistence of slow and fast chemical reactions

13.2.1 General statement

Let us call $\mathcal{S} = \{E_i,\ i = 1, ..., N\}$ the set of N chemical species of interest. Suppose these species are involved in a set of $L + 2J$ chemical reactions of the form

$$\nu_1^l E_1 + ... + \nu_N^l E_N \rightarrow \lambda_1^l E_1 + ... + \lambda_N^l E_N, \qquad 1 \leq l \leq L + 2J, \tag{13.1}$$

with ν_i^l and λ_i^l the stoichiometric coefficients. The first L chemical reactions in (13.1) are slow and the last $2J$ are J couples of fast reversible reactions that satisfy

$$\nu_i^{L+2j-1} = \lambda_i^{L+2j} \quad \text{and} \quad \lambda_i^{L+2j-1} = \nu_i^{L+2j}, \qquad j = 1, \ldots, J. \tag{13.2}$$

By considering a kinetic description of the equilibrium reactions and assuming that all of them are elementary, the problem that must be solved is

$$\frac{dy_i(t)}{dt} = \sum_{l=1}^{L}(\lambda_i^l - \nu_i^l)k_l \prod_{i=1}^{N} y_i^{\nu_i^l} + \sum_{j=1}^{J}(\lambda_i^{L+2j-1} - \nu_i^{L+2j-1})\Big[k_{L+2j-1}\prod_{i=1}^{N} y_i^{\nu_i^{L+2j-1}} - k_{L+2j}\prod_{i=1}^{N} y_i^{\lambda_i^{L+2j-1}}\Big] \tag{13.3}$$

where y_i, $i = 1, \ldots, N$ denotes the concentration of the i-th chemical species, k_l, $l = 1, \ldots, L$ is the rate constant for the l-th slow reaction and k_{L+2j-1} and k_{L+2j}, $j = 1, \ldots, J$, are the rate constants for the j-th fast reaction in the forward and backward directions respectively.

Since all the rate constants in (13.3) have different units, a scaling procedure must be applied in order to be able to compare them. In this way, the following dimensionless variables are defined

$$\hat{y}_i(\hat{t}) = \frac{y_i(t)}{Y_i} \qquad \text{and} \qquad \hat{t} = \frac{t}{T}, \tag{13.4}$$

where Y_i and T are the typical scales for the concentration and time in the problem. Equation (13.3) is transformed into

$$\frac{Y_i}{T}\frac{d\hat{y}_i}{d\hat{t}} = \sum_{l=1}^{L+2J}(\lambda_i^l - \nu_i^l)\hat{k}_l \prod_{i=1}^{N}\hat{y}_i^{\nu_i^l} + \sum_{j=1}^{J}(\lambda_i^{L+2j-1} - \nu_i^{L+2j-1})\Big[\hat{k}_{L+2j-1}\prod_{i=1}^{N}\hat{y}_i^{\nu_i^{L+2j-1}} - \hat{k}_{L+2j}\prod_{i=1}^{N}\hat{y}_i^{\lambda_i^{L+2j-1}}\Big], \tag{13.5}$$

The equivalence between the new rate constants $\hat{k}_l$, $\hat{k}_{L+2j-1}$ and $\hat{k}_{L+2j}$, and the old ones is not included for being trivial.

Let us assume that $\varepsilon > 0$ is a small positive parameter describing the ratio of fast time scales to slow ones. There exist two positive constants C_1 and C_2 such that

$$\hat{k}_l = \mathcal{O}(1), \quad l = 1, \ldots, L, \tag{13.6}$$

$$C_1\varepsilon^{-1} \leq \hat{k}_{L+2j-1} \leq C_2\varepsilon^{-1} \ \text{ and } \ C_1\varepsilon^{-1} \leq \hat{k}_{L+2j} \leq C_2\varepsilon^{-1},\ j = 1, \ldots, J, \ \text{for small enough } \varepsilon, \tag{13.7}$$

$$\hat{K}_j^e(\theta) = \frac{\hat{k}_{L+2j-1}}{\hat{k}_{L+2j}}, \quad j = 1, \ldots, J \qquad \text{is independent of } \varepsilon. \tag{13.8}$$

Under assumptions (13.7) to (13.8), the model can be written in the limit as

$$\left.\begin{array}{l} \mathbf{y}'(t) = \mathbf{f}(t, \mathbf{y}(t)) + \mathcal{A}\mathbf{p}(t), \\ \mathbf{g}(t, \mathbf{y}(t)) = 0, \\ \mathbf{y}(0) = \mathbf{y}_{init}. \end{array}\right\} \tag{13.9}$$

with $\mathbf{f}(t, \mathbf{y}(t))$ the contribution of the slow chemical reactions, $\mathcal{A}$ the $N \times J$ matrix of components $\mathcal{A}_{ij} = \frac{T}{Y_i}(\lambda_i^{L+2j-1} - \nu_i^{L+2j-1})$ and $\mathbf{g}(t, \mathbf{y}(t))$ the term that represents the contribution of the slow chemical reactions. Functions p_j, $j = 1, \ldots, J$ in equation (13.9) can be considered as Lagrange multipliers associated to restrictions $g_j(t, \mathbf{y}(t)) = 0$, $j = 1, \ldots, J$. Notice that the equality restriction $g_j(t, \mathbf{y}(t)) = 0$, $j = 1, \ldots, J$ implies that $g_j p_j = 0$, being p_j, $j = 1, \ldots, J$ either positive, negative or zero. The previous conditions are equivalent to $p_j \in \mathcal{H}(g_j)$, $\forall j = 1, \ldots, J$, where $\mathcal{H}$ is a multi-valued function,

$$\mathcal{H}(x) = \left\{ \begin{array}{lll} \emptyset & if & x < 0 \quad and \quad x > 0, \\ (-\infty, \infty) & if & x = 0, \end{array}\right. \tag{13.10}$$

where $\emptyset$ denotes the empty set. In addition, $p_j \in \mathcal{H}(g_j) \Leftrightarrow p_j = \mathcal{H}_\lambda(g_j + \lambda p_j) = p_j + \frac{1}{\lambda} g_j, \ \ \forall \lambda > 0$ and not necessarily a small number (cf. [3]). This equivalence is a general result for maximal monotone operators such as $\mathcal{H}$, with $\mathcal{H}_\lambda$ its Yosida approximation. Figure 13.1 depicts functions $\mathcal{H}(x)$ and $\mathcal{H}_\lambda(x)$.

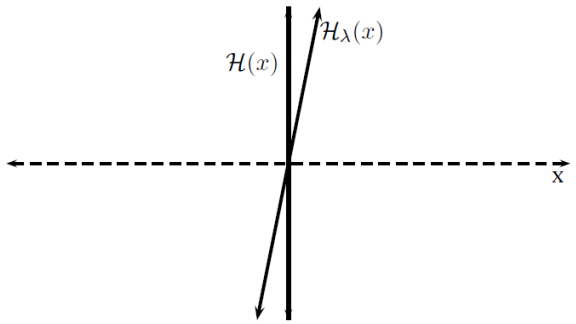

Figure 13.1: Functions $\mathcal{H}(x)$ and $\mathcal{H}_\lambda(x)$

When solubility reactions are also considered, some particularities arise that lead to Lagrange multipliers that only take positive values. The interested reader will find further explanations in [2].

13.2.2 Problem reduction and numerical resolution

The limit problem (13.9) is a good approximation of the original one (13.3) that can be directly solved for all the chemical species. However, it is stiff, meaning that it is expensive to solve. In order to eliminate its stiffness two reduction methods were proposed in the thesis that lead to a final statement of the problem that is similar to the one that can be found in the literature. The disadvantage of these methods is that they require a tedious algebraic treatment of the problem.

In any case, it has been demonstrated that the results of solving the complete and the reduced problems are the same.

13.3 A model for Limeisa open pit lake

All the theoretical considerations of the previous section were applied for the particular case of the Limeisa lake. The evolution of 112 chemical species was followed by accounting for the chemical reactions in which they were involved: 15 slow chemical reactions at the pit walls and at the water column (sulfide oxidation, silicate weathering and gas exchange with the atmosphere) and 72 fast reactions (homogeneous, solubility and adsorption equilibria).

The geochemical model was applied in two conceptual models for the future lake:

- **A stirred tank model:** a complete mixing of the water column is considered, being the water quality the same at any point. It represents the worst sittuation possible.
- **A three layer model:** it takes into account the seasonal patterns of vertical stratification/vertical mixing in the lake. In this case not only the geochemistry is important, but also the heat exchange with the atmosphere in order to calculate the density of each layer. Two adjacent layers will mix if the upper one is denser than the one below.

  According to this model, the water sources that feed the lake are separated into clean (low density) and polluted (higher density). The clean ones enter the lake through the surface and the polluted ones through the bottom. The geochemistry of each layer will depend on the specific chemical reactions that take place at that layer as well as the degree of mixing with the adjacent layers.

The results of both models from the beginning of the lake flooding to two years after its end (see the vertical line in the figures) with respect to the pH are shown in Figure 13.2. It must be mentioned that the lower the pH, the higher the water acidity and concentration of hazardous metals. According to the spanish law, pH values between 5.5 and 9 are acceptable.

Figure 13.2, left reproduces the results of the stirred tank model. It highlights the importance of the geochemistry on the future lake water quality by demonstrating that not accounting for chemical reactions at all (red line) or precipitation (blue line) leads to higher pH values.

Figures 13.2, center and right show the results of the three layer model by considering isolated layers or allowing vertical mixing, respectively. If no mixing is allowed, the bottom layer is more polluted than the surface one. On the other hand, if winter mixing occurs,the water column is more homogeneous, being just slight differences between the surface and the bottom layers observed during summer.

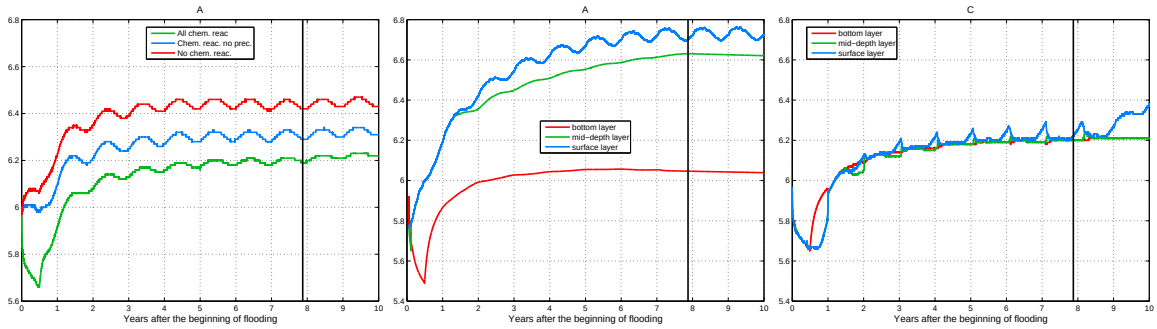

Figure 13.2: Model results for pH. **Left:** according to the stirred tank model, **center:** according to the 3-layer model with no mixing, **right:** according to the three layer model with mixing.

Bibliography

[1] A. Bermúdez, A. Continuum Thermomechanics, Birkhäuser, (2005)

[2] A. Bermúdez and L.M. GarcÃa-García Mathematical modeling in chemistry. Application to water quality problems, Applied Numerical Mathematics (2011). doi:10.1016/j.apnum.2011.05.002

[3] A. Bermúdez and C. Moreno Duality methods for solving variational inequalities, Comput. Math. Appl., 7 (1994),43-58.

[4] J.M. Castro and J.N. Moore Pit lakes: their characteristics and the potential for their remediation, Environmental Geology 39 (11), (2000), 1254-1260.

[5] A. Davis, W.B. Lyons and G.C. Miller Understanding the water quality of pit lakes, Environmental Science and Technology 30 (3), (1996), 118A-123A.

[6] F.M.M. Morel and J.G. Hering Principles and applications of Aquatic Chemistry John Wiley and Sons, (1993).

Special Sessions: Presentation of Industry Related Theses.

The Collision Avoidance Problem: Methods and Algorithms

F. Javier Martín-Campo
Thesis supervisors: Laureano F. Escudero and Antonio Alonso-Ayuso
University Complutense of Madrid and Rey Juan Carlos University
javier.martin.campo@ccee.ucm.es

Abstract

In this thesis, the Collision Avoidance problem for Air Traffic Management has been tackled. Two different models based on mathematical programming are presented in this thesis. The first one is a mixed integer linear model that solves realistic instances in short time (less than 5 seconds in very hard situations). The second model based on mixed 0-1 nonlinear optimization takes the time horizon explicitly in the constraints of the model in order to consider continuos maneuvers for solving the problem. This second model has been solved by using exact schemes by iteratively linearizing the nonlinear constraints and metaheuristic schemes because of the large-scale linearized models. Some instances are presented in this work in order to show the efficiency of the models.

14.1 Introduction

Aircraft conflict detection and resolution problem within the Air Traffic Management Problem is being studied tirelessly nowadays due to the demand growth. It consists of given a set of aircraft configurations where some parameters are known like velocity, altitude level, angle of motion, positions, etc. the aim of the problem is providing a new configuration such that all conflicts in the airspace are avoided. A conflict situation happens when two different aircraft lose the minimum safety distance that they have to keep. The standard distances are 5 nautical miles in the horizontal plane and 2000 feet in the vertical one.

Several approaches can be found in the literature, where different works tackle the problem from different points of view. In Kuchar and Yang (2000) [6] can be found several approaches until 2000. However, the developments from thereafter are very interesting. Some of the most important works can be found in Martín-Campo thesis (2010) [8]. For this work, the geometric construction presented in Pallottino et al. (2002) [9] helps us to detect the conflicts in the airspace.

The organization of the remainder of the note is as follows. First, Section 14.2 presents the guidelines for the first proposed model in the thesis, based on mixed integer linear optimization. Section 14.3 introduces the main features of the second proposed model, based on mixed 0-1 nonlinear optimization, as well as the schemes for solving it. And, finally, section 14.4 presents the main conclusions and future research lines.

14.2 The Velocity and Altitude Changes model (VAC)

The first model proposed in Martín-Campo [8] is the so-called "Velocity and Altitude Changes" (VAC). It is based on mixed integer linear optimization and it takes Fig. 14.1 as support for constraint modelization. This model takes into account the following aspects:

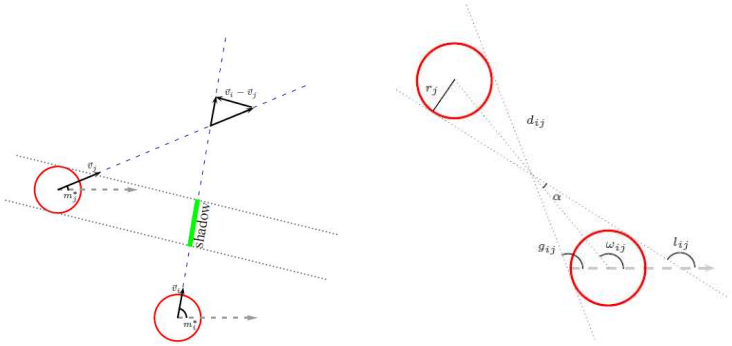

(a) Geometric construction for conflict avoidance constraints.

(b) Angles for the conflict avoidance constraints.

Figure 14.1: Geometric Construction for the VC problem.

- It avoids conflict situations by using the geometric construction in Fig. 14.1.
- It considers different safety radius for each aircraft in order to optimize the airspace.
- It detects situations in the preprocessing phase as "head to head" or "similar coordinates" in order to reduce the resolution time.
- It detects false conflict situations due to the geometric construction.
- It includes altitude changes in order to avoid conflict situations.
- It allows aircraft to climb or descend more than one altitude level.
- It solves a particular case due to a null denominator.

The VAC model has been tested with the case shown in Fig. 14.2(a). This case is bigger than the realistic ones, since notice that $F = 37$ aircraft in possible conflicts are considered. Also notice that there are two aircraft in both points (a) and (b). All aircraft fly with the same velocity, except aircraft (c) and (d) that fly with a higher velocity to test "pursuit cases". Aircraft (e), (f), (g) and (h) are in "false conflict" that implies an unnecessary velocity change. Aircraft (i), (j), (k), (l) and (m) are in an anomalous case.

Fig. 14.2(b) depicts the results of applying the VAC model for collision avoidance in the case depicted in Fig. 14.2(a) as follows:

- Seven velocity changes have been performed. The dotted line circles in the figure denote the positive variation of velocity, and the dashed line circle denotes the negative variation of velocity. In this case, all velocity changes are negative (slowdown). This is due to the same value of the costs $c_f^{q^+}$ and $c_f^{q^-}$.
- The points (a) and (b) still have two aircraft each, but the conflict has been avoided.
- The aircraft (e), (f), (g) and (h) have not changed their velocities, since they are in a "false conflict".
- There are eleven altitude level changes, four positive and seven negative, one of which descends two levels.

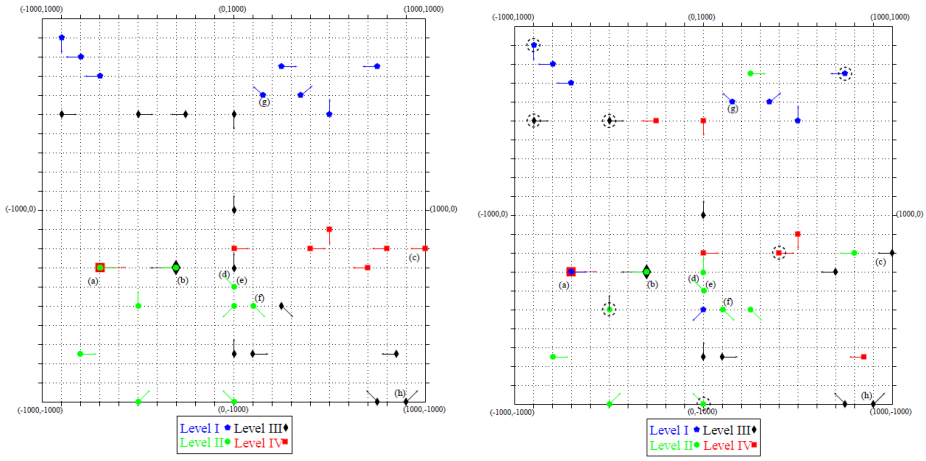

(a) Initial situation.

(b) Results for the VAC model.

Figure 14.2: Testing the VAC model.

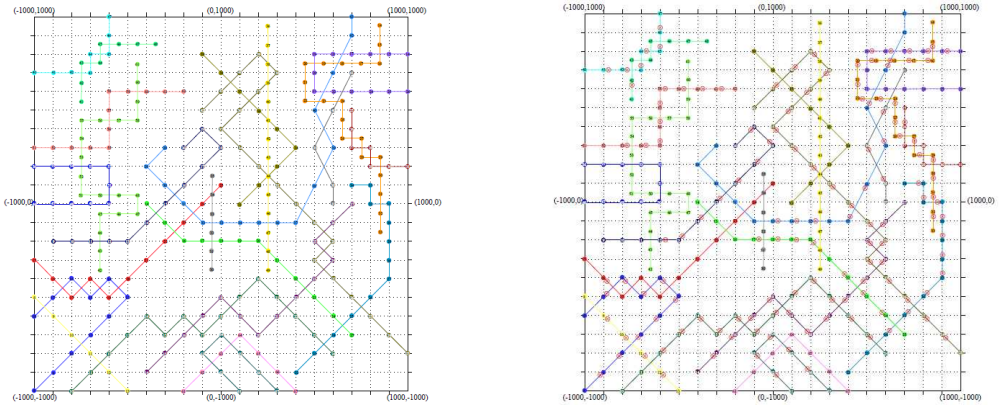

(a) Illustrative instance for testing the VCTP model. Initial situation

(b) Illustrative instance for testing the VCTP model. Resolution after 1st iteration

- The number of constraints, continuous and 0-1 variables in the reduced MIP have been 2998, 37 and 1963, respectively.
- The objective function value is 13.1124.
- The execution time was 8.42 seconds using the optimization engine CPLEX v.12.1 [5] (with the default options) in the following HW/SW platform: Intel Core 2 DUO P8400, 2.26GHz, 2GB RAM; Microsoft Windows 7 Professional SO.

See Martín-Campo (2010) [8] and Alonso-Ayuso et al. (2011a) [2] for the full model formulation and the extensive computational experience made.

14.3 The Velocity Changes through Time Periods model (VCTP)

The second model proposed in Martín-Campo (2010) [8] is the so-called "Velocity Changes through Time Periods" (VCTP), where continuous velocity changes are considered by using the Uniformly and

Accelerated Linear Motion (UALM). The same geometric construction presented in Fig. 14.1 is used, but the conflict avoidance constraints are nonlinear in this model, since the angles in Fig. 14.1(b) change depending on the positions of the aircraft. In this model the predicted configurations in different time periods for each aircraft are considered. This model extends the VAC in the sense of including nonlinear trajectories for aircraft. It results a model based on mixed 0-1 nonlinear optimization that cannot be solved by using directly standard nonlinear optimization engine. For solving the problem, the nonlinear constraints of the model has been linearized by using Taylor polynomials iteratively as Almiñana et al. (2008) [1] proposed for a nonlinear model. Therefore, due to the large-scale dimensions of the model, a metaheuristic so called "Variable Neighbourhood Decomposition Search" (Lazić et al. (2010) [7]) is used to find good solutions in short time.

The VCTP model has been tested by using the illustrative instance shown in Fig. 14.3(a) in order to prove that the conflicts are avoided. In this instance, 72 time periods with the same length (10 units) are considered. There exists several crossing conflicts in order to test the model. The computational experience was made by using the following HW/SW platform: Intel Core 2DUO P8400, 2.26GHz, 2GB RAM; Microsoft Windows 7 Professional SO. Only one iteration of the Taylor approach is presented for obtaining the results shown in Fig. 14.3(b), where:

- Several changes in the position have been made. The red circles with a cross denote the position after the resolution.
- The objective function value is 3.4238.
- The execution time has been 238 secs. by using CPLEX [5] (with the default options).

See Martín-Campo (2010) [8], Alonso-Ayuso et al. (2011b) [3] and Alonso-Ayuso et al. (2011c) [4] for studying the full model and the extensive computational experience that has been made.

14.4 Conclusions and future research

Two different models have been proposed in the thesis of Martín-Campo (2010) [8] in order to solve the Collision Avoidance for Air Traffic Management Problem. Both of them solve realistic problems by using optimization engine in short time. The first model is a static model since it solves problems without considering the future time. The second one assumes the time horizon explicitly in the model and it is able to solve realistic problems by considering continuous velocity changes. As future research, the next step will be to include altitude changes in the VCTP model and, on the other hand, to study angle changes as third maneuver to conflict avoidance.

Bibliography

[1] M. Almiñana, L. F. Escudero, M. Landete, J. F. Monge, A. Rabasa, and J. Sánchez-Soriano, On a mixed 0-1 separable nonlinear approach for water irrigation scheduling, IIE Transactions, 44 (4), (2008), 398-405.

[2] A. Alonso-Ayuso, L. F. Escudero, and F. J. Martín-Campo, Collision avoidance in the air traffic management: A mixed integer linear optimization approach, IEEE Transactions on Intelligent Transportation Systems, 12 (1), (2011a), 47-57.

[3] A. Alonso-Ayuso, L. F. Escudero, and F. J. Martín-Campo, A mixed 0–1 nonlinear approach for the collision avoidance in atm: Velocity changes through a time horizon, To be submitted, (2011b).

[4] A. Alonso-Ayuso, L. F. Escudero, and F. J. Martín-Campo, Variable neighbourhood decomposition search for the mixed 0-1 nonlinear collision avoidance problem, To be submitted, (2011c).

[5] IBM ILOG, CPLEX v12.1. User's Manual for CPLEX, (2009).

[6] J. K. Kuchar and L. C. Yang, A review of conflict detection and resolution modeling methods, IEEE Transactions on Intelligent Transportation Systems, 1, (2000), 179-189.

[7] J. Lazić, S. Hanafi, N. Mladenović, and D. Urošević, Variable neighbourhood decomposition search for 0-1 mixed integer programs, Computers & Operations Research, 37, (2010), 1055-1067.

[8] F. J. Martín-Campo, The collision avoidance problem: Methods and algorithms, Ph.D. dissertation, Department of Statistics and Operational Research, Rey Juan Carlos University, (2010).

[9] L. Pallottino, E. Feron, and A. Bicchi, Conflict resolution problems for air traffic management systems solved with mixed integer programming, IEEE Transactions on Intelligent Transportation Systems, 3 (1),(2002), 3-11.

Special Sessions: Presentation of Industry Related Theses.

Contributions to the mathematical study of some problems in magnetohydrodynamics and induction heating

Rafael Vázquez Hernández
Istituto di Matematica Applicata e Tecnologie Informatiche-CNR, via Ferrata 1, 27100, Pavia (Italy)
vazquez@imati.cnr.it

Abstract

The aim of the work is to numerically simulate an induction furnace in order to understand its behavior and to predict its performance under the variation of some parameters. An axisymmetric mathematical model consisting of coupled electromagnetic, hydrodynamic and thermal submodels is written before discretization. The thermal and hydrodynamic submodels are discretized by means of Lagrange-Galerkin methods, whereas the electromagnetic submodel is discretized with a mixed boundary element/finite element method. Iterative algorithms are also introduced to deal with the nonlinearities and the coupling terms. Numerical results of the simulation of an industrial induction furnace for melting are presented.

15.1 Motivation. The industrial problem

An induction furnace is a device designed to heat some material by electromagnetic induction. It consists mainly of a current generator and one inductor, to which an alternating electrical current is supplied. This induces eddy currents in the electrically conducting materials within the inductor, that are heated up by Joule effect. The real furnace we are interested in is similar to the one in Fig. 15.1, where the inductor is a helical-shaped coil, but since the scope is to melt the material, this must be put inside a crucible. Moreover, some thermally and electrically insulating materials surround the crucible (see Fig. 15.2), to avoid thermal losses without affecting the induction process. In this work we present the models and algorithms to simulate the induction process, taking into account the metal melting and the stirring of the molten material.

15.2 The coupled mathematical model

The mathematical model for the furnace consists of three coupled submodels: electromagnetic, thermal and hydrodynamic. We present now a brief description of each of them, and refer to [8, Ch. 3] for their detailed derivation.

15.2.1 The electromagnetic submodel

In order to solve the problem in an axisymmetric setting, the helical coil is replaced by m toroidal rings, where m is the number of windings of the coil. We denote by $\Omega_1, ..., \Omega_m$ the radial sections of the rings, by Ω_0 the radial section of the other electrically conducting parts of the furnace (the metal and

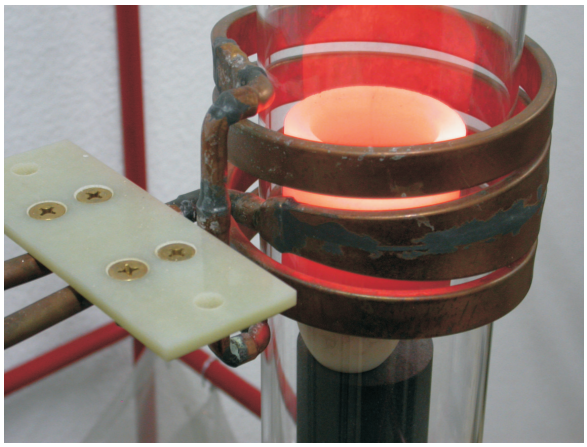

Figure 15.1: A simple induction furnace.

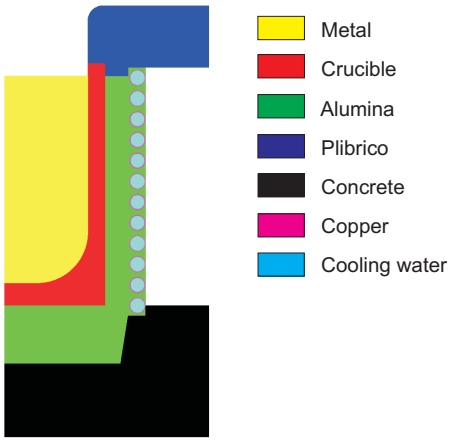

Figure 15.2: Materials of the furnace.

the crucible in Fig. 15.2), and define $\Omega = \cup_{i=0}^{m} \Omega_i$ the set of all conducting materials. We also denote by Γ the interface between Ω and its complementary in $\mathbb{R}^2$.

For our model we assume that an alternating current traverses the coil in the azimuthal direction, and that a different voltage current is applied in each radial section. Formulating the eddy-currents model in terms of the magnetic vector potential $\mathbf{A}$, the problem reduces to compute the azimuthal component A_θ and its normal derivative on the interface (see [4, 8] for details):

Given $\mathbf{V} = (V_1, \ldots, V_m) \in \mathbb{C}^m$, find $A_\theta : \Omega \longrightarrow \mathbb{C}$ such that

$$\mathrm{i}\omega \int_\Omega \sigma A_\theta \cdot \bar{\psi} r \, dr dz + \int_\Omega \frac{1}{\mu r} \frac{\partial (r A_\theta)}{\partial r} \frac{\partial (r \bar{\psi})}{\partial r} \, dr dz + \int_\Omega \frac{1}{\mu} \frac{\partial A_\theta}{\partial z} \frac{\partial \bar{\psi}}{\partial z} \, r \, dr dz$$
$$- \int_\Gamma \frac{1}{\mu_0} \frac{\partial (r A_\theta)}{\partial \mathbf{n}} \bar{\psi} \, d\gamma = -\frac{1}{2\pi} \sum_{k=1}^{m} V_k \int_{\Omega_k} \sigma \bar{\psi} \, dr dz \quad \forall \psi.$$

We notice that in these equations the electrical conductivity σ may depend on the temperature, which introduces a coupling with the thermal submodel.

We also remark that a different formulation has to be used if, instead of the voltages, the current intensities are given. It is also possible to use the power as the given data, but in this case a nonlinear problem must be solved. This approach is in fact the one that is used for the simulation, since in the real furnace the current intensity is automatically adjusted to attain a given power.

15.2.2 The thermal submodel

The thermal problem is solved in all the materials of the furnace (see Fig. 15.2). This includes the copper coil, but not the cooling water inside the coil, which is taken into account through suitable boundary conditions. The heat equation is written in terms of the enthalpy e, and assuming cylindrical symmetry it reads as follows:

$$\left(\frac{\partial e}{\partial t} + \mathbf{u} \cdot \mathbf{grad}\, e \right) - \frac{1}{r} \frac{\partial}{\partial r} \left(r k(r,z,T) \frac{\partial T}{\partial r} \right) - \frac{\partial}{\partial z} \left(k(r,z,T) \frac{\partial T}{\partial z} \right) = \frac{|J_\theta|^2}{2\sigma(r,z,T)},$$

where the current density J_θ is computed from the solution of the electromagnetic problem, and the velocity $\mathbf{u}$ from the solution of the hydrodynamic one, introducing new terms of coupling. Moreover,

the temperature dependence of the thermal conductivity k and the multi-valued nature of the enthalpy e introduce two nonlinear terms, that must be linearized before solving.

For the treatment of boundary conditions, convection conditions are taken in the external parts of the furnace, and in the interfaces with the cooling water. For the internal parts of the boundary, a radiation-convection boundary condition is chosen (an alternative is to use an internal radiation condition, as proposed in [2]). We remark that the radiation condition depends on the fourth power of temperature on the boundary. Moreover, the temperature of the cooling water must also be computed during the simulation. Both conditions introduce nonlinear terms in the equations.

15.2.3 The hydrodynamic submodel

In order to model the movement of the molten metal, Navier-Stokes equations are simplified using Boussinesq approximation, and considering also Smagorinsky's model for turbulent flows.

$$\rho_0 \left(\frac{\partial \mathbf{u}}{\partial t} + (\mathbf{grad}\,\mathbf{u})\mathbf{u} \right) - \mathrm{div}(\eta_{eff}(\mathbf{grad}\,\mathbf{u} + (\mathbf{grad}\,\mathbf{u})^t)) + \mathbf{grad}\,p = \mathbf{f},$$
$$\mathrm{div}\mathbf{u} = 0.$$

Notice that in these equations, the right-hand side $\mathbf{f}$ contains both buoyancy forces, caused by the temperature differences in the metal, and Lorentz forces, that are generated by the electromagnetic fields, introducing new terms of coupling. Moreover, the equations are only solved in the molten region of the metal, that is computed at every time step from the solution of the thermal problem.

15.3 Discretization and numerical results

In this section we give the main ideas about the algorithms for the discretization and the solution of the problem, that were implemented in a FORTRAN code. For more details about the algorithms we refer to [8, Ch. 4].

The electromagnetic equations, written in weak form, yield an integro-differential equation that is discretized by means of the mixed BEM/FEM method described in [1], with piecewise linear finite elements for A_θ, and piecewise constant boundary elements for its normal derivative.

The thermal and the hydrodynamic equations are discretized with Lagrange/Galerkin methods. In each equation, the convective term and the time derivative are summed up to rewrite the equations in terms of the material derivative, which is approximated with the method of characteristics [7]. Then, piecewise linear elements are used for the numerical approximation of the thermal problem, and the mini-element is chosen for the discretization of the hydrodynamic one (see, for instance, [5]). We notice that for the approximation of the material derivative it is necessary to solve an ordinary differential equation that depends on the velocity. This equation is numerically solved using the velocity at the previous time step, which allows to solve the hydrodynamic model decoupled from the other two.

Concerning the solution of the nonlinear and the coupling terms, a simple fixed point algorithm is introduced for the treatment of the thermoelectrical coupling, the temperature dependency of the physical properties, and for the computation of the temperature of the cooling water inside the coil. For the linearization of the enthalpy and the radiation boundary condition we use the iterative method introduced in [3]. To improve the convergence of the method, that depends on the particular choice of some parameters, we adopt the methodology proposed in [6].

The method has been applied for the simulation of the induction furnace in Fig. 15.2 under different conditions. For instance, the software has permitted us to test the performance of the furnace changing the power and the frequency of the electric current supplied to the coil, the size of the crucible and its relative position to the coil, or the distance between the windings of the coil. In this work we present a particular case, in which an electrical current at 500 Hz is supplied, and the power is fixed at 75 kW. In Fig. 15.3 we present the temperature in the furnace after three hours, when all the metal is already molten. It can be seen that the highest temperatures are attained in the lowest part of the crucible wall. It is also worth to note the high temperature differences in the insulator (from $50°$C near the coil to more than $1500°$C near the crucible), and for this reason a very fine mesh is required in this zone. In Fig. 15.4 we show the Joule effect in the crucible and the metal. Due to the skin effect, the Joule effect is concentrated near the walls, and a very fine mesh is also required in these zones.

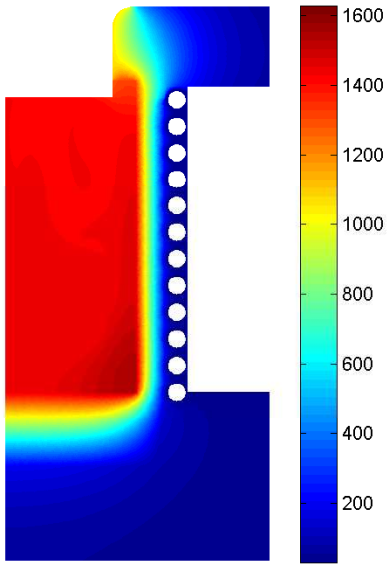

Figure 15.3: Temperature after 3 hours.

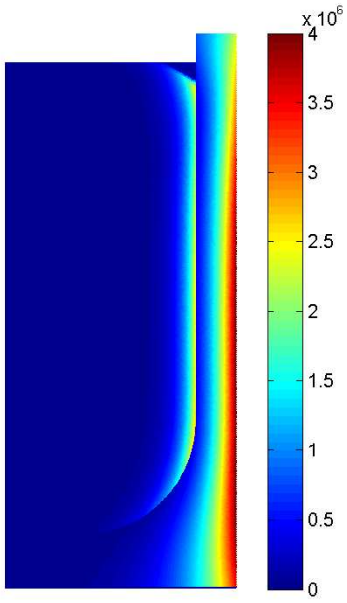

Figure 15.4: Joule effect in the metal and crucible.

Bibliography

[1] A. Bermúdez, D. Gómez, M. C. Muñiz, P. Salgado, A FEM/BEM for axisymmetric electromagnetic and thermal modelling of induction furnaces, Internat. J. Numer. Methods Engrg., 71 (2007), 856-878.

[2] A. Bermúdez, D. Gómez, M.C. Muñiz, R. Vázquez A thermoelectrical problem with a nonlocal radiation boundary condition, Mathematical and Computer Modelling 53, (2011), 63-80.

[3] A. Bermúdez, C. Moreno, Duality methods for solving variational inequalities, Comp. Math. Appl., 7 (1981), 43-58.

[4] C. Chaboudez, S. Clain, R. Glardon, D. Mari, J. Rappaz, M. Swierkosz, Numerical modeling in induction heating for axisymmetric geometries, IEEE Trans. Magn., 33 (1997), 739-745.

[5] V. Girault, P.-A. Raviart, *Finite element methods for Navier-Stokes equations. Theory and algorithms,* vol. 5 of Springer Series in Computational Mathematics, Springer- Verlag, Berlin, 1986.

[6] C. Parés, J. Macías, M. Castro, Duality methods with an automatic choice of parameters. Application to shallow water equations in conservative form, Numer. Math., 89 (2001), 161-189.

[7] O. Pironneau, On the transport-diffusion algorithm and its applications to the Navier-Stokes equations, Numer. Math., 38 (1982), 309-332.

[8] R. Vázquez Hernández, *Contributions to the mathematical study of some problems in magnetohydrodynamics and induction heating*, Ph.D. Thesis, Universidade de Santiago de Compostela, 2009.

BDF-α method: modification of the BDF2

E. Alberdi Celaya[1], **J. J. Anza Aguirrezabala**[2]

[1]Lea Artibai Ikastetxea, Av. Xemein 19, 48270 Markina-Xemein (Vizcaya), Spain

[2]Departamento de Matemática Aplicada, ETS de Ingeniería de Bilbao, Universidad del País Vasco, Alameda Urquijo s/n 48013 Bilbao, Spain

ealberdi@leartik.com

Abstract

After applying a multistep numerical method for solving Ordinary Differential Equations (ODE-s) to the test equation, $y' = \lambda y$, a difference equation is obtained which can be expressed matricially as:

$$Y_{n+k} = AY_{n+k-1} \tag{16.1}$$

where Y_{n+k-1}, Y_{n+k} are the variables or the unknowns and A is a matrix of dimension kxk which is called the amplification matrix or the amplification factor. The eigenvalues of A are the roots of the characteristic polynomial of the method: $p(r) = det\,(A - rI)$. The eigenvalue with largest module of A is called spectral radius and it is usually denoted by ρ:

$$\rho = max\,\{|\lambda_i| : \lambda_i\ eigenvalue\ of\ A\} \tag{16.2}$$

The method is stable if the eigenvalues of the amplification matrix are smaller or equal to one [2]. But an amplification factor close to cero makes the result less precise.

We have numerically simulated the solution of the linear wave equation, which is a Partial Differential Equation (PDE), using a Galerkin method [6] and the numerical methods BDF (Backward Differentiation Formulae), methods of orders 1:5 [1]. These methods have good stability properties but their amplification factor tends to cero when $h/T \to \infty$, where h is the step size and T the period. Unlike what happens with the modification Hilber-Hughes-Taylor [3], also known as HHT-α which was made to the Newmark's method [5], where a method with a smaller amplification factor is obtained, we have constructed a modification of the BDF2 method, which we have called BDF-α. This new method has order two and it is more precise than the BDF2 method. It also has an amplification factor greater than the one that the BDF2 has. In this way we have solved the wave equation in a more precise way than using the BDF2.

16.1 Newmark's method

This method was proposed by Newmark in [5]. The differential equation to which we apply the method is given by this equation: $Md'' + Cd' + Kd = F$, $d(0) = d_0$, $d'(0) = v_0$. The method consist of applying the next relations:

$$\begin{cases} d_{n+1} = d_n + \Delta t v_n + \frac{\Delta t^2}{2}\left[(1-2\beta)\,a_n + 2\beta a_{n+1}\right] \\ v_{n+1} = v_n + \Delta t\left[(1-\gamma)\,a_n + \gamma a_{n+1}\right] \end{cases} \tag{16.3}$$

It can be observed that when $\beta = 0.25,\ \gamma = 0.5$, Newmark's method (called the medium acceleration method) is converted into the trapezoidal method. To prove this, it is enough to substitute the values of β, γ in (16.3), to take out $(0.5a_n + 0.5a_{n+1})$ from the second equation and to substitute it in the first one to reach the trapezoidal method:

$$d_{n+1} = d_n + \Delta t \left(\frac{v_n + v_{n+1}}{2} \right) \tag{16.4}$$

Newmark's method can be expressed matricially in the next way:

$$X_{n+1} = AX_n \tag{16.5}$$

where: $X_{n+i} = \left(d_{n+i}, hv_{n+i}, h^2 a_{n+i}\right)^T$ for $i = 0, 1$, $h = \Delta t$ and A is given by: $A = \bar{A}_1^{-1} \cdot \bar{A}_2$, where:

$$\bar{A}_1 = \begin{pmatrix} 1 & 0 & -\beta \\ 0 & \frac{1}{h} & -\frac{1}{h}\beta \\ \omega^2 & \frac{2\xi\omega}{h} & \frac{1}{h^2} \end{pmatrix}, \bar{A}_2 = \begin{pmatrix} 1 & 1 & \frac{1}{2} - \beta \\ 0 & \frac{1}{h} & \frac{1}{h}(1-\gamma) \\ 0 & 0 & 0 \end{pmatrix}$$

As it is said in [4], that the order of the method is 2 when $\gamma = 1/2$.

16.2 HHT-α method

The HHT-α method is a modification made to the Newmark's method. The aim of the modification was to obtain more dissipation of the high frequencies. This method was proposed in [3] by Hilber-Hughes-Taylor and it is also known as HHT. The method consists of mantaining the two expressions of the Newmark's method (16.3) and varying the next equation:

$$Ma_{n+1} + (1+\alpha)\, Cv_{n+1} - \alpha Cv_n + (1+\alpha)\, Kd_{n+1} - \alpha Kd_n = F\left(t_{n+\alpha}\right) \tag{16.6}$$

where: $t_{n+\alpha} = (1+\alpha)\, t_{n+1} - \alpha t_n$

In the case that $\alpha = 0$, the HHT-α method is reduced to the Newmark's method. If the parameters are chosen in the way that $\alpha \in \left[-\frac{1}{3}, 0\right]$, $\gamma = \frac{1-2\alpha}{2}$, $\beta = \frac{(1-\alpha)^2}{4}$ the HHT-α method is a two-order method, unconditionally stable and high frecuency dissipation is obtained.

Figure 16.1 shows the spectral radius of some methods, such as: Newmark'a method, HHT-α method, Houbolt's method [4], Collocation [4] (among them the Wilson method which is a concrete case of the Collocation method) and Park's method.

16.3 BDF methods

The Backward Differentiation Formulae (BDF) where proposed in [1]. They are linear mustistep methods useful to solve ODE-s of order 1, such us $y' = f(t, y)$, and the expression of the BDF of order k is this one:

$$\sum_{j=1}^{k} \frac{1}{j} \nabla^j y_{n+k} = h f_{n+k} \tag{16.7}$$

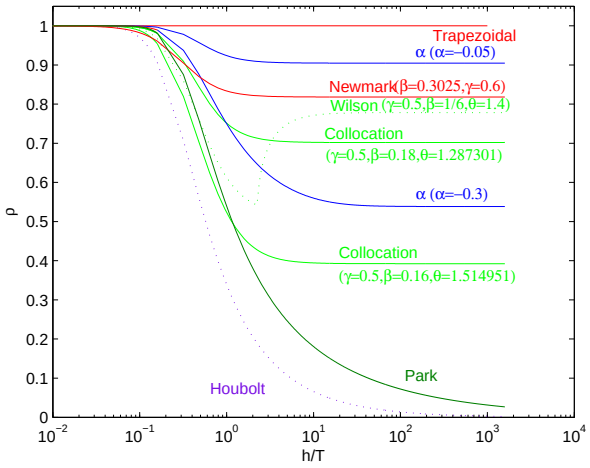

Figure 16.1: Spectral radius of some methods.

The BDF-s are unconditionally stable for orders 1 and 2. The stability properties of the BDF-s and their error constants can be seen in Table 16.1. Their stability regions and spectral radius are shown in Figures 16.2 and 16.3 respectively. It can be seen that the spectral radius of the BDF-s tends to 0 when $h/T \to +\infty$.

orden	1	2	3	4	5	6
α	90^o	90^o	86.03^o	73.35^o	51.84^o	17.84^o
C	-1/2	-1/3	-1/4	-1/5	-1/6	-1/7

Table 16.1: A(α)-stability and error constants of the BDF.

16.4 BDF-α

We have constructed a similar modification made to the Newmark's method in [3] called HHT-α method, but this time using the BDF-s as basis. The HHT-α method proposed by Hilber-Hughes-Taylor makes possible the dissipation of the high frequencies. In our case, we have seen before that the spectral radius of the BDF-s tends to 0 when $h/T \to +\infty$, so we have already maximum dissipation in high frequencies. We have constructed a method based in the BDF2 by ponderating the values of y, y', which offers many different rates of dissipation for high frequencies. The BDF2 is a two-order and A-stable method given by the next expression:

$$\frac{3}{2}y_{n+2} - 2y_{n+1} + \frac{1}{2}y_n = hf_{n+2} \tag{16.8}$$

The modification that we have done is expressed as:

$$\left(\frac{3}{2}+\alpha\right)y_{n+2} + (-2-2\alpha)\,y_{n+1} + \left(\frac{1}{2}+\alpha\right)y_n = h(1+\alpha)f_{n+2} - \alpha f_{n+1} \tag{16.9}$$

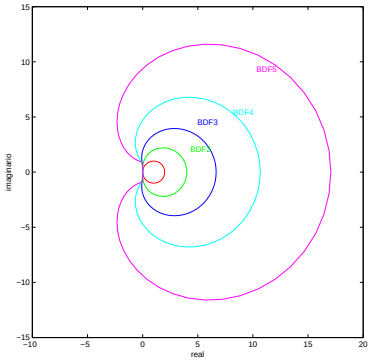

Figure 16.2: Stability regions of the BDF-s (exterior of the curves).

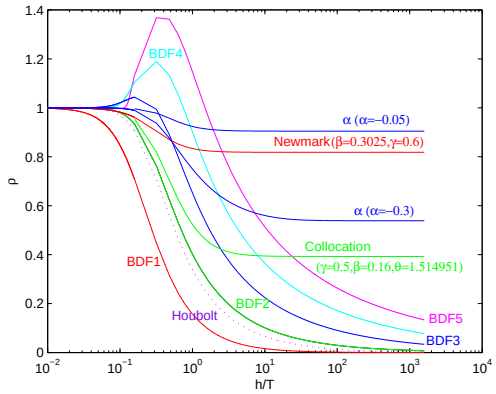

Figure 16.3: Spectral radius of the BDF-s.

Notice that if $\alpha = 0$ we obtain the BDF2 method and when $\alpha = -0.5$ we obtain the trapezoidal method. The error constant of the BDF-α method is this one:

$$C = \frac{-2 - 3\alpha}{6} \tag{16.10}$$

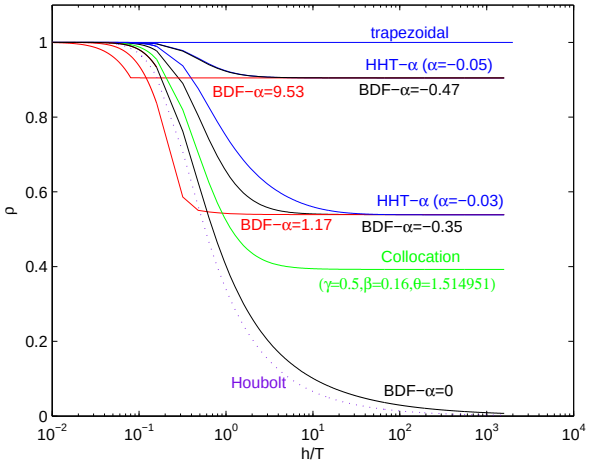

Figure 16.4: Spectral radius of BDF-α.

The BDF-α is a method of order two, A-stable for $\alpha \in [-0.5, +\infty)$ and it has a smaller error constant than the BDF2 for $\alpha \in [-0.5, 0)$. The parameter α of the BDF-α method makes also possible to take different values of the spectral radius as it can be seen in Figure 16.4.

Bibliography

[1] C.W. Gear, *Numerical initial value problems in Ordinary Differential Equations*, Prentice Hall, New Jersey, 1971.

[2] E. Hairer, G. Wanner, *Solving ordinary differential equations, I, Nonstiff problems*, Springer, 1993.

[3] H. M. Hilber, T. J. R. Hughes, R. L. Taylor, *Improved numerical dissipation for time integration algorithms in structural dynamics*, Earthquake engineering and structural dynamics, 5:283-292, 1977.

[4] Thomas J. R. Hughes, *The finite element method. Linear Static and dynamic finite element analysis*, Prentice-Hall International Editions, 1987.

[5] N. M. Newmark, *A method of computation for structural dynamics*, Journal of the Engineering mechanics division, ASCE, 85:67-94, 1959.

[6] R.L Taylor, J.Z. Zhu, O.C. Zienkiewicz, *The finite element method. Its basis & fundamentals*, Elsevier Butterworth-Heinemann, Oxford, 2005.

Contact melting of a three-dimensional phase change material on a flat substrate

Michelle M. De Decker and Tim G. Myers

Centre de Recerca Matemàtica, Campus de Bellaterra, Edifici C, 08193 Bellaterra (Barcelona), Spain
tmyers@crm.cat

Abstract

In this paper [1] a model is developed to describe the three dimensional contact melting process of a cuboid on a heated surface. The mathematical description involves two heat equations (one in the solid and one in the melt), the Navier-Stokes equations for the flow in the melt, a Stefan condition at the phase change interface and a force balance between the weight of the solid and the countering pressure in the melt. In the solid an optimised heat balance integral method is used to approximate the temperature. In the liquid the small aspect ratio allows the Navier-Stokes and heat equations to be simplified considerably so that the liquid pressure may be determined using an eigenfunction expansion and finally the problem is reduced to solving three first order ordinary differential equations. Results are presented showing the evolution of the melting process. Further reductions to the system are made to provide simple guidelines concerning the process. Comparison of the solutions with experimental data on the melting of n-octadecane shows excellent agreement.

17.1 Introduction

Contact melting is the process whereby a phase change material (PCM) is placed on a surface that is maintained above the phase change temperature. The heat from the surface causes the PCM to melt and it then rests on its own melt layer. The process may be easily observed by placing a piece of ice on a warm surface: after a short time the ice will sit on a thin layer of water. This layer is subject to the weight of the solid which induces a flow. The fluid layer remains thin since fluid is constantly being forced out from under the solid. Consequently the solid is always close to the substrate and so the melting process is relatively rapid. Industrially the process is exploited in thermal storage systems where energy is stored in the form of latent heat which is released upon melting.

Typically the thickness of the melted material is proportional to time. This may be contrasted to the standard one-dimensional Stefan problem, where weight is neglected, and the thickness is proportional to $\sqrt{t}$. For this reason contact melting, rather than melting a fixed solid, is exploited in thermal storage systems.

To describe the contact-melting process mathematically an account of the heat flow in the solid and liquid layers and the fluid flow is required.

The experimental work of Moallemi *et al.* involved a three-dimensional solid block on n-octadecane, insulated at the sides and top, so we will also compare our model with their data.

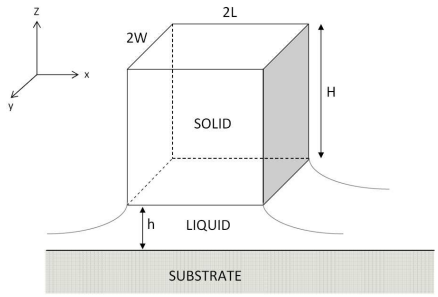

Figure 17.1: Problem configuration: Cuboid PCM floating on a liquid layer

17.2 Mathematical model

In order to solve the fluid flow equations we exploit the thinness of the layer and so impose the lubrication approximation:

$$\eta\frac{\partial^2 u}{\partial z^2}=\frac{\partial p}{\partial x}, \qquad \eta\frac{\partial^2 v}{\partial z^2}=\frac{\partial p}{\partial y}, \qquad \frac{\partial p}{\partial z}=0, \tag{17.1}$$

where η is the viscosity, the velocity vector is given by $\vec{u}_l=(u,v,w)$ for the x,y,z directions respectively and p is the pressure. The largest term that has been neglected is $\mathcal{O}(\epsilon^2 Re)$. Boundary conditions stipulate incompressible flow, no slip at the substrate, no slip in the x and y direction at the top of the liquid layer and the pressure is ambient at the edge of the block. The final condition required to solve the flow equations is derived from a momentum balance at $z=h$

$$w|_{z=h}=\frac{\partial h}{\partial t}-\frac{\rho_s}{\rho_l}\frac{\partial h_m}{\partial t}. \tag{17.2}$$

To relate the pressure to the height of the liquid layer, h, a force balance is introduced

$$\underbrace{4\rho_s LW[H_0-h_m(t)]}_{\text{mass of solid}}\,g=\int_{-L}^{L}\int_{-W}^{W} p\,dy\,dx\,. \tag{17.3}$$

The thermal problem in the solid and liquid is approximated by the following equations

$$T_{zz}=0, \qquad \theta_t=\alpha_s\theta_{zz}\,, \tag{17.4}$$

where the largest neglected term is $\mathcal{O}(\epsilon^2 Pe)$. A Stefan condition relates the height of the melted solid, h_m, to the heat flux across the boundary $z=h$,

$$\rho_s L_m\frac{dh_m}{dt}=k_s\left.\frac{\partial\theta}{\partial z}\right|_{z=h}-k_l\left.\frac{\partial T}{\partial z}\right|_{z=h}. \tag{17.5}$$

The melting process into 3 stages. The boundary conditions depend on which stage you are in. The first stage is the pre-melt stage, which occurs from the time the cuboid comes into contact with the heated surface until the bottom of the block reaches the melting temperature, T_m, and melting begins. This

first stage occurs for $t \in [0, t_1]$ where t_1 is determined by setting the temperature at $z = 0$ to T_m. Only BC for solid are needed during stage 1: A cooling condition is prescribed at $z = 0$,

$$\left.\frac{\partial\theta}{\partial z}\right|_{z=0} = \frac{-q + h_{ss}(\theta|_{z=0} - T_0)}{k_s}, \tag{17.6}$$

where T_0 is the substrate temperature and h_{ss} is the heat transfer coefficient between the substrate and the solid. The block is insulated at the top, $z = h + H$,

$$\left.\frac{\partial\theta}{\partial z}\right|_{z=h+H} = 0. \tag{17.7}$$

The second stage is that in which the liquid layer is first formed and the block begins to float upon it. This stage occurs for $t \in [t_1, t_2]$ and ends when the temperature at the top of the solid rises (noticeably) above the initial temperature, denoted θ_0. So t_2 is the time at which the temperature at the top of the block first exceeds θ_0 (according to the mathematical model). BC for both liq and solid are needed for stage 2: The cooling condition is now at $z = 0$ and we have temperature continuity at $z = h$,

$$\left.\frac{\partial T}{\partial z}\right|_{z=0} = \frac{-q + h_{sl}(T|_{z=0} - T_0)}{k_l}, \qquad T = \theta = T_m\,. \tag{17.8}$$

On the top surface (17.7) still holds.

Finally, stage 3 begins at t_2 and ends once all the block is melted, i.e. $t \in [t_2, t_m]$. Note, the distinction between stages 2 and 3 is a requirement of the mathematical model and a different approach may not require this. Stage 3 has same BC as stage 2, but now the temperature in the solid is above the initial temperature everywhere and this affects the analytical solution.

17.3 Analysis

The liquid velocities in the x and y directions can be calculated from equation (17.1). Applying the boundary conditions we find

$$u = \frac{p_x}{2\eta} z(z - h), \qquad v = \frac{p_y}{2\eta} z(z - h). \tag{17.9}$$

Integrating the incompressibility condition across $z \in [0, h]$, and applying (17.9) and (17.2) we have an expression for pressure in the form of Poisson's equation,

$$\nabla^2 p = \frac{12\eta}{h^3}\left(\frac{\partial h}{\partial t} - \frac{\rho_s}{\rho_l}\frac{\partial h_m}{\partial t}\right). \tag{17.10}$$

We found a solution using an eigenfunction expansions:

$$p = \sum_{n=1}^{\infty} b_n(\frac{y + W}{2}, t)\sin(\omega_n \frac{x + L}{2}), \tag{17.11}$$

where b_n is too cumbersone to report here.

Substituting the expression for pressure into the force balance (17.3) we obtain, an equation involving the two unknown heights, h and h_m,

$$\frac{dh}{dt} = \frac{\rho_s g L W}{3\eta\Phi} h^3[H_0 - h_m] + \frac{\rho_s}{\rho_l}\frac{dh_m}{dt}. \tag{17.12}$$

To close the system this must be coupled to the Stefan condition (17.5). However, this involves the temperature gradients which are as yet unknown. Consequently we analyse the thermal problem.

The main difference between the current and the previous analysis lies in the use of the heat balance integral method (HBIM) to solve for the temperature in the solid. There are many variations of the HBIM, but here we exploit a recent where the approximating function is chosen to minimise the error when the approximate temperature is substituted into the heat equation.

17.4 Results

We present results related to the experimental study of Moallemi *et al* [2]. Their work involved melting a block of n-octadecane on a substrate. The sides and top of the block were well insulated so melting primarily occurred at the bottom.

Fig. 17.2 shows a comparison of the experimental data (circles) reported by Moallemi [2] with the current model (solid line). Clearly, the agreement between the current model and experiment is excellent. To obtain such a close fit we set $h_{sl} = 3275\text{W/m}^2$. Note, this is the only parameter we are free to choose. The third curve (dotted) shown on the figure is the quasi-steady solution of equation (derived in paper, but not reported here). The quasi-steady solution is accurate during the initial stages, consistent with the requirement that $h_m \ll H_0$, but as h_m increases it overpredicts the melting rate. The comparison with experimental data allowed us to accurately determine the heat transfer coefficient h_{sl}. Now examine the whole process in more detail.

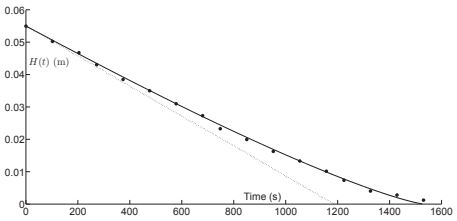

Figure 17.2: *The experimental data (circles) of $H(t)$ is compared to that of the 3D model with $h_{sl} = 3275W/m^2$ (solid line) and the quasi-steady solution (dotted line).*

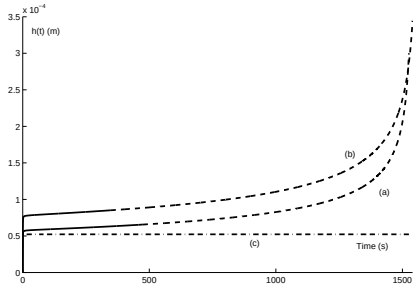

Figure 17.3: *Liquid height $h(t)$ for (a) 3D model with $h_{sl} = 3275\text{W/m}^2$, (b) 2D model with $h_{sl} = 7000\text{W/m}^2$, (c) quasi-steady solution. For curves (a), (b) stage 2 is the solid line, stage 3 is the dashed line.*

During the first stage, before melting occurs, the temperature may be well approximated by the Laplace transform solution, which provides a check on the accuracy of the HBIM solution. We found the HBIM and transform solutions matched well and the difference in predicting the melting time was less than 2%.

In Fig. 17.3 the height of the liquid layer is plotted for both stages 2 and 3. The different sets of lines represent (a) the 3D model with $h_{sl} = 3275\text{W/m}^2$, (b) the 2D model of Myers [4] with $h_{sl} = 7000\text{W/m}^2$, (c) the quasi-steady solution. Curves (a), (b) have two sections, stage 2 is the solid line, stage 3 is the dashed line. The liquid height for the 3D model is less than that for the 2D model, since the 3D model allows the liquid to escape in four directions. The quasi-steady solution has a constant height, h_q. The quasi-steady solution misses the final rise in $h(t)$ due to the neglect of h_m in the force balance. For curves (a) and (b), as $h_m \to H_0$ the weight of the solid tends to zero and so the solid is unable to squeeze out the water leading to a rapid increase in h. This increase in h also leads to a

greater insulating effect which then slows down the melting. This manifests itself in the solution of Fig. 17.2 through the slow upward curve of $H(t)$.

17.5 Conclusions

A model for a three-dimensional contact melting process has been presented. The work is an extension of the two-dimensional study of Myers (2008) [4] where the governing equations were reduced systematically, meaning that the terms neglected in the approximate solution are indeed negligible. As a result, our model reduced to solving three first order ordinary differential equations and the results showed excellent agreement when compared to experimental data. As expected the three-dimensional model requires a lower HTC than the two-dimensional model, although only by a factor of 2. This may be attributed to the fact that in the experiments a relatively large aspect ratio was used, $W/L = 6$. Reducing this value should increase the difference between two and three dimensional models.

Bibliography

[1] M.M. De Decker and T.G. Myers, Contact melting of a three-dimensional phase change material on a flat substrate. Submitted to Int. J. Heat Trans. 2011.

[2] M.K. Moallemi, B.W. Webb and R. Viskanta, An experimental and analytical study of close-contact melting. Int. J. Heat Trans. 1986; 108: 894 – 899.

[3] T.G. Myers, Optimizing the exponent in the Heat Balance and Refined Integral Methods. Int. Comm. Heat Mass Trans. 2009; 36(2): 143–147.

[4] T.G. Myers and S.L. Mitchell and G. Muchatibaya, Unsteady contact melting of a rectangular cross-section phase change material on a flat plate. Phys. Fluids. 2008; 20 103101: DOI:10.1063/1.2990751.

Microfluidic phase change valves

F. Font *, T.G. Myers and J. Low
Centre de Recerca Matemàtica, Campus de Bellaterra, Edifici C, 08193 Bellaterra, Barcelona, Spain
* ffont@crm.cat

Abstract

In this paper a mathematical model for the flow and solidification of a fluid in a narrow pipe is briefly presented. We show how the problem reduces to solving a single equation for the position of the solidification front. Then, we briefly highlight the extension to a model including curvature effects for narrow channels, where the phase change temperature decreases with the channel radius.

18.1 Introduction

Microfluidic valves are often miniature versions of their larger counterparts. However, due to obvious constraints, such as manufacturing difficulties on a small-scale or lack of space in the microfluidic device, there are also a number of valves that exploit technology not appropriate on a larger scale. One of these devices, namely the phase change valve, works by freezing the fluid within the channel, see the experimental studies in [2, 3, 4, 5]. To date theoretical studies of freezing flow in microchannels have been very limited and in order to make the analysis tractable involve highly restrictive assumptions (see [6], for example).

In the present work we analyse the flow in a circular cross-section pipe subject to a specified wall temperature. A model is developed for the combined flow and solidification which can then be used to determine the dominant forces driving the freezing and so provide guidelines for the design and operation of a phase change microvalve. In the second part of the work we refine the model to allow for variation of the phase change temperature due to the Gibbs–Thomson effect.

18.2 Mathematical Model

The configuration of the model is shown in figure 18.1. Fluid flows in the positive x–direction due to the action of a pressure gradient. The wall is cooled so that the fluid solidifies. The pipe is assumed to be sufficiently small such that gravity may be neglected.

In the liquid, the flow is governed by the Navier-Stokes equations (18.1a) and the heat equation (18.1b) which includes the advection term. In the solid, the heat equation with no advection holds in (18.1c). Finally, the interface between the solid and liquid layers is specified by a Stefan condition (18.1d).

$$\rho \frac{d\boldsymbol{u}}{dt} = -\nabla p + \mu \nabla^2 \boldsymbol{u} \tag{18.1a}$$

$$\frac{\partial T}{\partial t} + \boldsymbol{u} \cdot \nabla T = \alpha^l \nabla^2 T \qquad 0 < r < h(x,t) \tag{18.1b}$$

$$\frac{\partial \theta}{\partial t} = \alpha^s \nabla^2 \theta \qquad h(x,t) < r < 1 \tag{18.1c}$$

$$\rho_s L_f \frac{dh}{dt} = k^s \frac{\partial \theta}{\partial r}\bigg|_{r=h} - k^l \frac{\partial T}{\partial r}\bigg|_{r=h} \tag{18.1d}$$

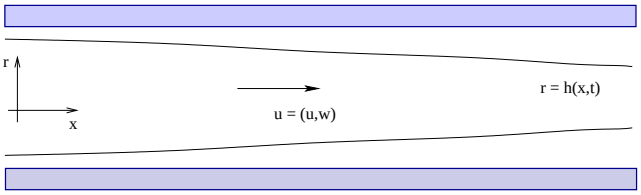

Figure 18.1: Problem configuration.

In these equations, $\boldsymbol{u}$ is the fluid velocity vector, T, θ are the temperatures in the liquid and solid layers (respectively) and subscripts s, l denote solid and liquid. The constants ρ, μ, c, L_f and k represent density, viscosity, heat capacity, latent heat and thermal conductivity, and $\alpha = k/(\rho c)$ is the thermal diffusivity.

In order to simplify the problem we non–dimensionalise equations (18.1a), (18.1b), (18.1c) and (18.1d). Note that the geometry is long and thin so standard lubrification scalings hold. Then, neglecting smaller terms the N-S equations (18.1a) become

$$\frac{1}{r}\frac{\partial}{\partial r}\left(r\frac{\partial u}{\partial r}\right) = \frac{\partial p}{\partial x} \qquad \frac{\partial p}{\partial r} = 0 \qquad \frac{\partial u}{\partial x} + \frac{\partial}{\partial r}(rw) = 0 \tag{18.2}$$

and heat equations (18.1b) and (18.1c) are now

$$\frac{1}{r}\frac{\partial}{\partial r}\left(r\frac{\partial \theta}{\partial r}\right) = 0 \qquad Pe\left(u\frac{\partial T}{\partial x} + w\frac{\partial T}{\partial r}\right) = \frac{1}{r}\frac{\partial}{\partial r}\left(r\frac{\partial T}{\partial r}\right) \tag{18.3}$$

where the time derivatives have been removed by assuming a large Stefan number (i.e. assuming a sensible temperature difference between the wall and the melting temperature) and Pe stands for the Péclet number. Finally, the Stefan condition changes to

$$h\frac{\partial h}{\partial t} = \left(\frac{\partial \theta}{\partial r} - k\frac{\partial T}{\partial r}\right)\Bigg|_{r=h(x,t)} \tag{18.4}$$

where k is a parameter assumed to be O(1). In addition, an important quantity for our analysis is the fluid flux

$$Q = 2\pi \int_0^h ru\, dr. \tag{18.5}$$

Equations (18.6) together with the flux expression lead to

$$u = \frac{p_x}{4}(r^2 - h^2) \qquad w = -\frac{1}{r}\frac{\partial}{\partial x}\left[\frac{p_x}{16}r^2\left(r^2 - 2h^2\right)\right] \qquad Q = -\frac{\pi}{8}h^4 p_x. \tag{18.6}$$

Now, fixing the position of the solidification front by setting $\hat{r} = r/h(x,t)$ and assuming $T = X(x)R(r)$ we are able to write the second equation in (18.3) as a separable problem

$$\frac{X'}{\gamma X} = \frac{1}{\hat{r}(1-\hat{r}^2)}\frac{\partial}{\partial \hat{r}}\left(\hat{r}\frac{\partial R}{\partial \hat{r}}\right) = -\lambda^2 \tag{18.7}$$

where $\gamma(t) = \pi/\left[2PeQ(t)\right]$[1]. The Sturm-Liouville problem for $R(r)$ defined by (18.7) has eigenfunctions

$$R_n = \frac{W_m(\lambda_n/4, 0, \lambda_n \hat{r}^2)}{\hat{r}} \tag{18.8}$$

[1]Note that after some considerations detailed in [1] we are able to assume $Q \approx Q(t)$.

where W_m is the Whittaker M function, see [7]. Hence, the temperature in the liquid will be given by

$$T = \sum_{n=1}^{\infty} A_n e^{-\lambda_n^2 \gamma(t) x} R_n(\hat{r}) \tag{18.9}$$

where the coefficients A_n are determined by the boundary conditions. The temperature in the solid is defined integrating first equation in (18.3), subject to appropiate boundary conditions

$$\theta = \frac{\ln \hat{r}}{\ln h}. \tag{18.10}$$

Finally, by means of (18.4) we are able to write the governing equation for the interface position

$$h \frac{\partial h}{\partial t} = \frac{1}{\ln h} - k \sum_{n=1}^{\infty} A_n e^{-\lambda_n^2 \gamma(t) x} \frac{dR_n}{dr}\bigg|_{\hat{r}=1}. \tag{18.11}$$

The above equation is easly solved numerically (the summation is truncated at $n = 9$, which provides sufficiently accuracy, see [1]).

18.2.1 Model including the Gibbs-Thomson effect

The lowering of the freezing point at a curved interface is known as the Gibbs–Thomson effect. This phenomena has been the object of numerous studies, both theoretical and experimental, ([8],[9]). Due to recent interest in modelling at the nanoscale it is becoming increasingly important given the role it plays concerning heat transfer at the nanoscale. The classical Gibbs–Thomson expression, [10], that relates the freezing point with the curvature of the physical system is

$$T_f = T_f^* - \Gamma \kappa \tag{18.12}$$

with capillary constant $\Gamma = \sigma T_f^* / \rho L_f$, where σ and T_f^* are the surface energy and the bulk freezing temperature, respectively. The curvature κ for spheres and cylinders is the inverse of the radius, so in our case $\kappa = 1/h(x,t)$. Therefore, the b.c. for the temperature in the solid–liquid interface is going to change according to

$$T(x,h,t) = T_f^* - \frac{\Gamma}{h}. \tag{18.13}$$

In the previous section the scaling used for T was $\hat{T} = (T - T_f^*)/\Delta T$ which defines $\hat{T} = 0$ at the boundary $h(x,t)$. By applying the same scaling in (18.13) we obtain $\hat{T}(x,h,t) = -\frac{\Gamma}{\Delta T h}$. Then, to avoid the inverse of the moving front $h(x,t)$ in the b.c. we propose the change of variable $\hat{T} = \tilde{T}/h$. This allows us to rewrite (18.13) as

$$\tilde{T}(x,h,t) = -\eta \tag{18.14}$$

where the constant $\eta = \Gamma / \Delta T$. The inclusion of the Gibbs–Thomson effect and the change of variable slightly modify the temperature profile in both phases

$$\begin{aligned} \hat{T} &= \sum_{n=1}^{\infty} A_n e^{-\lambda_n^2 \gamma(t) x} R_n(\hat{r}) \\ \theta &= \left(1 - \frac{\eta}{h}\right) \frac{\ln \hat{r}}{\ln h} - \frac{\eta}{h} \end{aligned} \tag{18.15}$$

and consequently the governing equation for the interface position becomes

$$h\frac{\partial h}{\partial t} = \left(1 - \frac{\eta}{h}\right)\frac{1}{\ln h} - k\sum_{n=1}^{\infty} A_n e^{-\lambda_n^2 \gamma(t) x}\frac{dR_n}{dr}\bigg|_{\hat{r}=1}. \tag{18.16}$$

Fig. 18.2 shows a typical evolution of the freezing front $h(x,t)$, obtained through the numerical solution of (18.11) and (18.16) (i.e. with and without the G–T effect). As the channel narrows, and so h decreases, the increasing importance of G–T becomes clear.

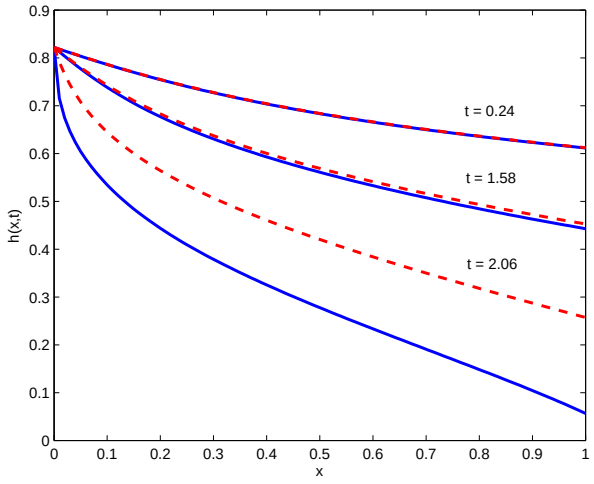

Figure 18.2: Evolution of $h(x,t)$ for a typical solidification example. Blue solid line: numerical solution of (18.11). Red dashed line: Numerical solution of (18.16).

18.3 Conclusions

In this paper we have briefly sumarized the mathematical model for solidification in a cylindrical pipe subject to a fixed temperature boundary condition developed in [1]. In addition, we have established the governing equation for the freezing front when the channel becomes sufficiently narrow to experience the Gibbs–Thomson effect. Finally, we have been able to solve numerically the governing equation for $h(x,t)$ in both cases, which clearly shows the importance of the G–T effect when dealing with nanochannels.

Bibliography

[1] Myers T.G., Low J., *An approximate mathematical model for solidification of a flowing liquid in a microchannel*, Microfluidics and Nanofluidics., (2010), DOI: 10.1007/s10404–011–0807–4.

[2] Bevan C.D., Mutton I.M., *Freeze–thaw flow management: a novel concept for high performance liquid chromatography capillary electrophoresis, electrochromatography and associated techniques*, J. Chromatogr. A 697, (1995), 541–548.

[3] Bevan C.D., Mutton I.M., *Use of freeze-thaw flow controlling and switching tubes*, Anal. Chem. 67, (1995), 1470–1473.

[4] Chen Z., Wang J., Qian S., Bau H.H., *Thermally-actuated, phase change flow control for microfluidic systems*, Lab. Chip. 5, (2005), 1277–1285.

[5] He Y., Zhang Y.H., Yeung E.S., *Capillary-based fully integrated and automated system for nanoliter polymerase chain reaction analysis directly from cheek cells*, J. Chromatogr. A 924, (2001), 271–284.

[6] Gui L., Liu J., *Ice valve for mini/micro flow channel*, J. Micromech. Microeng. 14, (2004), 242–246.

[7] Abramowitz M., Stegun I.A., *Handbook of mathematical functions with formulas, graphs, and mathematical tables*, 9th Edition, Dover Inc., New York 1972.

[8] Wu B., Tillman P., McCue S.W., Hill J.M., *Nanoparticle melting as a Stefan moving boundary problem*, J. Nanosc. Nanotech. 9 (2), (2009), 885–888.

[9] Buffat P., Borel J–P., *Size effect on the melting temperature of gold particles*, Physical Rev. A 13 (6), (1976), 2287–2298.

[10] Alexiades V., Solomon A.D., *Mathematical Modelling of Freezing and Melting processes*, 1st Edition, Hemisphere Publishing Corporation, Washington DC 1993.

Least Squares methods for attitude determination from GPS data

Alejandro P. Nicolás

Departamento de Matemática Aplicada. Universidad de Valladolid, Spain

Michael González-Harbour, Laureano González-Vega[1]

Departamento de Matemáticas, Estadística y Computación. Universidad de Cantabria. Spain

Raúl Arnau Prieto, Daniel Bolado Guerra, María Campo-Cossio Gutiérrez, Alberto Puras Trueba

Fundación Centro Tecnológico de Componentes. Santander, Spain

Abstract

The aim of this work is to study the behaviour of instantaneous methods for attitude determination using data from non-dedicated GPS receivers. These methods use L1 carrier phase-double differences obtained from real GPS signals and provide an instantaneous estimation of the attitude. However, they are very sensitive to experimental errors as can be seen in the presented experimental results.

19.1 Introduction

The problem of using GPS signals for attitude determination has been discussed by many authors. There are two approaches for dealing with it: those performing instantaneous estimation of the attitude see [6, 4] and those which exploit the redundancy present in measurements (see LAMBDA method in [5]). The first one are faster but they can present lack of accuracy, specially if we are working with real data measured near the Earth. On the other hand, the second one are more accurate but computationally more expensive.

If we start with the phase data from the GPS receivers, the substantial problem is an integer ambiguity in the receiver carrier phase measurement. A GPS receiver can only measure a fraction of carrier phase cycle ($-\pi$ to π in radians or $-\lambda/2$ to $\lambda/2$ in range), so the number of cycles is unknown. Notice that both approaches work with double phase differences for removing the offset error in measurements.

The principal difference between instantaneous and LAMBDA methods lies on data processing. While for the first one a unique measurement is used at each step (epoch), for the second one several epochs are processed at the same time. Moreover, the instantaneous methods make use of the available information, such as the length of the baselines, for reducing the ambiguity search (three-dimensional search is reduced to a two-dimensional one), whereas LAMBDA approach performs integer least squares for solving ambiguities. We will use this last method only for validation purposes.

[1]Partially supported by the spanish MICINN grant MTM2008-04699-C03-03 (Algorithms in Algebraic Geometry for Curves and Surfaces)

19.2 Mathematical approach

As it is referred in the previous section, the instantaneous method used for ambiguity resolution is based on the ideas exposed in [6] and [4]. We use information about base lines for reducing the ambiguity search space. Thus, the method performs only a two dimensional search of the ambiguities instead of a three-dimensional one.

Let $\{s_i : i = 1, \ldots, 4\}$ be the set of unit vectors from master antenna to GPS satellites. Let us suppose that the set $\{s_1 - s_2, s_2 - s_3, s_3 - s_4\}$ is linearly independent, and so, a base of $\mathbb{R}^3$. Using the Gram Smidt orthogonalization method we can construct a new set $\{v_k : k = 1, \ldots, 3\}$ of orthogonal vectors. For $j = 1, \ldots, 3$, the base line b_j can be written as a linear combination of these orthogonal vectors as $b_j = \sum_{k=1}^{3} \mu_{jk} v_k$. Notice that base lines are known from the experimental device. On the other hand, the projections $r_{ij} = s_i \cdot b_j$ are experimentally known from carrier phase measurements. In fact, if n_{ij} is the integer ambiguity, we have that $r_{ij} = \overline{r}_{ij} + n_{ij}$ for $i = 1, \ldots, 4$ and $j = 1, \ldots, 3$. The value $\overline{r}_{ij}$ is a module measurement of a single (normalize) phase difference and satisfies $-1/2 < \overline{r}_{ij} < 1/2$.

For each base line j, the coefficients μ_{jk} can be calculated from the experimental double differences $\Delta\,\overline{r}_{kj} = \overline{r}_{kj} - \overline{r}_{k+1\,j}$ making an exhaustive two dimensional search over all possible values of $\Delta\, n_{kj}$ for $k = 1, 2$. Since the length of the base lines, l_j, is known, we can predict the integer $\Delta\, n_{3j}$ and so, reduce the ambiguity search space. For each $j = 1, \ldots, 3$ and each $\Delta\, n = (\Delta\, n_{1j}, \Delta\, n_{2j}, \Delta\, n_{3j})$, the goodness of fit against the base line b_j is estimated with

$$\varepsilon_j^{\Delta n} = a_{11}\,\hat{\mu}_{j1}^2 + a_{22}\,\hat{\mu}_{j2}^2 + a_{33}\,\hat{\mu}_{j3}^2 - l_j^2,$$

where $\hat{\mu}_{jk}$, $k = 1, \ldots, 3$, are the estimated μ_{jk} and $a_{kk} = v_k \cdot v_k$ for $k = 1, \ldots, 3$.

Suppose that we have a total of N choices for each base line. Then, by this process, we will obtain three lists of N possible values ordered by decreasing ε. The next step consists on finding a combination of three estimated base lines, one for each list, which leads to the best fitting with respect to the real data.

Let us define the virtual base line difference $\Delta\, l_{ij}$ as $\Delta\, l_{ij} = l_i - l_j$. This value will be compared with the estimated virtual base line difference $\Delta\, \hat{b}_{ij}^{k_1 k_2} = \hat{b}_i^{k_1} - \hat{b}_j^{k_2}$, where $\hat{b}_i^{k_1}$ denotes the k_1 estimated i'th base line, that is, the k_1 position in the i'th list. This comparison is made for all possible base line differences $\Delta\, l_{ij}$, $1 \le i < j \le 3$ and all possible combinations $\Delta\, \hat{b}_{ij}^{k_1 k_2}$, $1 \le i < j \le 3$, $1 \le k_1, k_2 \le N$. Goodness of fit is measured by the parameter

$$\varepsilon_{tot} = \sum \| \hat{b}_i^k \|^2 + \sum \| \Delta\, \hat{b}_{ij}^{km} \|^2 - \sum \| l_i \|^2 - \sum \| \Delta\, l_{ij} \|^2.$$

This last process can be seen as the construction of most likely tetrahedron from the available data. Notice that we are working with norms, so this equation is valid either the vectors b, Δb, l and Δl are expressed in the same reference system or not.

LAMBDA method is described in [5]. We start from the linearized double phase differences $\lambda\, \Phi_{AB}^{ij}(t) = A(t)\, b + \Lambda\, N$, where λ is the wavelength, $\Lambda = \mathrm{diag}(\lambda, \ldots, \lambda)$, $A(t)$ is the design matrix, b is the vector of all base lines, which are all unknown, and N is a vector with all integer ambiguities, also unknown. Unrestricted least squares adjustment is performed to obtain the *float solution*. It consists on a estimation of ambiguities, $\hat{N}$, and base lines, $\hat{b}$. At this step, the estimated ambiguities $\hat{N}$ are real numbers. Also, we obtain the covariance matrix

$$Q_{\hat{N}} = \begin{bmatrix} Q_{\hat{b}} & Q_{\hat{b}\hat{N}} \\ Q_{\hat{N}\hat{b}} & Q_{\hat{N}} \end{bmatrix}.$$

Notice that since we only have phase data, we need to consider more than one epoch in order to consider a system with more equations than unknowns. In fact, for each epoch we can state $n_b\,(n_{sat}-1)$ equations with $n_b\,(n_{sat}+2)$ unknowns, where n_b is the number of base lines and n_{sat} the number of observed satellites.

Once the float solution is obtained, an integer least squares minimization is performed. That is, a solution of the problem

$$\min_{N\in\mathbb{Z}^n} \|\hat{N}-N\|^2_{Q^{-1}_{\hat{N}}}$$

is found. This minimization yields the integer least-squares estimate for the ambiguities: $\check{N}$. The final solution, with the ambiguities fixed to their integer estimates are $\check{b}=\hat{b}-Q_{\hat{b}\hat{N}}\,Q^{-1}_{\hat{N}}(\hat{N}-\check{N})$. For both instantaneous and LAMBDA method, attitude is calculated as the solution of Wahba's problem (see [3]) $L(C)=\frac{1}{2}\sum_i a_i\,|b_i-Cr_i|^2$, where b_i, $1\leq i\leq n_b$, are the base lines measured in the body frame system and r_i, $1\leq i\leq n_b$, are the corresponding unit vectors in a reference frame. The weights a_i are non-negative and are chosen to be inverse variances σ_i^{-1}. The matrix C is orthogonal and gives the attitude of the system. It is found using Davenport's Q-method (see [1, 2] for details).

19.3 Some experimental results

Now, we present some experimental results obtained from L1 carrier phase measurements. They were collected from a device consisting of four GPS receivers lying on the same plane. If the master antenna is labeled as 1, the coordinates of the other ones, referred to the body frame reference system with origin at 1, and their respective base lines lenghts (also measured from 1) are:

Antenna	Position	Base Line Length
2	$(0,-0.958,0)$	0.958 m
3	$(-0.958,0,0)$	0.958 m
4	$(-0.958,-0.958,0)$	1.355 m

The instantaneous method works with data coming from a single epoch. There are 11 possible wavelength integers for the shorter base lines and 8 for the longer one. The double phase differences give, respectively, a total of 21 and 29 integer elections. We only need to compute 1281 possible solutions, whereas 42911 trials should be computed if we perform a three-dimensional search of the ambiguities. For each epoch, we select the four satellites with maximum elevation. Since the exact attitude of the experimental device is unknown, an estimation has been performed using LAMBDA. We have used data received from 6 satellites, which have been processed in sets of 120 epochs each. That is, each attitude determination results from a measure of about 2 minutes. All calculations were made with MATLAB. LAMBDA implementation was provided by the Delft Geodetic Computing Centre. We have used data from two different captures. The first one consists on 2996 measurements while the second one consists on 6958. The following results for the attitude (roll, pitch and yaw angles) of the experimental device were obtained from LAMBDA method after removing outliers. They are displayed in Figure 19.1.

Capture	Attitude (degrees)	Standard Deviation
1	$(0.1241,-1.1986,-166.2053)$	$(0.1313,0.2296,0.0765)$
2	$(-0.0884,-0.2306,10.9227)$	$(0.2845,0.1506,0,0913)$

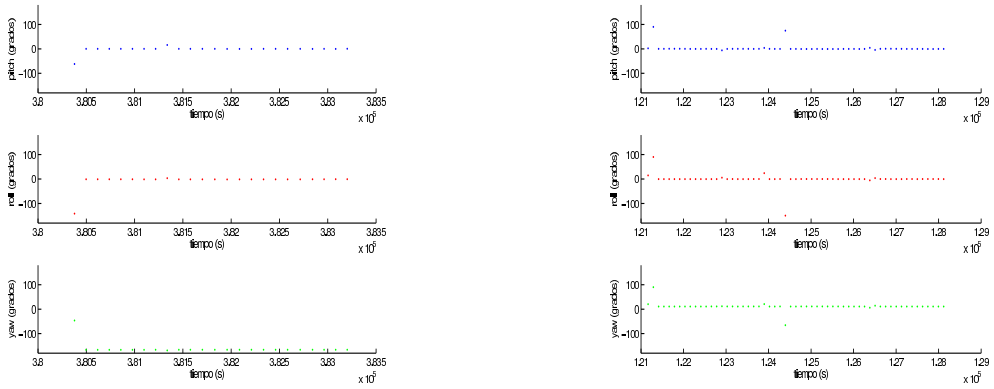

Capture 1 Capture 2

Figure 19.1: LAMBDA Method

On the other hand, Figure 19.2 displays the behaviour of the instantaneous method. There is an important lack of accuracy in the results, due to the reduction of the information used for calculating attitude. Data coming from only four satellites can be insufficient for attitude determination, as can be appreciated in these figures. Moreover, the goodness of fit provided by ε_{tot} used for choosing the correct ambiguities, gives sometimes wrong solutions. This bad behaviour was reported in [4]. However, this problem can be overcome if data are not very noisy.

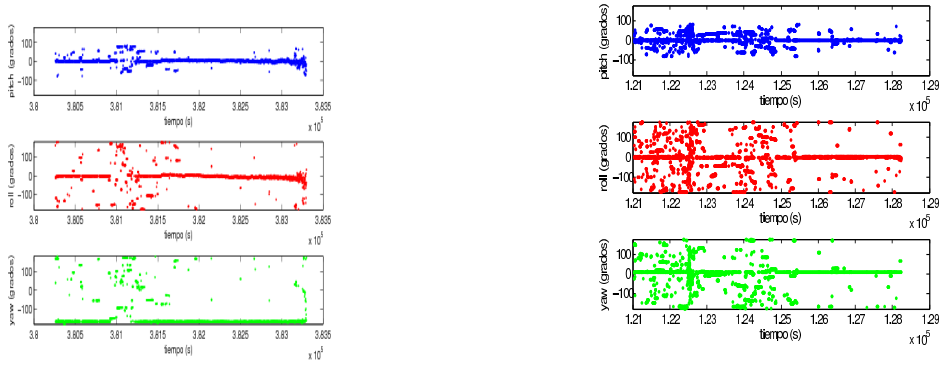

Capture 1 Capture 2

Figure 19.2: Instantaneous Method

If we are working with real data, we can also see that the method can provide wrong solutions for a long period of time. Since there is no validation of the solution given at each single epoch, it is very likely that these errors will be unnoticed.

Bibliography

[1] F. L. Markley, Fast Quaternion Attitude Estimation From Two Vector Measurements, Journal of Guidance, Control and Dynamics, 5(2), (2002), 411-414.

[2] F. L. Markley, Optimal Attitude Matrix for Two Vector Measurements, Journal of Guidance, Control and Dynamics, 31(3), (2008), 765-768.

[3] Grace Wahba, A Least Squares Estimate of Spacecraft Attitude, SIAM Review, 7(3), (1965), 409.

[4] M. S. Hodgart and S. Purivigraipong, New approach to resolving instantaneous integer ambiguity resolution for spacecraft attitude determination using GPS signals, In Position Location and Navigation Symposium, IEEE 2000, (2000), 132-139.

[5] P. De Jonge and CCJM Tiberius (1996). *The LAMBDA method for integer ambiguity estimation: implementation aspects*. LGR Series 12, Delft Geodetic Computing Centre, Delft University of Technology, The Netherlands 1996.

[6] S. Purivigraipong, M. S. Hodgart and M. J. Unwin, An approach to resolve integer ambiguity of GPS carrier phase difference for spacecraft attitude determination, In TENCON 2005. 2005 IEEE Region 10, (2005), 1-6.

Modelos matemáticos para la planificación de industrias culturales

Francisco A. Ortega Riejos, Miguel A. Pozo Montaño y Emma Torres Luque
Departamento de Matemática Aplicada I. E. T. S. de Arquitectura. Universidad de Sevilla
riejos@us.es, miguelpozo@us.es, emma.torres@juntadeandalucia.es

20.1 Introducción

A mediados del siglo XX, la Escuela Filosófica de Frankfurt acuñó el término Industria Cultural para explicar cómo la mercantilización poía regir el mecanismo de transmisión de la cultura ([6]). Actualmente, las manifestaciones culturales como el cine, el teatro, la ópera, los certámenes, congresos y el turismo cultural, se han consolidado en la sociedad actual como un dinamizador económico de gran interés. El sistema de flujos económicos que genera este sector cultural y las posibilidades de intervención pública han favorecido la aparición de un nuevo mercado de la cultura con nuevas posibilidades para agentes e instituciones, tanto en el sector público como en el privado ([5]).

Un espacio escénico es un edificio o lugar destinado a la representación de obras dramáticas y otros espectáculos de música o danza, que requiere el equipamiento propio del escenario teatral. En Andalucía existe un centenar de espacios escénicos de titularidad pública. La propagación de la cultura a través de éstos espacios escénicos requiere, además de un edificio físico, la existencia de una red de penetración que sea funcionalmente eficiente para los gestores de dichos recintos, económicamente sostenible por parte de la administración, socialmente rentable para los organismos públicos responsables y económicamente atractiva para los productores escenográficos ([9]). En [2] se enumeran 21 redes de ámbito internacional para la gestión coordinada de objetivos culturales.

Desde su creación en 1996, los Circuitos de Espacios Escénicos andaluces constituyen un instrumento para la democratización de la cultura, con el objetivo prioritario de que ésta llegue a todos los territorios de la región, tal y como establecen la Constitución española y el Estatuto de autonomía de Andalucía. Los actuales circuitos se articulan en torno a cuatro líneas temáticas: Música, Teatro y Danza, Abecedaria (contenidos formativos), y Cine. La adhesión de los municipios a dichos circuitos les garantiza una serie de prestaciones de asesoramiento y financiación compartida de gastos para la realización de eventos. En 2009 la actividad de los Espacios Escénicos presentó una gran dispersión en sus niveles de actividad, contraviniendo el objetivo político inicial de lograr una equidad en la oferta cultural extendida a todo el territorio. Al objeto de combatir la marginalidad cultural que actualmente se produce en determinados municipios y racionalizar la aportación de subvenciones, el Instituto Andaluz de las Artes y las Letras (IAAL) ha establecido en 2010 un sistema de créditos con los que cuantificar el caché de cada compañía teatral, de modo que cada municipio disponga de un mismo número de créditos (165) para ”gastar” en la contratación de las formaciones escénicas y de esta forma poder confeccionar una agenda cultural propia a lo largo del calendario anual. El sistema de créditos vigente incluye un descuento por repetición sucesiva de funciones en un mismo teatro. Así, el coste acumulativo en créditos derivado de la repetición de representaciones no es lineal, sino que va descendiendo conforme aumenta el grado de multiplicidad de la función. Otra variante que suele incorporar la Administración en su sistema de créditos es la obligatoriedad de los municipios a tener que elegir un mínimo número de espectáculos para cada una de las modalidades artísticas ofertadas, que en el caso de Andalucía son las cuatro anteriormente citadas de Música, Teatro y Danza, Abecedaria, y Cine.

La particular etnografía en torno a cada municipio, los objetivos de los gestores municipales, los intereses de los productores de las compañías itinerantes y los criterios globales de calidad defendidos por el organismo público responsable de la difusión cultural, suponen puntos de vista que pueden entrar en conflicto. La producción de la compañía tiende a lograr el máximo beneficio económico, eligiendo como sedes para su actuación aquellos espacios escénicos más prometedores en las fechas más convenientes. No obstante, la intervención de un organismo supramunicipal (como empresa pública de gestión de programas culturales de la Consejería de Cultura de la Junta de Andalucía) puede hacer que se modifiquen las preferencias de los productores de las compañías, al aplicar distintas tasas o exenciones fiscales dependiendo del municipio considerado y otras circunstancias (calendarios de actividades, rutas seguidas en las giras de las compañas, capacidades de los recintos, condicionantes arquitectónicos de las salas, etc.).

Excepción hecha de la configuración con criterios de optimalidad de calendarios deportivos en redes de estadios, no existen apenas referencias bibliográficas de modelos de optimización específicamente orientados a la planificación y gestión de una industria cultural, si bien continuamente se reclaman resultados en este campo que provengan del análisis y la investigación ([3]). Identificando (por lo que comparten como recintos singulares) el espacio escénico con un quirófano de hospital, podría establecerse un paralelismo entre la confección de la agenda cultural del municipio y la planificación eficiente de uso de un quirófano como "teatro de operaciones" ([4]). Abundando en la existencia de contextos similares, la programación de torneos deportivos de carácter regional-nacional ([8]) tiene como objetivo el diseño de rutas factibles para los equipos que compiten en estadios sujeto a un calendario y a una amplia gama de restricciones. La determinación de calendarios deportivos con criterios de optimalidad en los estadios guarda una clara analogía con la visión de la entidad pública responsable de favorecer que la actividad teatral alcance la máxima difusión posible sobre los espacios escénicos encomendados. En el presente trabajo se formulan un conjunto de modelos de optimización lineal para asesorar la toma de decisiones de dos agentes que concurren en este contexto: los gestores municipales y los productores de las compañías teatrales.

20.2 Modelos de decisión asociados

Perspectiva del Municipio

Dado un municipio $h \in H$, éste tendrá que administrar un presupuesto C (cuantificado en créditos) para emplear en la elaboración de su agenda cultural a partir de un conjunto de compañías ofertadas por el mercado. Asumamos un beneficio social (expresado en el número de usuarios interesados en asistir a la representación escénica), si la compañía k es elegida por el decisor municipal. La función objetivo debe maximizar el beneficio que se obtiene tanto por la selección de compañías realizada como por su número de actuaciones. Este objetivo es básicamente un Problema Mochila no acotado ([7]). Si consideramos las denominadas "ofertas de descuento" por la repetición de funciones, utilizaremos un nuevo índice $j \in J$ que indicará las veces que tiene lugar una representación en un mismo municipio. Asumamos una secuencia decreciente de costes $c_{kj} \geq 0$ para cada espectáculo en función de los j días que lleve de representación. Con una estructura similar, el beneficio social derivado de la j-ésima actuación de la compañía k se denota $b_{kj} \geq 0$. La variable binaria de decisión x_{kj} será igual a 1 si y solo si la compañía k es elegida por el municipio para realizar una j-ésima actuación. Por último, si se obliga al municipio a tener que elegir un mínimo de espectáculos entre varias modalidades (por ejemplo, las anteriormente mencionadas Abecedaria, Cine, Música, Teatro y Danza) entonces el modelo Mochila se transforma en el Problema de la Dieta ([10]) que consiste en determinar una dieta (agenda cultural del municipio) que satisfaga ciertos requerimientos nutricionales (número mínimo de representaciones por

cada modalidad n_q).

En el modelo que sigue, la función objetivo (1) maximiza el beneficio social del calendario de representaciones seleccionado para el municipio. La restricción (1.a) impide que los municipios sobrepasen en su elección el número de créditos establecidos. La restricción (1.b) establece que para que una compañía actúe por j-ésima vez en el municipio, haya tenido que actuar anteriormente en dicho municipio. La restricción (1.c) obliga al municipio a tener que elegir al menos n_q compañías de la modalidad q. La restricción (1.d) identifica el carácter entero de la variable que establece el número de actuaciones a realizar por la compañía k. La partición en las distintas modalidades escénicas del conjunto de compañías K se recoge en la restricción (1.e).

$$Max \sum_{k\in K}\sum_{j\in J} b_{kj}x_{kj} \tag{1}$$

sujeto a:

$$\sum_{k\in K}\sum_{j\in J} c_{kj}x_{kj} \leq C \tag{1.a}$$

$$x_{k(j-1)} \geq x_{kj} \qquad k \in K,\ j \in J,\ j \neq 1 \tag{1.b}$$

$$\sum_{k\in K_q}\sum_{j\in J} x_{kj} \geq n_q \qquad q \in Q \tag{1.c}$$

$$x_{kj} \in \{0,1\} \qquad k \in K \tag{1.d}$$

$$K = K_1 \cup K_2 \cup \cdots \cup K_{|Q|} \tag{1.e}$$

Perspectiva del Productor de la Compañía.

El punto de vista del productor de la compañía artística consiste en trazar un tour que maximice sus ingresos. En el caso más sencillo, no se considera la posible interacción con otras compañías, ni tampoco los costes de desplazamiento de manera directa. La decisión a adoptar será sencillamente elegir los municipios donde actuar y decidir el número de días de permanencia ininterrumpida. En este modelo usaremos una nueva variable real positiva y_j^{ht} para representar el beneficio obtenido por la compañía si decide actuar en el municipio h por j-ésima vez consecutiva a partir del día t. Esta opción del productor estará caracterizada por la asignación del valor 1 a la variable binaria correspondiente x_j^{ht}. Los máximos beneficios esperables por municipio y por municipio-día son respectivamente Y^h e Y^{ht}.

La función objetivo (2) del modelo que sigue maximiza el beneficio de la compañía obtenido en el tour óptimo. La restricción (2.a) impide que la compañía pueda actuar más de una vez en el mismo día (se podría ampliar la limitación a 2 conservando la validez del modelo). La restricción (2.a') es un requisito alternativo al anterior, ya que establece que una compañía no pueda actuar más de una vez en el mismo municipio el mismo día. La restricción (2.b) obliga a realizar un descanso por parte de la compañía de al menos un día entre actuaciones realizadas en distintos municipios. La restricción (2.c) establece que para que una compañía actúe por j-ésima vez en un municipio, haya tenido que hacerlo antes una (j-1)-ésima vez en dicho municipio. Las restricciones (2.d) y (2.e) marcan valores máximos para los beneficios que pueda lograr la compañía respectivamente, por actuaciones según municipio y día o por la totalidad de representaciones en un mismo municipio. Las restricciones (2.f) identifican el tipo de variables empleadas en el modelo.

$$Max \sum_{h\in H}\sum_{j\in J}\sum_{t\in T} y_j^{ht} \tag{2}$$

sujeto a:

$$\sum_{h\in H}\sum_{j\in J} x_j^{ht} \leq 1 \qquad t \in T \tag{2.a}$$

$$\sum_{j\in J} x_j^{ht} \leq 1 \qquad h \in H,\ t \in T \tag{2.a'}$$

$$\sum_{j\in J} x_j^{ht} + \sum_{h\in H\ (h\neq h')}\sum_{j\in J} x_j^{h'(t+1)} \leq 1 \qquad h \in H,\ t \in T \tag{2.b}$$

$$x_j^{ht} \leq \sum_{t\in T\ (t<t')} x_{(j-1)}^{ht'} \qquad h \in H,\ t \in T,\ j \in J(j \neq 1) \tag{2.c}$$

$$y_j^{ht} \leq x_j^{ht} Y_j^{ht} \qquad h \in H,\ t \in T,\ j \in J \tag{2.d}$$

$$\sum_{j\in J}\sum_{t\in T} y_j^{ht} \leq Y^h \qquad h \in H \tag{2.e}$$

$$x_j^{ht} \in \{0,1\},\ y_j^{ht} \in R^+ \qquad h \in H,\ t \in T,\ j \in J \tag{2.f}$$

20.3 Conclusiones

Los modelos de programación lineal entera permiten dotar de un soporte científico a la planificación de circuitos culturales sobre la base de una red de espacios escénicos ([11]). Las variables de diseño definidas en estos modelos tienen la capacidad de identificar las soluciones, con el apoyo de parámetros de tipo espacial, temporal y de preferencias por parte de los espectadores. La incorporación de otros parámetros no considerados en este artículo, como los gastos de desplazamiento entre diferentes nodos, gastos de personal para la compañía durante la representación y gastos de adecuación de los teatros (personal y material) y de publicidad para el gestor local del espacio escénico, puede favorecer la comprensión del punto de vista económico de las compañías y la detección de zonas cultural mal atendidas en el territorio ([1]), que deberán ser objeto de aplicación de políticas de intervención económica (actuando sobre los cánones) o de rehabilitación arquitectónica para ampliar la capacidad de los aforos.

Agradecimientos

Este artículo ha sido patrocinado con la subvención del Centro de Estudios y Experimentación de Obras Públicas (Ministerio de Fomento) asignada al proyecto PT-2007-003-08-CCPP. La información sobre las actuaciones llevadas a cabo por la Junta de Andalucía en relación al programa de Rehabilitación de Teatros Públicos y al Programa de Infraestructuras Escénicas de Andalucía, ha sido facilitada por la Dirección General de Innovación e Industrias Culturales de la Consejería de Cultura.

Bibliography

[1] Arriola, R., Ortega, F. A., Pozo, M. A., Torres, E. *Evaluación de la Accesibilidad Cultural a la red de Espacios Escénicos de Andalucía.* Actas de las III Jornadas sobre Modelos de Optimización Aplicados a la Planificacición Robusta y a la Gestión de los Servicios de Transporte en Caso de Emergencia (MORE 2010) (ISBN: 13:978-84-693-4034-9), 128-139, 2010.

[2] Casacuberta, D., and Mestres, A. *Redes Culturales: una introducción*. Boletín Gestión Cultural Nº 14: Redes culturales (ISSN:1697-073X), julio 2006. Portal Iberoamericano de Gestión Cultural (www.gestioncultural.org).

[3] Castells, R. *¿Es viable la gestión privada de la cultura?*. Boletín Gestión Cultural Nº 18: La Gestión Cultural desde el ámbito Empresarial Privado (ISSN:1697-073X), julio 2009. Portal Iberoamericano de Gestión Cultural (www.gestioncultural.org).

[4] Fei, H., Meskens, N. and Chu, C. A planning and scheduling problem for an operating theatre using an open scheduling strategy, Computers and Industrial Engineering 58 (2010), 221-230.

[5] Herrero, L.C. *La Economía de la Cultura en España: Una disciplina incipiente*. Revista Asturiana de Economía 23, Universidad de Valladolid, Valladolid (España) 2002.

[6] Horkheimer, M., and Adorno Th., *Dialéctica de la Razón. La Industria Cultural. Iluminismo como mistificación de las masas*. Editorial Sudamericana, Buenos Aires (Argentina) 1949.

[7] Poirriez, V., Yanev, N., and Andonov, R. A Hybrid Algorithm for the Unbounded Knapsack Problem. Discrete Optimization 6 (2009), 110-124.

[8] Russel, R. A., and Urban, T. L. A constraint programming approach to the multiple-venue sport-scheduling problem. Computers and Operations Research 33 (2006), 1895-1906.

[9] Sempere, A. M. *La Economía de la Cultura en España: Una disciplina incipiente*. Circuitos. Revista de Espacios Escénicos, 11, 2009.

[10] Stigler, G. J. The cost of subsistence. J. Farm Econ. 27 (1945), 303-314.

[11] Ortega, F. A., Pozo, M. A., and Torres, E. *Optimización en el Diseño de Rutas Culturales a través de los Espacios Escénicos Andaluces.* Actas del Seminario de Innovación e Investigación en la ETSAS. Escuela Técnica Superior de Arquitectura de Sevilla (ISBN: 978-84-937904-9-3), 185-195, 2010.

Minisymposium: Numerical simulation of processes in the metallurgical industry

Numerical simulation of an alloy solidification problem

A. Bermúdez[1], **M. C. Muñiz**[2] **and M. V. Otero**[3]

[1,2] Departamento de Matemática Aplicada, Universidade de Santiago de Compostela.
[3] Departamento de Métodos Matemáticos e de Representación, Universidade da Coruña.
e-mail: [1] alfredo.bermudez@usc.es, [2] mcarmen.muniz@udc.es, [3] vickyo@udc.es

Abstract

In this work two different models are considered in order to simulate temperature and solute concentration of an alloy during its solidification. Firstly, a general model consisting of two coupled enthalpy-type partial differential equations valid on the entire domain is numerically solved. Under certain assumptions, we obtain an entalphy equation for the temperature together with a Scheil-like equation for the solute concentration in a three-dimensional domain variable with time in order to simulate a continuous casting process for slab formation.

21.1 Introduction

In many industrial processes involving metal solidification, the solidifying material is usually an alloy, that is, a mixture consisting of a material (solvent) with a small concentration of impurity (solute). In order to obtain a final product with suitable characteristics, it is interesting to know the temperature and solute concentration of the material along the entire solidification process (see [6]).

In a solidification process there exists a free boundary separating both solid and liquid phases. The mathematical modeling of this free boundary problem takes into account the mass and the heat transfer at the different phases. The main differences between the solidification of an alloy and the classical two-phase Stefan problem arise in the behavior at the free boundary, where the latent heat of fusion is released —as in the Stefan problem— but there is a redistribution of impurities as well due to the rejection of solute from the solid to the liquid (see [4, 9]). Besides, the solidification temperature is not a constant but also depends on the solute concentration through the so-called *phase diagram*.

In this work we numerically solve two models in order to simulate this problem. In Section 21.2 a coupled model is considered, consisting in a system of two nonlinear partial differential equations for both temperature and solute concentration in a fixed domain. In Section 21.3 both unknowns are numerically calculated in a time-dependant three dimensional domain to simulate the formation of cilindrical slabs, taking into account some physical assumptions that simplify the resulting mathematical model.

21.2 A coupled model for temperature and solute concentration

We denote $\Omega \subset \mathbb{R}^N$, $N \leq 3$, the domain occupied by the alloy. We want to obtain the temperature and the solute concentration, $T(\mathbf{x}, t)$ and $C(\mathbf{x}, t)$, respectively, at each spatial point $\mathbf{x} \in \Omega$ and at each time $t \in [0, t_{\rm f}]$ which corresponds to the time interval of the process.

Following [3], we consider an entalphy formulation for the temperature in the entire domain Ω and an analogous formulation for a new unknown W defined from the solute concentration. The physical meaning of $W(\mathbf{x}, t)$ is the phase change temperature of point $\mathbf{x}$ according to the concentration of this point at time t. We obtain

$$\frac{\partial u}{\partial t} - \operatorname{div}\left(k(T, W)\,\nabla T\right) = 0 \ \text{ in } Q, \ \ u \in H_W(T), \tag{21.1}$$

$$\frac{\partial v}{\partial t} - \operatorname{div}\left(d(T, W)\,\nabla W\right) = 0 \ \text{ in } Q, \ \ v \in G_T(W), \tag{21.2}$$

where $Q = \Omega \times (0, t_{\mathrm{f}})$ and the parameters $k(T, W)$ and $d(T, W)$ being the thermal conductivity and a modified diffusion coefficient for the solute, respectively. The function H_W is the enthalpy density given by:

$$H_W(T) = \begin{cases} \Phi(T), & T < W, \\ \left[\Phi(W),\ \Phi(W) + \rho(W)\,L(W)\right], & T = W, \\ \Phi(T) + \rho(W)\,L(W), & T > W, \end{cases} \tag{21.3}$$

with

$$\Phi(v) = \int_0^v \rho(s)\,c(s)\,\mathrm{d}s. \tag{21.4}$$

The parameters ρ, c and L are the density, specific heat and latent heat of fusion of the material, respectively. Moreover, G_T is the multi-valued function defined by

1. if $T \le T_{\mathrm{sol}}^{\mathrm{p}}$,

$$G_T(W) = \begin{cases} -\sigma_l\,(W - T_{\mathrm{sol}}^{\mathrm{p}}), & W < T, \\ \left[-\sigma_l\,(W - T_{\mathrm{sol}}^{\mathrm{p}}),\ -\sigma_s\,(W - T_{\mathrm{sol}}^{\mathrm{p}})\right], & W = T, \\ -\sigma_s\,(W - T_{\mathrm{sol}}^{\mathrm{p}}), & W > T, \end{cases} \tag{21.5}$$

2. if $T > T_{\mathrm{sol}}^{\mathrm{p}}$,

$$G_T(W) = \begin{cases} -\sigma_l\,(W - T_{\mathrm{sol}}^{\mathrm{p}}), & W \le T_{\mathrm{sol}}^{\mathrm{p}}, \\ -\sigma_s\,(W - T_{\mathrm{sol}}^{\mathrm{p}}), & W > T_{\mathrm{sol}}^{\mathrm{p}}, \end{cases} \tag{21.6}$$

where $T_{\mathrm{sol}}^{\mathrm{p}}$ is the solidification temperature of the pure component and σ_l, σ_s are the slopes of the liquidus and the solidus lines in the phase diagram, respectively. Suitable boundary and initial conditions are considered to complete the model, see [7].

The weak formulation of the previous equations consists of two coupled nonlinear partial differential equations. In order to numerically solve this problem, a semi-implicit scheme is considered for the time discretization that allows to tackle the nonlinearities due to k and d. In [3, 7] an existence result for the time semidiscretized problem is given by obtaining two sequences that converge to the minimal and the maximal solution. Based on this proof, an iterative algorithm is considered, uncoupling the nonlinear equations for T and W. The remaining nonlinearities due to the functions H_W and G_T are treated by means of the duality algorithm introduced in [1]. Finally, a finite element method (FEM) is considered for space discretization. In [7] some numerical results are shown.

21.3 A three dimensional simplified model

In the metallurgical process of the ingot or slab formation, the three dimensional domain grows with time; indeed, during this process, the liquid alloy is continuously poured on the top of the forming slab being regularly cut downwards in order to obtain the desired slab size.

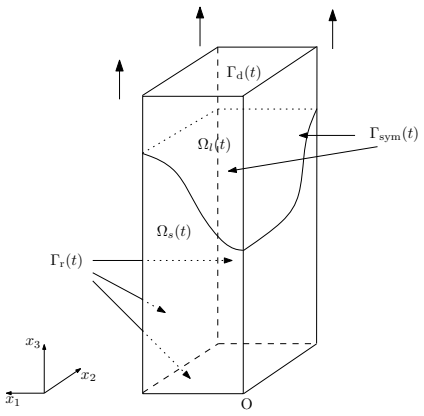

Figure 21.1: Three dimensional computational domain, $\Omega(t)$.

Taking into account the symmetry conditions of this problem, let $\Omega(t)$ be a quarter of the slab at time $t \in [0, t_{\rm f}]$ (see Figure 21.1). The main assumptions we consider to simplify the problem are the following:

A1. The solute transport in the solid can be neglected.

A2. The solute concentration in the liquid does not depend on the spatial variable as occurs in a *stirred tank*.

A3. The thermal conductivity, k, and the diffusion coefficient, d, only depend on temperature and concentration, respectively.

Under these assumptions the equations for the heat and mass transfer are uncoupled and the former is a simple ODE for the solute concentration.

Taking into account the previous assumptions and following [5], we obtain an enthalpy formulation for the temperature

$$\frac{\partial e}{\partial t} - \text{div}\,(k(T)\,\nabla T) = 0 \ \text{ in } \Omega(t),\ \forall\, t \in (0, t_{\rm f}), \tag{21.7}$$

$$e \in H(T) \ \text{ in } \Omega(t),\ \forall\, t \in (0, t_{\rm f}), \tag{21.8}$$

where $H(T)$ is the enthalpy per unit volume defined by (21.3) with $W = T_{\rm sol}$, the constant solidification temperature of the material.

We denote $\Gamma(t) = \Gamma_{\rm d}(t) \cup \Gamma_{\rm r}(t) \cup \Gamma_{\rm sym}(t)$ the boundary of the domain $\Omega(t)$, $\Gamma_{\rm d}(t)$ being the upper boundary of the slab, $\Gamma_{\rm sym}(t)$ the symmetry boundaries and $\Gamma_{\rm r}(t)$ the lower and remaining lateral boundaries of $\Omega(t)$, shown in Figure 21.1. The boundary and initial conditions are the following:

$$k(T)\,\frac{\partial T}{\partial \mathbf{n}} = \alpha(T_{\rm e} - T) \quad \text{on } \Gamma_{\rm r}(t),$$

$$k(T)\,\frac{\partial T}{\partial \mathbf{n}} = 0 \quad \text{on } \Gamma_{\rm sym}(t),$$

$$T(\mathbf{x}, t) = T_{\rm d}(\mathbf{x}, t) \quad \text{on } \Gamma_{\rm d}(t),$$

$$T(\mathbf{x}, 0) = T_0(\mathbf{x}) \quad \text{in } \Omega(0),$$

$\mathbf{n}$ being the unit outward normal vector to the boundary, $\alpha(\mathbf{x}, t)$ the convective heat transfer coefficient and $T_{\rm e}(\mathbf{x}, t)$ the temperature of the surrounding air. Besides, $T_{\rm d}$ and T_0 are known temperatures.

First we eliminate the nolinearity of the term $k(T)$ in (21.7) by means of the *Kirchhoff transformation* (see [8]). The resulting problem presents two nonlinearities: one due to the entalphy term and the other one introduced by the Kirchhoff transformation on $\Gamma_{\rm r}(t)$ boundary condition. In order to solve these nonlinearities, we apply the duality algorithm introduced in [1]. The problem is discretized in time using an implicit Euler scheme and in space by means of a FEM on a tetrahedral mesh of the domain. Taking into account that the domain $\Omega(t)$ grows with time, we obtain a tetrahedral mesh of the domain

$\overline{\Omega(t^{n+1})}$ adding to the previous mesh of $\overline{\Omega(t^n)}$ the tetrahedra corresponding to the amount of alloy poured during this time step (see [2]).

Regarding the solute concentration, under the assumptions A1, A2 and A3, we deduce the following Scheil-like equation for the liquid solute concentration:

$$\frac{d}{dt}\left(C_l(t)\, V_l(t)\right) = -K\, C_l(t)\, \frac{dV_s}{dt}(t) + C_{\text{in}}(t)\, q_{\text{in}}(t), \tag{21.9}$$

$V_l(t)$ and $V_s(t)$ being the liquid and solid volume, respectively, at time t, $q_{\text{in}}(t)$ the poured liquid flow rate and $C_{\text{in}}(t)$ its solute concentration. The distribution coefficient K is equal to the ratio between the solute concentration in the solid and in the liquid. We notice that $V_l(t)$ and $V_s(t)$ can be obtained from the thermal simulation prior to the solute concentration simulation. Finally, an initial condition $C_l(0)$ is considered.

21.4 Numerical results

In this section we numerically solve the thermal problem with phase change introduced in the previous section by using an Euler implicit scheme and a FEM for time and spatial discretization, respectively. In Figure 21.2 the distribution of temperature in a growing solid slab is shown where the upper surface corresponds to the solid-liquid interphase.

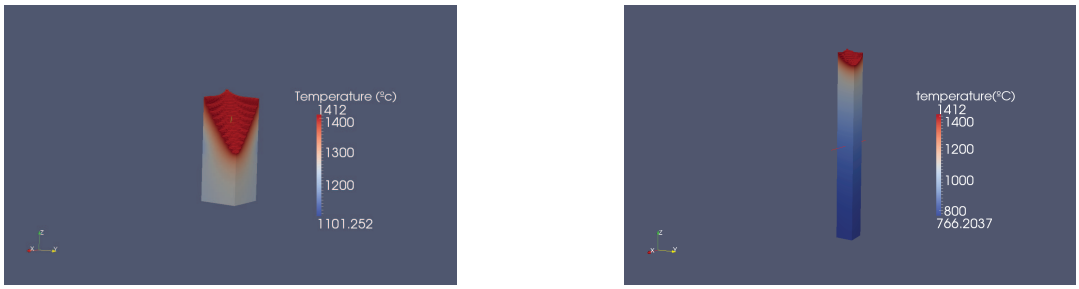

Figure 21.2: Distribution of temperature in growing solid slab at two different times.

Finally, knowing the evolution of the solid and liquid volumes and taking the input solute concentration as a constant, equation (21.9) is discretized by an Euler method in order to obtain P and B evolution of solute in the liquid, see Figure (21.3) and, using the distribution coefficient, in the solid as well.

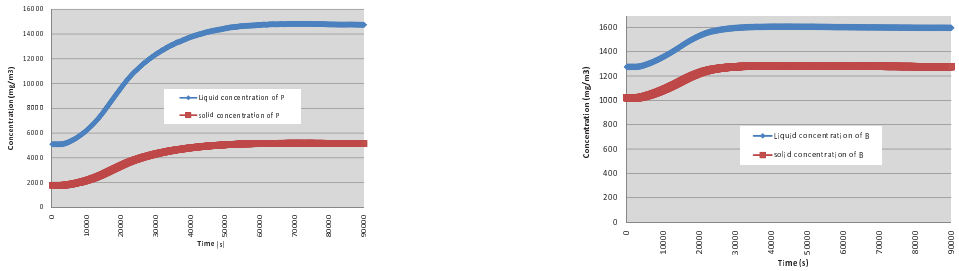

Figure 21.3: Evolution of solute concentration of P (left) and B (right).

Bibliography

[1] A. Bermúdez, C. Moreno, Duality methods for solving variational inequalities, Comput. Math. Appl. 7 (1), (1981), 43-58.

[2] A. Bermúdez, M. V. Otero, Numerical solution of a three-dimensional solidification problem in aluminium casting, Math. Models Methods Appl. Sci. 40, (2004), 1885-1906.

[3] A. Bermúdez, C. Saguez, Etude numérique d'un probleme de solidification d'un alliage, Rapports de Recherche 104, INRIA, Rocquencourt, France (1981).

[4] S. Chakraborty, P. Dutta, Three-dimensional double-diffusive convection and macrosegregation during non-equilibrium solidification of binary mixtures. International Journal of Heat and Mass Transfer 46, (2003), 2115-2134.

[5] C. M. Elliot, J. R. Ockendon, Weak and variational methods for moving boundary problems. Research notes in mathematics 59, Pitman, London (1982).

[6] I. L. Ferreira, V. R. Voller, B. Nestler, A. Garcia, Two-dimensional numerical model for the analysis of macrosegregation during solidification. Computational Materials Science 46, (2009), 358-366.

[7] M. V. Otero, *Estudio matemático y resolución numérica de modelos que surgen en el estudio de una colada de aluminio*. Ph.D. Thesis, Universidade de Santiago de Compostela 2004.

[8] M. N. Ozisik, *Boundary value problems of heat conduction*. Dover Publications Inc., New York 1968.

[9] D. Sanyal, P. Ramachandrarao, O. P. Gupta, A fast strategy for simulation of phase change phenomena at multiple length scales. Computational Materials Science 37, (2006), 166-177.

Minisymposium: Numerical simulation of processes in the metallurgical industry

Steel Heat Treating in Industry: modeling and numerical simulation

J. M. Díaz Moreno[†], C. García Vázquez[†], M. T. González Montesinos[‡] & F. Ortegón Gallego[†]

[†]Departamento de Matemáticas, Universidad de Cádiz, 11510 Puerto Real, Cádiz, Spain
josemanuel.diaz@uca.es, concepcion.garcia@uca.es,
francisco.ortegon@uca.es

[‡]Departamento de Matemática Aplicada I, Universidad de Sevilla, Avda. de Reina Mercedes, s/n,
41012 Sevilla, Spain
mategon@us.es

Abstract

The goal of steel heat treatment is to attain a satisfactory hardness over certain boundary layers on the workpiece and at the same time keeping its ductility properties all over the rest. To do so, the workpiece is heated up till austenization is reached, followed by an immediate cooling process, called aqua-quenching. This heating-cooling process produces changes in the microconstituents of steel which have different hardness properties. Though the physical phenomena involved in the industrial process of steel heat treating are well understood, the same cannot be said for a full mathematical description. We use a mathematical model for the description of the heating-cooling industrial process of a steel workpiece. The model consists of a nonlinear coupled system of PDEs/ODEs involving the electric potential, the magnetic vector potential, the temperature, the stress tensor, the displacement field, and the steel phase fractions. We also give some numerical results of a simpler model.

22.1 Introduction

Steel is an alloy of iron and carbon, though other alloying elements may be present depending on its final intended use. For instance, Cr and V in tools steels, or Si, Mn, Ni and Cr in stainless steels. Most structural components in mechanical engineering are made of steel. Some of these components, such as toothed wheels, bevel gears, pinions and so on, engage each others in order to transmit some kind of (rotational or longitudinal) movement. As a result the contact surfaces of these components are particularly stressed. The goal of heat treating of steel is to attain a satisfactory hardness over the workpiece boundary layers which are intended to be engaged to other structural components. Prior to heat treating, steel is a soft and ductile material. Without a hardening treatment, and due to the surface stresses, the gear teeth will soon get damaged and they will no longer engage properly.

Here we are interested in the mathematical description and the numerical simulation of the hardening procedure of a car steering rack (see Figure 22.1). This particular situation is one of the major concerns in the automotive industry. In this case, the goal is to increase the hardness of the steel along the tooth line and at the same time maintain the rest of the workpiece soft and ductile in order to reduce fatigue.

From a microscopic point of view, steel may be present in different solid phases, namely austenite, martensite, bainite, pearlite and ferrite. For a given wt% of carbon content up to 2.11, all steel phases are transformed into austenite provided the temperature has been raised up to a certain range. The

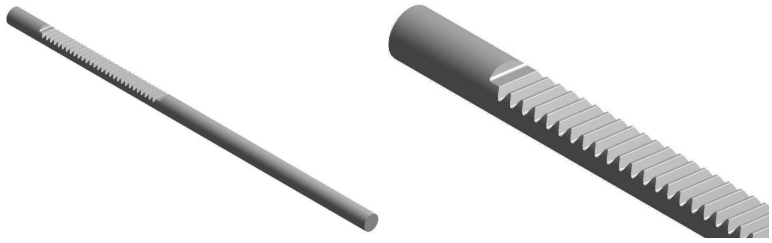

Figure 22.1: Car steering rack.

minimum austenization temperature (727°) is attained for a carbon content of 0.77 wt% (eutectoid steel). Upon cooling, the austenite is transformed back into the other phases (see Figure 22.2), but its distribution depends strongly on the cooling strategy ([2, 9]).

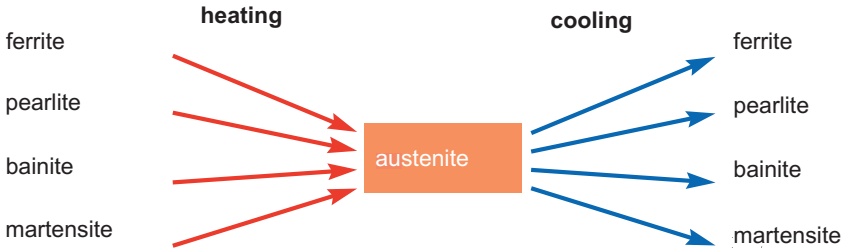

Figure 22.2: Microconstituents of steel. Upon heating, all phases are transformed into austenite, which is transformed back to the other phases during the cooling process. The distribution of the new phases depends strongly on the cooling strategy. A high cooling rate transforms austenite into martensite. A slow cooling rate transforms austenite into pearlite.

Martensite is the hardest constituent in steel, but at the same time is the most brittle, whereas pearlite is the softest and more ductile phase. Martensite derives from austenite and can be obtained only if the cooling rate is high enough. Otherwise, the rest of the steel phases will appear.

22.2 Mathematical modeling

We consider the setting corresponding to Figure 22.3. The domain Ω^{c} represents the inductor (made of copper) whereas Ω^{s} stands for the steel workpiece to be hardened. Here, the coil is the domain $\Omega = \Omega^{\mathrm{s}} \cup \Omega^{\mathrm{c}} \cup S_0$. In this way, the workpiece itself takes part of the coil.

In order to describe the heating-cooling process, we will distinguish two subintervals forming a partition of $[0, T]$, namely $[0, T] = [0, T_{\mathrm{h}}) \cup [T_h, T_{\mathrm{c}}]$, $T_{\mathrm{c}} > T_{\mathrm{h}} > 0$. The first one $[0, T_{\mathrm{h}})$ corresponds to the heating process. All along this time interval, a high frequency electric current is supplied through the conductor which in its turn induces a magnetic field. The combined effect of both conduction and induction gives rise to a production term in the energy balance equation, namely $b(\theta)|\boldsymbol{\mathcal{A}}_t + \nabla\phi|^2$. This is Joule's heating which is the principal term in heat production. In our model, we will only consider three steel phase fractions, namely austenite (a), martensite (m), and the rest of phases (r). In this way,

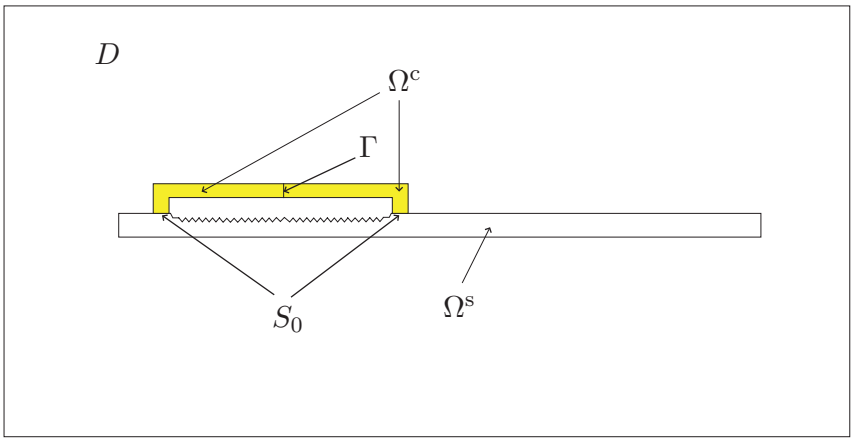

Figure 22.3: Domains D, $\Omega = \Omega^{\rm s} \cup \Omega^{\rm c} \cup S_0$ and the interface $\Gamma \subset \Omega^{\rm c}$. The inductor $\Omega^{\rm c}$ is made of copper. The workpiece contains a toothed part to be hardened by means of the heating-cooling process described below. It is made of a hypoeutectoid steel.

we have $a + m + r = 1$ and $0 \leq a, m, r \leq 1$ in $\Omega^{\rm s} \times [0, T]$. At the initial time we have $r(0) = 1$ in $\Omega^{\rm s}$. Upon heating only austenite can be obtained. In particular $m = 0$ in $\Omega^{\rm s} \times [0, T_{\rm h}]$ and the transformation to austenite is derived at the expense of the other phase fractions (r).

At the instant $t = T_{\rm h}$, the current is switched off and during the time interval $[T_h, T_{\rm c}]$ the workpiece is severely cooled down by means of aqua-quenching.

The heating model

The current passing through the set of conductors $\Omega = \Omega^{\rm c} \cup \Omega^{\rm s} \cup S_0$ is modeled with the aid of an auxiliary smooth surface $\Gamma \subset \Omega^{\rm c}$ cutting the inductor $\Omega^{\rm c}$ into two parts, each one of them having a surface contact over the boundary of the workpiece $\Omega^{\rm s}$ (see Figure 22.3). The heating model involves the following unknowns: the electric potential, ϕ; the magnetic vector potential, $\boldsymbol{\mathcal{A}} = (\boldsymbol{\mathcal{A}}_1, \boldsymbol{\mathcal{A}}_2, \boldsymbol{\mathcal{A}}_3)$; the stress tensor, $\boldsymbol{\sigma} = (\boldsymbol{\sigma}_{ij})_{1 \leq i,j \leq 3}$, $\boldsymbol{\sigma}_{ij} = \boldsymbol{\sigma}_{ji}$ for all $1 \leq i, j \leq 3$; the displacement field $u = (u_1, u_2, u_3)$; the austenite phase fraction, a; and the temperature, θ. Among them, only $\boldsymbol{\mathcal{A}}$ is defined in the domain D containing the set of conductors Ω. On the other hand, since the inductor and the workpiece are in close contact, both ϕ and θ are defined in Ω. Since phase transitions only occur in the workpiece, we may neglect deformations in $\Omega^{\rm c}$. This implies that $\boldsymbol{\sigma}$, u and a are only defined in the workpiece $\Omega^{\rm s}$. The heating model is written in terms of a nonlinear coupled system of PDEs ($\phi, \boldsymbol{\mathcal{A}}, \boldsymbol{\sigma}, u, \theta$) and ODEs ($a, m$) ([1, 4, 7, 8, 5]).

The cooling model

The heating process ends, the high frequency current passing through the coil is switched-off and aqua-quenching begins. The quenching is just modeled via a Robin boundary condition.

We put $a_{T_{\rm h}} = a(T_{\rm h})$, that is, $a_{T_{\rm h}}$ is the austenite phase fraction distribution at the final heating instant $T_{\rm h}$. In the same way, we define $\theta_{T_{\rm h}} = \theta(T_{\rm h})$. Obviously, these functions will be taken as the initial phase fraction distribution and temperature, respectively, in the cooling model.

During the cooling stage, both the electric potential and the magnetic vector potential are dropped out in the mathematical modeling ([4]).

22.3 Numerical simulation

We use the Freefem++ package ([6]) to carry out some numerical simulations for the approximation of the solution to the resulting heating-cooling models. In these simulations we did not consider mechanical effects ($\boldsymbol{\sigma} = 0$, $u = 0$) and we are interested in the evolution of the temperature, the austenization process and the martensite transformation ([3]). We want to describe the hardening treatment of a car steering rack during the heating-cooling process. The goal is to produce martensite along the tooth line together with a thin layer in its neighborhood inside the steel workpiece. The martensite phase can only derive from the austenite phase. Thus we need to transform first the critical part to be hardened (the tooth line) into austenite. For our hypoeutectoid steel, austenite only exists in a temperature range close to the interval $[1050, 1670]$ (in K). During the first stage, the workpiece is heated up by conduction and induction (Joule's heating) which renders the tooth line to the desired temperature. In order to transform the austenite into martensite, we must cool it down at a very high rate. This second stage is accomplished by spraying water over the workpiece. In this simulation, the final time of the heating process is $T_{\mathrm{h}} = 5.5$ seconds and the cooling process extends also for 5.5 seconds, that is $T_{\mathrm{c}} = 11$. We have used the finite elements method for the space approximation and a Crank-Nicolson scheme for the time discretization. At $t = 5.5$ the heating process ends and the computed temperature shows that the temperature along the rack tooth line lies in the interval $[1050, 1670]$ (K).

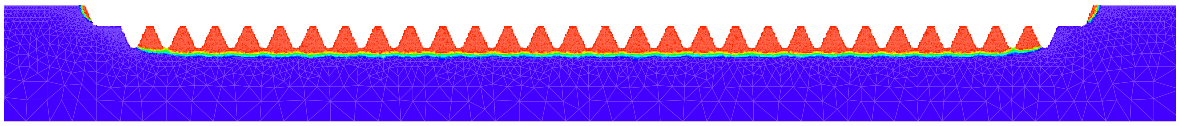

Figure 22.4: Heating process. Austenite at $t = 5.5$s along the rack tooth line.

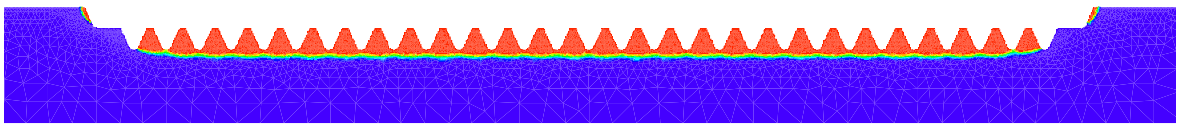

Figure 22.5: Cooling process. Martensite transformation at the final stage of the cooling process $t = 11$s.

Acknowledgements

This research was partially supported by Ministerio de Educación y Ciencia under grant MTM2010-16401 with the participation of FEDER, and Consejería de Educación y Ciencia de la Junta de Andalucía, research group FQM–315.

Bibliography

[1] K. Chełminski, D. Hömberg and D. Kern, *On a thermomechanical model of phase transitions in steel,* WIAS preprint, **1125,** Berlin 2007.

[2] J. R. Davis *et al. ASM Handbook: Heat Treating,* vol. **4,** ASM International, USA, 2007.

[3] J. M. Díaz Moreno, C. García Vázquez, M. T. González Montesinos and F. Ortegón Gallego, *Numerical simulation of a Induction-Conduction Model Arising in Steel Hardening model arising in steel hardening,* Lecture Notes in Engineering and Computer Science, World Congress on Engineering 2009, volume II, July 2009, 1251–1255.

[4] J. M. Díaz Moreno, C. García Vázquez, M. T. González Montesinos and F. Ortegón Gallego, *On an electrothermomechanical model arising in steel heat treating,* Proceedings of the XIV Spanish-French Jacques-Louis Lions School, A Coruña, 2010, 265–281.

[5] J. Fuhrmann, D. Hömberg and M. Uhle, *Numerical simulation of induction hardening of steel,* COMPEL, **18,** No. 3, 482–493, 1999.

[6] F. Hecht, O. Pironneau, A. Le Hyaric, K. Ohtsuda, *Freefem++,* `http://www.freefem.org/ff++`.

[7] D. Hömberg, *A mathematical model for induction hardening including mechanical effects,* Nonlinear Analysis: Real World Applications, **5,** 55–90, 2004.

[8] D. Hömberg and W. Weiss, *PID control of laser surface hardening of steel,* IEEE Transactions on Control Systems Technology, **14,** No. 5, 2006, 896–904.

[9] G. Krauss, *Steels: Heat Treatment and Processing Principles,* ASM International, USA, 2000.

Minisymposium: Numerical simulation of processes in the metallurgical industry

Numerical Simulation and Reduced Order Modelling of Steel Products Heating in Industrial Furnaces

E. Martín*, C. Mourenza, F. Varas****

* Departamento de Ingeniería Mecánica, Máquinas y Motores Térmicos y Fluidos, and
** Dpto de Matemática Aplicada II
Universidad de Vigo, Campus Lagoas-Marcosende, 36310 Vigo, SPAIN
emortega@uvigo.es, curro@dma.uvigo.es, cmourenza@dma.uvigo.es

Abstract

Numerical simulation of the steel product heating process in industrial furnaces exhibits several potencial profits both in the design of the operation conditions and in the furnace control. However, the great complexity needed to accurately reproduce the main involved phenomena leads to prohibitive computational costs, only affordable for certain specific purposes. To deal with *real time* calculations (where *real time* alludes to a computational cost compatible with the characteristic times of a process simulation software package or a control strategy) a set of numerical tools based on some reduced order modelling techniques is proposed. This set includes finite element solution of simplified models, higher order singular value decomposition based analysis of simulation databases and proper orthogonal decomposition techniques to integrate partial differential equations. Two specific applications are presented. The first of them deals with the prediction of the forged steel axle heating process in a heat treatment furnace operating under steady conditions. Reduced order modelling is then used to predict axle heating under a particular set of operations conditions. The second example is related to the prediction of steel products heating in a reheating furnace designed to feed a rolling mill and operating under rather variable conditions. Heating prediction computations are then incorporated in the furnace regulation scheme in order to control the temperature of the pieces being fed to the rolling mill.

23.1 Introduction

Important recent studies deal with the heating of steel pieces in heat treatment and reheating furnaces, among others, those from C. Zhang et al. ([1], [2], [4] y [3]), J.G. Kim et al. ([5] y [6]) and M.Y. Kim et al. ([7], [8] y [9]). In spite of the successful advances achieved, the tremendous computacional effort necessary, prevents this type of implementations in the design of operation conditions of the furnaces. On the other hand, there are a lot of works that tackle simplified dynamical models based on physical principles that describe very variable operation conditions of reheating furnaces ([12], [13]). Recently, very efficient interpolation techniques, based on generalized singular value decomposition ([10]) and use of reduced order models (ROM) based on proper orthogonal decomposition (POD) and its implementation on *snapshots* ([11]) give the chance of dealing with the modelling of two different applications: heat treatment of forged automotive axles under steady operation conditions, and billets reheating furnace in hot rolling plant usually submitted to very varying operation conditions. The work will be organized as follows: The analysis of furnace configuration and operation conditions for the heat treatment of forged axles can be find in section §23.2, where the simplified models used

for the numerical simulation and its comparison with the experimental data are also explained. Then, the explotation of a basis of snapshots to obtain heating prediction for given operation conditions will be presented. Regarding the reheating furnace in a hot rolling plant, section §23.3 shows both the description of the mathematical ROM used to obtain a dynamical tool to predict *instantaneous* heating, and its preliminary validation tests. In §23.4 the main conclusions and on-going and future lines of this work are summarized.

23.2 Analysis of furnace configuration and operation conditions for the heat treatment of forged axles

Numerical simulations of a two dimensional quasi-steady model, corresponding to a central section of an specific heat treatment furnace where carried out. The three different coupled submodels (including equations, boundary and initial conditions): steady furnace walls heating, steady thermofluid dynamics for the gases and unsteady heating of the axles are shown in equations (23.1)-(23.5), where a surface to surface model was used to obtain the radiative internal heat fluxes in the furnace and an appropiate total power balance between convective and radiative fluxes was imposed for each flame surface. A standard k-ε model was used to solve the fluid turbulence.

•Furnaces walls model:

$$\text{div}(k_e \vec{\nabla} T_e) = 0 \tag{23.1}$$

Outer b.c.: $k_e \dfrac{\partial T_e}{\partial n} = h(T_e - T_\infty)$, Inner b.c.: $k_e \dfrac{\partial T_e}{\partial n} = q_{conv} + q_{rad}$

•Thermofluid dynamics model for the gases:

$$\text{div}(\rho_g \vec{U}) = 0 \tag{23.2}$$

$$\text{div}(\rho_g \vec{U} \otimes \vec{U}) + \vec{\nabla} P - \text{div}(\mu(\vec{\nabla}\vec{U} + (\vec{\nabla}\vec{U})^T) = \text{div}\tau^R \tag{23.3}$$

$$\text{div}(\rho_g \vec{U} T_g) - \text{div}((k + k_T)\nabla T_g) = 0 \tag{23.4}$$

B.c.: refractory and axles: wall laws, flame surfaces: velocity and temperature

•Axles heating model for the n-th axle position

$$\rho_p c_p \frac{\partial T_p}{\partial t} - \text{div}(k_p \vec{\nabla} T_p) = 0, \quad \text{for } t \in (0, t_{res}), \tag{23.5}$$

Initial c.: $T_p^n(\vec{x}, 0) = T_p^{n-m}(\vec{x}, t_{res})$ B.c.: $-k_p \dfrac{\partial T_p}{\partial n} = q_{rad} + q_{conv}$

For given operation conditions, that is, feeding velocity of the axles (e.g. 720 s) and power of each group of burners (e.g. group I: 6 burners of nominal power 1.15 MW, group II: 7 burners of nominal power of 0.66 MW), the simulation was implemented with the finite element software Elmer (http://www.csc.fi/english/pages/elmer) with a total mesh of approximately 65000 nodes, providing us the temperature along the furnace, as can be seen in the left picture of figure 23.1. Validation of the model was done through experiments in the furnace, where quite a good agreement was achieved, as displayed in the right picture of figure 23.1. In order to make a fast heating prediction for the axles under different operation conditions a simulation database (DB) was storaged for 29 different operation conditions, corresponding to the combinations of three different residences times (540, 720, 900 s) and three group I and II burner powers (50%,75%,100% and 50%,55%,60%, respectively), where the output variable stored from the numerical simulations was the axles temperature. Interpolation for

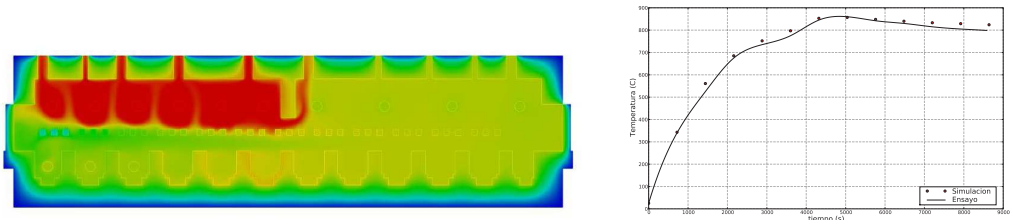

Figure 23.1: Numerical simulation results for the temperature field along the furnace (left), experimental and numerical temperature at the axle center vs. time (rigth)

operation conditions not present in the database was made using higher order singular value decomposition (HOSVD) [10], allowing us to predict the axles heating in less that 0.1s with an accuracy of ± 5 K, as figure 23.2 shows.

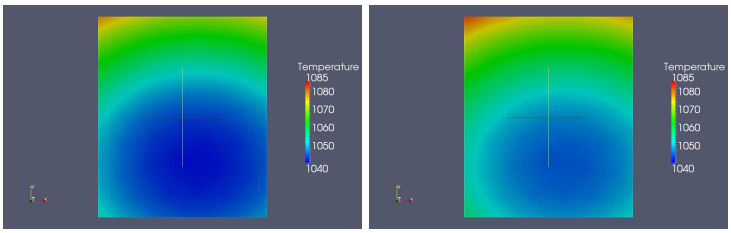

Figure 23.2: Axle heating prediction (central position) for operation conditions of 630 s, 85% and 58%: Direct numerical simulation (left) vs DB/HOSVD prediction (rigth)

23.3 Heating prediction under dynamical conditions for a reheating furnace in a hot rolling plan

The very variable operation conditions common to this type of furnaces (usually because the furnace is slaved to the rolling plant that gets stacked quite often) forces us to obtain a dynamical prediction of the heating of the billets. To do so, ROM for both the furnace walls and the billets heating are obtained. The equations used to derived the models are an unsteady version of (23.1) and (23.5), with a surface to surface model for radiation fluxes. To take into account the presence of gaps, a neutral radiation condition is introduced for each gap, that is $0 = \sum_{k=1}^{N_{hollow}} q_{net}^{k}$. Both structure and billets models are discretized in time (with a step time of 1 s) and integrated along one minute of operation. Radiative fluxes are recalculated for each time with the instantaneous temperature on each surface, while the convective fluxes are obtained from numerical simulations of steady operation conditions (as in the previous section) and then correlated with the "instantaneous"powers of the burners. Proyection of the variables (e.g. temperature of the furnace walls T_h) and equations were made with a choice of functions $\Phi_i(\vec{x})$ extracted from the snapshots of the numerical simulations under steady operation

conditions. Variables are expanded in the base functions, $T_h(\vec{x},t) = \sum_{i=1}^{N_{base}} \alpha_i(t)\Phi_i(\vec{x})$, and inserted in the model equations, as in equation (23.6)

$$\sum_{i=1}^{N_{base}} \frac{d\alpha_i}{dt} \int_\Omega \rho c_p \Phi_i \Phi_j \, d\Omega + \sum_{i=1}^{N_{base}} \alpha_i \int_\Omega k\vec{\nabla}\Phi_i \cdot \vec{\nabla}\Phi_j \, d\Omega = \int_{\partial\Omega} q\Phi_j \, dS, \quad \forall j = 1,2,\dots N_{base} \tag{23.6}$$

to obtain a set of matrix problems of the form $M\frac{d\vec{\alpha}}{dt} + K\vec{\alpha} = \vec{b}$, where unknows $\vec{\alpha}$ have to be solved. The generation of the ROM basis was made using only 6 modes for the furnaces walls and each billet. For the input operation variables (actual power of each burner sampled every second, times of movement of the walking beam system and times of charge and temperature of new billets) and with the initial values of the mean temperature of the billets (obtained from the previous minute of computation), the dynamical system provides the mean temperature of the billets along the following minute of operation. To validate the results of the dynamical model, comparison between numerical results and two different experiments (with thermocouples inserted in the billets) were implemented. The computation time of the dynamical model necessary to mimic each experiment was less than 1 s. The upper figure of 23.3, shows the predicted temperature of the model and the thermocouples temperatures vs. time for the first experiment, while the rest of the pictures correspond, respectively, to each group instantaneous burners powers, total instantaneous burner power in the furnace and walking beam movement signal. Results are in good agreement with the experiment and deviations are lower than 50 K throughout the whole experiment. Unfortunately, the second experiment was not as succesful as the first one, and final deviations of the billet temperature were of 100 K, with a maximum deviation of 200 K approximately.

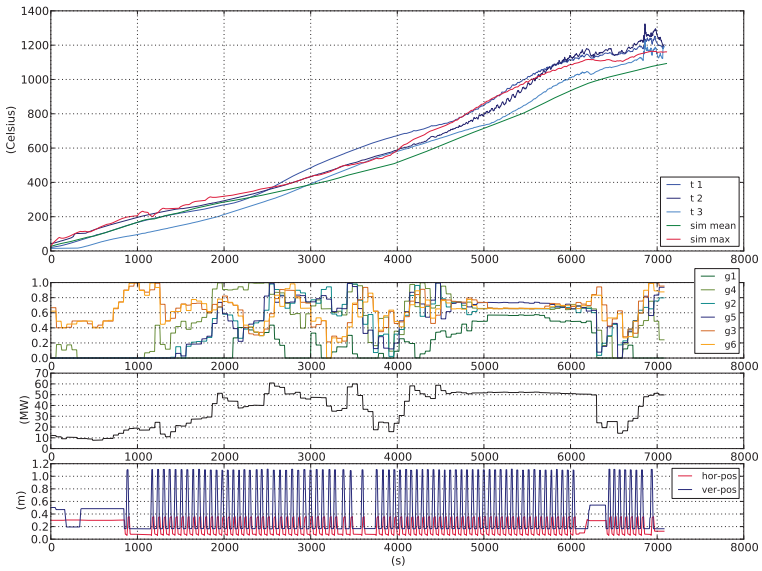

Figure 23.3: Dynamical model prediction vs thermocouple signals. Mean power during test:28 MW. Total furnace power: 80 MW

23.4 Conclusions and future work

We obtain very accurate numerical predictions for the heating of axles under steady operation conditions. We also achieve very fast and quite good heating predictions using simulation databases allowing direct design of operation conditions for the process. The next step we are working on is the implementation of trust region methods in combination with DB/HOSVD models.

We developed a numerical simulation tool that allows us to have "real time"temperature predictions for variable operation conditions of a reheating furnace. Although we obtain poor numerical predictions under "very"variable operation conditions, a regulation of a furnace using an early implementation of this dynamical model gave a reduction of consumption of natural gas of more that 10%. Future lines of work include the ROM of thermofluid dynamics and implementation of adaptive control techniques.

Bibliography

[1] C. Zhang, T. Ishii, S. Sugiyama Numerical modeling of the thermal performance of regenerative slab reheat furnaces Numerical Heat Transfer, Part A 32: 613-631 (1997)

[2] C. Zhang, T. Ishii, Y. Hino, S. Sugiyama The Numerical and Experimental Study of Non-Premixed Combustion Flames in Regenerative Furnaces Journal of Heat Transfer 122: 287-293 (2000)

[3] N. Stockwell, C. Zhang, T. Ishii, Y. Hino Numerical Simulations of Turbulent Non-premixed Combustion in a Regenerative Furnace ISIJ (The Iron and Steel Institute of Japan) International 41:1272-1282 (2001)

[4] T. Ishii, C. Zhang, Y. Hino Numerical Study of the Performance of a Regenerative Furnace Heat Transfer Engineering 23:23-33 (2002)

[5] J.G. Kim, K.Y. Huh, I.T. Kim Three-dimensional analysis of the walking-beam-type slab reheating furnace in hot strip mills Numerical Heat Transfer, Part A 38:589-609 (2000)

[6] J.G. Kim, K.Y. Huh Prediction of Transient Slab Temperature Distribution in the Re-heating Furnace of a Walking-beam Type for Rolling of Steel Slabs ISIJ (The Iron and Steel Institute of Japan) International 40:1115-1123 (2000)

[7] M.Y. Kim A heat transfer model for the analysis of transient heating of the slab in a direct-fired walking beam type reheating furnace International Journal of Heat and Mass Transfer 50:3740-3748 (2007)

[8] C.T. Hsieh, M.J. Huang, A.T Lee, C.H. Wang Numerical modeling of a walking-beam-type slab reheating furnace Numerical Heat Transfer, Part A 53: 966-981 (2008)

[9] S.H. Han, S.W. Baek, M.Y. Kim Transient radiative heating characteristics of slabs in a walking beam type reheating furnace International Journal of Heat and Mass Transfer 52:1005-1011 (2009)

[10] L. de Lathauwer, B. de Moor, J. Vanderwalle A multilinear singular value decomposition SIAM J. Matrix Anal. Appl. 21:1253-1278 (2000)

[11] N. Sirovich Turbulence and the dynamics of coherent structures Quarterly of Applied Mathematics 45: 561-571 (1987)

[12] A. Jacklic, F. Vode, T. Kolenko Online simulation model of the slab-reheating process in a pusher-type furnace Applied Thermal Engineering 27:1105-1114 (2007)

[13] P. Marino, A. Pignotti, D.Solís Numerical Model of Steel Slab Reheating in Pusher Furnaces Latin American Applied Research 32:257-261 (2002)

Minisymposium: Projects in technology centers of the Basque Country

Mathematical Image Segmentation. Variational and Level Set Techniques.

Adrián Galdrán[1,2], **David Pardo**[2,3], **Artzai Picón**[1]

[1]Tecnalia Research & Innovation, Parque Tecnológico de Bizkaia, Zamudio, Spain.
[2]Basque Country University (UPV/EHU), Bilbao, Spain. [3]IkerBasque Foundation, Bilbao, Spain.

Abstract

In this joint project between the University of the Basque Country and Tecnalia Research Corporation, we focus on the deep understanding and implementation of existing variational techniques for image segmentation. In the field of Variational Image Segmentation, mathematical methods coming from the area of numerical analysis and PDE can be combined with statistical and probabilistic techniques, yielding powerful generalistic algorithms that in many aspects overcome other previous techniques in the area. In here we provide a review on some basic topics in the area, that configure the starting point of our work.

24.1 Introduction

An image is a representation of a collection of measurements made over a two or three-dimensional space. Following [1] we can classify images according to the kind of values that measurement takes. Common images, the ones we can find in a newspaper or a book are Light Intensity (LI) images. But there is a number of image types. For example, in Magnetic Resonance (MRI) images, what we represent is the frequency of resonance of the atomic nuclei when exposed to certain magnetic field. X-Ray images measure the quantity of absorbed radiation, and Ultra-Sound images, acoustic pressure.

Another possible classification can be made following the type of mathematical data associated to each pixel. If we only relate a number to each pixel, we are dealing with scalar images; archetypical examples are black and white images. But to each point we can also associate a vector of arbitrary dimension, leading to a vectorial image. An RGB image would be the main example; there, to each pixel we assign a vector in $\mathbb{R}^3$ determining the quantity of red,green, and blue. However, there exist much more complex possibilities. For example, there are color systems based on more than three components, for example. In Diffusion Tensor Imaging (DTI), employed in neurology, a tensor is assigned to each pixel, i.e., a matrix, whose eigenvalues determine the rate of diffusion of water molecules in each direction. This information is of great value to understand the structure and organization of neurones, and the connections in the central nervous system.

To sum up, the great variety of existing images types (see figure 24.1) demands sophisticated processing techniques.

Now, what is image segmentation? There is not a universal definition. Informally speaking, it is the process of classification of the pixels, according to wether they share certain common characteristics, such as intensity or texture. Equivalently, it can be looked at as the process of finding the boundaries between different regions of interest inside the image. In what follows, we give an overview of how can this be tackled with Variational mechanisms, and what is the contribution of Level Set Techniques to the field.

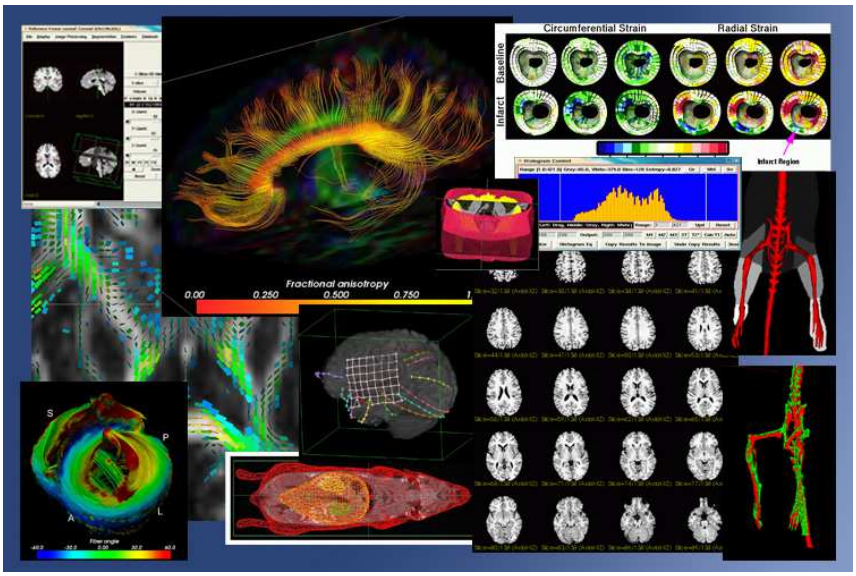

Figure 24.1: Biomedical Images extracted form the Bioimage Suite of image processing developed at Yale University, `www.bioimagesuite.org`

24.2 Variational Image Segmentation

Nowadays, the variational approach is in the core of many Artificial Vision problems nowadays, [2, 3]. The main idea is to define a functional whose minimum provides a solution of the problem.

Introducing in the image segmentation problem the variational point of view provides many advantages. Mainly, it allows to impose on the solution some criteria that needs to be satisfied, such as smoothness of the extracted contours, homogeneity of the different regions, or correspondence with certain a priori knowledge that we can have about the ideal result of the segmentation.

The first variational approach to image segmentation appears in the literature in 1988 in [4]. It was given the name of "Snakes" because of the way in which the curves evolved across the image until they arrived to a segmentation of it. The functional to be minimized was:

$$E_{snakes}(c) = \alpha \int_0^1 |c'(s)|^2 \, ds + \beta \int_0^1 |c''(s)|^2 \, ds - \lambda \int_0^1 |G_\sigma * \nabla I(c(s))|) \, ds$$

where I is the image to be segmented, $I : \Omega \subset \mathbb{R}^2 \to \mathbb{R}$, G_σ is a Gaussian of standard deviation σ, that acts as a filter of the noise on the image, and c is a parametric curve. When minimizing E_{snakes} , the first two terms account for the smoothness of the contours, while the third one depends on the gradient of the image: the model will tend to carry the curve to the locus of the image where it takes higher values, i.e., where there is more image variation. This is where we expect to find the borders of the objects that we want to segment. The parameters α, β, and γ are manually tuned to control the weight of each term in the minimization process.

The trend of modeling image segmentation as the search of a minimum of certain functional went on with the definition of the Mumford-Shah functional in 1989, in [5]:

$$E_{MS}(f, \Gamma) = \mu^2 \int \int_\Omega (f - I)^2 \, dxdy + \int \int_{\Omega - \Gamma} \|\nabla f\|^2 \, dxdy + \nu \, |\Gamma|$$

where E_{MS} is minimized in a space made up of pairs (f, Γ), being f a piecewise continuous approximation of the image I, and Γ a set of discontinuities over the image, that identifies the contours of the segmentation. The smaller is E_{MS}, the better is I segmented by (f, Γ). Notice that:

- The first term requires f to be an approximation of I.
- The second term enforces that f (and as a consequence, I) varies as little as possible across the interior and the exterior of Γ.
- The third term pushes the process to obtain boundaries Γ with the lesser longitude possible. This leads to additional regularity.

The Mumford-Shah functional turns to be a very hard problem, as it usually shows many local minima, and in addition it couples geometric entities of different dimensionality. However, many of the most popular variational segmentation models derive from this one, as simplifications of it, [6, 7, 8].

After introducing as examples the two most classic variational segmentation models, we give a brief overview of the Level Set Techniques, and their contribution to the field.

24.3 The Level Set Method

The introduction of the Level Set Method in [9] for the evolution of the geometry deeply influenced the success of the variational models, since it allowed for robust and versatile implementation of the minimization of the functionals.

The main strategy for the minimization of a functional such as the described above is the implementation of a gradient descent: we compute the (variational) derivative of the functional. That gives as a differential equation of the type:

$$\frac{\partial c}{\partial t} = V,$$

where V is the velocity field at which the curve evolves (in the minimization space) to decrease the value of the functional. When we arrive to a stationary point, the functional must have a minimum.

However, if we approach directly the minimization of a functional such as, for example, E_{snakes}, by parameterizing the curve c and discretizing the differential equations obtained after finding the derivative of the functional, we encounter a series of numerical difficulties: small initial errors rapidly propagate in the numerical process [10]. Besides, parametrization may become poor within the time evolution, and marker points can get too close to each other, or too far apart. Remedies to these drawbacks require complicated strategies [11].

All these difficulties can be overcome by implementing a Level Set method. The idea is to build a family of functions $\phi : \Omega \times [0, T] \rightarrow \mathbb{R}$ that, rather than following the evolution of the curve, capture it. Let us assume we have an initial curve $c(p, t) = (x(p, t), y(p, t))$, parameterized by p, that is moving across the image following a velocity field $\vec{V} : \Omega \subset \mathbb{R}^n \rightarrow \mathbb{R}^n$. The parameter t controls the temporal evolution. If we want the function ϕ to have as its zero-level set the points lying on the trace of the curve c, we will have (omitting the parameter p) $\phi(c(t), t) = 0$, and if we take derivatives in both sides,

$$\phi_t(x(t), y(t), t) + \frac{\partial \phi}{\partial x}\frac{\partial x}{\partial t} + \frac{\partial \phi}{\partial y}\frac{\partial y}{\partial t} = \nabla \phi \cdot \left(\frac{\partial x}{\partial t}, \frac{\partial y}{\partial t}\right) = 0$$

Of course, the time derivative of c is the velocity at which it is evolving, so:

$$\phi_t + \nabla\phi \cdot \vec{V} = 0.$$

But if we now decompose the velocity field in its normal and tangential components, $\vec{V} = V_n\,\mathbf{n} + V_t\,\mathbf{t}$, and have into account that the gradient of the function ϕ always points in the normal direction to its level sets, we get:

$$\phi_t + \nabla\phi \cdot \vec{V} = 0.$$

So, finally, the evolution of the functions ϕ is governed by the following Partial Differential Equation:

$$\boxed{\phi_t + V_n|\nabla\phi| = 0}$$

This is known as the Fundamental Level Set Equation [12]. In figure (24.2) we can see an example of how the functions ϕ capture the evolution of the curve towards a segmentation of an image of two lungs.

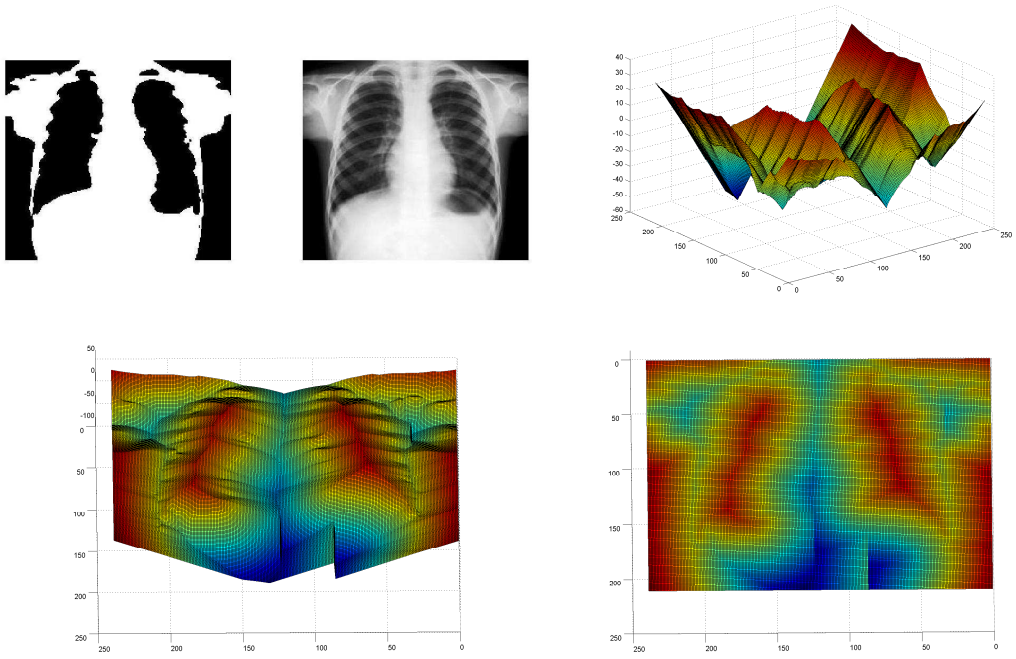

Figure 24.2: Level Set Segmentation

Bibliography

[1] N. Pal and S Pal A review on image segmentation techniques, Pattern Recognition 9 (26), (1993), 1277–1294.

[2] G. Aubert and P. Kornprobst, *Mathematical Problems in Image Processing.* Springer, 2001.

[3] O. Scherzer, M. Grasmair, H. Grossauer, M. Haltmeier,F. Lenzen, *Variational Methods in Imaging.* Springer Verlag, New York 2009.

[4] M. Kass, A. Witkin, D. Terzopoulos, Snakes: Active contour models, International Journal of Computer Vision 1 (4),(1988), 321-331.

[5] D. Mumford, J. Shah, Optimal Approximations by piecewise smooth functions and associated variational problems, Communications in Pure and Applied Mathematics 42,(1989), 577-685.

[6] T. Chan, L. Vese, Active contours without edges, IEEE Transactions on Image Processing, 2, (2001), 266-277.

[7] T. Chan, L. Vese, A Multiphase Level Set Framework for Image Segmentation Using the Mumford and Shah Model, International Journal of Computer Vision, 50, (2002), 271-293.

[8] A. Tsai, A. Yezzi, A.S. Willsky, Curve evolution implementation of the Mumford-Shah functional for image segmentation, denoising, interpolation, and magnification, IEEE Transactions on Image Processing, 10 (8), (2002), 1169-1186.

[9] J. Sethian, Curvature and the evolution of fronts, Communications in Mathematical Physics 4, (1985), 487-499.

[10] J. Sethian, *Level Set Methods and Fast Marching Methods: Evolving Interfaces in Computational Geometry, Fluid Mechanics, Computer Vision, and Materials Science.* Cambridge University Press 1999.

[11] T. Mcinerney, D. Terzopoulos, Topologically Adaptable Snakes, Medical Image Analysis, 4, (1995), 840-845.

[12] S. Osher, R.Fedkiw, *Level Set Methods and Dynamic Implicit Surfaces.* Springer 2002

Minisymposium: Projects in technology centers of the Basque Country

Gestión, optimización y estimación del consumo eléctrico doméstico condicionado por la oferta de incentivos

Carlos Gorria y Mikel Lezaun
Universidad del Paí s Vasco
carlos.gorria@ehu.es, mikel.lezaun@ehu.es

Joseba Jimeno, Iñaki Laresgoiti y Nerea Ruiz
Tecnalia Corporation
jjimeno@labein.es, lares@labein.es, nruiz@labein.es

Abstract

En el mercado energético la electricidad es un factor estratégico por su gran implantación en el sector industrial y doméstico y porque, en parte, procede de fuentes renovables y poco contaminantes. Sus mayores inconvenientes son la imposibilidad de almacenamiento a gran escala y la respuesta limitada ante la fluctuación aleatoria de la demanda. Mientras que las necesidades energéticas por parte de los servicios básicos y sociales son prácticamente invariables, la demanda doméstica tiene cierta flexibilidad en las horas de encendido de algunos electrodomésticos. Una redistribución horaria del consumo en esos aparatos, estimulada mediante incentivos, contribuiría a la estabilidad de la red, y redundaría en un beneficio para el cliente y la compañía. El Gestor de la Demanda es un sistema atomático que propone a cada cliente su perfil de consumo diario óptimo y ajusta el consumo global estimado. Para ello utiliza técnicas de investigación operativa y de regresión. En este trabajo se alían la experiencia de una empresa tecnológica como Tecnalia y los conocimientos teóricos de un equipo de la Universidad del País Vasco UPV/EHU, para desarrollar las herramientas matemáticas aplicadas en este modelo.

25.1 Introduction

La creciente preocupación por disminuir las emisiones contaminantes que aceleran el cambio climático está obligando a impulsar las fuentes de energía renovable. Es por ello que en el actual mapa de la energía de los países industrializados la electricidad juega un papel prioritario. Es bien sabido que uno de los obstáculos a los que se enfrenta es que las fuentes "limpias", como la eólica o la solar, sufren bruscas variaciones en la producción. Este hecho se suma a la intrínseca aleatoriedad de la demanda eléctrica donde, en espacios cortos de tiempo, se suceden los temidos periodos "valle" y "pico" de consumo. Ambos factores desestabilizan la red y ocasionan fallos en el suministro y sobreproducciones que se traducen en pérdidas. En este contexto se hace imprescindible mejorar los métodos de previsión y control del consumo eléctrico, dada la ineficiencia del modelo actual. El objetivo es diseñar un sistema robusto que reaccione en un tiempo reducido a las variaciones de la demanda y consiga adaptarla a la capacidad de generación de la red evitando otras medidas más costosas.

Una posibilidad para homogeneizar la demanda eléctrica es proponer a los consumidores domésticos una programación diaria de su distribución de cargas eléctricas desplazables de manera que compensen los periodos pico y valle. Como cargas desplazables se consideran las de los electrodomésticos que tienen un consumo significativo pero sólo se utilizan en momentos puntuales, como la lavadora, el

lavavajillas o la secadora, y su encendido es susceptible de ser diferido a lo largo del día. También se puede considerar desplazable el aire acondicionado en el sentido de que la temperatura de confort T^c puede ser variada. Tanto el cambio de horario de encendido de los electrodomésticos como la variación de la temperatura de confort suponen cierta molestia para el cliente, que puede asumirla en la medida en que se ofrezca una contrapartida, como por ejemplo un incentivo económico a cambio de un consumo reducido, $Q < \gamma$. En este punto entra en juego el Gestor de la Demanda, que es un sistema automático que analiza estadísticamente la previsión global de la demanda eléctrica de cada instante y propone a cada cliente un mapa de consumo diario óptimo utilizando técnicas de investigación operativa.

Para finalizar, el Gestor de la Demanda también incorpora un módulo que estima la redistribución de la demanda provocada por el sistema de incentivos, calculando por una parte la reducción del consumo en los momentos incentivados y por otra el desembolso total que hará la compañía para lograrlo. En la figura (25.1) se observa un esquema de las interrelaciones que supervisa el Gestor de la Demanda. Los datos recogidos de experiencias piloto desarrolladas con clientes voluntarios, a los que se lanzarán diferentes tipos de incentivos en cuantía, instante y duración, conformarán una base de datos sobre la cual aplicar métodos de regresión para aproximar la tendencia del consumo en función de los incentivos.

25.2 Metodología

Se comienza dividiendo las 24h del día en 96 intervalos de de 15', $h_i \in [t_{i-1}, t_i),\ i = 1, \ldots, 96$, donde t_0 =0:00 y t_{96} =24:00 y asumiendo un precio unitario p_i por Kw/h. En el modelo más sencillo se consideran como desplazables las cargas eléctricas ligadas a los electrodomésticos cuya puesta en marcha puede diferirse, es decir, la lavadora, el lavavajillas y la secadora. La potencia inducida por intervalo temporal a partir de su encendido es respectivamente $(P_1^L, \ldots, P_l^L)$, $(P_1^V, \ldots, P_v^V)$, $(P_1^S, \ldots, P_s^S)$, siendo l, v y s las duraciones en número de intervalos de 15' del ciclo de cada electrodomestico. La potencia que el regulador térmico (aire acondicionado) necesita para pasar de una temperatura T_i en el instante t_i a T_{i+1} en el siguiente instante depende de la capacidad calorífica β, la eficiencia del aparato ERR, la dispersión térmica α y la tempreatura exterior T_i^o y se puede expresar como

$$Q_i^{AC} = \frac{1}{\Delta t \cdot ERR}\left(\frac{T_i - T_{i+1}}{\beta} + \alpha \Delta t (T_i^o - T_i)\right). \tag{25.1}$$

La decisión de los instantes de encendido de la lavadora, el lavavajillas o la secadora se representan mediante las respectivas variables binarias y_i, z_i, u_i, $i = 1, \ldots, 96$, que pueden valer 1 en el caso de que el correspondiente electrodoméstico se encienda en el intervalo i o 0 en caso contrario. Por lo tanto la potencia demandada por cada uno de ellos en el intervalo i, por ejemplo la de la lavadora, vale

$$Q_i^L = y_{i-l+1}P_l + \cdots + y_{i-1}P_2 + y_i P_1 = \sum_{j=0}^{l-1} y_{i-j}P_{j+1}. \tag{25.2}$$

La demanda total es la suma de la carga básica no desplazable Q_i^B y el resto de elementos

$$Q_i^T = Q_i^B + Q_i^L + Q_i^V + Q_i^S + Q_i^{AC}. \tag{25.3}$$

Para formular el problema de optimización hay que construir la función lineal $f(x, y, z, u, T^c)$ a minimizar y las restricciones lineales, donde x es la variable binaria que indica si se cumplen las condiciones para el cobro del incentivo I, $x = 1$, o no se cumplan, $x = 0$. El óptimo para este problema se alcanzará en un valor que combinará cierto compromiso entre el mínimo gasto económico y la mínima

incomodidad para el cliente. Una opción que tiene en cuenta estos aspectos es

$$f = \sum_{i=0}^{96} Q_i^T p_i - xI + \lambda_L \sum_{i=0}^{96-i_1^B} i \cdot y_{i_1^B+i} + \lambda_V \sum_{i=0}^{96-i_2^B} i \cdot z_{i_2^B+i} + \lambda_S \sum_{i=0}^{96-i_3^B} i \cdot u_{i_3^B+i} + \lambda_{AC} \sum_{i=0}^{97} w_i \quad (25.4)$$

Aquí $\lambda_L,\ \lambda_V,\ \lambda_S$ y λ_{AC} son los parámetros que modulan respectivamente el esfuerzo que supone para cada cliente el aplazamiento del encendido de lavadora, lavavajillas, secadora y la diferencia de la temperatura con respecto a la de confort. Estos valores se fijan según las prioridades del cliente siendo su magnitud mayor cuanto más importancia tenga en su patrón de uso básico sin incentivos. En cualquier caso serán pequeños para que el término que refleja el interés por obtener el incentivo, $-xI$, domine en la minimización. Los índices i_1^B, i_2^B e i_3^B corresponden a los instantes de encendido básicos de los electrodomésticos según cada cliente. Los términos finales son $w_i = \max(T_i - T_i^c, T_i^c - T_i)$.

La solución cumplirá las restricciones estructurales, como son el uso a diario de los electrodomésticos y los límites del termostato, de la potencia del regulador térmico y de la potencia total contratada,

$$\sum_{i=1}^{96} y_i = \sum_{i=1}^{96} z_i = \sum_{i=1}^{96} u_i = 1, \quad T_i^{\min} \leq T_i \leq T_i^{\max}, \quad 0 \leq Q_i^{AC} \leq Q^{AC}, \quad Q_i^T < Q^{cont}. \quad (25.5)$$

Las restricciones de cobro del incentivo cuando $Q_i^T = Q_i^B + Q_i^L + Q_i^V + Q_i^S + Q_i^{AC} < \gamma$ implican $x = 1$ o en caso contrario $x = 0$. Con la ayuda de una constante M grandese pueden hacer lineales

$$\begin{cases} \gamma < Q_i^T + Mx \\ Q_i^T \leq \gamma + M(1-x) \end{cases} \Longrightarrow \begin{cases} Q_i^T \leq \gamma,\ x = 1 \\ Q_i^T > \gamma,\ x = 0 \end{cases} \quad (25.6)$$

El Gestor de la Demanda busca una solución óptima del problema de optimización planteado mediante técnicas clásicas de programación lineal, ver [1]. A cada cliente del experimento se le anuncia una propuesta de planificación similar a la de la figura (25.2). En el ejemplo se ha considerado un hogar con lavadora y lavavajillas. La curva roja indica el patrón de consumo habitual con dos elevaciones correspondientes al uso de estos dos electrodomésticos y la curva verde es la programación que minimiza su función de consumo con una señal de incentivo de 0.03 euros entre las 13:00h y las 14:00h por cada intervalo de 15' en que consuma menos de 1 kw/h.

Teniendo en cuenta que no todos los clientes adaptarán su consumo doméstico diario a la sugerencia del Gestor de la Demanda y que la probabilidad de aceptarla dependerá de la cuantía del incentivo y de la hora a la que se oferte, es importante construir un modelo que estime el seguimiento de la propuesta en función de los incentivos. Una opción para obtener estos datos es aplicar una regresión lineal por mínimos cuadrados, donde las variables explicativas son los incentivos aplicados durante el día y el resultado es el consumo medio en cada franja horaria $\langle Q_i^T \rangle$. Más concretamente, para cada cliente $n = 1, \ldots, N$, su gasto total aproximado en la franja i es

$$Q_{n,i}^T = \beta_{i,0} \cdot 1 + d_n^L Q_i^L + d_n^V Q_i^V + d_n^S Q_i^S + d_n^{AC} Q_i^{AC} + \epsilon_{n,i}, \quad (25.7)$$

donde las variables binarias d_n^L, d_n^V y d_n^S valen 1 si dicho cliente tiene lavadora, lavavajillas o secadora respectivamente y 0 en caso contrario y $\epsilon_{n,i}$ es el residuo aleatorio. Experiencias anteriores en el análisis del consumo eléctrico publicados en [2], [3] y [4] sugieren tratar de manera independiente en la regresión el consumo de cada electrodoméstico, por lo que se desglosan

$$Q_i^L = \beta_{i,0}^W \cdot 1 + \beta_{i,1}^W \cdot I_i + \beta_{i,2}^W I_i^{(prev)} + \beta_{i,3}^W I_i^{(post)} + \beta_{i,4}^W I_i^{(out)} \quad (25.8)$$

para la lavadora $W = L$, el lavavajillas $W = V$ y la secadora $W = S$. Dado que un incentivo en un intervalo horario contribuye al desplazamiento de las cargas hacia otras horas, el consumo acumulado en cada instante dependerá principalmente del incentivo aplicado en dicha hora I_i y de la suma de incentivos aplicados respectivamente en la hora anterior $I_i^{(prev)}$, en la hora posterior $I_i^{(post)}$ y en el resto del día $I_i^{(out)}$. La regresión se hace para cada una de las 96 franjas horarias h_i. El ajuste por mínimos cuadrados encuentra los valores de los parámetros $\beta_{i,j}^W$ que minimizan los residuos,

$$\min_{\beta_i} \sum_{n=1}^{N} \epsilon_{n,i}^2 = \min_{\beta_i} \sum_{n=1}^{N} (Q_{n,i}^T - \vec{\beta_i} \cdot d_n \vec{I}_i)^2 \tag{25.9}$$

La solución del problema (25.9) se obtiene de las ecuaciones normales $\mathbf{A_i}^t \mathbf{A_i} \vec{\beta_i} = \mathbf{A_i}^t \vec{Q_i}$ para cada intervalo $h_i,\ i = 1, \ldots, 96$, despues de eliminar las columnas linealmente dependientes. El valor de estos coeficientes se puede actualizar según aumente la base de datos de los clientes. Finalmente, para una señal de incentivos, se construyen los observables en cada franja, $I_i,\ I_i^{(prev)},\ I_i^{(post)},\ I_i^{(out)}$ y las medias de penetración de los electrodomésticos $\langle d \rangle$ y se calcula la estimación del consumo medio

$$\langle Q_i^T \rangle \approx (\langle d \rangle \vec{I})^t \cdot \vec{\beta_i} \tag{25.10}$$

Analicemos un experimento ejecutado con datos sintéticos para una señal de incentivo de 0.03 euros entre los instantes 53 (13:15h) y 57 (14:15h) como se muestra en la figura (25.3). Por ejemplo, la regresión sobre el intervalo h_{55} ha generado unos coeficientes $\beta_{55,0} = 0.918$, $\beta_{55,2} = -23.781 :\ \beta_{55,3} = 5.333$, $\beta_{55,4} = -1.882$, $\beta_{55,5} = 0.091$, etc. Apartamos $\beta_{55,1} = 0$ ya que todos los clientes poseían lavadora, con lo que la columna asociada a $\beta_{55,1} = 0$ en la matriz de observables es la misma que la de $\beta_{55,0}$ y debe eliminarse de las ecuaciones normales. El resto de términos reflejan que la aplicación del incentivo en el instante 55 y en la hora posterior contribuyen a reducir el consumo en ese momento, pero los incentivos aplicados en la hora anterior o en el resto del día desplazan cierta carga hacia ese instante.

Los cálculos de la optimización y de la regresión se han realizado con el software libre *octave* [6] aunque para problemas de optimización en los que aumente el número de variables y restricciones pueden ser recomendables el software, también libre, *LPSOLVE* [5] o incluso el software con licencia *LINGO* [7].

25.3 Conclusiones

Las soluciones matemáticas aportan información indudablemente útil a procesos industriales de fabricación, distribución, transporte, etc. En este trabajo se estudia un problema de distribución en el mercado eléctrico en presencia de incentivos al consumo doméstico limitado durante periodos críticos. El objetivo es suavizar en lo posible la curva de demanda global. Los métodos de optimización ofrecen al cliente una planificación individual del uso de la electricidad que le permita captar los incentivos, minimizando las incomodidades causadas. Los métodos de regresión estiman el índice de seguimiento de estas señales y las tendencias relativas. Ambas herramientas han aportado resultados satisfactorios para los objetivos del proyecto y aún son susceptibles de mejora utilizando métodos de estimación más ajustados a la problemática del modelo como la regresión logística.

25.4 Figures

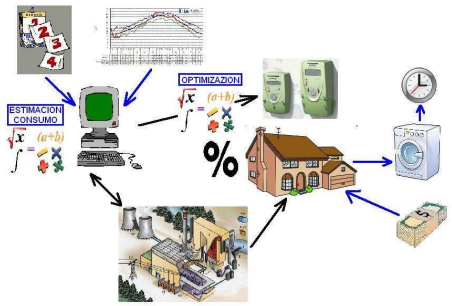

Figure 25.1: Esquema de los factores que influyen en las decisiones del Gestor de la Demanda.

Figure 25.2: Propuesta de consumo (verde) a un cliente con un perfil básico (rojo) en el que intervienen la lavadora y el lavavajillas con una señal de incentivo aplicado de 13:00h a 14:00h de 0.03 euros/15'.

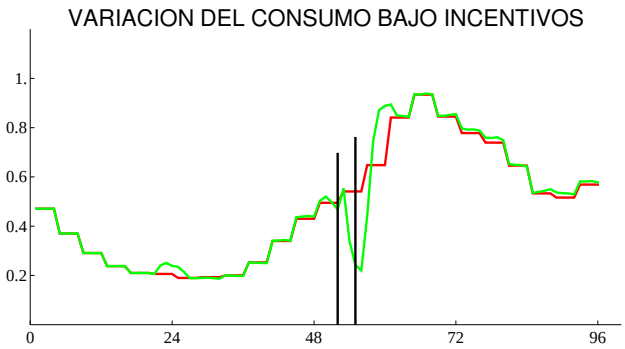

Figure 25.3: Variación media del consumo en Kw/h con una señal de incentivo de 0.03 euros entre los instantes 53 (13:15h) y 57 (14:15h).

Bibliography

[1] J. Nocedal and S.J. Wright *Numerical Optimization*. Springer Series in Operations Research, Springer Verlag, 2006

[2] P.C. Reiss and M.W. White, Household Electricity Demand, Revisited, Review of Economic Studies, 72(3),(2005), 853-883.

[3] J.A. Dubin and D.L. Mcfadden, An Econometric Analysis of Residential Electric Appliance Holdings and Consumption, Econometric, 52(2),(1984), 345-362.

[4] R. Bartels and D.G. Fiebig, Residential End-Use Electricity Demand: Results from a Designed Experiment, Energy Journal, 21(2),(2000), 51-81.

[5] LPSOLVE http://lpsolve.sourceforge.net/

[6] OCTAVE (GLPK package) http://octave.sourceforge.net/

[7] LINGO http://www.lindo.com/

Minisymposium: Projects in technology centers of the Basque Country

Estratificación de la población: matemáticas para una atención sanitaria con enfoque poblacional

Maider Mateos, Jon Orueta, Irantzu Barrio, Roberto Nuño
O+berri, Instituto Vasco de Innovación Sanitaria
maider@bioef.org, www.bioef.org

Abstract

La respuesta a las necesidades de las personas que padecen enfermedades crónicas constituye actualmente uno de los principales retos para el Sistema Sanitario Vasco. Con el objetivo de avanzar hacia una atención sanitaria con enfoque poblacional que analice el nivel de morbilidad de la población y la segmente a fin de planificar los recursos para cubrir los diferentes requerimientos de manera adaptada y proactiva, se está llevando a cabo en Euskadi el proyecto *Estratificación de la Población*.

A través de técnicas estadísticas, principalmente modelos two-part, y basándose en variables demográficas y clínicas, se calcula una predicción para el coste sanitario que tendrá cada persona en el futuro. Esta predicción permitirá clasificar a las personas e identificar candidatos a beneficiarse de intervenciones diseñadas para ser dirigidas a pacientes cuyo estado de salud cumpla unas características determinadas.

26.1 Introducción

Como consecuencia del aumento en la esperanza de vida y de las mejoras en la atención socio-sanitaria, entre otros factores, se está produciendo un crecimiento progresivo de la prevalencia de enfermedades crónicas. Este tipo de patologías son la principal causa de mortalidad, conllevan un empeoramiento en la calidad de vida de las personas que las padecen y, además, el coste de su atención representa una parte más que relevante del gasto sanitario total.

Con el fin de proporcionar un cuidado de mayor calidad a los pacientes crónicos, de prevenir estas enfermedades y de avanzar hacia un sistema sanitario más sostenible, el Departamento de Sanidad y Consumo del Gobierno Vasco publicó en julio de 2010 la *Estrategia para afrontar el reto de la cronicidad en Euskadi* [1]. En el marco de esta estrategia se han diseñado diversas intervenciones que se adaptan a las necesidades de atención de los pacientes. Una premisa para la adecuada implantación de estas intervenciones es seleccionar correctamente a las personas susceptibles de beneficiarse de las mismas. Esto es, precisamente, lo que el proyecto *Estratificación de la población en Euskadi* pretende.

Basándose en técnicas estadísticas, este proyecto permitirá clasificar a las personas en función de su nivel de morbilidad e identificar a aquellos pacientes cuyas características de salud respondan al perfil para el que fueron concebidas las intervenciones.

26.2 Métodos

La población de estudio está constituida por todas las personas mayores de 13 años adscritas a Osakidetza (Servicio Vasco de Salud) por un intervalo mínimo de 6 meses en el año comprendido entre el

1/09/2007 y el 31/08/2008. De todas ellas se han recogido datos correspondientes a un periodo de dos años. Los relativos a los primeros 12 meses se han utilizado para construir las variables independientes y engloban tanto la información demográfica (edad y sexo) como la clínica (diagnósticos y fármacos). Con los datos del segundo año se ha calculado, a nivel individual, el coste sanitario total, que se tomará como variable respuesta.

A través de modelos estadísticos y partiendo de la información del primer año se pretende predecir el coste sanitario de cada persona en el segundo periodo. Dada la extrema asimetría de la variable respuesta (mientras que la mitad de la población consume solamente un 4% del gasto total, el 10% de los pacientes más consumidores requiere un 63% del presupuesto) se ha optado por recurrir a los modelos *two-part* [2] [3] [4]. Estos modelos se construyen en dos fases. En primer lugar, se lleva a cabo una regresión logística que, para cada individuo, proporciona la probabilidad de tener coste no nulo en el segundo año. Posteriormente, se ajusta un modelo normal multivariante con la variable respuesta transformada por el logaritmo dejando fuera a los no consumidores, es decir, considerando únicamente aquellos pacientes que tuvieron coste.

Combinando de manera adecuada los resultados de ambas fases se obtiene una predicción para el coste del segundo periodo. A partir de ella se calcula la probabilidad de pertenecer al grupo de personas con riesgo de alto consumo de recursos considerando como personas de alto consumo aquéllas cuyo coste sanitario total supera el percentil 95.

26.3 Resultados

Si bien todavía los análisis no han finalizado, la Tabla 26.1 muestra los resultados preliminares obtenidos para tres de los modelos evaluados. La primera fila corresponde al modelo más simple, que tiene como variables independientes sólo la edad y el sexo de los pacientes. La segunda es relativa al modelo que incorpora la información clínica procedente de los diagnósticos (Dx) y los fármacos (Rx) que se les han prescrito y, por último, aparece el modelo que incluye también el coste sanitario del año previo. Para cada uno de ellos se presenta el coeficiente de determinación R^2 de la segunda fase del modelo two-part y el área bajo la curva ROC que nos indica la capacidad de la predicción obtenida para identificar a los individuos con riesgo elevado de alto consumo de recursos sanitarios.

	$\mathbf{R^2}$ **de la fase 2**	**AUC**
Edad + Sexo	0.201	0.767
Edad + Sexo + Dx+ Rx	0.373	0.828
Edad + Sexo + Dx + Rx + Coste año previo	0.444	0.840

Table 26.1: Resultados para modelos two-part

Se comprueba que tanto las variables de naturaleza clínica (más de 160) como el coste del año anterior resultan estadísticamente significativas ($p < 0.05$) y provocan una mejoría notable en la capacidad explicativa y de discriminación del modelo. Además, lo dotan de significado clínico.

A pesar de que los valores del coeficiente de determinación no parecen elevados desde el punto de vista estadístico, nuestros resultados son similares a los logrados en estudios llevados a cabo en otros países y ponen de manifiesto que el coste sanitario individual es una variable difícil de predecir. No obstante, los valores del área bajo la curva ROC indican que la identificación de pacientes que tendrán altas necesidades de atención puede realizarse de manera satisfactoria a través de este tipo de procedimientos.

26.4 Discusión

Entre las políticas incluidas en la *Estrategia para afrontar el reto de la cronicidad en Euskadi* se encuentra la adopción de un enfoque de salud poblacional que dé respuesta a las necesidades actuales de los ciudadanos. El proyecto de estratificación resuelve esta cuestión permitiendo clasificar a las personas según su nivel de morbilidad y requerimientos de atención. De este modo, se puede llevar a cabo una selección proactiva de pacientes candidatos a ser incluidos en programas diseñados específicamente para enfermos con un determinado perfil.

No se debe olvidar que en el futuro la herramienta resultante será utilizada por profesionales de la salud. Gracias a la inclusión de la información proporcionada por los diagnósticos y los fármacos, los modelos adquieren un significado clínico que facilita su interpretación por parte del personal sanitario. Asimismo, la identificación de pacientes con determinados problemas de salud, como ancianos en estado de fragilidad o pacientes polimedicados, puede hacerse de manera inmediata.

En un futuro próximo la estratificación empezará a ser empleada, por ejemplo, en el pilotaje de una nueva figura de enfermería: la enfermera de competencias avanzadas para la gestión de casos complejos. Entre sus funciones destacan coordinar, gestionar y unificar la atención sanitaria, así como proporcionar cuidados clínicos personalizados a pacientes vulnerables en su domicilio. Cada profesional de enfermería incluido en este pilotaje atenderá a 50 pacientes con necesidades de cuidados muy altas, que serán identificados por medio de los modelos de estratificación.

Otra aplicación de esta herramienta se encuentra en el programa Batera Zainduz concebido para mejorar los resultados en el tratamiento a enfermos de diabetes. El programa cuenta con tres paquetes de cuidados dirigidos a diabéticos de distintas características. La determinación de qué paquete aplicar a cada paciente se realizará con la estratificación.

26.5 Conclusiones

Como vemos, la estadística proporciona fundamentos para construir un instrumento de ayuda a la toma de decisiones muy útil y de gran aplicabilidad. Gracias a él Osakidetza dispone de información adicional para seleccionar pacientes que presentan situaciones de riesgo tales como ancianos en estado de fragilidad, pacientes polimedicados o crónicos complejos con grandes necesidades futuras de atención sanitaria.

Bibliography

[1] *Estrategia para Afrontar el Reto de la Cronicidad en Euskadi*. Departamento de Sanidad y Consumo del Gobierno Vasco, julio 2010.

[2] Buntin M.B., Zaslavsky A.M., *Too much ado about two-part models and transformation? Comparing methods of modeling medicare expenditures*. Journal of Health Economics 23, 2004, 525-542.

[3] Diehr P., Yanez D., Ash A., Hornbrook M. Lin D.Y., *Methods for Analyzing Health Care Utilization and Costs*. Annu. Rev. Public Health, 1999, 20:125-144.

[4] Mullahy J., *Much ado about two: reconsidering retransformation and the two-part model in health econometrics*. Journal of Health Economics 17, 1998, 247-281.

[5] Weir S., Aweh G., Clark R.E., *Case Selection for a Medicaid Chronic Care Management Program.* Heath Care Financing Review 30 (1), 2008, 61-74.

[6] Winkelman R., Mehmud S., *A Comparative Analysis of Claims-Based Tools for Health Risk Assessment.* A Research Study Sponsored by the Society of Actuaries, 2007.

Minisymposium: Transfer Problems of Statistics and Operations Research

Técnicas de Estadística e Investigación Operativa aplicadas al Ciclo Integral del Agua: planificación y optimización de bombeos

David Ibarra Gómez, Miguel Molina Peralta

Aqua Ambiente Ingeniería de Sistemas (Grupo AGBAR). Calle Beato Diego de Cádiz, 32 Alicante
dibarra@agbar.es, mmolinap@agbar.es

Abstract

Se describe un ejemplo real de la aplicación de técnicas estadísticas y de investigación operativa sobre un bombeo de agua potable. Las técnicas estadísticas tienen que ver con la predicción de consumos de agua y las de investigación operativa con la resolución de un problema de planificación en condiciones de incertidumbre. Para la consecución de los objetivos se han desarrollado e interconectado las herramientas software necesarias para automatizar la toma de decisiones. El resultado de la aplicación se traduce en un ahorro en la factura eléctrica de un veinte por ciento comparado con la estrategía anterior.

27.1 Introducción

Aqua Ambiente es la empresa de Ingeniería y Tecnología dentro del Grupo Agbar. El grupo Agbar es líder en la gestión del ciclo integral del agua en España, además de tener una destacada presencia internacional: México, Cuba, Chile, Colombia, Reino Unido, Argel, Arabia Saudí o China.

Aqua Ambiente está encargada de proporcionar soluciones tecnológicas dentro del ciclo integral del Agua. En este ámbito participamos, sobre todo como implementador tecnológico, en distintos proyectos internacionales que aplican investigaciones realizadas en el mundo del agua.

Presentamos a continuación un ejemplo de aplicación de las matemáticas en nuestro ámbito del ciclo integral del agua.

27.2 Realidad modelada

Habitualmente, las redes de distribución de agua se dividen en sectores para mejorar la eficiencia hidráulica del abastecimiento. Esto permite reducir pérdidas de agua, facilita la localización de incidencias y mejorar los tiempos de localización y reacción frente a las mismas. Normalmente los sectores se alimentan de agua a través de depósitos situados en las zonas más altas, para presurizar la red.

Es en el llenado de este depósito donde se pueden ahorrar costes energéticos. El llenado de estos depósitos se hace mediante bombas que consumen grandes cantidades de energía, y como grandes consumidores, disponen de contratos en los cuales el coste energético es dependiente de la hora de consumo.

Además hay que tener en cuenta otros factores y/o restricciones, entre otros:

- Cumplir las ecuaciones de red o abastecer la demanda, para lo cual hay que conocerla previamente (factor estocástico)
- Respetar los parámetros operación del grupo de bombeo: Si se arranca debe permanecer un tiempo mínimo en marcha que dé tiempo a poner la bomba en régimen, no puede arrancarse demasiadas veces consecutivas para evitar su deterioro, ...
- Calidad: El agua estancada pierde su calidad (cloro)
- El depósito debe mantener un nivel válido operacionalmente

27.3 Predicción de la demanda

A los sistemas de telecontrol que gobiernan el funcionamiento de estas instalaciones llegan medidas de distintos parámetros, en nuestro caso pueden ser interesante el nivel del depósito o el valor leído por el caudalímetro de salida.

Todos estos datos llegan en bruto y están expuestos a diferentes tipos de fallos, como por ejemplo pérdidas de comunicación con el centro de control o fallos en los sensores. Además no tienen porque llegar con una cadencia determinada.

Para poder aplicar técnicas de predicción haciendo uso de series temporales es muy interesante realizar una detección y corrección de estos fallos (missing, outliers), pero además es necesario[1] realizar una regularización de la cadencia de los datos de forma que se entregue una serie temporal regular, por ejemplo una muestra cada 5 minutos.

Se ha programado un proceso automatizado que analiza y corrige todos estos "errores" de forma automática.

Por otro lado, y también de forma desatendida, tomando los últimos datos de la serie "corregida", cada hora se selecciona y ajusta un modelo de series temporales, para producir una predicción con un horizonte a 24 horas vista.

27.4 Estrategía de funcionamiento

Cada hora se calcula la consigna de funcionamiento del bombeo para las siguientes 24 horas utilizando el nivel actual del depósito y la predicción disponible en ese momento, enviándose al autómata que controla el bombeo.

El programa que se resuelve cada hora es un programa lineal entero mixto, que apoyandose en la predicción, entrega las horas de arranque y parada del bombeo para todo el día.

Dado que la predicción suele ser acertada, la planificación inicial no varía para el día, sin embargo la revisión del problema cada hora permite responder a situaciones anómalas como pueda ser un pico inesperado de demanda.

[1] Al menos para las técnicas de series temporales más comúnes

27.5 Aplicación

Todos estos bloques de software se han puesto en funcionamiento, no sólo como herramienta de soporte a la decisión, si no como operador de red automático en un depósito real. El resultado se traduce en un ahorro de un veinte por ciento sobre la factura eléctrica en comparación con el mejor de los métodos anteriores tradicionales.

Además, gracias al servicio de predicción de la demanda se han detectado comportamientos anómalos en la red como son fugas.

27.6 Otros problemas

Esta sección cita someramente otros campos sobre los que se trabaja actualmente. Se pretende despertar el interés y que sirvan como ejemplo de problemas en los que colaborar, por ejemplo para presentar propuestas conjuntas para la obtención de ayudas a nivel nacional o europeo:

- Modelos de envejecimiento/fiabilidad/supervivencia de tuberías (se usan como criterio para la priorización de renovación del patrimonio).
- Detección de fugas en redes hidráulicas.
- Gestión de modelos hidráulicos a nivel global, conjuntos de depósitos.
- Modelización de la cinética del cloro en redes hidráulicas, detección de anomálias.
- Estimación y caracterización por muestreo del consumo de agua.
- Gestión de redes de saneamiento.
- Predicción de lluvias, modelado de cuencas hidráulicas.

Minisymposium: Transfer Problems of Statistics and Operations Research

Crew rostering at passenger rail operators

Mikel Lezaun, Gloria Pérez, Eduardo Sáinz de la Maza
Departamento de Matemática Aplicada, Estadística e Investigación Operativa
Facultad de Ciencia y Tecnología. Universidad del País Vasco
Barrio Sarriena s/n, 48940 Leioa, España
e-mail: mikel.lezaun@ehu.es, gloria.perez@ehu.es, eduardo.sainzdelamaza@ehu.es

Abstract

This presentation revisits projects conducted for Metro Bilbao, *EuskoTren* and FEVE which entailed the modelling and operational resolution of the problem of assigning working days and tasks fairly to employees over the year. At Metro Bilbao and *EuskoTren* the rostering is for train drivers, while at FEVE it is for station personnel. In all three cases, final rostering entails solving various binary programming problems. This is done on a PC running commercially available software.

28.1 Introduction

The assigning of work to drivers at railway passenger service operators is a complex task. Conventionally, it has been done in two phases: in phase one day-to-day work is divided into working days with tasks to be performed individually. These working days must meet a number of requirements in terms of their duration and start/end times. This process is known as *crew scheduling*. As a result the year is divided into two or three seasons, and employees have a pattern of working days that is repeated week by week throughout the period. These seasons are often identified as "summer" and "winter", though summer is sometimes subdivided into "August" and the rest. At all three companies working days are normally divided into three shifts: morning, afternoon and night. Within a single season weekdays are usually all the same, while Saturdays and Sundays are different, though in some cases Fridays may also be different from other weekdays. On the same calendar day there may be different types of working day in terms of tasks and duration, which may run from 6 to 9 hours.

In phase two, lists of working days and rest days are drawn up and assigned to workers. This is known as *crew rostering*. Given that the pattern of working days is repeated week by week in each season of the year, the number of drivers on active duty (neither on vacation nor on standby as replacements) is the same in each week within a season. This means that the most natural rostering system is one in which the lists of working days and rest days are cyclical, and based on a rota drawn up for that purpose. This is known as *cyclic crew rostering*.

This is precisely what is done in the cases of drivers at Metro Bilbao (cf. [5]) and *EuskoTren* (cf. [6]). In the case of FEVE the personnel covered are station personnel, so the rostering process is different (cf. [7]). For one thing, the rota for each station is based on four-month patterns, but this does not entail any major drawbacks because the number of employees at each station is low. For another, it is envisaged that employees can be seconded from one station to another (with provisions to ensure that such secondments and the distances involved in them are minimised) to cover rest days and holidays.

There are not many papers that deal specifically with the cyclic crew rostering problem (CCRP). Caprara et al. ([1]) examine this problem at Italian rail operator Ferroviale dello Stato SpA. Sodhi and Norris ([11]) develop a method for solving the CCRP at the London Underground and Hartog et al. ([4]) do likewise for Netherlands Railways. Esclapés ([3]) provides an overview and an extensive bibliography on rostering problems. Mesquita et al. ([10]) presents an integer mathematical formulation to describe the integrated vehicle-crew-rostering problem. The paper by Ernst et al. ([2]) presents a review of staff scheduling and rostering.

28.2 Assigning of working days to drivers

Working days are assigned to drivers in various stages.

- Assigning of weeks' holidays and standby duty

The first thing that the company does is assign the drivers their weeks of holidays. Once these weeks are distributed, there are more drivers available in each season of the year than required for active duty, so to even out working time Metro Bilbao and *EuskoTren* assign drivers weeks on standby duty, seeking to ensure as far as possible that each has the same number of such weeks over the full year. This is done by setting up and solving a binary programming problem. The same problem also takes into account drivers' preferences as regards the distribution of standby duty weeks (adjacent to holiday weeks or otherwise, in groups of two or three weeks or in single weeks).

- Constructing the rotas

Working days over the year are assigned on the basis of two rotas with weekly multi-shift patterns: one for the winter season and one for the summer. A rota can be seen as a table of rows and columns in which the columns represent the days of the week and the rows are the weekly working patterns of the drivers. The number of rows - i.e. the number of patterns - is equal to the number of drivers on active duty. Each pattern represents the working days and rest days of one driver. The full table shows all the working days in the week. These tables must be such that drivers can run through them week by week, following the table in order and starting again from the first pattern when they complete the last one. It is essential to draw up good rotas if the annual work load is to be distributed evenly among all drivers. And drawing up good tables, especially when they are large, is a complicated problem faced by all passenger rail operators.

There are three types of constraint covering requirements imposed by collective bargaining agreements and workers' preferences. The first set, which only affect each weekly pattern, are the following: each pattern must have between four and six working days; it may not include two working days on the same day of the week; it may not include a morning-shift working day immediately after an afternoon-shift day; it may not include a working day immediately following a night-shift working day; and it may not include single, isolated morning- or afternoon-shift working days. Moreover, there are more Saturday working days than Sunday working days, so if a pattern includes a rest day on a Saturday then the Sunday must also be a rest day, and if there is a morning- or afternoon-shift working day on a Sunday then the Saturday must have a similar working day. The second set comprise constraints that affect two consecutive patterns: if a pattern schedules an afternoon shift on Sunday then the following pattern may not schedule a morning shift on Monday; if a pattern schedules a night shift on Saturday then the following pattern must schedule a rest day on Monday; there may be no isolated morning or afternoon-shift working days in the transition between any two consecutive patterns; no two consecutive patterns may contain more than seven consecutive working days, or two weekends off; there may not be two consecutive patterns with Saturday night shifts; and when alternating between shift types they

must between them have at least one morning shift and one afternoon shift. The third set comprise constraints that affect more than two consecutive pattern: there may not be more than one night shift in four consecutive patterns; there may not be three consecutive patterns with weekends worked; and in every five consecutive patterns there must be at least two weekends off.

The overall construction of these rotas is highly complicated, so they are drawn up in two stages. In phase 1 a simplified version is constructed in which only the type of shift in the working days is maintained. In phase 2 shifts are associated with tasks and their corresponding durations in hours. This second phase is relatively easy to work out using a binary programming program. The main difficulties in phase 1 are due to the need to impose a certain rotation in the table between shift types, weekends worked and weekends off, especially when large numbers of drivers are involved.

Three ways of obtaining rotas of this type can be considered. In the first a rota is obtained by directly setting a binary programming problem that covers all the constraints referring to bargaining agreements (cf. [6]). In the second it is obtained by resolving an integer linear programming problem based on a pre-set catalogue of weekly patterns that comply with the first group of constraints described above. This reduces the constraints to be implemented and mans that this method entails less effort than the previous one. The procedure also assigns weights to patterns so that the most favourable ones are fostered (cf. [5]). The third method entails the least effort in terms of computation. It is broken down into two stages: in stage 1 the patterns that are to make up the table and the transitions from one pattern to another are selected from the catalogue. This is once again done by resolving an integer linear programming problem. In stage 2 the patterns and transitions obtained are used to construct the rota using a program in Visual Basic. Like method 2, this method prioritises certain patterns, but in this case certain transitions from one pattern to another are also prioritised (cf. [11] and [8]). In principle this method enables no more than two consecutive patterns to be controlled, but if the right weights are selected for the transitions, solutions can be obtained that meet the constraints covering three or four consecutive patterns. Using this third method tables can be obtained almost instantaneously, even for large-scale problems. Article [8] compares the three methods.

Once the tables with the types of shift are obtained, a simple binary programming program assigns tasks to shifts, seeking insofar as possible to assign the same tasks to consecutive shifts, and to ensure that the hours worked in weekly patterns are similar.

- Annualised assigning of weekly patterns

Weekly patterns are assigned to drivers on a rota basis, running through the table for each season row by row, taking into account that changes in tables from one season to another must also meet the constraints on consecutive patterns. In these terms, this assignment is highly inflexible. However, some degree of freedom is available in the fact that drivers coming back from holiday or standby duty can be assigned any of the patterns left vacant by those who are taking holidays or moving onto standby weeks, so as to ensure that the annualised work-load of each driver is similar in terms of hours, days, shifts and weekends worked. This is done by drawing up and solving a binary programming problem.

- Correcting assignments for public holidays and local festivals

The annualised assignment of weekly patterns is deployed on a day to day basis to obtain a daily assignment of shifts and rest days. At both Metro Bilbao and *EuskoTren*, services are reduced on public holidays to the level of the Sunday service in the ongoing season. There are also numerous special days during the year, especially during the festivals in honour of local patron saints during the summer, when additional services are run, especially at night. Of course, it is harder to add more services and to reduce them, but in both cases the same strategy and program are used, adapted to suit each circumstance. On days when no changes in services are required the rota is left untouched, and on the others further working days are assigned so that drivers who have a rest day on a public holiday maintain it, and

those who have a working day on a festival day continue to work. The aforementioned constraints must always be observed. Once again, the changes are made by solving a binary programming problem, striving also to maintain or increase the egalitarian nature of the drivers' work-load.

Drivers are entitled to two rest days after a night shift, so the most complicated situation arises on those days when several night-shift working days have to be added. In such cases it is advisable also to modify the assigning of the next two days. Even then, it may not be possible to assign all the shifts required, i.e. the problem may be intractable. To prevent a collapse, fictional drivers are added and assignment of work to those drivers is heavily penalised so that they are assigned work only when it is absolutely unavoidable. In that case, the working days of the fictitious drivers are considered as not covered, and must be worked by drivers on standby duty. Finally, the two Festival Weeks in Bilbao and San Sebastián are special cases. Specific assignments are set up for them and inserted into the annualised assignment.

- Computational results

The integer programming problems are solved using commercially available Lingo software ([9]) on a PC. The problem of standby weeks and the drawing up of rotas with the third method are easy to solve. The biggest problem is the annualised assignment of weekly patterns at the Amara residency at *EuskoTren*. This problem has 96701 integer variables, 221463 constraints and 1012798 non-zero elements. As the requirement for equality in the work-load of drivers begins to become strict, completing the assignment for the full year become a very long process. It was therefore decided to split the year into three parts. CPU time was thus reduced to a total of 9 minutes. The reduction in services on public holidays is a simple problem. The problem of increased services on festival days is handled in daily sections and does not pose any particular difficulty.

28.3 Assigning of working days to station personnel

The annualised assignment of shifts to station personnel is based on tables with a number of cycles equal to the number of employees at each station. These tables cover complete four-week periods running from Monday to Sunday, and contain the working days and rest days for the relevant station. Many different shifts are worked at different stations. Some stations have a single morning and afternoon shift, some have several morning and afternoon shifts, some have a single split shift, some are closed on Saturdays or Sundays, and some have night shifts on Saturdays. At some stations there is a staff surplus, so their patterns are scheduled to contain relief shifts intended to cover shifts left vacant due to rest days or holidays at their home station or at nearby stations. The rotas are agreed with employees and feature working and rest day conditions similar to those described above for drivers.

The four-week patterns are assigned to station personnel on a rota basis (cf. [7]). Each employee must work 13 patterns per year. Once the annualised assignment of patterns is completed, each employee is given 30 working days' holiday. A "working day" is defined for this purpose by whether the agent has a shift assigned to him/her in the initial assignment. Employees must take these 30 days in one full month and one full fortnight, both of which are preset.

Once holidays have been assigned, the shifts that remain vacant must be reassigned to employees on relief shifts. This is done for each 28-day cycle by setting up and solving a binary programming problem so that the assignment meets all the working and rest day conditions agreed, and the distance travelled between stations is as short as possible. To complete the year this binary programming problem must be solved 13 times. In the case of Asturias, the largest geographical area involved, the period which took longest to solve has 411,853 integer variables, 92,484 constraints and 7,257,117 non-zero elements. Lingo ([9]) required two hours of CPU time to solve it.

Bibliography

[1] A. Caprara, M. Fischetti, P.L. Guida, P. Toth and D. Vigo, *Solution of large-scale railway crew planning problems: the italian experience*. In: Wilson N H M (ed.). Computer-Aided Transit Scheduling. Lecture Notes in Economics and Mathematical Systems 471: 1-18, 1999.

[2] A. Ernst, H. Jiang, M. Krishnamoorthy and D. Sier, Staff scheduling and rostering: A review of applications, methods and models, Eur. J. Oper. Res. 153, (2004), 3-27.

[3] C. Esclapés, *Asignación de conductores a jornadas de trabajo en empresas de transporte colectivo*. PhD Thesis, Universitat Politecnica de Catalunya, Spain 2000.

[4] A. Hartog, D. Huisman, E.J.W. Abbink and L.G. Kroon, Decision support for the crew rostering at NS, Public Transp. 1, (2009), 121-133.

[5] M. Lezaun, G. Pérez and E. Sáinz de la Maza, Crew rostering problem in a public tranport company, J. Oper. Res. Soc. 57, (2006), 1173-1179.

[6] M. Lezaun, G. Pérez and E. Sáinz de la Maza, Rostering in a rail passenger carrier, J. Scheduling 4-5, (2007), 245-254.

[7] M. Lezaun, G. Pérez and E. Sáinz de la Maza, Staff rostering for the station personnel of a railway company, J. Oper. Res. Soc. 61, (2010), 1104-1111.

[8] M. Lezaun and E. Sáinz de la Maza, The Railway Cyclic Crew Rostering Problem, *in preparation*.

[9] Lindo Systems Inc., *Lingo User's Guide*, Chicago 2003.

[10] M. Mesquita, M. Moz, A. Paias, P. Paixão, M. Pato and A. Respicio, A new model for the integrated vehicle-crew-rostering problem and a computacional study on rosters, J. Scheduling (2010), DOI 10.1007/s10951-010-0195-8.

[11] M. Sodhi and S. Norris, A Flexible, Fast, and Optimal Modeling Approach Applied to Crew Rostering at London Underground, Ann. Oper. Res. 127, (2004), 259-281.

Minisymposium: An experience on transfer within the CENIT program: numerical simulation of electrical machines

Design methodology for multipolar PM machines

G. Almandoz*, J. Poza*, G. Ugalde*, A. Escalada+
* University of Mondragon/Faculty of Engineering, Mondragon, (Spain)
+ ORONA Elevator Innovation Centre, Hernani, (Spain)
galmandoz@mondragon.edu, jpoza@mondragon.edu, gugalde@mondragon.edu, aescalada@orona.es

Abstract

This work is part of the mini-symposium: Transfer experience within the Cenit program: Numerical simulation of electric machines. The purpose of this mini-symposium is to show a transfer experience within a Cenit project framework: Lifting Technology Research "Net Zero" (NET0LIFT). This is an interdisciplinary project funded by the Basque company Orona and supported by the Ministry of Science and Innovation through the CDTI. Orona is a leading group of international standing in the European market whose business focuses on the design, manufacture, installation, maintenance and modernization of mobility solutions, such as elevators. The goal of the project was the development of technology aimed at achieving "a sustainable lift" (zero energy elevators), with the participation of several companies, universities and institutions. In particular, the task assigned to the Electrical Machines research team of the University of Mondragon was aimed at developing advanced design methodologies for permanent magnet synchronous machines.

29.1 Introduction

In the last years, computer aided electric machine designs are becoming more attractive. Analytical and numerical software oriented to the electromagnetic and thermal design of electric machines are involved in a continuous development. The technological progress of personal computer and powerful work stations that are able to deal with large amount of computation load in relatively short time periods, make computer aided designs to grow substantially. Some authors prefer to develop their own analytical and numerical tools instead of using commercial software solutions. That provides more flexibility in the sense that it is possible to manipulate the design tools in order to adequate them for the requirements of each design process.

Generally almost all of the electric machine designs found in the literature combine analytical tools with numerical tools based on the Finite Element Method (FEM) [1], [2]. These tools are rather extended among electric machine designers. However the rate of utilization and the interaction between them are not well defined. Although there are some authors who define a specific design methodology for PM machines [3], [4], actually there is a significant lack of scientific contributions in this matter.

In order to fulfil this scientific need, the main contribution of this research work is the definition of a design methodology for PM machines. The next are the main characteristics or goals of the proposed design methodology:

- The design methodology combines analytical design tools along with numerical tools based on the FEM

- The grade of interaction between different design tools is defined for each design stage
- Different physical phenomena such as electromagnetic, thermal and mechanical phenomena are considered all together, taking into account the interactions between them.

As shown in the Fig. 29.1, the proposed design methodology is structured mainly in three steps:

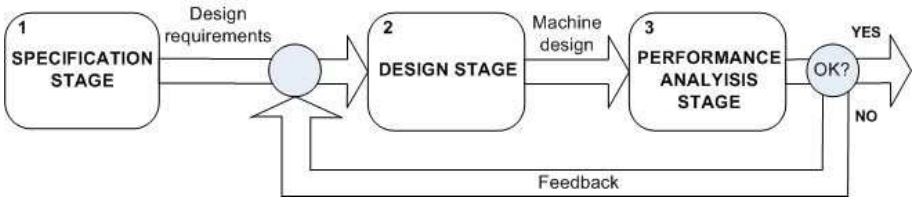

Figure 29.1: Main block diagram of the proposed design methodology

- Specification Stage: Analysis of the application and identification of the design requirements
- Design Stage: Design of the electric machine
- Performance analysis Stage: Experimental evaluation of machine performances and validation of the machine design for the application

29.2 Specification Stage

The first stage consists in the identification of the design requirements for the electrical machine and it is described in the Fig. 29.2. For that purpose, the application is analyzed in depth taking into account different operation aspects such as the speed vs. torque requirement, transient and continuous functioning conditions or working cycles.

The motor performance can be strongly influenced by the converter in the sense that the current ripple caused by chopped voltage can increase the magnetic losses and the harmonic content of the torque ripple. The inverter topology, the DC bus voltage level or the switching frequency of semiconductors are some of the important characteristics of the power supply to take into consideration.

29.3 Design Stage

The design stage of the electrical machine is an iterative process which is carried out in 4 steps (Fig. 29.3). In the first stage an initial electromagnetic design for the motor is performed using basic design sizing equations. This pre-design consists in the selection of the adequate topology, the sizing of the machine and the design of electric and magnetic circuits.

In the second stage the initial machine design is optimized by advanced analytic tools. The electromagnetic optimization is performed using mathematical models of PM machines based on Fourier series [5]. The electromagnetic model of the machine based on Fourier series is a very useful tool to evaluate the influence of certain design parameters on the performance of the machine, in a relatively fast and easy way. This feature is possible because the spatial variables, which are defined as the sum of spatial

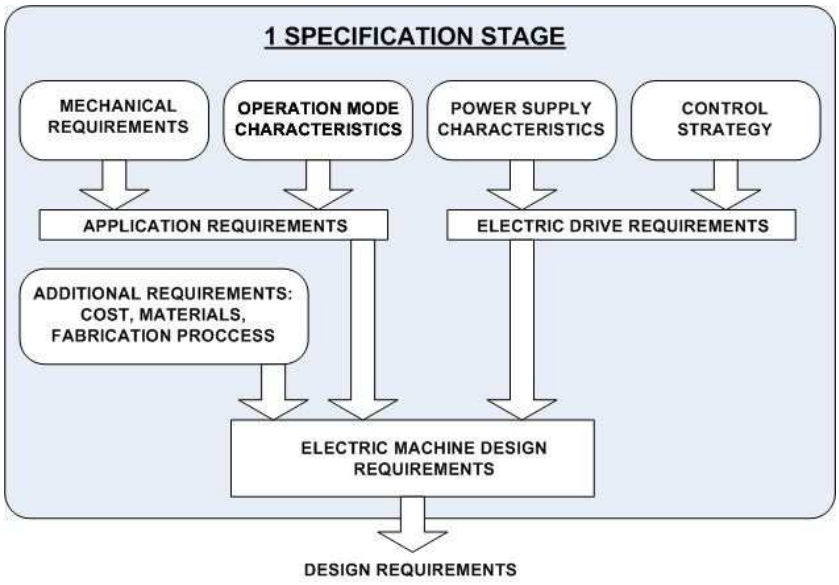

Figure 29.2: Block diagram of the specification stage

components, are related to different design parameters. In this second step, there is a strong interaction between electromagnetic and thermal simulations. Magnetic properties of the magnets or electric properties of the copper are strongly influenced by the temperature. This interaction between electromagnetic and thermal phenomena cannot be neglected, so it is necessary to deal with them together.

In the third step, the higher level optimization of the design is carried out. In the first two steps the machine is designed approximately in 80%. After that, the machine design is adjusted by high accuracy numerical tools based on the FEM. Non-linear phenomena caused by saturations which are complicated to implement in analytic models are evaluated in this stage. The effects of the stator slots, which can be significant depending on the machine configuration, or the iron losses are evaluated accurately.

Finally, the iterative design process concludes with the performance evaluation of the machine. Numerical and analytical tools are combined in this design stage. The electromagnetic performance of the machine in terms of torque capability and quality or induced electro-motive force is evaluated and the lumped parameters of the electrical equivalent circuit are obtained using the FEM [6]. Moreover, the thermal behavior of the machine is evaluated under the operation mode imposed by the application, considering the working cycles and the losses increase caused by the Pulse Width Modulation (PWM) voltage depending on its switching frequency and modulation index. In this stage multi-physic co-simulations are also proposed as a useful tool to study the behavior of the whole drive system. Using this kind of tools it is possible to identify possible interactions between the different elements such as the inverter, the electric machine or the mechanical system which comprise the overall application. The usefulness and some examples of multi-physic simulations are reported in [7].

29.4 Conclusions

In this paper a design methodology for the PMSM is presented. This methodology is based on the combination of analytical and numerical tools. The rate of utilization of analytical and numerical tools is distributed in such a way that the majority of the iterative design process is carried out by analytical

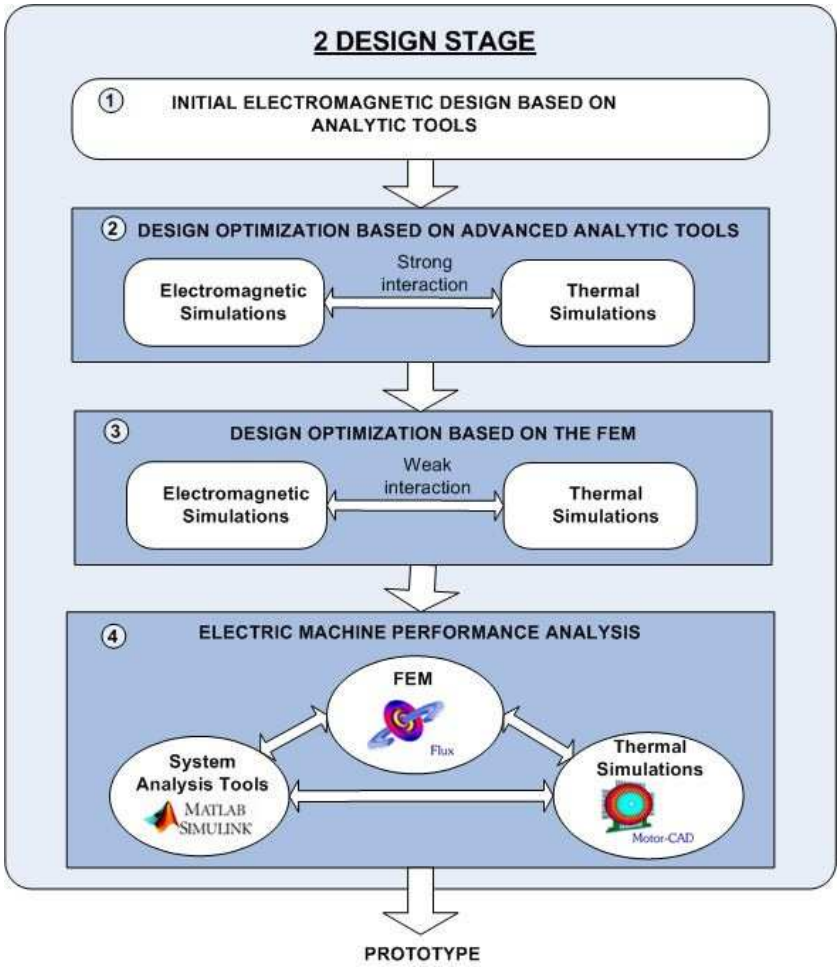

Figure 29.3: Block diagram of the design stage

tools. This way the time consumption of the process is reduced substantially. Then numerical tools are used to optimize the design and to evaluate and to validate the final performance of the machine design.

This design methodology allows reducing the number of prototypes before obtaining an industrial solution.

Bibliography

[1] C. Schlensok, M. H. Gracia, K. Hameyer, Combined Numericalal and Analytical Method for Geometry Optimization of a PM Motor, *IEEE Transactions on Magnetics*, 42 (4), (2003), 1211-1214.

[2] F. Libert,J. Soulard, Design Study of Low Speed Direct Driven Permanent Magnet Motors With Concentrated Windings, 6th International Symposium on Advanced Electromechanical Motion Systems, ELECTROMOTION, 2005.

[3] Z. Makni, M. Besbes, C. Marchand, Multiphysics Design Methodology of Permanent-Magnet Synchronous Motors, *IEEE Transactions on Vehicular Technology*, 56 (4), (2007), 1524-1530.

[4] L.Gasc, S.Astier, M.Fadell, L.Calegari, Design to modeling of Permanent Magnet Motors, International Conference on Electrical Machines, ICEM 2002.

[5] G. Almandoz, J. Poza, M. A. Rodriguez, A. Gonzalez, Analytic Model of a PMSM Considering Spatial Harmonics, International Symposium on Power Electronics, Electrical Drives, Automation and Motion SPEEDAM 2008.

[6] G. Almandoz, J. Poza, M. A. Rodriguez, A. Gonzalez, Modelling of Cross-Magnetization Effect in Interior Permanent Magnet Machines, International Conference on Electrical Machines, ICEM 2008.

[7] G. Almandoz, J. Poza, M. A. Rodriguez,A. Gonzalez, Co-Simulation Tools for the Permanent Magnet Machine Design Oriented to the Application, in EUROCON 2007.

Minisymposium: An experience on transfer within the CENIT program: numerical simulation of electrical machines

Losses computation in laminated magnetic cores

A. Bermúdez, D. Gómez, P. Salgado
Departamento de Matemática Aplicada. Universidade de Santiago de Compostela. Spain
{alfredo.bermudez,mdolores.gomez,mpilar.salgado}@usc.es

Abstract

This work is part of the mini-symposium: *Transfer experience within the Cenit program: Numerical simulation of electric machines*. The purpose of this mini-symposium is to show a transfer experience within a Cenit project framework: *Lifting Technology Research "Net Zero" (NET0LIFT)*. This is an interdisciplinary project funded by the Basque company Orona and supported by the Ministry of Science and Innovation through the CDTI. Orona is a leading group of international standing in the European market whose business focuses on the design, manufacture, installation, maintenance and modernization of mobility solutions, such as elevators. The goal of the project was the development of technology aimed at achieving "a sustainable lift" (zero energy elevators), with the participation of several companies, universities and institutions. In particular, the task assigned to the USC research group was aimed at developing mathematical tools adapted to the electromagnetic and thermal analysis performed in the design stage. This presentation deals with the first of these objectives.

30.1 Introduction

An important practical challenge when designing electrical machines is to develop methods of predicting power losses in the core of the device. These losses are traditionally known as iron losses and are due to the fact that the magnetic field variations in the ferromagnetic materials produce energy dissipation. Traditionally, iron losses computation was based on data sheets provided by the manufactures where total core losses density are given for typical values of the flux density $\mathbf{B}$ and the frequency f. However, in practical applications, the operating conditions as well as the geometry are often different from those of the data sheets and then numerical simulation becomes important. In the last years, there has been a vast amount of research in this field and it is an up-to-date topic of great interest both from industrial and academic points of view. On the one hand, for producers seeking to improve the properties of materials; on the other hand, for manufacturers of electrical machines, with a view to choosing a material for optimizing the size, and the limitation of losses in order to avoid anomalous heating of the machine and the wider attention to the problem of energy saving as a global index of the device quality. From the academic point of view, the interest is mainly focused on the modeling of the electromagnetic phenomena and the ferromagnetic materials behavior.

At the macroscopic level, the total iron losses are the sum of two main components: the *hysteresis losses* and the *eddy-current losses*. Hysteresis losses are due to the intrinsic nature of the ferromagnetic materials and it is related to the fact the relationship between the magnetic induction $\mathbf{B}$ and the magnetic field $\mathbf{H}$ is not only non-linear but also depends on the history of the magnetic field. The main characteristic of this fact is the observation of the so-called hysteresis loops (see Fig. 30.1). One of the most complicated problems is just the modeling of the hysteresis and its inclusion in numerical

methods. Even if there exist some mathematical models which deal with this phenomena, the problem is still open (see, for instance, [14]). Most of commercial finite element codes use a one-to-one relationship between $\mathbf{B}$ and $\mathbf{H}$ based on different approaches and calculate the losses from the magnetic flux density by using an a posteriori hysteresis model.

Our work was mainly concerned with the computation of the eddy current losses. These losses are essentially due to the Joule effect from eddy currents induced in the material by time-varying magnetic flux. Their power density at point $\mathbf{x} = (x, y, z)$ and time t are given by $\sigma^{-1}|\mathbf{J}(\mathbf{x}, t)|^2$ where σ denotes the electrical conductivity of the material and $\mathbf{J}$ is the current density. In order to compute the magnetic field an eddy current model in a 3-D domain including the device and the air around it should be solved. Numerical computation of eddy currents by using the Maxwell quasi-static partial differential equations is now a well established subject, even in the 3-D where edge finite elements are very useful (see for instance [3] and references therein). In this case, the main difficulty comes from the fact that the domain is a laminated media in order to reduce the eddy-currents so discretizing each sheet along its thickness is computationally unnafordable. In the last decades a great number of papers have been devoted to develop numerical methods [8, 9, 14] or approximate formulas [4, 10, 12] for the computation of both hysteresis and eddy current losses. In industrial applications, some authors propose simplified 2D methods combined with classical analytical formulas to compute the eddy current losses which are only valid under certain assumptions. Then the losses computation is carried out applying these analytical formulas to fields that have been experimentally measured or numerically computed. This is the case of some commercial packages.

30.2 Computation of losses: developed tools and obtained results

One of the objectives of our work was the determination of a simple analytical expression to calculate the magnetic losses in soft ferromagnetic materials. The most employed model in the work published over the last decades is based on that developed by Bertotti ([4, 5, 10], where the specific iron losses are a summation of hysteresis, classical eddy-current and excess (or anomalous) losses. The formula involves several coefficients (assumed to be constant) which are determined from the measured data for a certain frequency by using the least square method. Nevertheless, the results obtained using this model illustrate the fact that, in some cases, the loss coefficients need to be dependent of both flux density and frequency and that the usual approach of constant coefficients can lead to unpredictable and significant numerical errors. The search for alternative formulas was carried out following some requirements established by our partners from the Mondragon University. In particular, the coefficients of the different terms involved in the losses should depend on frequency f and magnetic induction $\mathbf{B}$. Moreover, the formula should be valid for arbitrary operating voltages, and in particular, for Pulse With Modulated (PWM) voltages (see Fig. 30.1). Once the formula was established, the next step was to develop a Matlab code that implements the selected formula and allows the calculation of the total losses from the magnetic induction field calculated with the commercial package Flux2D®. Finally, we should compare the losses thus calculated with those provided by other methods implemented in commercial packages and, in particular, with the Loss Surface Model [7] implemented in Flux2D®.

After an exhaustive bibliographical review, the formulas proposed by Mthombeni and Pillay [12] for the case of harmonic excitations, and Boglietti et al. [6], for the case of PWM excitations, were selected. In particular, the authors in [6] use a model where classical and anomalous losses are grouped into an eddy-current loss term and both hysteresis and eddy-current loss coefficients are allowed to vary with frequency level and induction. The effect of the PWM supply voltage over the core losses is modeled using factors that depend on the average rectified and rms voltage values. However, just as happens

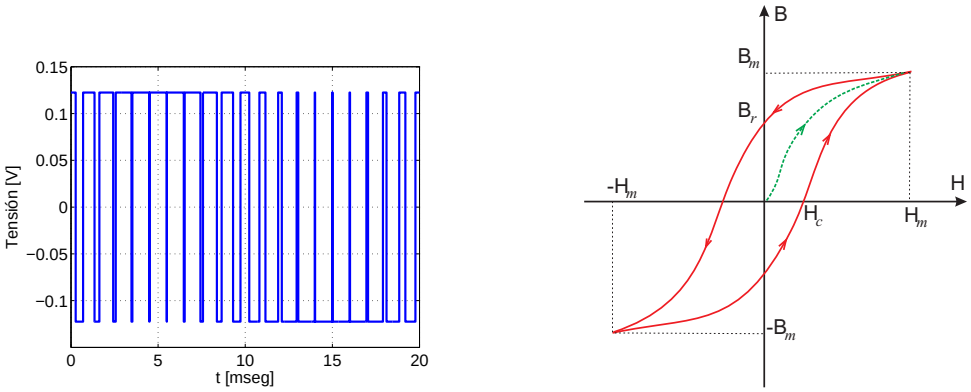

Figure 30.1: PWM tension (left) and example of hysteresis curve (right)

with most of the formulas found in the literature, the model does not account either for skin effect or for the so-called minor hysteresis loops. Even if this formula is also valid for harmonic excitations, in this case the one developed in [12] is better since more adjusting parameters are involved.

Parallel to the development of this task other works were carried out. In particular, we were interested in comparing the eddy-current losses provided by these simplified methods with the "exact" values obtained by numerical simulation. Thus, a transient non linear eddy current model based on Maxwell's equations was considered. In order to be able to make accurate numerical simulations of a true 3-D domain, we assume axisymmetrical toroidal geometry in the model as the one represented in Fig. 30.2. It consists of N sheets of rectangular section and thickness d and we have denoted by R_1 and R_2 the internal and external radius of the core, respectively. Let n_e be the number of turns of the coil and $I(t)$ the current intensity at time t. The coil will be considered as infinitely thin so it will be modeled as a surface current. We use cylindrical coordinates in order to exploit the cylindrical symmetry of the problem. In particular, both the magnetic and the induction fields have only azimuthal components, here denoted by H_θ and B_θ, respectively. It is not difficult to prove that, in this case, it is possible to write exact boundary conditions on the surface of each sheet and hence to solve the problem in a meridian section $\Omega = [R_1, R_2] \times [0, d]$ of it with a fine mesh. The problem to be solved is the following one

$$\frac{\partial B_\theta}{\partial t} - \frac{\partial}{\partial r}\left(\frac{1}{\sigma r}\frac{\partial (r H_\theta)}{\partial r}\right) - \frac{\partial}{\partial z}\left(\frac{1}{\sigma}\frac{\partial H_\theta}{\partial z}\right) = 0 \ \text{ in } (0,T)\times\Omega, \tag{30.1}$$

$$B_\theta(r,z,t) \in \mathcal{B}(r,z,H_\theta(r,z,t)) \text{ a.e. in } (0,T)\times\Omega, \tag{30.2}$$

$$H_\theta = n_e\, I(t)/(2\pi r) \ \text{ in } (0,T)\times\partial\Omega, \tag{30.3}$$

$$B_\theta(r,z,0) = B_0(r,z) \ \text{ in } \Omega, \tag{30.4}$$

where $I(t)$ and B_0 are given data. The non-linear behavior of the material is defined through its anhysteretic B-H curve which can have very high slope or even to be multi-valued. This fact is expressed by equation (30.2), where $\mathcal{B}(r,z,\cdot)$ stands, for a.e. (r,z), a (possibly multi-valued) non-linear mapping in $\mathbb{R}$. In [2], a numerical method to solve this transient problem based on a finite element method combined with the implicit Euler time discretization and an iterative algorithm to handle the nonlinear term is proposed. The results show that, for harmonic excitation sources and at high frequency, the skin effect can be important and in this case the analytical expressions could overestimates the eddy-current losses (see [2] for details).

In practical situations it is not so easy to define the eddy current problem in a laminated media because we do not know the value of the magnetic field on the surface of the sheet in terms of the source current.

Figure 30.2: Toroidal laminated magnetic core (left) and sketch of its radial section (right)

This lack of boundary conditions has led to several authors to introduce different methods to compute eddy-current losses in laminates based on solving 2-D or 3-D electromagnetic problems which avoid the discretization of each sheet along its thickness. Some of them are based on the concept of equivalent conductivity (see, for instance, [11]). The idea is to replace the laminated cores with a homogeneous media having either isotropic or anisotropic conductivity. In this sense, other task developed along the project was to analyze, in a linear harmonic case, some methods and formulas existing in the literature to determine an equivalent electric conductivity and to compare their accuracy against the values obtained by solving the exact model by numerical methods. (see [1] for details).

30.3 New research lines

As a consequence of the works described in previous section some new research lines have been opened in the group. The main one is the inclusion of a hysteresis model in a finite element method for numerical simulation of electrical machines. This problem is being addressed by a PhD student. On the other hand the group experience in mathematical and numerical analysis of electromagnetic problems, leads us to think that this is a field where we could make interesting contributions.

Finally, in [2] the authors also show how to solve the eddy-current problem in case where the source is given by the voltage instead of the current intensity. Of particular difficulty is the case of PWM voltage supply, because it is a discontinuous function with great number of discontinuities in each period, thus requiring the use of very small time steps and thereby a great computational cost (see Fig. 30.1). The problem is more serious because the calculation of losses requires to obtain the stationary electromagnetic field corresponding to a periodic PWM potential source which, in principle, is only reached after simulating a certain number of cycles unless the initial intensity is properly chosen. One of the objectives of present work is to introduce a procedure to calculate the initial intensity corresponding to the periodic solution thus allowing to integrate the equations along just one period.

Bibliography

[1] A. Bermúdez, D. Gómez, P. Salgado, Eddy-current losses in laminated cores and the computation of an equivalent conductivity, *IEEE Trans. Magn.*, 44 (12), (2008), 4730–4738.

[2] A. Bermúdez, D. Gómez, P. Salgado, Numerical solution of transient non-linear axisymmetric eddy-current models, *In preparation*.

[3] A. Bermúdez, B. López-Rodríguez, R. Rodríguez, P. Salgado, Numerical solution of transient eddy current problems with input current intensities as boundary data. *To appear in IMA J. Numer. Anal.*

[4] G. Bertotti, General properties of power losses in soft ferromagnetic materials, *IEEE Trans. Magn.*, 24 (1), (1988), 621–630.

[5] G. Bertotti, *Hysteresis in Magnetism*, Academic Press, San Diego. 1998.

[6] A. Boglietti, A. Cavagnino, M. Lazzari, M. Pastorelli, Predicting iron losses in soft magnetic materials with arbitrary voltage supply: An engineering approach, *IEEE Trans. Magn.*, 39 (2),(2003), 981-989.

[7] T. Gautreau, *Estimation des pertes fer dans les machines électriques*. Thèse de Doctorat. Institut National Polytechnique de Grenoble. 2005.

[8] P. Dular, J. Gyselinck, L. Kräenbühl A time-domain finite element homogenization technique for laminated stacks using skin effect sub-basis functions, *COMPEL*, 25 (1), (2006), 6–16.

[9] L.R. Dupré, O. Bottauscio, M. Chiampi, M. Repetto Modeling of electromagnetic phenomena in soft magnetic materials under unidirectional time periodic flux excitations, *IEEE Trans. Magn.*, 35(5), 4171–4184, (1999).

[10] F. Fiorillo, A. Novikov, An improved approach to power losses in magnetic laminations under nonsinusoidal induction waveform, *IEEE Trans. Magn.*, 26 (5), (1990), 2904-2910.

[11] P. Hahne, R. Dietz, B. Rieth and T. Weiland, "Determination of anisotropic equivalent conductivity of laminated cores for numerical computation", *IEEE Trans. Magn.*, 32 (3), (1996) 1184–1187.

[12] T.L. Mthombeni, P. Pillay, Physical basis for the variation of lamination core loss coefficients as a function of frequency and flux density, IECON, France, 2006.

[13] K. Preis, O. Biro, I. Ticar, FEM analysis of Eddy Current Losses in Nonlinear Laminated Iron Cores, *IEEE Trans. Magn.*, 41 (5), (2005), 1412-1415.

[14] R. Van Keer, L. Dupré, J. Melkebeek, Computational methods for the evaluation of the electromagnetic losses in electrical machinery, *Arch. Comp. Meth. Eng.*, 5 (4), (1999), 385-443.

Minisymposium: An experience on transfer within the CENIT program: numerical simulation of electrical machines

An application of the Galerkin lumped parameter method for electric machines

A. Bermúdez, F. Pena

Departamento de Matemática Aplicada, Universidade de Santiago de Compostela, 15782 Santiago de Compostela, Spain
alfredo.bermudez@usc.es, fran.pena@usc.es

Abstract

This work is part of the mini-symposium: *Transfer experience within the CENIT program: Numerical simulation of electric machine*s. The purpose of this mini-symposium is to show a transfer experience within a CENIT project framework: Lifting Technology Research "Net Zero" (Net0lift). This is an interdisciplinary project funded by the Basque company ORONA COO. The main objective is the thermoelectrical simulation of electrical machines in order to optimize its performance.

In this work we show an application of a Galerkin lumped parameter method (GLPM) to simulate the thermal behavior of an electric motor, assuming that the electric losses are known. In GLPM, the domain is decomposed into several sub-domains and a time-independent adapted reduced basis is calculated solving elliptic problems in each sub-domain. The method solves the Galerkin approximation of the original problem in the space spanned by this basis. This approach is useful for electric motors, since the decomposition into several pieces is natural. A practical implementation of this method is described and numerical results are shown.

31.1 Introduction

In this work we are interested in the thermal modeling of an electric motor. This type of machines are composed of a large amount of pieces, each of them can be made of a different material. The GLPM, introduced in [1], takes advantage of this decomposition to calculate a reduced basis adapted to it. Since the basis is time-independent, it remains unchanged when the source heat varies with time. Therefore, GLPM can present an advantage in time calculation respect to the classical Galerkin methods.

Besides, the classical lumped parameter method used in heat transfer in electric machines exchanges the computational domain by a network that represents the main heat transfers paths (see, for instance, [2], [5]). The geometrical information of each piece is reduced to a parameter called 'capacitance'. In contrast, GLPM constructs the reduced basis solving a Galerkin approximation of weak formulations of the original distributed parameter problem.

Techniques for reduced-order modeling like proper orthogonal decomposition ([3]) and reduced basis methods ([4]) are similar to the GLMP method. While these methods are particularly useful for optimization, the main goal of GLPM is to solve time dependent partial differential equations by reducing them to lumped parameters models.

31.2 Statement of the problem

Let us consider a body Ω whose boundary Γ is divided into three parts:

- $\Gamma^P = \cup_{l=1}^{n^P} \Gamma_l^P$ are the *ports*, i.e., the surfaces of the domain that connect two or more sub-domains. We assume that each Γ_l^P is a connected component of Γ^P.
- $\Gamma^C = \cup_{l=1}^{n^C} \Gamma_l^C$ are the *convective boundaries*, where to apply convective heat transfer conditions.
- Γ^A, are the isolated surfaces.

Now, we introduce the following transient heat transfer problem in Ω:

Find the temperature field $\theta(x,t)$ satisfying

$$\rho\, c\, \frac{\partial \theta}{\partial t} \,-\, \mathrm{div}(k\, \mathbf{grad}\, \theta) = f \quad \text{in } \Omega \times [0,T], \tag{31.1}$$

$$\theta(x,t) = \theta_l^P(x,t) \text{ on } \Gamma_l^P,\ l = 1, \ldots, n^P, \tag{31.2}$$

$$k\, \frac{\partial \theta}{\partial \mathbf{n}}(x,t) \,+\, \alpha_l(\theta(x,t) - \theta_l^C(x,t)) = 0 \text{ on } \Gamma_l^C,\ l = 1, \ldots, n^C, \tag{31.3}$$

$$k\, \frac{\partial \theta}{\partial \mathbf{n}} = 0 \text{ on } \Gamma^A, \tag{31.4}$$

$$\theta(x,0) = \theta_0(x) \quad \text{in } \Omega. \tag{31.5}$$

Instead of solving the previous problem by a classical finite element method, we will take an alternative approach, which is very popular in some engineering areas like electromagnetism or thermal analysis. The idea is to employ the so-called *lumped parameters models* and to look for approximate solutions in a very low dimension approximation space. This model requires the choose of a reduced adapted basis.

31.3 The reduced basis adapted to the domain decomposition

In order to calculate the reduced basis, we decompose domain Ω into sub-domains Ω_i, $i = 1, \ldots, N$, connected among them through boundaries called *ports*. Thus, in the boundary of each sub-domain Ω_i, called Γ_i, we distinguish three parts: *the ports*, $\Gamma_i^P = \bigcup_{j=1}^{n_i^P} \Gamma_{ij}^P$, *the convective boundary*, $\Gamma_i^C = \bigcup_{j=1}^{n_i^C} \Gamma_{ij}^C$, and the *the isolated boundary*, Γ_i^A.

The basis for the i-th sub-domain consists of $n_i^P + n_i^C$ elements, to be called $\varphi_{ij}^P :\ j = 1, \cdots, n_i^P$, and $\varphi_{ij}^C :\ j = 1, \cdots, n_i^C$ which are defined as the unique solutions to the following stationary boundary-value problems:

- *For $i = 1, \cdots, N$ and $j = 1, \cdots n_i^P$ find $\varphi_{ij}^P \in H^1(\Omega_i)$ satisfying,*

$$-\,\mathrm{div}(k\, \mathbf{grad}\, \varphi_{ij}^P) = 0 \quad \text{in } \Omega_i, \tag{31.6}$$

$$\varphi_{ij}^P(x) = \delta_{jl} \text{ on } \Gamma_{il}^P,\ l = 1, \ldots, n_i^P, \tag{31.7}$$

$$k\, \frac{\partial \varphi_{ij}^P}{\partial \mathbf{n}} \,+\, \alpha_l \varphi_{ij}^P = 0 \text{ on } \Gamma_{il}^C,\ l = 1, \ldots, n_i^C, \tag{31.8}$$

$$k\, \frac{\partial \varphi_{ij}^P}{\partial \mathbf{n}} = 0 \text{ on } \Gamma_i^A. \tag{31.9}$$

- *For* $i = 1, \cdots, N$ *and* $j = 1, \cdots n_i^C$ *find* $\varphi_{ij}^C \in H^1(\Omega_i)$ *satisfying,*

$$-\operatorname{div}(k\,\mathbf{grad}\,\varphi_{ij}^C) = 0 \quad \text{in } \Omega, \tag{31.10}$$

$$\varphi_{ij}^C(x) = 0 \text{ on } \Gamma_{il}^P,\ l = 1, \ldots, n_i^P, \tag{31.11}$$

$$k\,\frac{\partial \varphi_{ij}^C}{\partial \mathbf{n}} + \alpha_l(\varphi_{ij}^C - \delta_{jl}) = 0 \text{ on } \Gamma_{il}^C,\ l = 1, \ldots, n_i^C, \tag{31.12}$$

$$k\,\frac{\partial \varphi_{ij}^C}{\partial \mathbf{n}} = 0 \text{ on } \Gamma_i^A. \tag{31.13}$$

Thus, the approximation space to functions defined in the whole domain Ω is composed by two types of functions:

- the elements w_l^P that coincide with φ_{ij}^P in Ω_i when the l-th global port is the j-th local port of Ω_i and is zero otherwise;
- the elements w_l^C that coincide with φ_{ij}^C in Ω_i when the l-th global convective boundary is the j-th local convective boundary of Ω_i and is zero otherwise.

Let us call $\mathcal{V} \subset H^1(\Omega)$ the linear space spanned by the above set of $n^P + n^C$ functions. The lumped parameter model is defined as the Galerkin approximation of the weak formulation of problem (31.1)–(31.5) corresponding to this basis, namely,

LP. *For* $t \in [0, T]$, *find* $\tilde{\theta}(., t) \in \mathcal{V}$ *satisfying*

$$\int_\Omega \rho\, c\, \frac{\partial \tilde{\theta}}{\partial t}\, \tilde{\psi}\, dx + \int_\Omega k\ \mathbf{grad}\,\tilde{\theta} \cdot \mathbf{grad}\,\tilde{\psi}\, dx + \sum_{l=1}^{n^C} \int_{\Gamma_l^C} \alpha_l\ \tilde{\theta}\ \tilde{\psi}\ d\Gamma$$

$$= \int_\Omega f\tilde{\psi}\, dx + \sum_{l=1}^{n^C} \int_{\Gamma_l^C} \alpha_l\ \tilde{\theta}_i^C\ \tilde{\psi}\, d\Gamma\ \forall \tilde{\psi} \in \mathcal{V} \tag{31.14}$$

$$\tilde{\theta}(x, 0) = \tilde{\theta}_0(x) \ \text{ in } \Omega, \tag{31.15}$$

where $\tilde{\theta}_0$ denotes a projection of the initial condition θ_0 on the space $\mathcal{V}$.

By writing

$$\tilde{\theta}(x, t) = \sum_{l=1}^{n^P} \theta_l^P(t) w_l^P(x) + \sum_{l=1}^{n^C} \theta_l^C(t) w_l^C(x),$$

problem (31.14), (31.15) becomes an ordinary differential system of dimension $n^P + n^C$. Here, θ_l^P and θ_l^C denote the temperature at the ports and the convective boundary, respectively.

31.4 Numerical results

The GLPM has been implemented by using Matlab. The program consists of two parts, that can be executed independently: in the first one, functions φ_{ij}^P and φ_{ij}^C are calculated as solution of systems (31.6)–(31.9) and (31.10)–(31.13); in the second one, function $\tilde{\theta}$ is calculated as solution of an ordinary differential system of equations equivalent to (31.14)–(31.15).

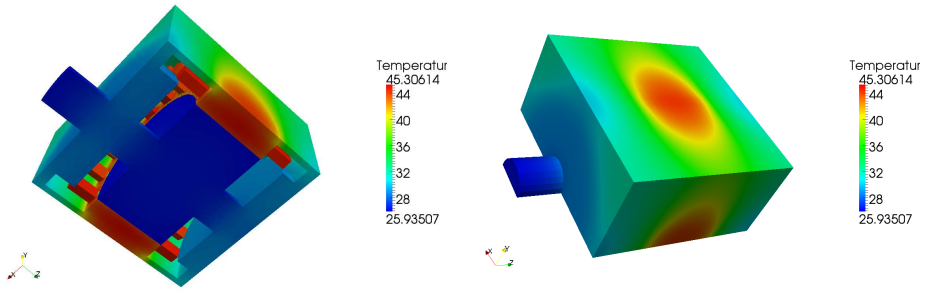

Figure 31.1: Solution calculated by the finite element method.

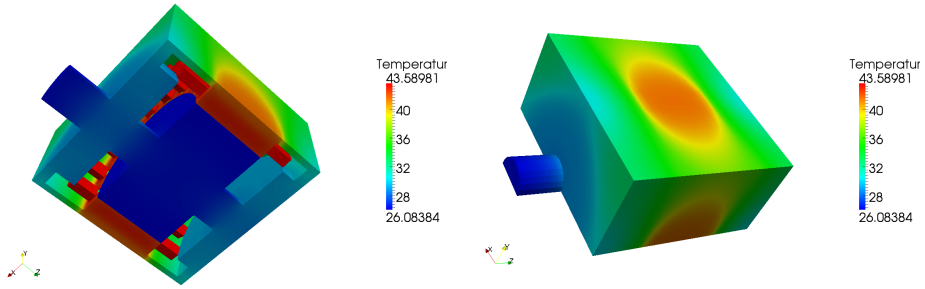

Figure 31.2: Solution calculated by the lumped parameter method.

A comparison between the lumped parameter method and the classical finite element method has been carried out in a electric motor, designed by the University of Mondragon and the Orona company.

Figure 31.1 shows the solution of the finite element method , whereas Figure 31.2 shows the solution of the lumped parameter method at time same time. We have compared the solution obtained by the finite element method with the one of the GLPM. The relative error in the $L^2([0,T];\Omega)$ norm was 2.056%.

Bibliography

[1] Bermúdez, A. and Pena, F. Galerkin lumped parameter methods for transient problems, To appear in Int. J. Numer. Meth. Engng.

[2] Boglietti, A.; Cavagnino, A.; Staton, D,; Shanel, M.; Mueller, M. and Mejuto, M. Evolution and Modern Approaches for Thermal Analysis of Electrical Machines, IEEE Trans. on Ind. Electronics 56 (3), (2009), 871–882.

[3] Kunisch, K.; Volkwein, S. Galerkin proper orthogonal decomposition methods for parabolic problems, Numer. Math. 90 (1), (2001), 117–148.

[4] Maday, Y.; Ronquist, M. A reduced-basis element method, J. Sci. Comput. 17 (1–4), (2002), 447-459.

[5] Quarteroni, A.; Valli, A., *Numerical Approximation of Partial Differential Equations*. Springer-Verlag Berlin Heidelberg. 2008.

Posters

Logistic management in a livestock feed cooperative: model, heuristic, and case study

Mikel Álvarez Mozos
Department of Statistics and Operations Research, University of Santiago de Compostela
mikel.alvarez@usc.es

María Luisa Carpente Rodríguez
Department of Mathematics, University of La Coruña
luisacar@udc.es

Balbina Virginia Casas Méndez
Department of Statistics and Operations Research, University of Santiago de Compostela
balbina.casas.mendez@usc.es

Manuel Alfredo Mosquera Rodríguez
Department of Statistics and Operations Research, University of Vigo
mamrguez@uvigo.es

Abstract

The research on the vehicle routing problems is an active topic given its vast applications in real world logistic problems. This work considers a real decision problem faced by an actual livestock feed cooperative. The cooperative receives demands from stockbreeders on each of the four livestock feeds available. The stockbreeders might be served by multiple trucks, moreover, the trucks can make several routes in each day, all of them starting and ending in the cooperative headquarters. In this situation the cooperative has to plan the routes of each truck. Additional constraints of the situation concern the fact that the fleet consists of trucks with different load capacity and this load capacity is divided in hoppers of different sizes. Moreover, each hopper can contain just a type of feed that has to be served to just one stockbreeder. A programming model is introduced in order to reduce costs. We test the resolution of the problem programming our model in AMPL and solving it with KNITRO. Solving the model for actual size instances is computationally burdensome. Hence, we introduce and implement one heuristic algorithm to reduce the computational time. The heuristic is applied to the real case of the cooperative "AIRA" with a large number of stockbreeders. The numerical results show that the heuristic can solve large instances effectively with reasonable computational effort.

32.1 Introduction

The study of decision support systems for logistics is an extremely active area of research and applications in modern Operations Research. In this framework, the planning and scheduling of routes for different purposes is a main topic. From a mathematical point of view, such problems are complex and very difficult to solve exactly. Therefore, many heuristic algorithms have been proposed to overcome

these difficulties taking advantage of the underlying combinatorial structure of each particular problem. To delve deeper into this topic see the survey [1] and the seminal papers [4] and [3].

This work is motivated by a real problem faced by a livestock feed company. AIRA is an agricultural cooperative located in Taboada, a town in the Spanish north western region of Galicia. They produce four different kinds of livestock feeds and serve them to their customers. There are 1500 stockbreeders (customers) spread in about 60 municipalities of the rather vast surrounding area as we can see in Figure 32.1.

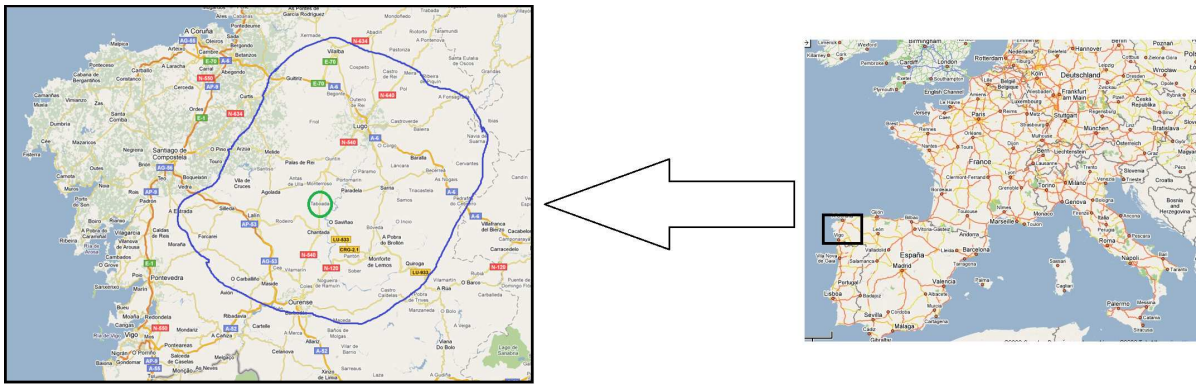

Figure 32.1: Localisation of the cooperative and area of delivery.

The stockbreeders place their orders for the different feeds with the cooperative and each order is either urgent, which means that they need to be served the following day, or has a three or four days window to deliver it. Urgent orders are more expensive for the customers. Usually, stockbreeders order once or twice a month and most of the times, they are only in need of one type of feed. The distribution of feeds is carried out by the fleet of trucks owned by the cooperative and each truck driver is paid depending on the distance covered and the load carried. Additionally, the trucks have different size and are compartmentalized in several hoppers (three to five) which have distinct capacities. Furthermore, given their size, some trucks cannot access some livestock farms. In order to simplify the delivery process, the cooperative demands that no stockbreeder can be served by more than one truck per day. Moreover, for technical reasons, each hopper can only contain one type of feed and cannot be shared among stockbreeders. The goal of this study is to provide the cooperative a tool that automatically proposes routes for each truck that satisfying the restrictions, first maximizes the total food delivered per working day and second minimizes the transportation cost of that amount. Besides, the transportation cost paid to each truck driver is a fixed amount for each unloading plus another amount which is proportional to the distance covered and the amount of feed carried on each route. Furthermore, the ratio of this proportion depends on the distance covered.

A research group of Agroforestry Engineering of the University of Santiago de Compostela designed a Global Positioning System (GPS) to monitor the routes of the trucks but the cooperative managers are hoping to improve the whole system in the years to come. Indeed, this routing project is part of a bigger one which aims at automating the whole distribution process of the cooperative. The GPS that are currently being used provide us all the geographical data we are using to solve this problem, that is to say the distance between all the partners and the cooperative but also the corresponding time necessary to make this route. The other data used here are the quantities of feeds ordered, the capacities of the hoppers and whether or not a truck can reach a barn.

Figure 32.2: Facilities and trucks of the cooperative AIRA.

[9] is also inspired by the real problem of another Spanish cooperative that manufacturates animal feed. Their approach generates all feasible routes by means of an implicit enumeration algorithm, in a first step, and secondly they use and integer programming model that selects the optimum routes. In this scope, we treat the problem through a nonlinear multiobjective model that is solved by the lexicographic procedure. In this way, we confront the task of adapting more classical vehicle routing models to the specific one of AIRA. The facilities and the trucks of this cooperative are shown in Figure 32.2.

32.2 Formulation of the problem

32.2.1 Problem data

In order to model our problem, we use a set of stockbreeders, a set of trucks and for each truck, its corresponding sets of routes and hoppers. As for the data, we know the capacities of each hopper, the demand of the different customers and the urgence of their order as well as the distances between stockbreeders and the time it takes to go from one to another. We also know whether a truck is able to reach a specific barn and its maximum charge authorized. Moreover, the cooperative provided us with all the cost related data such as the price of each unloading and the variable cost of the transportation of a certain quantity of feed on a given distance.

32.2.2 Decision variables

The problem as we modeled it involves two different kinds of variables. The first one is a set of binary variables which equals 1 if there is a route that a truck follows to go from a stockbreeder to another, and 0 otherwise. The second one is a set of continuous variables, in [0,1], which represents the percentage of a certain hopper that is filled by a feed for a certain stockbreeder.

32.2.3 Objective functions

The objective of this problem is to minimise the cost of food transportation when we try to meet each stockbreeder's order as well as possible. For doing so, we need to divide the problem in two steps: first

we maximize the quantity of food carried by the different trucks and then we minimize the cost of the deliveries. In this second step, the term that we minimise is the sum of: the cost generated by each unloading, which is proportional to the number of stockbreeders visited, and the cost generated by the transportation of the feeds which itself is the sum of a fixed cost proportional to the amount of food carried and a variable cost that depends of the distance covered on the route and the quantity of food carried on this route. We should note that, actually, the fixed cost of the food transportation is not taken into account in the minimisation as it is considered as constant once it was determined by the previous maximisation.

32.2.4 Constraints

The most common constraint of a vehicle routing problem is the flow condition. Here, every truck that visits a stockbreeder leaves afterwards and all the routes start from the cooperative headquaters. This way, we are sure that if a route really exists, it will end back at the cooperative. In order to avoid pointless trips, we ask that if a truck goes to a stockbreeder, it is carrying food for him. If a truck cannot reach a barn, we make sure that it does not visit the corresponding stockbreeder. A truck driver cannot work for more than 9 hours a day, so each truck cannot travel more than 9 hours. A truck cannot cover more than a certain amount of kilometres a day. The load of each truck on each route is bounded. To the stockbreeders whose order is urgent (no days left to deliver), we give the quantity they asked for. To the stockbreeders whose order is less urgent and could still be delivered another day, we give as much as possible. Each stockbreeder is to be visited only once so each order has to be delivered by the same truck. A hopper cannot be shared among stockbreeders and cannot contain different type of feeds. Thus, each hopper contains only one feed for one stockbreeder.

32.3 The heuristic algorithm and first results

For solving the real problem efficiently, we introduce an heuristic algorithm and design a JAVA application (see [7]) that can be readily used by the technician of the cooperative. The heuristic algorithm has a first part in which we define an initial solution by following the so-called insertion procedure as it is introduced by [10] but taking into account distances and occupation criterions instead of time ones. The second part is devoted to ask for better solutions by using the Tabu methodology. This is a well known type of heuristic algorithm that we can see explained in detail in [6] and [8], among others (in Figure 32.3 a brief schedule of the algorithms is presented). [1]

In order to illustrate the model we elaborated and the algorithm we introduced, we consider a small instance of arbitrary data. We chose to work with a fleet of 2 trucks, a little one with 2 hoppers who can respectively contain up to 4 and 3 tons of feeds and a bigger one with 3 hoppers whose capacities are 5, 4 and 4 tons of feeds. The first truck cannot be carrying more than 6 tons while the other is allowed to carry up to 13 tons at the same time. Moreover, there are 5 stockbreeders located in the towns of Orense, Begonte, Sarria, A Estrada and Friol. We assume that the bigger truck is unable to deliver food to the ones located in Begonte and Sarria. The orders are as shown in Table 32.1. We also consider the distance among the different barns, the time to go from one to the other, the maximum distance covered by a truck daily, the cost of an unloading, the fixed cost of food transportation, and the variable cost of food transportation.

[1] Detailed mathematical formulation of the non linear programming model, its implementation with AMPL, the heuristic algorithm, and the JAVA application can be obtained from authors under request.

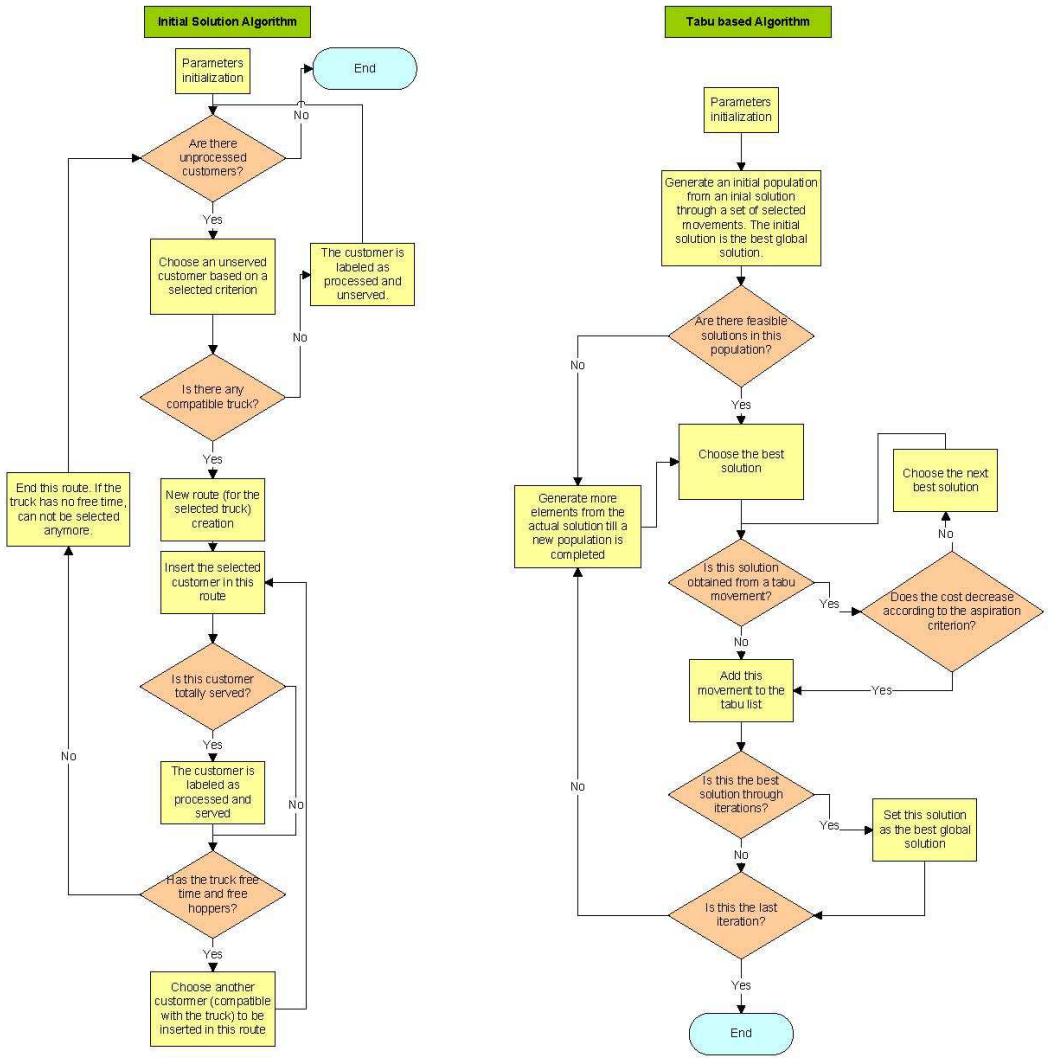

Figure 32.3: Flow charts of the algorithms.

The implementation of the model was done in the language AMPL (see [5]). We let the resolution of the problem to a free version of the solver KNITRO 6.0.0 (see [2]), which uses a version of the interior point algorithm for non linear problems, obtained in the NEOS server[2]. When dealing with integer variables, the solver uses a branch and bound algorithm which can only give a locally optimal solution. In the example, the solver gives us a locally optimal solution after 9278 secs (about 2 hours and a half).

For instance, if we run the same example tested with AMPL, the heuristic algorithm achieves the optimal solution with the initial solution algorithm in 0.0001 secs. Figure 32.4 shows the results as they are provided by the Java application.

Finally, we can conclude by explaining that in this setup we are using the model and the algorithm with real data with the goal of achieving an economic analysis, comparing our results with previous planning human-based and assessing the possible utilization of our application in the cooperative AIRA.

[2]For more details visit http://www-neos.mcs.anl.gov/.

Table 32.1: Orders of the different stockbreeders (in tons of feed).

Orders	Feed 1	Feed 2	Feed 3	Feed 4	Days left to deliver
Orense			4.5		0
Begonte	4				0
Sarria				2	3
A Estrada				3.5	0
Friol		3			2

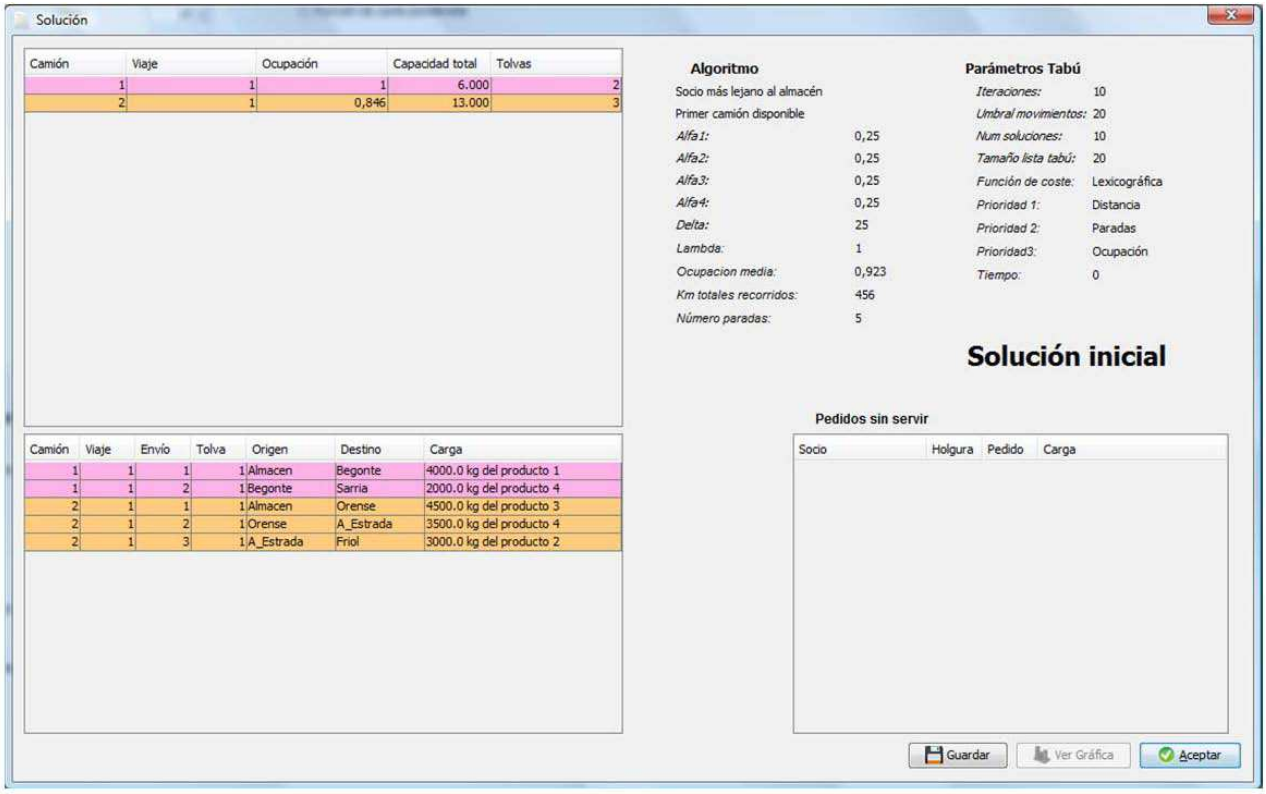

Figure 32.4: Some results provided by the JAVA application.

32.4 Acknowledgements

The authors wish to thank the interesting suggestions, comments and computing support made by C. Amiama, I. Fernández González, I. García Jurado, X. C. Hermida, and M. C. Perrot. This research received financial support from Spanish Ministry for Science and Technology through Project ECO2008-03484-C02-02 and from Xunta de Galicia through Project INCITE09-207-064-PR.

Bibliography

[1] C. Archetti, M.G. Speranza, The split delivery vehicle routing problem: a survey, The Vehicle Routing Problem: Latest Advances and New Challenges, Springer US. 43 (2008), 103-122.

[2] R.H. Byrd, J. Nocedal, R.A. Waltz, KNITRO : An integrated packages for nonlinear opimization, in G. di Pillo and M. Roma, eds. Large-scale Nonlinear Optimization, Springer- Verlag (2006).

[3] G. Clarke, J.W. Wright, Scheduling of vehicles from a central depot to a number of delivery points, Operations Research 12 (1964), 568-581.

[4] G.B. Dantzig, J.H. Ramser, The truck dispatching problem, Management Science 6 (1959), 80-91.

[5] R. Fourer, D.M. Gay, B.W. Kernighan, AMPL. A modeling language for mathematical programming, Thomson, Brooks/Cole, second edition (2003).

[6] F. Glover, Tabu search-Part I, ORSA Journal on Computing 1 (1989), 190-206.

[7] J. Gosling, B. Joy, G. Steele, G. Bracha, The Java Language Specification, Addison-Wesley, third edition (2005).

[8] S.C. Ho, D. Haugland, A tabu search heuristic for the vehicle routing problem with time windows and split deliveries, Computers & Operations Research 31 (2004), 1947-1964.

[9] R. Ruiz, C. Maroto, J. Alcaraz, A decision support for a real vehicle routing problem, European Journal of Operational Research 153 (2004), 593-606.

[10] M.M. Solomon, Algorithms for the vehicle routing and scheduling problems with time window constraints, Operations Research 35 (1987), 254-265.

Optimal placement of river sampling stations

L.J. Alvarez-Vázquez[(1)] **A. Martínez**[(1)], **M.E. Vázquez-Méndez**[(2)], **M.A. Vilar**[(2)]

(1) Depto. de Matemática Aplicada II, E.I. Telecomunicación, Univ. de Vigo, 36310 - Vigo, Spain.
lino@dma.uvigo.es, aurea@dma.uvigo.es

(2) Depto. de Matemática Aplicada, E.P.S., Univ. de Santiago de Compostela, 27002 - Lugo, Spain.
miguelernesto.vazquez@usc.es, miguel.vilar@usc.es

Abstract

Usual methods for controlling river pollution include establishing water pollution monitoring stations located along the length of the river. The point where each station is located (*sampling point*) is of crucial importance if we want to obtain representative information about the pollution in the whole river. In this work, the optimal location of sampling points is studied by means of a combination of numerical simulation and optimization techniques. Based on a one-dimensional system of partial differential equations, a mathematical formulation of the optimization problem is proposed, and it is solved for a real case on Neuse River (State of North Caroline, U.S.A.).

33.1 Introduction

At present, all wastewater discharged into a river must be first treated in a purifying plant, in order to reduce its pollutants level. Wastewater purification at each plant must be strong enough so that the river basin be capable of assimilating all the wastewater disposed there. In order to be sure that the river can assimilate the discharges, we have to choose some simple indicators of pollution levels, and design an adequate sampling technique giving us information about the values of these indicators along the river. For instance, if we want to control pollution in terms of pathogenic microorganisms coming from domestic wastewater, one of the most common indicators is the concentration (in $units/m^3$) of faecal coliform (FC) bacteria because its concentration in wastewater discharges is much greater than any other microorganism concentration. A standard technique to control the concentration of coliform bacteria in rivers consists of dividing it into several sections - according to the morphology of the river basin and the number, type and location of the discharges - and to take samples of water at one point of each section. The point where the station sampling is located (sampling point) is of crucial importance in order to obtain representative information about the pollution in the whole section. Thus, the optimal sampling point will be that one at which the concentration of coliform bacteria over time is as similar as possible to the averaged concentration in the whole section (an overview of the entire sampling process can be seen, for example, in [2]). The main objective of this work is to show the advantages of using numerical simulation and optimization techniques to achieve optimal sampling points. In order to do it, we formulate the problem from a mathematical viewpoint (section 33.2) and solve it in a real case posed in the Neuse River (section 33.3).

33.2 Mathematical formulation

Let us consider a river L meters in length, with V_a tributaries flowing into the river and V_{ar} domestic wastewater discharges coming from purifying plants ($V = V_a + V_{ar}$). We suppose that the river is

divided into N sections, consecutively numbered from the source, and we denote by Δ_i the length of the i-th zone ($i = 1, 2, \ldots, N$). Let T (in seconds) be the total time for pollution control. Then, for each $(x,t) \in [0,L] \times [0,T]$, we denote by $\rho(x,t)$ the FC concentration in the transversal section, x meters from the source and t seconds from the moment the control is initiated. We define $a_0 = 0$ and, for $i = 1, 2, \ldots, N$,

$$a_{i+1} = a_i + \Delta_i, \qquad c_i(t) = \frac{\displaystyle\int_{a_{i-1}}^{a_i} \rho(x,t)\, dx}{\Delta_i}.$$

Thus, the optimization problem (P) consists of finding the sampling points $p_i \in [a_{i-1}, a_i]$, for $i = 1, 2, \ldots, N$, such that minimize the cost function

$$J(p) = \sum_{i=1}^{N} \int_0^T \left(\rho(p_i,t) - c_i(t)\right)^2 \, dt, \qquad \text{with } \; p = (p_1, p_2, \ldots, p_N).$$

If we neglect the effect of molecular diffusion, the FC concentration is given by the following hyperbolic boundary value problem:

$$\left.\begin{array}{ll} \dfrac{\partial \rho}{\partial t} + u\dfrac{\partial \rho}{\partial x} + k\rho = \dfrac{1}{A}\displaystyle\sum_{j=1}^{V} m_j \delta(x - v_j) & \text{in } \; (0,L)\times(0,T) \\ \rho(0,t) = \rho_0(t) & \text{in } \; [0,T], \\ \rho(x,0) = \rho^0(x) & \text{in } \; [0,L], \end{array}\right\} \tag{33.1}$$

where $\delta(x-b)$ denotes the Dirac measure at point b, $v_j \in (0,L)$ and $m_j(t)$ are, respectively, location and mass FC flow rate for $j-$th discharge (including tributaries and wastewater discharges), k is the loss rate for FC and, finally, $A(x,t)$ and $u(x,t)$ denote, respectively, the area of the section occupied by water (*wet section*) and the averaged velocity in that section. They can be experimentally known but also can be obtained by numerical simulation, solving the following hyperbolic system:

$$\left.\begin{array}{ll} \dfrac{\partial A}{\partial t} + \dfrac{\partial (Au)}{\partial x} = \displaystyle\sum_{j=1}^{V_a} q_j \delta(x - v_j) & \text{in } \; (0,L)\times(0,T) \\ \dfrac{\partial (Au)}{\partial t} + \dfrac{\partial (Au^2)}{\partial x} + gA\dfrac{\partial h}{\partial x} = \displaystyle\sum_{j=1}^{V_a} q_j U_j \cos(\alpha_j)\delta(x - v_j) + S_f & \text{in } \; (0,L)\times(0,T) \\ A(L,t) = A_L(t), \quad u(0,t) = u_0(t) & \text{in } \; [0,T], \\ A(x,0) = A^0(x), \quad u(x,0) = u^0(x) & \text{in } \; [0,L], \end{array}\right\} \tag{33.2}$$

where:

- $q_j(t)$, $U_j(t)$ and α_j denote flow rate, velocity and gate angle for the j-th tributary.
- g and S_f denote, respectively, gravity and bottom friction stress.
- $h(x,t) = H(x,t) + b(x)$ is the height of water with respect to a fixed reference level (see figure 33.1). It is worthwhile remarking here that, if the geometry of the river is known, $h(x,t)$ can be written in terms of the unknown $A(x,t)$. In effect, for each $x \in [0,L]$, the geometry of the river gives us a positive function $b(x)$ and a strictly increasing and positive function $S(.,x)$ verifying

$$A(x,t) = S(H(x,t), x) \quad \text{in } \; [0,L]\times[0,T], \tag{33.3}$$

in such a way that

$$\frac{\partial h}{\partial x}(x,t) = \frac{\partial}{\partial x} S^{-1}(A(x,t), x) + b'(x). \tag{33.4}$$

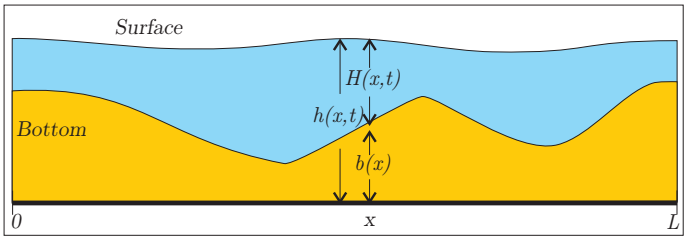

Figure 33.1: Longitudinal cut of a river at time t.

The first step in the numerical resolution of problem (P) is to obtain the velocity field and the area of the wet section in every point and at every time. With this data we proceed to solve the problem (33.1), which give us the function $\rho(x,t)$ in $[0,L]\times[0,T]$ and, consequently, $c_i(t)$ in $[0,T]$, for $i=1,2,\ldots,N$. Then, the problem is reduced to solve N one-dimensional minimization problems. A detailed algorithm to solve problem (P) can be seen in [1].

33.3 Numerical results

Above problem (P) has been solved to determine the optimal sampling points in the segment of the Neuse River (North Caroline, U.S.A.) which can be seen in figure 33.2.

Figure 33.2: Case of study: Neuse River (North Caroline, U.S.A.)

We run multiple model scenarios including different types of storms that cause the flooding of Neuse River and the contamination by the hog waste lagoons (see [3] for more details). In this section we only present numerical results for a typical situation where the segment (53534 meters in length) has been divided into three sections: [0,9740], [9740,25685] and [25685,53534]. The optimal sampling points achieved in the optimization process have been $p_1 = 8616\,m$, $p_2 = 20675\,m$, $p_3 = 38738\,m$. The quality of these points can be seen in figure 33.3, where averaged FC concentration in each section are compared with FC concentration at optimal sampling points.

Acknowledgments

This work was supported by Projects MTM2009-07749 of Ministerio de Ciencia e Innovación (Spain) and INCITE09-291-083 of Xunta de Galicia. The authors are grateful to J. Jeffrey Peirce and Adam W.

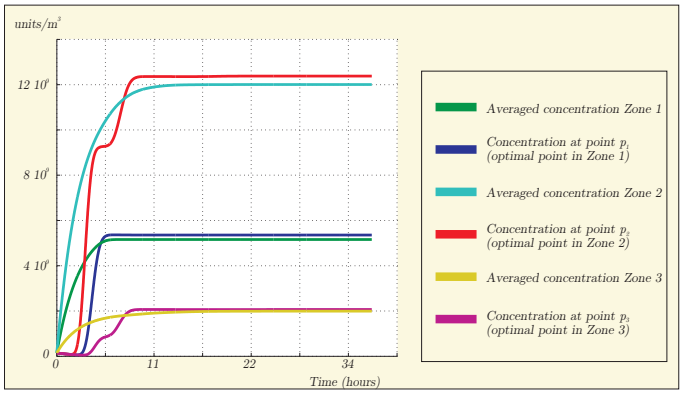

Figure 33.3: Comparison between averaged FC concentration and FC concentration at optimal sampling points

Pollak (Duke University, U.S.A.) for experimental data and useful comments about Neuse River.

Bibliography

[1] L.J. Alvarez-Vázquez, A. Martínez, M.E. Vázquez-Méndez and M.A. Vilar, Optimal location of sampling points for river pollution control, Mathematics and Computers in Simulation 71,(2006), 149-160.

[2] K.D. Harsham, *Water sampling for pollution regulation.* Gordon and Breach Publishers, Luxembourg, 1995.

[3] A.W. Pollak, J.J. Peirce, L.J. Alvarez-Vázquez and M.E. Vázquez-Méndez, Methodology for identifying optimal water quality sensor locations in river systems (In progress).

Posters

Modelo predictivo de mala evolución en pacientes con exacerbación de EPOC e implementación en herramienta tecnológica de uso en los servicios sanitarios

I. Barrio[1], I. Arostegui[2], J.M. Quintana[3], A. Bilbao[4] y V. Núñez-Antón[5]

[1,3]Hospital de Galdakao - Usansolo. Unidad de Investigación
e-mail: irantzubarrio@gmail.com
josemaria.quintanalopez@osakidetza.net

[2]UPV-EHU. Departamento de Matemática Aplicada, Estadística e Investigación Operativa
e-mail: inmaculada.arostegui@ehu.es

[4]Fundación Vasca de Investigación e Innovación Sanitarias (BIOEF)
e-mail: abilbao@bioef.org

[5]UPV-EHU. Departamento de Econometría y Estadística (E.A.III)
e-mail: vicente.nunezanton@ehu.es

Abstract

Los modelos predictivos son una herramienta estadística que facilita la toma de decisiones en la práctica clínica. En este trabajo proponemos una metodología basada en regresión logística, combinada con modelos aditivos y árboles de clasificación, para el desarrollo de modelos predictivos. Proponemos la validación cruzada como método de validación. Aplicamos la metodología propuesta para desarrollar y validar un modelo predictivo de mala evolución en pacientes con exacerbación de la EPOC. El resultado es un modelo válido y fiable que va a permitir desarrollar una herramienta tecnológica que servirá de apoyo en la toma de decisiones en la práctica clínica.

34.1 Introducción

En la medicina en general y más aún en los tiempos actuales, se requieren opciones individualizadas para el desarrollo de test diagnósticos o tratamientos diferenciados en la toma de decisiones médicas. Los médicos y gestores sanitarios necesitan realizar predicciones en el pronóstico y/o en la probabilidad de brote de una enfermedad y en su toma de decisiones. Actualmente, inmersos en la era de la medicina basada en la evidencia y en la toma de decisiones compartida, los modelos predictivos son de gran relevancia.
Los modelos de predicción clínica proporcionan estimaciones de la probabilidad individual del riesgo y el beneficio [1]. La predicción es básicamente un problema de estimación y contraste de hipótesis. La correcta selección de factores predictivos de una variable respuesta requiere una modelización estadística. Además, un modelo predictivo se crea con el objetivo de ser utilizado para la toma de decisiones individualizada, de manera que el desarrollo debe tener en cuenta aspectos relacionados con el sobre-ajuste o la sobre-dependencia de la muestra utilizada.

En este trabajo se presenta una metodología de desarrollo y validación de modelos predictivos basada en la regresión logística. La metodología propuesta se aplica para predecir la evolución de pacientes que acuden a un servicio de urgencias con una exacerbación de la enfermedad pulmonar obstructiva crónica (EPOC).

La EPOC, afecta al 10% de la población adulta en Europa y a un 9% en nuestro medio, oscilando entre un 4.9% y un 18%, siendo la cuarta causa de mortalidad detrás del cáncer, las cardiopatías y las enfermedades cerebrovasculares. De estas enfermedades, la EPOC es la única que está aumentando en prevalencia, y se espera que siga haciéndolo en los próximos 25 años. La exacerbación de la EPOC, se define como un empeoramiento agudo de los síntomas respecto a la situación basal del paciente, lo que implica que sea necesario realizar cambios en su medicación habitual.

34.2 Metodología: Desarrollo y Validación de Modelos Predictivos

Los resultados más comúnmente considerados en predicción médica son el diagnóstico (presencia de la enfermedad); el pronóstico (p.e morbi-mortalidad, complicaciones, etc) o la evolución. En este trabajo hemos considerado modelos predictivos para la respuesta binaria definida como mala evolución a corto plazo en un paciente que acude a la urgencia con una exacerbación de la EPOC. La regresión logística es la técnica estadística más extendida para modelizar respuesta de tipo binario en medicina. Esta técnica, flexible en cuanto a la incorporación de variables predictoras categóricas y/o continuas, términos de interacción y transformaciones no lineales, viene definida por la ecuación 34.1, donde la función $logit$ es la función enlace de un modelo lineal generalizado, siendo θ un parámetro que toma valores en el intervalo $[0, 1]$ y representa la probabilidad de mala evolución, $\boldsymbol{x} = \{1, x_1, \ldots, x_p\}$ el vector de variables predictoras y $\boldsymbol{\beta} = (\beta_0, \beta_1, \ldots, \beta_p)^T$ el vector de coeficientes de regresión.

$$logit(\theta) = log(\frac{\theta}{1-\theta}) = log\frac{P(Y=1|X=\mathbf{x})}{P(Y=0|X=\mathbf{x})} = \boldsymbol{\beta^T}\mathbf{x} \tag{34.1}$$

Hemos modelizado la relación funcional de los predictores continuos con la variable respuesta mediante modelos generales aditivos [2], buscando una estimación mediante funciones suaves y puntos de corte que han permitido categorizar las variables continuas de forma óptima (ver ejemplo en Figura 34.1 (a)). Hemos empleado los árboles de clasificación y regresión [3] para detectar interacciones estadística y clínicamente significativas que posteriormente han sido introducidas en el modelo de regresión logística. Las variables predictoras se han seleccionado mediante comparación de modelos anidados y los parámetros se han estimado mediante el método de máxima verosimilitud. Se ha evaluado la capacidad predictiva del modelo mediante el parámetro denominado *area under the curve* (AUC). La calibración del modelo se ha contrastado mediante el test de Hosmer-Lemeshow [4]. Finalmente, el modelo obtenido se ha validado clínicamente mediante validación aparente y estadísticamente mediante validación cruzada. Se ha utilizado una validación cruzada de 10 hojas. Este método consiste en dividir los datos en deciles (conteniendo cada partición 1/10 parte del total de la muestra), el modelo se ajusta en 9 de lo 10 grupos y se valida en el décimo. Este proceso se repite hasta que los 10 grupos han sido utilizados para la validación, de esta forma, todos los casos han sido utilizados una vez para la validez del modelo [5].

La ventaja principal de la validación cruzada frente a la validación basada en la partición es que en este caso se puede utilizar mayor número de casos de la muestra original (p.e 90 %) para el desarrollo del modelo.

34.3 Resultados Obtenidos

Las variables significativas en la predicción de mala evolución en pacientes con una exacerbación de la EPOC son, el PH, la PCO2 (cantidad de dióxido de carbono liberado en la sangre) y la frecuencia

Table 34.1: Resultados del modelo predictivo de regresión logística

	β	OR	IC(OR)95%	P
PCO2 (a la llegada)				<0,0001
Normal	-	-	-	
Alterado	1,22	3,40	(2,14 a 5,41)	
Muy Alterado	2,20	9,06	(5,32 a 15,44)	
FRECUENCIA RESPIRATORIA (toma decisión)				0,0006
Normal	-	-	-	
Alterada	0,68	1,98	(1,21 a 3,24)	
Muy Alterada	0,95	2,59	(1,59 a 4,22)	
EVOLUCIÓN PH (llegada - decisión)				<0,0001
Estable	-	-	-	
Inestabilidad Leve	0,91	2,48	(1,61 a 3,83)	
Alterado a la llegada	1,96	7,07	(3,21 a 15,54)	
Alterado en la decisión	3,59	36,28	(9,89 a 133,06)	

OR: Odds Ratio; IC: Intervalo de confianza

respiratoria en la toma de decisión. La tabla 34.1 muestra los resultados del modelo de regresión logística.

Una de las variables que más influye en la mala evolución de los pacientes con EPOC exacerbada a la llegada a la urgencia, es el cambio en el PH. Como ejemplo de interpretación de los resultados obtenidos, diremos que un paciente cuyo PH está alterado en la toma de decisión, es casi 36 veces, más probable (odds ratio (OR) 36,28) que sufra mala evolución que un paciente con el PH estable.

El modelo resultante tiene una buena capacidad predictiva, con un AUC de 0,853 con intervalo de confianza al 95% (0,823-0,883), siendo el punto de corte óptimo de 0,09 (ver Figura 34.1 (b)). Finalmente, el modelo está bien calibrado, con un p-valor de 0,3075 en el test de Hosmer Lemeshow.

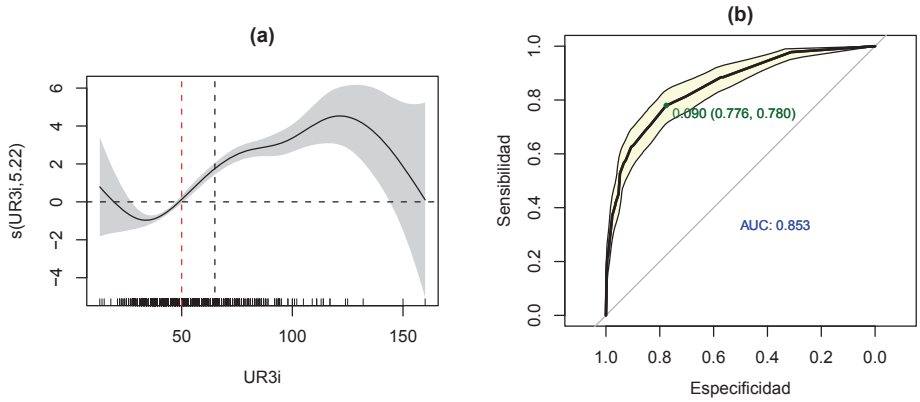

Figure 34.1: (a) Función Suave (b) Curva ROC del modelo

34.4 Conclusiones

La metodología propuesta ha permitido desarrollar un modelo válido y fiable para predecir la evolución de pacientes con una exacerbación de la EPOC. Por lo tanto, estos resultados facilitarán la toma de decisiones en la práctica clínica. En la práctica, la aplicación de los resultados obtenidos del modelo propuesto va a permitir desarrollar una herramienta tecnológica de uso en los servicios sanitarios que permita a los clínicos conocer el riesgo individual de mala evolución de un paciente que llega a la urgencia con una exacerbación de la EPOC.

Agradecimientos

Este trabajo se ha realizado con financiación del Gobierno Vasco, la Universidad del País Vasco (UPV-EHU) y el Ministerio de Ciencia e Innovación (UE09+/62, GIU10/21 y MTM2010-14913) y ha sido presentado en parte como trabajo fin de master realizado en la UPV/EHU dentro del programa Master en Modelización Matemática, Estadística y Computación.

Bibliography

[1] Steyerberg, E. W. *Clinical Prediction Models*. Springer - Verlag, New York. 2009.

[2] Wood, N.S *Generalized Additive Models. An Introduction with R*. Chapman & Hall /CRC. 2006.

[3] Zhang, H. and Singer, B. *Recursive Partitioning in the Health Sciences*. Springer - Verlag, New York. 1999.

[4] Hosmer, D. and Lemeshow, S. *Applied Logistic Regression*.John Wiley & Sons, New Jersey. 2000.

[5] Hastie, T., Tibshirani, R. and Friedman, J. *Elements of Statistical Learning. Data Mining, Inference and Prediction*. Springer, New York. 2009.

Posters

A second-order pure lagrange-galerkin method for convection-diffusion problems

M. Benítez

Dpto. de Economía Aplicada II, Universidade da Coruña, Facultad de Economía y Empresa, Campus de Elviña, CP. 15071, A Coruña
e-mail: marta.benitez@udc.es

A. Bermúdez

Dpto. de Matemática Aplicada, Universidade de Santiago de Compostela, Facultad de Matemáticas, Campus sur, CP. 15782, Santiago de Compostela
e-mail: alfredo.bermudez@usc.es

Abstract

In this work we present a second order pure Lagrange-Galerkin for variable coefficient convection-(possibly degenerate) diffusion equations with mixed Dirichlet-Robin boundary conditions. In [1] and [2] this method is rigorously introduced and analyzed. Stability is proved and error estimates of order $O(\Delta t^2) + O(h^k)$ are obtained. In this work, firstly, after statement the problem, the strong formulation of the convection-diffusion Cauchy problem is written in Lagrangian coordinates. Next, to test the proposed methods, a numerical example is presented which has a solution developing a steep layer and a velocity field which is not divergence-free.

35.1 Introduction

Linear convection-diffusion equations model a variety of important problems from different fields of engineering and applied sciences. In many cases the diffusive term is much smaller than the convective one, giving rise to the so-called convection dominated problems. For convection-diffusion problems with dominant convection, methods of characteristics for convective term discretization, are extensively used (see [5], [3]).
Characteristics methods are based on time discretization of the material time derivative. For space discretization, they has been combined with finite differences [6], finite elements ([5], [7], [8]), spectral finite elements ([9]), discontinuous finite elements ([10]), and so on. When combined with finite elements they are also called Lagrange-Galerkin methods. In particular, when the characteristic methods are formulated in Lagrangian coordinates (respectively, Eulerian coordinates) they are called Lagrangian methods (respectively, semi-Lagrangian methods). In the present work we will consider the combination of Lagrangian and semi-Lagrangian methods with a spatial discretization by using finite elements spaces.

After the present section, we introduce the strong problem and the Lagrangian strong problem. Next, a numerical test is presented to assess the performance of the numerical method described in the present work.

35.2 Statement of the problem and the discretized scheme

Let Ω be a bounded domain in $\mathbb{R}^d$ ($d = 2, 3$) with Lipschitz boundary Γ divided into two parts: $\Gamma = \Gamma^D \cup \Gamma^R$, with $\Gamma^D \cap \Gamma^R = \emptyset$. Let T be a positive constant and $X_e : \overline{\Omega} \times [0,T] \longrightarrow \mathbb{R}^d$ be a motion in the sense of Gurtin [11] and P its reference map. We call $\Omega_t = X_e(\Omega, t)$, $\Gamma_t = X_e(\Gamma, t)$, $\Gamma_t^D = X_e(\Gamma^D, t)$ y $\Gamma_t^R = X_e(\Gamma^R, t)$, for $t \in [0,T]$. We assume that $\Omega_0 = \Omega$. Let us introduce the *trajectory* of the motion

$$\mathcal{T} := \{(x,t) : x \in \overline{\Omega}_t,\ t \in [0,T]\},$$

and the set $\mathcal{O} := \bigcup_{t\in[0,T]} \overline{\Omega}_t$. Let us consider the following initial-boundary value problem.

(SP) **STRONG PROBLEM**. *Find a function* $\phi : \mathcal{T} \longrightarrow \mathbb{R}$ *such that*

$$\rho(x)\frac{\partial \phi}{\partial t}(x,t) + \rho(x)\mathbf{v}(x,t)\cdot \operatorname{grad}\phi(x,t) - \operatorname{div}\left(A(x)\operatorname{grad}\phi(x,t)\right) = f(x,t), \tag{35.1}$$

for $x \in \Omega_t$ *and* $t \in (0,T)$, subject to the boundary conditions

$$\phi(\cdot,t) = \phi_D(\cdot,t) \text{ on } \Gamma_t^D, \tag{35.2}$$

$$\alpha\phi(\cdot,t) + A(\cdot)\operatorname{grad}\phi(\cdot,t)\cdot\mathbf{n}(\cdot,t) = g(\cdot,t) \text{ on } \Gamma_t^R, \tag{35.3}$$

for $t \in (0,T)$, and the initial condition

$$\phi(x,0) = \phi^0(x) \text{ in } \Omega. \tag{35.4}$$

In the above equations, $\mathbf{v} : \mathcal{T} \longrightarrow \mathbb{R}^d$ is the velocity, $A : \mathcal{O} \longrightarrow Sym$ denotes the diffusion tensor field, where Sym is the space of symmetric tensors in the d-dimensional space, $\rho : \mathcal{O} \longrightarrow \mathbb{R}$, $f : \mathcal{T} \longrightarrow \mathbb{R}$, $\phi^0 : \Omega \longrightarrow \mathbb{R}$, $\phi_D(\cdot,t) : \Gamma_t^D \longrightarrow \mathbb{R}$ and $g(\cdot,t) : \Gamma_t^R \longrightarrow \mathbb{R}$, $t \in (0,T)$, are given scalar functions, and $\mathbf{n}(\cdot,t)$ is the outward unit normal vector to Γ_t. We define the material description Ψ_m of a spatial field Ψ by

$$\Psi_m(p,t) = \Psi(X_e(p,t),t). \tag{35.5}$$

Throughout this work, we use the notation

$$\begin{aligned}
\widetilde{A}_m(p,t) &:= F^{-1}(p,t)A_m(p,t)F^{-T}(p,t)\det F(p,t) \quad \forall (p,t) \in \overline{\Omega}\times[0,T],\\
\widetilde{m}(p,t) &:= |F^{-T}(p,t)\mathbf{m}(p)|\det F(p,t) \quad \forall (p,t) \in \Gamma\times[0,T],
\end{aligned}$$

being $F(\cdot,t)$ the Jacobian matrix of the deformation $X_e(\cdot,t)$ and $\mathbf{m}$ the outward unit normal vector to Γ. We recall that, according to the standard formalism of continuum mechanics, $x = X(p,t)$ is the position at time t of the material point p, while the reference map $P(x,t)$ yields the material point located at position x at time t. We assume that $X_e(p,0) = p$, $\forall p \in \overline{\Omega}$. We are going to write the problem (35.1)-(35.4) in Lagrangian coordinates p. For this, we introduce the change of variable $x = X_e(p,t)$ and use the chain rule, obtaining (see [12])

(LSP) **LAGRANGIAN STRONG PROBLEM**. *Find a function* $\phi_m : \overline{\Omega}\times[0,T] \longrightarrow \mathbb{R}$ *such that*

$$\rho_m(p,t)\dot{\phi}_m(p,t)\det F(p,t) - \operatorname{Div}\left[\widetilde{A}_m(p,t)\nabla\phi_m(p,t)\right] = f_m(p,t)\det F(p,t), \tag{35.6}$$

for $(p,t) \in \Omega\times(0,T)$, subject to the boundary conditions

$$\phi_m(p,t) = \phi_D(X_e(p,t),t) \text{ on } \Gamma^D\times(0,T), \tag{35.7}$$

$$\alpha\widetilde{m}(p,t)\phi_m(p,t) + \widetilde{A}_m(p,t)\nabla\phi_m(p,t)\cdot\mathbf{m}(p) = \widetilde{m}(p,t)g(X_e(p,t),t) \text{ on } \Gamma^R\times(0,T), \tag{35.8}$$

and the initial condition

$$\phi_m(p,0) = \phi^0(p) \text{ in } \Omega. \tag{35.9}$$

We consider the standard weak formulation associated with this pure Lagrangian strong problem. We introduce the number of time steps, N, the time step $\Delta t = T/N$, and the mesh-points, $t_n = n\Delta t$ for $n = 0, 1/2, 1, \ldots, N$. The time discretization scheme we are going to consider is a Crank-Nicholson-like scheme. It arises from approximating the material time derivative at $t = t_{n+\frac{1}{2}}$, for $0 \leq n \leq N-1$, by a centered formula and using a second order interpolation formula involving values at $t = t_n$ and $t = t_{n+1}$ to approximate the rest of the terms at the same time $t = t_{n+\frac{1}{2}}$. Regarding the space discretization we use the piecewise quadratic finite elements space. Since usually the characteristic curves cannot be exactly computed, in practice, we replace the exact characteristic curves and gradient tensors by accurate enough approximations. More precisely, we use a second order Runge-Kutta approximation of X_e. In [1] and [2] stability and error estimates of order $O(\Delta t^2) + O(h^2)$ are proved in the $l^\infty(H^1)$-norm.

Thus, we shall denote this Lagrangian method by $(\mathcal{LG})_2$. Furthermore, we shall denote by $(\mathcal{SLG})_2^1$ the semi-Lagrangian scheme analogous to $(\mathcal{LG})_2$, but re-initializing the transformation to the identity at the beginning of each time step (see [12] for more details).

35.3 Numerical results

We consider the following example to compare the numerical results obtained with semi-Lagrangian and (full) Lagrangian methods.
The spatial domain is $\Omega = (0,1) \times (0,1)$, $T = 1$, and $\mathbf{v} = \nabla\psi, \quad \nu = \sigma_1, \quad f = 0$, being $\psi = (1 - cos(2\pi x_1))(1 - cos(2\pi x_2))$ and $\sigma_1 = 0.001$. The initial data varies between $\phi^0(0,0) = 0$ and $\phi^0(1,1) = 1$ according to the following expression:

$$\phi^0(x_1,x_2) = \begin{cases} 0 & \text{if } \xi < 0, \\ \frac{1}{2}(1 - cos(\pi\xi)) & \text{if } 0 \leq \xi \leq 1, \\ 1 & \text{if } 1 < \xi, \end{cases} \tag{35.10}$$

where $\xi = x_1 + x_2 - 1/2$. We impose Dirichlet boundary conditions given by the initial data. Moreover, in order to obtain an approximate solution of ϕ^n in Eulerian coordinates, we are going to calculate the spatial description of material field $\phi^n_{m,\Delta t,h} \sim \phi^n_m$. More precisely, we calculate $\widehat{\phi_{\Delta t,h}} \sim \widehat{\phi}$ as follows

$$\phi^n_{\Delta t,h}(x) := \phi^n_{m,\Delta t,h}(P^n_{RK}(x)) \quad \forall x \in \overline{\Omega},\ 0 \leq n \leq N, \tag{35.11}$$

being P^n_{RK} the second order Kunge-Kutta approximation of P^n. In Figure 35.1 we plot the velocity field and the initial data. This example has been solved in [13] with a semi-Lagrangian method combined with a discontinuous Galerkin discretization, and also with a standard Galerkin scheme. The Gibbs phenomena is observed for both methods. The oscillations produced by the standard Galerkin scheme are observed even far from the transition layer.

Here we solve this problem with the Lagrangian method $(\mathcal{LG})_2$ and the semi-Lagrangian scheme $(\mathcal{SLG})_2^1$.

In Fig. 35.2 and 35.3 we represent the numerical solution contours at final time $T = 1$ and the section $x_1 \longrightarrow \phi^N_{\Delta t,h}(x_1, 1/2)$, computed by using the $(\mathcal{SLG})_2^1$ and $(\mathcal{LG})_2$ methods, respectively. The semi-Lagrangian method presents oscillations near the transition layer, so Gibbs phenomena is observed, while the Lagrangian method is accurate even in the steep layer around the diagonal. These features can be observed on the plots of the sections.

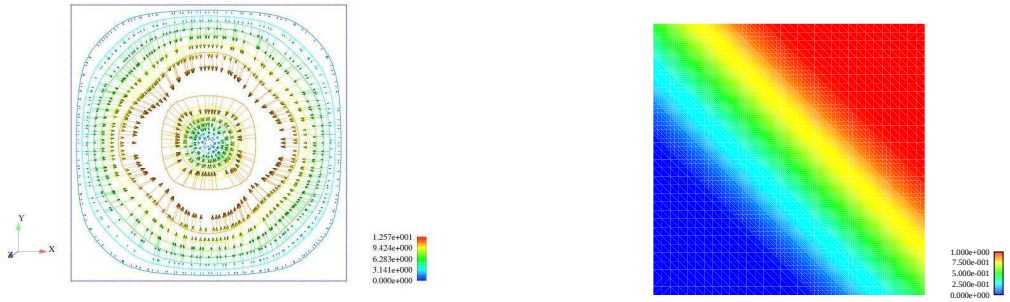

Figure 35.1: Velocity field (left) and initial date (right).

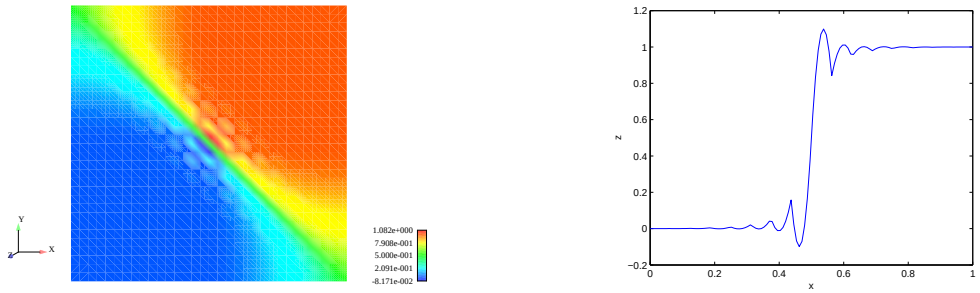

Figure 35.2: Numerical solution contours at $T = 1$ (left) and the section $x_1 \longrightarrow \phi^N_{\Delta t,h}(x_1, 1/2)$ (right) for the $(\mathcal{SLG})^1_2$ scheme, $h = 1/16$, $\Delta t = 1/60$.

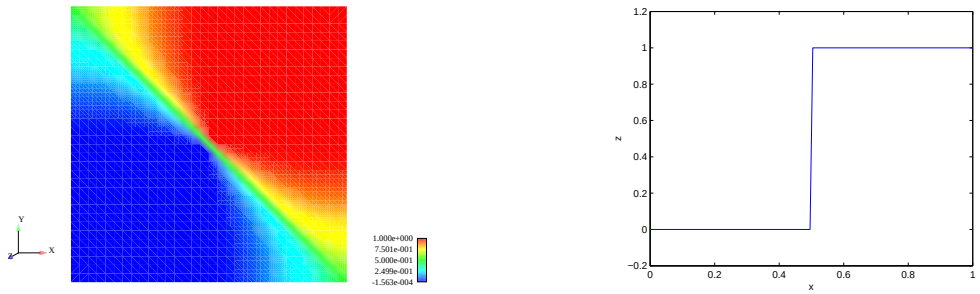

Figure 35.3: Numerical solution contours at $T = 1$ (left) and the section $x_1 \longrightarrow \phi^N_{\Delta t,h}(x_1, 1/2)$ (right) for the $(\mathcal{LG})_2$ scheme, $h = 1/16$, $\Delta t = 1/60$.

Bibliography

[1] M. Benítez and A. Bermúdez, *Numerical Analysis of a second-order pure Lagrange-Galerkin method for convection-diffusion problems. Part I: time discretization*. Submitted.

[2] M. Benítez and A. Bermúdez, *Numerical Analysis of a second-order pure Lagrange-Galerkin method for convection-diffusion problems. Part II: fully discretized scheme and numerical results*. Submitted.

[3] M. Benítez and A. Bermúdez, *A second order characteristics finite element scheme for natural convection problems*. Journal of Computational and Applied Mathematics, 235:3270–3284, 2011.

[4] G. de Vahl Davis, *Natural convection of air in a square cavity: a benchmark numerical solution*. Internat. J. Numer. Methods Fluids, 3:249–64, 1983.

[5] O. Pironneau, *On the Transport-Diffusion Algorithm and Its Applications to the Navier-Stokes Equations*. Numer. Math., 38:309–332, 1982.

[6] J. Douglas, Jr. and T.F. Russell, *Numerical methods for convection-dominated diffusion problems based on combining the method of characteristics with finite element or finite difference procedures*. SIAM J. Numer. Anal., 19:871–885, 1982.

[7] M. Bercovier, O. Pironneau and V. Sastri, *Finite elements and characteristics for some parabolic-hyperbolic problems*. Appl. Math. Modelling, 7:89–96, 1983.

[8] K.W. Morton, A. Priestley and E. Süli, *Stability of the Lagrange-Galerkin Method with non-exac integration*. M2AN Math. Model. Numer. Anal., 22:625–653, 1988.

[9] M.D. Baker, E. Süli and A.F. Ware, *Stability and convergence of the spectral Lagrange-Galerkin method for mixed periodic/non-periodic convection-dominated diffusion problems*. IMA J. Numer. Anal., 19:637–663, 1999.

[10] J. Baranger and A. Machmoum, *A "natural" norm for the method of characteristics using discontinuous finite elements: 2D and 3D case*. Math. Model. Numer. Anal., 33:1223–1240, 1999.

[11] M.E. Gurtin, *An Introduction to Continuum Mechanics*. Mathematics in Science and Engineering, Academic Press, San Diego, 158, 1981.

[12] M. Benítez, *Métodos numéricos para problemas de convección difusión. Aplicación a la convección natural*. Ph.D. Thesis, Universidade de Santiago de Compostela. http://dl.dropbox.com/u/14459353/tesis_benitez.pdf, 2009.

[13] K. Chrysafinos and N.J. Walkington, *Lagrangian and moving mesh methods for the convection diffusion equation*. M2AN Math. Model. Numer. Anal., 42:25–55, 2008.

Posters

Optimizing size of large tonnage fish farm design

Ibán Constenla Rozados, Alfredo Bermúdez de Castro, José Luis Ferrín González
Applied Maths Department, University of Santiago de Compostela (Spain)
e-mail: iban.constenla@mundo-r.com, alfredo.bermudez@usc.es, joseluis.ferrin@usc.es

Abstract

The main objective of this project is to analyse the hydraulic behaviour of turbot fish farms using computer fluid dynamics tools. Several design scenarios are proposed. Firstly, steady state water flux is simulated using a 3D model and considering fishes such as a porous zone. Water is supposed incompressible and Newtonian. Secondly, emptying for cleaning is simulated in order to obtain information about sediment transport and their evacuation out of the tank. This process is transient. Thirdly, feed particles distribution on water surface is simulated in order to check their uniformity. Finally, water flux stop is analysed. During this operation, it is necessary to introduce an additional oxygen source to ensure fish survival. The oxygen comes through four small tubes placed at the bottom of the tank. All simulations are made using Ansys Fluent software.

This project has been developed by the Department of Applied Mathematics of the University of Santiago de Compostela, under the supervision of Alfredo Bermúdez de Castro and Juan José Casares Long, and with the collaboration of José Luis Ferrín González and Ibán Constenla Rozados. It has been proposed by IMPULSO Engineering, Architecture and Consulting services.

36.1 Model equations

Every proposed scenario needs different groups of equations, which are described here. The water flux is simulated under the assumption of constant density. In this case, incompressible Navier–Stokes equations are employed. The mass (36.1) and momentum (36.2) conservations are shown next:

$$\nabla \cdot \vec{v} = 0, \tag{36.1}$$

$$\rho \nabla \vec{v}\vec{v} = -\nabla p + \nabla \cdot \bar{\bar{\tau}} + \rho \vec{g}. \tag{36.2}$$

For modeling turbulence, the standard $k-\epsilon$ model is selected. This method is based on model transport equations (equations (36.3) and (36.4)) for the turbulence kinetic energy,k, and its dissipation rate, ϵ.

$$\rho \dot{k} - \nabla \cdot \left[\left(\mu + \frac{\mu_t}{\sigma_k} \right) \nabla k \right] = P_k - \rho \epsilon, \tag{36.3}$$

$$\rho \dot{\epsilon} - \nabla \cdot \left[\left(\mu + \frac{\mu_t}{\sigma_\epsilon} \right) \nabla \epsilon \right] = C_{1\epsilon} \frac{\epsilon}{k} P_k - C_{2\epsilon} \rho \frac{\epsilon^2}{k}. \tag{36.4}$$

The porous media used for modeling the presence of fishes is included into the model as a source term using Darcy's law. Anisotropic case is considered (see (36.5)) and porosity, ϕ, is calculated (see (36.6)).

$$S = -\mu K^{-1} \vec{v}, \tag{36.5}$$

$$\phi = \frac{V_{total} - V_{fishes}}{V_{total}}. \tag{36.6}$$

Transitory term is necessary to be included into the mass and momentum conservation equations for the emptying tank process as follows

$$\frac{\partial \vec{v}}{\partial t} + \nabla \cdot \vec{v} = 0, \tag{36.7}$$

$$\rho \frac{\partial \vec{v}}{\partial t} + \rho \nabla \vec{v}\vec{v} = -\nabla p + \nabla \cdot \bar{\bar{\tau}} + \rho \vec{g}. \tag{36.8}$$

The water surface boundary condition was set under the assumption of equal velocity for all its points. The emptying rate was determined using the Bernoulli's principle between points 1 and 2, such as it is shown in Figure (36.3) and equation (36.9). Applying mass conservation, equation (36.10) is obtained for characterizing the height of water level. Its solution is a function of time (see (36.11)) and the total emptying time ($z(t_{emptying}) = 0$) can be calculated, leading to (36.12).

$$\rho \frac{{v_1}^2}{2} + P_1 + \rho g(z(t) - H) = \rho \frac{{v_2}^2}{2} + P_2 + \rho g(h_c - H) + K\rho \frac{{v_2}^2}{2}, \tag{36.9}$$

$$\frac{dz}{dt} = -\frac{A_2}{A_1}\sqrt{\frac{2\left(\frac{P_1 - P_2}{\rho} + g(z(t) - h_c)\right)}{1 + K - (A_2/A_1)^2}}, \tag{36.10}$$

$$z(t) = h_c + \frac{1}{2g}\left[\frac{2(P_2 - P_1)}{\rho} + \left(\sqrt{\frac{2(P_1 - P_2)}{\rho} + g(H - hc)} - \frac{(A_2/A_1)gt}{\sqrt{1 + K - (A_2/A_1)^2}}\right)^2\right], \tag{36.11}$$

$$t_{emptying} = \frac{\sqrt{g(H - h_c)(1 + K - (A_2/A_1)^2)}}{A_2 g/A_1}. \tag{36.12}$$

The feeding process does not introduce new equations to solve. An injection of particles associated to the water surface is defined for modeling the feed. The presence of the particles do not modify the flux (it supposes less than 10% of the total mass), so interaction between solid and liquid phases is not consider.

The oxygen distribution is a transient process due to the fact that this system is activated when normal water flux inside the tank is interrupted. The oxygen is introduced in the tank through four nozzles placed over the tank floor, letting fishes continue breathing. In this case, water flux and oxygen concentration are calculated in a separate way. Firstly, turbulent flux equations are solved, saving results at several time steps. Secondly, oxygen distribution is calculated using the obtained data from the previous stage.

The oxygen consumption inside the tank is due to several processes: the fishes's breath, the carbon waste degradation and the nitrification processes. Both degradation and nitrification are less important than breath, so they are not considered in the simulations. An experimental expression (see (36.13)) proposed by Maceira [2] is adopted for modeling this term. It can be adopted for turbot which range of weight is 4-1000 g and for water temperatures between 7 and 16 °C.

$$Q_{O_2} = (68.281 \cdot T - 398.87)p^{-0.25} \tag{36.13}$$

The mass transfer between phases is taken into account in the model. The different concentration level of oxygen between phases acts as driving force in the process (see (36.14)).

$$J = k_{ol}(C_s - C) \tag{36.14}$$

Parameters such as saturation concentration of water (36.15), salinity S or water gas pressure (36.17) are necessary to complete the full model. All of them are obtained through experimental correlations.

$$\begin{aligned} C_s &= \frac{1}{0.2099}\exp[-139.34411 + 1.575701\cdot 10^5/T - 6.642308\cdot 10^7/T^2 + \\ &\quad + 1.2438\cdot 10^{10}/T^3 - 8.621949\cdot 10^{11}/T^4 - \\ &\quad - S\cdot(1.7674\cdot 10^{-2} - 10.754/T + 2140.7/T^2)]\cdot\frac{P-P_{wv}}{1-P_{wv}}\cdot\frac{1-\theta\cdot P}{1-\theta}, \quad (36.15) \\ \theta &= 0.000975 - 1.426\cdot 10^{-5}\cdot(T-273.15) + 6.436\cdot 10^{-8}\cdot(T-273.15)^2, \quad (36.16) \\ P_{wv} &= \exp(11.8571 - 3840.7/T - 216961/T^2) \quad (36.17) \end{aligned}$$

The model adopted for bubbles was proposed by Wüest et al. [3]. Bubbles have a rise tendency within a fluid due to the difference between water and oxygen densities. Rise velocity v_b and mass transfer coefficient k_{ol} are both dependent of bubble ratio.

$$k_{ol} = \begin{cases} 0.6\cdot r & \text{if } r < 6.67\cdot 10^{-4} \\ 4\cdot 10^{-4} & \text{if } r \geq 6.67\cdot 10^{-4} \end{cases} \quad (36.18)$$

$$v_b = \begin{cases} 4474\cdot r^{1.357} & \text{if } r < 7\cdot 10^{-4} \\ 0.23 & \text{if } 7\cdot 10^{-4} \leq r < 5.1\cdot 10^{-3} \\ 4.202\cdot r^{0.547} & \text{if } r \geq 5.1\cdot 10^{-3} \end{cases} \quad (36.19)$$

Finally, a differential equation for modeling bubbles mass lost is obtained. Spherical bubbles are taken as assumption in this job.

$$\frac{dm_{O_2}}{dt} = -A_p\cdot M_{O_2}\cdot k_{ol}\cdot(C_s - C_{O_2}(t))^+, \quad (36.20)$$

$$V_p = \frac{m_{O_2}}{\rho_{O_2}} = \frac{4}{3}\pi r^3(t) \Rightarrow r(t) = \left(\frac{3m_{O_2}(t)}{4\pi\rho_{O_2}}\right)^{1/3}. \quad (36.21)$$

36.1.1 Figures

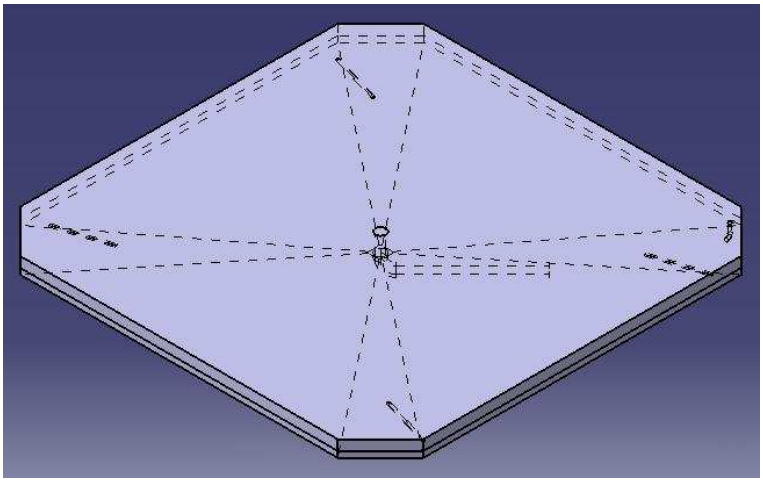

Figure 36.1: Geometry of 15x15 tank

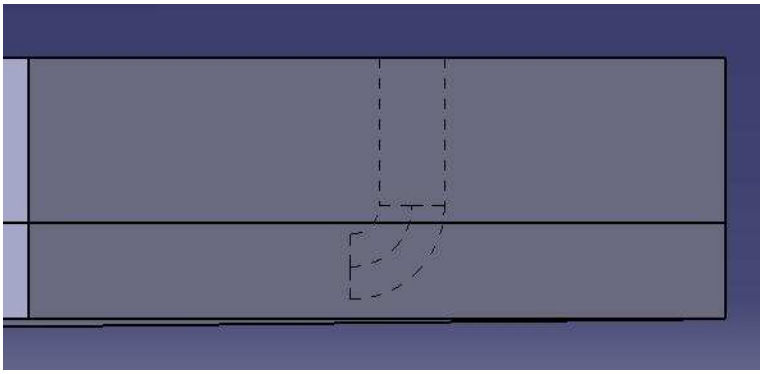

Figure 36.2: Water entry pipe (detail)

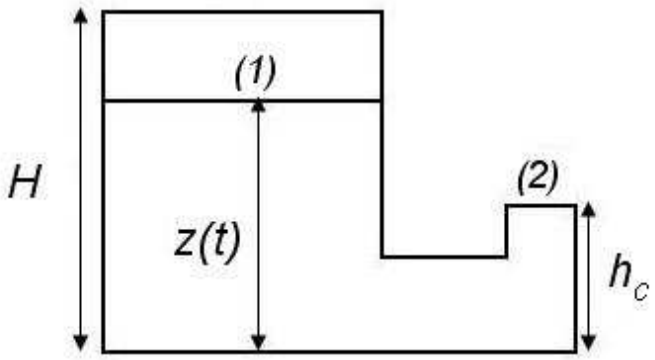

Figure 36.3: Emptying scheme of the tank

Bibliography

[1] Standard Methods, *Technical Report 20th Ed.*, APHA, American Public Health Association, 1998.

[2] Maceira Fernández, P., *Análisis y modelización de procesos de flujo de oxígeno y nitrógeno en sistemas de acuicultura*, PhD Thesis, Escola Técnica Superior de Enxeñería, Dpto. de Enxeñería Química, Santiago de Compostela, Spain, 2005.

[3] Wüest, A. and Brooks, N. H. and Imboden, D. M., *Bubble Plume Modeling for Lake Restoration*, Water Resources Research, 28(12), 3235–3250, 1992.

Posters

An optimized simulated annealing algorithm for GPUs with application to a SABR model in finance [1]

A. Ferreiro, J.A. García, J.G. López-Salas, C. Vázquez

Departamento de Matemáticas, Universidade da Coruña

e-mail: aferreiro@udc.es, jagrodriguez@udc.es, josegsalas@gmail.com, carlosv@udc.es,

http://dm.udc.es/m2nica/

Abstract

We present a generic and efficient implementation of a simulated annealing algorithm for GPUs, that is suitable for calibrating financial models to market prices at almost real time.

37.1 Introduction

As in many industrial sectors, mathematical models are widely used nowadays in quantitative finance. These pricing models usually depend on many parameters that must be previously calibrated to fit certain market data. This calibration process is usually posed in terms of a nonlinear optimization problem, involving a highly demanding computational task. Moreover, these problems are specially well suited to take advantage of the recent GPU technologies.

The main objective of the present work is to develop a generic and highly optimized version of a simulated annealing algorithm in CUDA [8] and its application to the calibration of the static SABR stochastic volatility model [1, 4]. For this purpose, first the more efficient versions of simulated annealing presented in [2, 5] have been analyzed, tested and adapted to the GPU technology. After testing the software with academic examples, as the motivation comes from the practical requirement of speeding up financial computations, the calibration of the recently proposed SABR stochastic volatility model has been considered . Thus, the static version of the model has been analyzed.

37.2 Simulated annealing and parallel GPU implementation

37.2.1 Simulated annealing algorithm

Let us consider the global minimization problem: $\min_{x \in V} f(\boldsymbol{x})$, where f is the cost function and V is the search space. The annealing process can be described as follows: starting from some maximum temperature, T_0, we consider a sequence of decreasing temperatures. At each one the system is allowed to reach thermal equilibrium, in which the probability of the system to be in some state with energy E is given by the Boltzmann distribution. The main steps of the simulated annealing algorithm are the following (see [2] for details):

- **Step 1**: Start with a given temperature, T_0, and an initial point, $\boldsymbol{x}_0$, with energy of configuration $E_0 = f(\boldsymbol{x}_0)$.

[1] This project has been proposed by Analistas Financieros Internacionales (AFI) and it has been developed in collaboration with J.L. Fernández (U. Autónoma de Madrid). It is also partially supported by I-Math Consolider Project (Reference: COMP-C6-0393) and by MICINN (MTM2010-21135-C02-01).

- **Step 2**: Select randomly a coordinate of $\boldsymbol{x}_0$ and a random number to modify the selected coordinate to obtain another point $\boldsymbol{x}_1 \in V$ in a neighborhood of $\boldsymbol{x}_0$.

- **Step 3**: Compare the function value at the two previous points, by using the Metropolis criterion as follows: let $E_1 = f(\boldsymbol{x}_1)$ and select a sample of a random uniform variable $U(0,1)$. Then, move the system to the new point if and only if $U < \exp(-(E_1 - E_0)/T)$, where T is the current temperature. Thus, $E_1 - E_0$ is compared with an exponential random variable with mean T. Note that we always move to the new point if $E_1 < E_0$, and that at any temperature there is a chance for the system to move "upwards". Note that we need 3 uniform random numbers: one to choose the coordinate, one to change the selected coordinate and one for the acceptance criterion.

- **Step 4**: Either the system has moved or not, repeat steps $2-3$. At each stage we compare the function at new points with the function at the present point until the sequence of accepted points fulfills some test of achieving an equilibrium state.

- **Step 5**: Once an equilibrium state has been achieved for a given temperature, the temperature is decreased according to the annealing schedule (in our case we update temperature with a decreasing factor λ with $0 < \lambda < 1$, usually λ close to one) and step 2 starts again, with the last iteration of the algorithm as initial state. The iteration procedure continues until a stopping criterion considering the system as frozen is achieved.

  Since we continue steps $2-3$ until an equilibrium state, the starting values in step 1 have no effect on the solution. The algorithm can be implemented in numerous ways.

The pseudo-code of the previous algorithm can be sketched as follows:

```
x = x_0 ; T = T_0;
for i = 1 to NumberOfTemperatureReduction do
    for j = 1 to N do
        x' = ComputeNeighbour( );
        ΔE = f(x') − f(x); //Energy increment
        if (ΔE < 0 or AcceptWithProbability P(ΔE, T))
            x = x'; //The trial is accepted
    end for
    T = λT ; with λ < 1
end for;
```

37.2.2 Some GPU implementation details

The SA algorithm has a very high computational cost; thus, in this section, we present its parallelization using modern GPUs. A GPU consists of a great number of processors that can work in parallel, together with a memory bus that can perform memory transfers (read/write operations) in parallel with certain restrictions. Each processor can execute several threads simultaneously (see [7]). We will work with Nvidia GPUs. There is an API for programming Nvidia GPUs called CUDA that consists of some drivers for the card, a compiler and a language consisting of extensions to C/C++ language to control the GPU (the memory transfers, the job assignment to processors and the synchronization tasks).

The parallelization of the previous algorithm is not straightforward. We take the following approach (see [3]): at each temperature level we perform NT Markov chains. These are independent processes and can be distributed among the GPU processors: each Markov process will be executed by one thread in the GPU and thus, each thread returns one final state. We then choose the best state among the NT computed ones, advance to the next temperature level and use the obtained state as starting point for the next NT Markov processes. This technique is also more effective than usual SA algorithm, even when

performed sequentially in CPU. This is because updating the starting point at every certain number of Markov chains makes the algorithm to converge more precisely to the optimum. We have implemented this version of the SA, both in CPU and GPU, so both codes perform the same operations, explore the same points and return the same result, and thus can be compared.

From the parallel implementation point of view, we remark that for each temperature level, each thread computes a Markov chain starting from the best state of the previous state space. The Nvidia CURAND CUDA library has been used as random number generator: the random numbers are generated at each temperature level. In order to take advantage of the texture cache, the random numbers are stored in memory using textures , so that we perform parallel reads from the GPU memory. The reduction to pass from one temperature level to another is performed at GPU, following the most efficient implementation of the Nvidia reduction [8]. Next, the best state is stored in constant memory. As it is used as starting point for all the threads in the next temperature step, storing it in constant memory allows to benefit from broadcasting. The implementation has been performed in single precision and double precision. The results presented in this paper are for the single precision case.

37.3 Numerical Experiments: academic test and SABR model

In this section several experiments are presented to asses the correctness and performance of our CUDA implementation of simulated annealing. The CUDA implementation has been developed from an optimized C code, following the idea of section 37.2.2, so both codes perform exactly the same operations and their performance can thus be compared [2]

Academic test: a typical benchmark for optimization techniques is the Normalized Schwefel function [9]:

$$f(\boldsymbol{x}) = -\frac{1}{n}\sum_{i=1}^{n} x_i \cdot \sin(\sqrt{|x_i|}, \quad -512 \leq x_i \leq 512, \qquad \boldsymbol{x} = (x_1, \ldots, x_n). \tag{37.1}$$

For any n, the global minimum is achieved at $\overline{x}_i = 420.9687$, $i = 1, \ldots, n$, and $f(\overline{\boldsymbol{x}}) = -418.982887$. Table 37.1 shows the accuracy for three tests with different SA parameters. Notice that as soon as the T is decreased, and T_0, λ, the number of threads and the Markov chain length are increased, the accuracy and the computational cost increases. This can be allowed by the GPU technology and provides an accurate result. Table 37.2 shows the performance of the GPU implementation with respect a one core CPU.

SABR model: this stochastic volatility model is derived in [4] and it allows to obtain immediately the market price from Black Scholes's formula. It also provides fine, and sometimes spectacular, fits of the market implied volatility surfaces and captures the dynamics of the smile. The model is given by:

$$dF_t = V_t F_t^{\beta} dW_t, \qquad dV_t = V_t \nu dZ_t, \tag{37.2}$$

where $F_t = S_t e^{(r-q)(T-t)}$ is the forward price of asset S (r and q being the interest rate and the dividend yield), and V_t denotes the asset volatility. The spot values S_0 and $V_0 = \alpha$ are the initial conditions. W_t, Z_t are two correlated Brownian processes with correlation $-1 < \rho < 1$. The spot value of volatility, $\alpha \geq 0$, the elasticity of variance, $\beta \in [0, 1]$, and the volatility of volatility, $\nu > 0$, are constants. The model parameters to be calibrated are α, β, ν and ρ. A great advantage of SABR model is the asymptotic expression for the volatility. The implied volatility is the value of the lognormal volatility in Black Scholes model and it is given by an analytical formula (see [4] and [6], for example).

[2] The numerical experiments have been performed with the following hardware and software configuration: a GPU Nvidia Geforce GTX470, a recent CPU Xeon E5620 clocked at 2.4 Ghz with 16 GB of RAM, CentOS Linux, Nvidia CUDA SDK 3.2 and GNU C++ compiler 4.1.2.

	Test 1	Test 2	Test 3
x_1	423.235474	420.950195	420.967255
x_2	419.037170	420.961792	420.978210
x_3	419.975250	420.999695	420.984650
x_4	423.326172	420.997253	420.999115
x_5	420.853394	420.979065	420.986816
x_6	421.988647	421.007874	420.955261
x_7	421.221191	420.939178	420.982971
x_8	422.035004	420.938171	420.990631
x_9	421.060028	420.971497	420.980896
x_{10}	420.850159	420.959167	420.976135
x_{11}	420.532379	420.957062	420.990265
x_{12}	421.783997	421.006927	420.978882
x_{13}	422.096436	420.936279	420.938324
Error	$2.9328 \cdot 10^{-3}$	$6.0229 \cdot 10^{-5}$	$4.2443 \cdot 10^{-5}$

Table 37.1: Exact vs. computed solution for different SA parameters. Test 1 ($NT = 8192, N = 5, T_0 = 100, T_{min} = 1, \lambda = 0.7$), Test 2 ($NT = 16384, N = 10, T_0 = 1000, T_{min} = 0.1, \lambda = 0.99$) and Test 3 ($NT = 16384, N = 100, T_0 = 1000, T_{min} = 0.01, \lambda = 0.99$), where NT is the number of paths/threads, N is the thread length, T_0 is the starting temperature and T_{min} is the final temperature. Error is measured in $\|\cdot\|_2$.

	Test 1	Test 2	Test 3
CPU Time (s)	0.388	101.287	1301.283
GPU Time (s)	$1.0822 \cdot 10^{-2}$	$8.9932 \cdot 10^{-1}$	9.260071
Speedup	35.85	112.62	140.52

Table 37.2: Performance of CUDA version vs. sequential version with one CPU core.

We present a test for calibrating a real volatility surface. We have market data data given by Banesto and stored in an EXCEL data-sheet, containing historical series of the volatility surface for EUR-USD. Thus we have the Black Scholes market quoted volatilities $\sigma(K,T)$ and we compute the Black Scholes, $\sigma_{model}(K,T)$, given by the SABR model. The objective is to adjust the model parameters so that $\sigma_{model}(K_j,T_i) \equiv \sigma(K_j,T_i)$, or more precisely, so that the following mean quadratic error is minimized:

$$f(\boldsymbol{x}) = \sum_{i,j} \Big(C_{model}(K_i,T_j) - C(K_i,T_j) \Big)^2.$$

Table 37.3 shows the performance of GPUs in a SABR calibration example with four different SA parameter configurations. The computed parameters for Test 4 are $\alpha = 1.79512309$, $\nu = 0.5901644239$ and $\rho = -1$, while we take $\beta = 0.8$. The relative error in $\|\cdot\|_2$ between the calibrated model results and the market volatility surface is $7 \cdot 10^{-3}$.

	Test 1	Test 2	Test 3	Test 4
Time CPU	16.767	581.667	11647.2564	46523.130600
Time GPU	0.244171	8.2428	159.454172	503.106656
Speedup	68.669	70.566	73.04453	92.4717

Table 37.3: Performance CUDA version vs. sequential one with one CPU core for the SABR model. Test 1 ($NT = 8192, N = 5, T_0 = 1000, T = 0.01, \lambda = 0.7$), Test 2 ($NT = 8192, N = 5, T_0 = 1000, T = 0.01, \lambda = 0.99$), Test 3 ($NT = 8192, N = 100, T_0 = 1000, T = 0.01, \lambda = 0.99$) and Test 4 ($NT = 16384, N = 200, T_0 = 1000, T = 0.01, \lambda = 0.99$).

Bibliography

[1] B. Bartlett, Hedging under SABR Model. Wilmott Magazine (2009).

[2] S.B. Brooks, B.J.T. Morgan. Optimization using simulated annealing, The Statistician 44 (2),(1995), 241-257.

[3] A. Debudaj-Grabysz, and R. Rabenseifner. Nesting OpenMP in MPI to Implement a Hybrid Communication Method of Parallel Simulated Annealing on a Cluster of SMP Nodes, EuroPVM/MPI, Sorrento, September 19, 2005

[4] P.S. Hagan, D. Kumar, A.S. Lesniewski, D.E. Woodward. Managing the smile risk, Wilmott Magazine (2002), 84-108.

[5] P.J.M van Laarhoven, E.H.L.Aarts. Simulated Annealing: Theory and Applications, Kluwer Academic Publishers (1987).

[6] J. Obloj. Fine-tune your smile: Correction to Hagan *et al*, Wilmott Magazine (May 2008).

[7] J. Sanders, E. Kandrot. CUDA by Example: An Introduction to General-Purpose GPU Programming (2011).

[8] Nvidia Coorp. CUDA 4.0 Programming guide (2011).

[9] `http://www.it.lut.fi/ip/evo/functions/node10.html`

Posters

Simulación del reparto de gas y carbón por dedos del quemador en función de la posición del concentrador de carbón

J. L. Ferrín[(1)], **L. Saavedra**[(2)]

(1) Dpto. Matemática Aplicada, Facultad de Matemáticas, Universidade de Santiago de Compostela
joseluis.ferrin@usc.es

(2) Dpto. Fundamentos Matemáticos, E.T.S.I. Aeronáuticos, Universidad Politécnica de Madrid
laura.saavedra@upm.es

Resumen

En este póster presentamos los resultados obtenidos en el proyecto final del Master en Ingeniería Matemática de la Universidad de Santiago de Compostela de L. Saavedra [4]. En él se realizaron simulaciones de Mecánica de Fluidos Computacional (CFD) para predecir el reparto de gas y carbón por dedos del quemador, en función de la posición del concentrador en una caldera de una Central Térmica. La empresa que ha propuesto el proyecto es Endesa Generación, S.A. y, de forma más precisa, la Central Térmica de As Pontes.

38.1 Descripción del problema

El carbón pulverizado, utilizado como combustible en la caldera de la Central Térmica, es arrastrado hacia el interior de la misma por una corriente de gases de combustión recirculados del proceso. De este modo, se consigue una atmósfera inerte que evita que la combustión del carbón comience antes de entrar en la parte de la caldera diseñada para este proceso, llamada el hogar.

Los cuatro conductos por los que entra la mezcla de gases de recirculación y carbón se denominan dedos. Uniendo la zona del molino con los dedos está la llamada caja de vientos que reparte la mezcla que viene del molino entre los cuatro niveles de quemadores. En el interior de este conducto se encuentra una pieza llamada concentrador formada por unos álabes direccionales que pueden adoptar distintos ángulos. En función de la posición de dichos álabes se obtienen distintos repartos de carbón en los dedos del quemador, priorizando unos niveles frente a los otros. En la Figura 38.1 se puede ver la caja de vientos y la geometría del concentrador con sus álabes sin inclinación (posición 0^o).

38.2 Modelización matemática

Queremos simular un flujo que consta de dos fases: la fase gaseosa formada por una mezcla de gases no reactivos cuya composición, temperatura y viscosidad permanecen constantes desde la salida del molino hasta la entrada en el hogar de la caldera, y, por otro lado, la fase sólida formada por las partículas de carbón. Los gases que arrastran las partículas son pobres en oxígeno y su temperatura es tan baja que no se inicia ninguna reacción de gasificación o liberación de volátiles; por lo tanto, la masa y la temperatura de las partículas no varían hasta su llegada al hogar, es decir, consideraremos las partículas como inertes. Además, como la fase sólida es dispersa y su fracción volumétrica es pequeña comparada con la del gas, sus efectos sobre la cantidad de movimiento de la mezcla gaseosa serán despreciables.

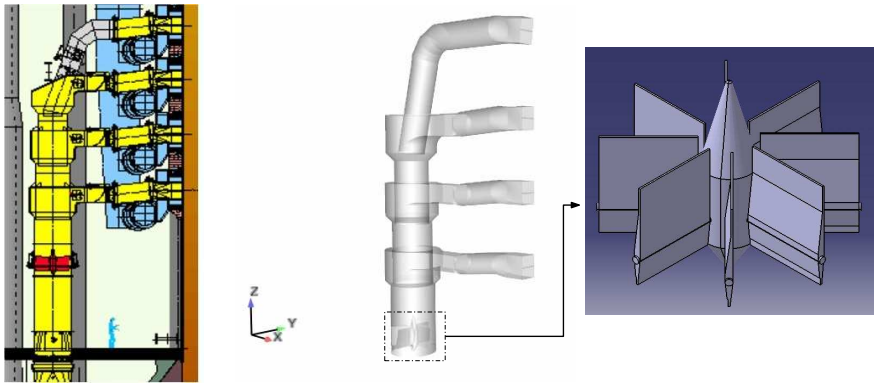

Figure 38.1: Geometría del dominio computacional y detalle del concentrador

En consecuencia, podemos considerar la fase gaseosa desacoplada de la fase sólida y resolverla hasta alcanzar el estado estacionario. Una vez resuelta la fase gaseosa con la velocidad obtenida para la mezcla podremos utilizar un modelo para calcular la trayectoria de las partículas.

38.2.1 Fase gaseosa

Consideramos un flujo turbulento incompresible. Para modelizar la turbulencia elegiremos un modelo tipo RANS (Reynods Average Navier Stokes), concretamente el modelo $k-\epsilon$ estándar. En este tipo de modelos se descompone la velocidad como suma de una media y una fluctuación, $\mathbf{v} = \overline{\mathbf{v}} + \mathbf{v}'$, y se promedian las ecuaciones de Navier-Stokes obteniendo el modelo:

$$\operatorname{div}(\overline{\mathbf{v}}) = 0, \tag{38.1}$$

$$\overline{\mathbf{v}} \cdot \nabla\overline{\mathbf{v}} - \operatorname{div}(\nu(\nabla\overline{\mathbf{v}} + (\nabla\overline{\mathbf{v}})^t)) - \operatorname{div}\left(\nu_t\left(\nabla\overline{\mathbf{v}} + (\nabla\overline{\mathbf{v}})^t\right) - \frac{2}{3}k\mathrm{I}\right) + \nabla\overline{\pi} = 0, \tag{38.2}$$

$$\overline{\mathbf{v}} \cdot \nabla k - \operatorname{div}\left[\left(\nu + \frac{\nu_t}{\sigma_k}\right)\nabla k\right] = P_k - \epsilon, \tag{38.3}$$

$$\overline{\mathbf{v}} \cdot \nabla \epsilon - \operatorname{div}\left[\left(\nu + \frac{\nu_t}{\sigma_\epsilon}\right)\nabla \epsilon\right] = C_{1\epsilon}\frac{\epsilon}{k}P_k - C_{2\epsilon}\frac{\epsilon^2}{k}, \tag{38.4}$$

con $\nu_t = C_\mu \frac{k^2}{\epsilon}$ la viscosidad turbulenta, $P_k = \frac{1}{2}\nu_t\|\nabla\mathbf{v} + (\nabla\mathbf{v})^t\|^2$ la producción de la energía cinética turbulenta y $C_{1\epsilon},\ C_{2\epsilon},\ \sigma_k,\ \sigma_\epsilon$ y C_μ constantes del modelo cuyos valores se pueden consultar en [3].

38.2.2 Fase sólida

La velocidad de las partículas se obtiene resolviendo el problema de valor inicial:

$$\frac{d\mathbf{v}_p}{dt} = F_A\left(\mathbf{v} - \mathbf{v}_p\right) + \mathbf{g}\frac{\rho_p - \rho}{\rho_p}, \quad \mathbf{v}_p(0) = \mathbf{v}_{p0}, \tag{38.5}$$

donde $\mathbf{v}_p$ es la velocidad de la partícula, ρ_p su densidad y F_A la fuerza de arrastre por unidad de masa dada por

$$F_A = \frac{18}{24}\frac{\mu}{\rho_p d_p^2}C_D Re, \tag{38.6}$$

siendo μ la viscosidad dinámica del gas, d_p es el diámetro de la partícula, Re el número de Reynolds relativo a la partícula y C_D es el coeficiente de arrastre aerodinámico para partículas esféricas. La expresión de estos dos últimos parámetros se puede ver en [3].

38.3 Resultados

Para realizar las simulaciones de este proyecto se ha utilizado CATIA (generación de la geometría de la caja de vientos), GAMBIT (mallado del dominio) y FLUENT (resolución de las ecuaciones de los modelos, tanto de la fase gaseosa como de las partículas de carbón, para cada una de las posiciones del concentrador).

En primer lugar, mostramos algunos de los resultados obtenidos cuando la inclinación de los álabes del concentrador es de -5^{o}. A continuación, se compararán los repartos de gas y carbón a los dedos del quemador que predicen las simulaciones, para las diferentes posiciones del concentrador, con los que se han medido en la central térmica.

38.3.1 Posición -5º

En la Figura 38.2 se pueden ver los contornos de velocidad y energía cinética turbulenta obtenidas en la simulación en un plano vertical que corta a la caja de vientos por la mitad. Los caudales de gas y carbón obtenidos en cada uno de los niveles se muestran en la Figura 38.3, donde se comparan con las medidas realizadas.

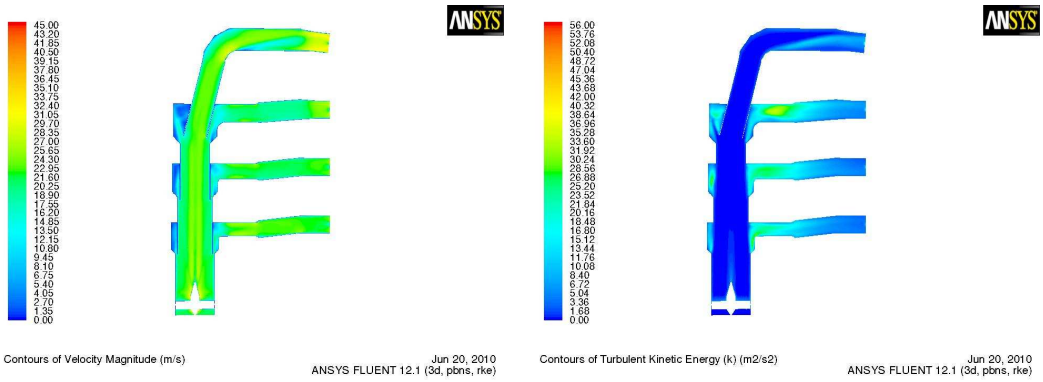

Figure 38.2: Velocidad $(\mathrm{m/s})$ y energía cinética turbulenta $(\mathrm{m^2/s^2})$

38.3.2 Resultados globales

Las Figuras 38.4 y 38.5 muestran los caudales de gas y carbón, respectivamente, en función de la inclinación de los álabes del concentrador para cada uno de los niveles del quemador. Además se comparan estos caudales con los que se han obtenido experimentalmente.

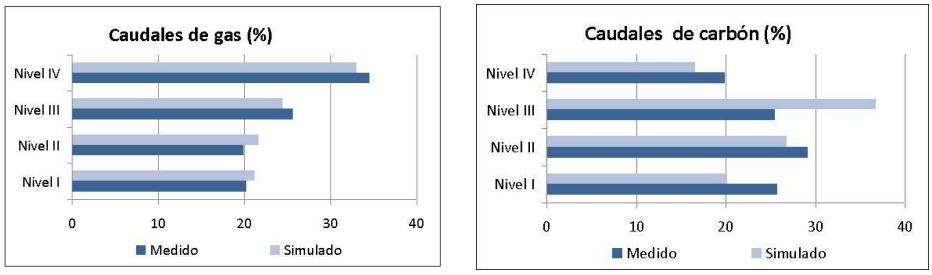

Figure 38.3: Comparación de los caudales de gas y carbón en los distintos niveles

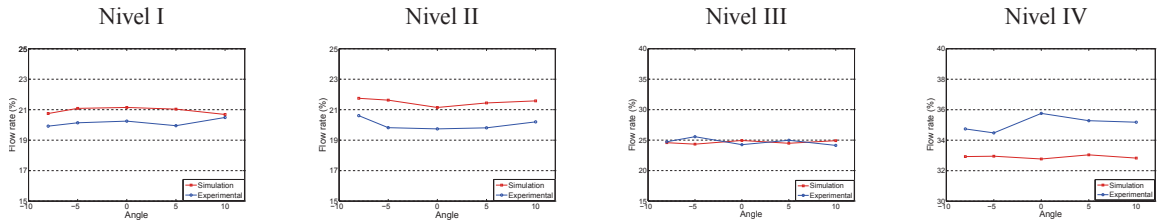

Figure 38.4: Reparto de gas a dedos del quemador

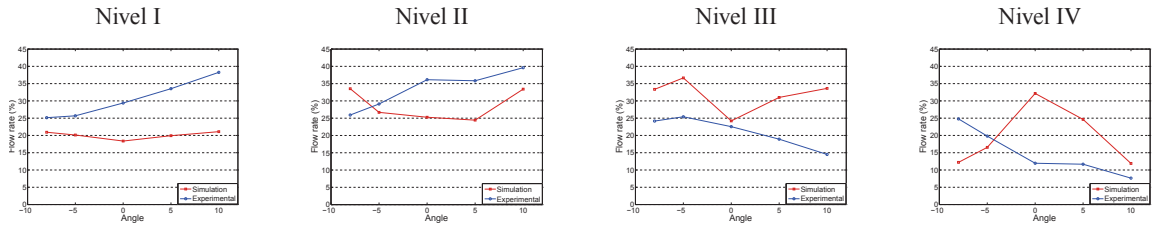

Figure 38.5: Reparto de carbón a dedos del quemador

38.4 Conclusiones

Como hemos visto, los resultados de las simulaciones CFD se ajustan bien a los valores experimentales en el reparto de los caudales de gas que salen por cada nivel de quemadores. Sin embargo, el reparto de carbón a dedos del quemador obtenido con las simulaciones muestra valores diferentes a los obtenidos con las medidas experimentales (sobre los que existen numerosas incertidumbres). Los datos de las simulaciones y los experimentales en cada nivel solo se parecen en algunas posiciones y la tendencia de los datos experimentales es siempre monótona (creciente o decreciente) mientras las simulaciones muestran comportamientos algo más simétricos.

Bibliography

[1] A. Bermúdez. *Continuum thermomechanics*. Birkhäuser Verlag, 2005.

[2] M. G. del Río Cidoncha, M. E. Martínez Lomas, J. Martínez Palacios, and S. Pérez Díaz. *El libro de CATIA V5*. Tébar, 2007.

[3] Ansys. Inc. *Ansys Fluent 12.0 User's Guide*. 2009.

[4] L. Saavedra. Obtener como resultado de una simulación CFD el reparto de gas y carbón por dedos del quemador en función de la posición del concentrador de carbón. Proyecto del Master de Ingeniería Matemática, 2010.

The RSME Conference on Transfer and Industrial Mathematics is supported by the Royal Spanish Mathematical Society, a scientific society for the promotion of mathematics and its applications as well as the encouragement of research and teaching at all educational levels. The three-day conference presents successful experiences in the field of mathematical knowledge transfer to industry and focuses on the following issues:

— Showing how collaboration with industry has opened up new lines of research in the field of mathematics providing high quality contributions to international journals and encouraging the development of doctoral theses.
— How the promotion of existing infrastructures has contributed to enhance the transfer of mathematical knowledge to industry.
— The presentation of postgraduate programs offering training in mathematics with industrial applications.

The conference includes talks from researchers and industry representatives who present their different points of view and experiences with regards to the transfer of mathematical knowledge to industry.

REAL SOCIEDAD MATEMÁTICA ESPAÑOLA CENTENARIO 1911//2011
mat+i Grupo de Investigación en Ingeniería Matemática
nodo.cesga (i-math) Red Mathematica Consulting & Computing de Galicia
i-math ingenio mathematica consolider ingenio 2010
GOBIERNO DE ESPAÑA MINISTERIO DE CIENCIA E INNOVACIÓN
XUNTA DE GALICIA
USC UNIVERSIDADE DE SANTIAGO DE COMPOSTELA